VŠB - Technical University of Ostrava
Faculty of Mechanical Engineering
Department of Control Systems and Instrumentation
Czech Republic

CLOSED-LOOP CONTROL OF MECHATRONIC SYSTEMS

Prof. Ing. Antonín Víteček, CSc., Dr.h.c.
Prof. Ing. Miluše Vítečková, CSc.

Ostrava 2013

CLOSED-LOOP CONTROL OF MECHATRONIC SYSTEMS

ISBN 978-80-248-3149-7

PREFACE

The educational module the „Closed-loop Control of Mechatronic Systems“ is devoted to the bases of automatic control. The main emphasis is put on the principle of a negative feedback and its use in the control of mechatronic systems. It covers the most important area of analog automatic control and very briefly also describes digital control.

Since the educational module is concerned with the basic concepts automatic control, any precise proofs in the module are therefore not given. For deepening and extending the study material the below mentioned references are recommended:

DORF, R.C., BISHOP, R. *Modern Control Systems.* 12th Edition. Prentice-Hall, Upper Saddle River, New Jersey 2011

FRANKLIN, G.F., POWELL, J.D. – EMAMI-NAEINI, A. *Feedback Control of Dynamic Systems.* 4th Edition. Prentice-Hall, Upper Saddle River, New Jersey, 2002

LANDAU, I. D., ZITO, G. *Digital Control Systems. Design, Identification and Implementation*. Springer – Verlag, London, 2006

NISE, N. S. *Control Systems Engineering*. 6th Edition. John Wiley and Sons, Hoboken, New Jersey, 2011

The authors give thanks to Mr Mark Landry for the English language correction.

The textbook is determined for students who are interested in control engineering and mechatronics.

CONTENTS

List of basic notations and symbols ... **6**

1. Introduction to closed-loop control ... **12**

2. Mathematical models of dynamic systems ... **19**

2.1 General mathematical models ... 19

2.2 Linear dynamic systems ... 22

3. Mathematical models of linear dynamic systems ... **25**

3.1 Basic linear mathematical models ... 25

3.2 Linear dynamic system classification ... 37

3.3 Block diagram algebra ... 46

4 Mathematical model simplification ... **57**

4.1 Linearization ... 57

4.2 Plant transfer function modification ... 62

5 Closed-loop control systems ... **73**

5.1 Controllers ... 73

5.2 Stability ... 84

6 Closed-loop control system synthesis ... **101**

6.1 Control performance ... 101

6.2 Controller tuning ... 110

6.3 Digital control ... 149

6.4 Cascade control ... 155

7 State space control ... **168**

7.1 State space controller ... 168

7.2 State observer ... 175

Appendix A – Laplace transform ... **184**

References ... **203**

LIST OF BASIC NOTATIONS AND SYMBOLS

$a, a_i, b, b_i, \ldots$ constants

a_i coefficients of left side of differential equation, coefficients of transfer function denominator

A, A_i, B, B_i constants, coefficients

$A(\omega) = \mathrm{mod}G(j\omega) = |G(j\omega)|$ frequency transfer function modulus, plot of $A(\omega)$ = magnitude response

A_o modulus of open-loop (control system) frequency transfer function

A_C modulus of controller frequency transfer function

A_P modulus of plant frequency transfer function

A_{wy} modulus of closed-loop control system frequency transfer function

$\boldsymbol{A}$ system (dynamics) matrix of order n [$(n\times n)$]

b set-point weight for proportional component (term)

b_i coefficients of right side of differential equation, coefficients of transfer function nominator

$\boldsymbol{b}$ input state vector of dimension n

c set-point weight for derivative component (term)

$\boldsymbol{c}$ output state vector of dimension n

C capacitance

d transfer constant

e control error

$e_v(\infty)$ steady-state error caused by disturbance variable

$e_w(\infty)$ steady-state error caused by desired (reference) variable

f general function

$f = \dfrac{\omega}{2\pi}$ frequency

$g(t)$ impulse response

$g_P(t)$ plant impulse response

$G(s)$ transfer function, transform of impulse response

$G(j\omega) = P(\omega) + jQ(\omega) = A(\omega)\mathrm{e}^{j\varphi(\omega)}$ frequency transfer function, plot of $G(j\omega)$ = frequency response

G_F filter transfer function

G_o open-loop (control system) transfer function

G_C controller transfer function

G_P plant transfer function

G_{vy} disturbance variable-to-controlled variable transfer function

G_{ve} disturbance variable-to-control error transfer function

G_{wy} closed-loop (control system) transfer function

G_{we} desired (reference) variable-to-control error transfer function

$h(t)$ step response

$h_P(t)$ plant step response

$h_v(t)$ step response caused by disturbance variable

$h_w(t)$ step response caused by desired (reference) variable

H_i Hurwitz determinants (subdeterminants, minors)

$\boldsymbol{H}$ Hurwitz matrix

$H(s)$ transform of step response

i interacting coefficient, current

I_i integral criteria of control performance ($i = IE, IAE, ISE, ITAE$)

$j = \sqrt{-1}$ imaginary unit

k relative discrete time

k_i gain

kT discrete time

K_D weight of controller derivative component (term)

K_I weight of controller integral component (term)

K_P controller gain, weight of controller proportional component (term)

K_{Pc} ultimate controller gain

$\boldsymbol{k}$ vector of state space controller

L inductance

L operator of direct Laplace transform

L^{-1} operator of inverse Laplace transform

$L(\omega) = 20\log A(\omega)$ logarithmic modulus of frequency transfer function

L_o logarithmic modulus of open-loop (control system) frequency transfer function

L_C logarithmic modulus of controller frequency transfer function

L_{wy} logarithmic modulus of closed-loop (control system) frequency transfer function

$\boldsymbol{l}$ Luenberger observer gain vector, correction vector

m degree of polynomial in transfer function nominator, motor torque, mass

m_A gain margin

m_l load torque

$m_L = 20\log m_A$ logarithmic gain margin

M polynomial in transfer function nominator (roots = zeros)

M_S maximum value of sensitivity function modulus

n degree of characteristic polynomial, degree of polynomial in transfer function denominator, dimension of state variable vector $\boldsymbol{x}$

N characteristic polynomial or quasipolynomial, polynomial or quasipolynomial in transfer function denominator (roots = poles)

$N(j\omega)$ Mikhailov function (hodograph, characteristic)

$N_P(\omega) = \mathrm{Re}N(j\omega)$ real part of Mikhailov function

$N_Q(\omega) = \mathrm{Im}N(j\omega)$ imaginary part of Mikhailov function

p number of controller adjustable parameters

$P(\omega) = \mathrm{Re}G(j\omega)$ real part of frequency transfer function

pp proportional band

q order of integral system, control system type

$Q(\omega) = \mathrm{Im}G(j\omega)$ imaginary part of frequency transfer function

$\boldsymbol{Q}_{co}$ controllability matrix of order n [$(n\times n)$]

$\boldsymbol{Q}_{ob}$ observability matrix of order n [$(n\times n)$]

r order of derivative system

R resistance

$s = \alpha + j\omega$ complex variable, independent variable in Laplace transform

s_i roots of polynomial with complex variable s

S complementary area over step response

$S(j\omega)$ sensitivity function

t (continuous) time

t_m time of reaching value y_m (peak value)

t_r rise time

t_s settling time

$t_\varphi = \dfrac{\varphi}{\omega}$ time corresponding to phase φ

$T = \dfrac{2\pi}{\omega}$ period

T sampling period, period

T_d time delay (dead time)

T_D derivative time

T_I integral time

T_{Ic} ultimate integral time

T_i (inertial) time constant

$T_c = \dfrac{2\pi}{\omega_c}$ ultimate period

T_n substitute time constant

T_p transient time

T_Σ summary time constant

T_u substitute time delay (dead time)

$T(j\omega)$ complementary sensitivity function

$\boldsymbol{T}_c$, $\boldsymbol{T}_o$ transformation matrices of order n [$(n \times n)$]

u manipulated variable, control variable, input variable (input), voltage

u_T formed (stair case) manipulated variable

v disturbance variable (disturbance)

w desired (reference, command) variable, set-point value

x state variable (state)

$\boldsymbol{x}$ state vector (state) of dimension n

y controlled (plant, process) variable, output variable (output)

$y_m = y(t_m)$ maximum value of controlled variable (peak value)

y_v regulatory response

y_w servo response

y_T transient part of response

y_S steady-state part of response

Z impedance

α stability degree, coefficient in DMM, minimum segment slope

$\alpha = \mathrm{Re}\, s$ real part of the complex variable s

β coefficient in DMM, maximum segment slope

γ phase margin

δ relative control tolerance

$\delta(t)$ unit Dirac impulse

Δ difference, control tolerance

$\eta(t)$ unit Heaviside step

$\omega = 2\pi f$ angular frequency, angular speed

$\omega = \mathrm{Im}\, s$ imaginary part of complex variable s

ω_b cut-off angular frequency

$\omega_c = \dfrac{2\pi}{T_c}$ ultimate angular frequency

ω_g gain crossover angular frequency

ω_p phase crossover angular frequency

ω_R resonant angular frequency

ω_0 natural angular frequency

$\varphi(\omega) = \arg G(j\omega)$ phase of frequency transfer function, plot of $\varphi(\omega)$ = phase response

φ_o phase of open-loop (control system) transfer function

ξ_i relative damping

κ overshoot

τ_j time constant

Upper indices

* recommended, optimal

-1 inverse

T transpose

Symbols over letters

. (total) derivative with respect to time

$\wedge$ estimation

Relation signs

$\approx$ approximately equal

$\doteq$ after rounding equal

$\triangleq$ correspondence between original and transform

$\Rightarrow$ implication

$\Leftrightarrow$ equivalence

Graphic marks

○ single zero

◎ double zero

× single pole

⋇ double pole

nonlinear system (element)

linear system (element)

⟶ single variable (signal)

➡ multiple variable (signal), disrete (digital) variable (signal)

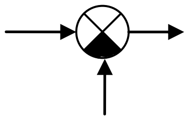

summing node (filled segment expresses minus sign)

Shortcuts

arg	argument
dB	decibel
const	constant
dec	decade
det	determinant
dim	dimension
Im	imaginary, imaginary part
lim	limit
max	maximum
min	minimum
mod	modulus
Re	real, real part
sign	sign

DMM	**d**esired **m**odel **m**ethod
DOF	**d**egree **o**f **f**reedom
GGM	**g**ood **g**ain **m**ethod
MOM	**m**odulus **o**ptimum **m**ethod (criterion)
QDM	**q**uarter-**d**ecay **m**ethod
SIMC	**S**kogestad **i**nternal **m**odel **c**ontrol
SOM	**s**ymmetrical **o**ptimum **m**ethod (criterion)
TLM	**T**yreus – **L**uyben **m**ethod
UEM	**u**niversal **e**xperimental **m**ethod
ZNM	**Z**iegler – **N**ichols **m**ethod

1 INTRODUCTION TO CLOSED-LOOP CONTROL

We meet control all the time. We can find control systems in every complex equipment or machine, which more often operate in a closed-loop. These systems are so common that we aren´t often conscious of their existence. For example, today´s compact cameras contains automatic focusing, automatic image stabilization, automatic white balancing, automatic aperture and shutter setting, automatic tracking of an object, etc. Home appliances such as radios and televisions, refrigerators, freezers, washing machines, dryers, microwave and electric ovens, deep fryers, electric irons, room thermostats, etc., also contain simple or more complex control systems.

Control systems can be found in modern toys, such as remote controlled cars, boats, helicopters, planes, etc. Advanced control systems are present in today's means of transport, i.e. cars, boats, airplanes, and of course various military technology, equipment and weapons.

Most of these systems can be included in a very broad group of mechatronic systems, which are characterized by the synergetic integration of the advantages and characteristics of various branches, such as mechanics, electromechanics, electronics, cybernetics, as well as technology and mechanical design.

We will explain the control problem in an **open-loop control** and **closed-loop control** on a simplified example of the angular speed (rotational speed) control of a direct current (DC) motor with permanent magnets, see Figs 1.1 and 1.2, where: $\omega(t)$ is the actual angular speed of the motor shaft [rad s^{-1}], $\omega_w(t)$ – the desired angular speed of the motor shaft [rad s^{-1}], $u(t)$ – the motor armature voltage [V], $u_w(t) = k_\omega \omega_w(t)$ – the output voltage of the setting device [V], $u_\omega(t) = k_\omega \omega(t)$ – the output voltage of the tachogenerator [V], k_ω – the tachogenerator gain [V s rad^{-1}], $m_l(t)$ – the load torque [N m].

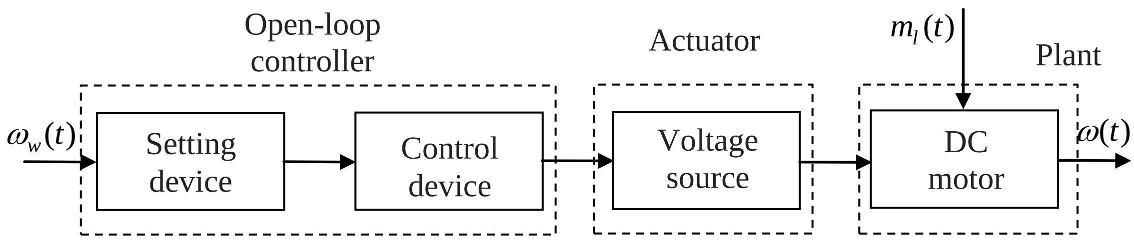

Fig. 1.1 Open-loop speed control of a DC motor

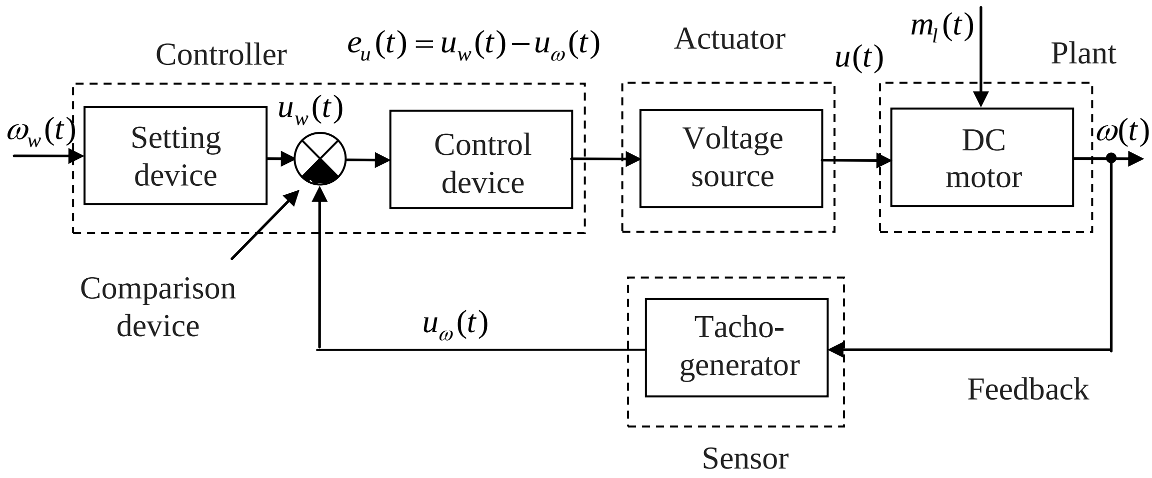

Fig. 1.2 Closed-loop speed control of a DC motor

The setting device is often added to the control device and then both devices form the **open-loop controller** (Fig. 1.1) or the (**closed-loop) controller** (Fig. 1.2).

The **control objective** consists in the fact that at the actual angular speed of the motor shaft (**plant**, **process**) $\omega(t)$ at each time t was kept on (ideally equal to) the desired angular speed $\omega_w(t)$ regardless of the varying load torque $m_l(t)$, i.e.

$$\omega(t) \to \omega_w(t)\,. \tag{1.1a}$$

It is obvious that the control objective (1.1a) can be expressed in the equivalent form

$$e(t) = \omega_w(t) - \omega(t) \to 0\,, \tag{1.1b}$$

where $e(t)$ is the **control error**.

In the **open-loop control** (Fig. 1.1) the controller must generate via the voltage source (**actuator**) such the armature voltage $u(t)$ in order for the angular speed of the motor shaft $\omega(t)$ to approach the most the desired angular speed $\omega_w(t)$. It follows from this that the DC motor properties must be very well known. Any inaccuracy in the knowledge of motor properties appears in angular speed $\omega(t)$. Also it is obvious that the controller cannot remove the influence of the load torque $m_l(t)$ on the angular speed $\omega(t)$. The load torque $m_l(t)$ causes the **irremovable disturbance.**

For that reason the open-loop control can be only used for very simple control tasks.

These simple open-loop control systems are e.g. in street traffic lights, washing machines, dryers, microwave and electric ovens, etc. The control task is set by the choice of preprogrammed operating modes. The open-loop controller contains simple and most often logical systems.

In the **closed-loop control** (Fig. 1.2) the control error

$$e_u(t) = u_w(t) - u_\omega(t) = k_\omega \omega_w(t) - k_\omega \omega(t) = k_\omega e(t) \tag{1.2}$$

is created and the controller tries to remove it by generating the suitable armature voltage $u(t)$ by means of a voltage source (actuator).

It does not matter if the control error (1.2) was caused by lack of motor behaviour or its change or by actuating the load torque $m_l(t)$. It is important that the contoller has such ability to always try as quickly as possible to minimize, preferably to completely remove the control error (1.2).

The tachogenerator (**sensor**) in the feedback (Fig. 1.2) generates in its output the voltage

$$u_\omega(t) = k_\omega \omega(t) \tag{1.3}$$

and it is obvious that its dynamic behaviour would be negligible. The accuracy of the relation (1.3), therefore the accuracy of the tachogenerator (sensor) determines the resulting control accuracy. ***Control accuracy cannot be higher than sensor accuracy is***.

From the above mentioned it follows that the closed-loop control is much better than the open-loop control. That is why we will further deal with closed-loop control.

Since the **feedback** rises in the control system in Fig. 1.2, the closed-loop control is called the **feedback control** or the **regulation**. It is clear that the ***feedback must be negative***.

The block diagram of the closed-loop control system, i.e. the feedback control system in Fig. 1.2 is substituted for purposes of its analysis and synthesis by the simplified diagram in Fig. 1.3.

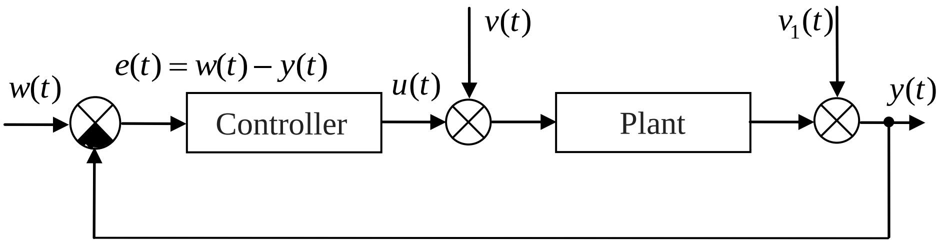

Fig. 1.3 Block diagram of the closed-loop control system

The setting and control devices create the controller. The plant (in our case a DC motor) is controlled machinery or a process. The actuator and the sensor are often added to the plant. Sometimes these devices are added to the controller. It depends on the realization of all elements of the feedback control systems.

Disturbance variables are aggregated to one or two disturbance variables, e.g. $v(t)$ and $v_1(t)$. The **desired** (reference, command) variable is marked as $w(t)$ and the **controlled** (process) variable as $y(t)$. The controller output variable $u(t)$ is called the **manipulated** (actuating, control) variable.

The **control objective** for the control system in Fig. 1.3 can be expressed in the form

$$y(t) \to w(t) \tag{1.4a}$$

or equivalently

$$e(t) \to 0. \tag{1.4b}$$

From both relations two controller functions follow. The first function consists in the tracking of the desired variable $w(t)$ by the controlled variable $y(t)$ and the second one consists in the rejection of the negative influence of the disturbances $v(t)$ and $v_1(t)$ on the control system operation. The first function is called the **servo problem** (set-point tracking) and the second one is called the **regulatory problem**.

The behaviour of open-loop and closed-loop control will be shown in two simple examples.

Example 1.1

It is necessary to analyse open-loop control (the open-loop control system) in Fig. 1.4, where K_P is the open-loop controller gain, k_1 – the plant gain. It is assumed that the plant gain k_1 may change by $\pm \Delta k_1$.

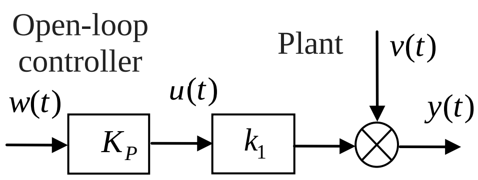

Fig. 1.4 Simple open-loop control system – Example 1.1

Solution:

For the open-loop control system it holds

$$y(t) = K_P k_1 w(t) + v(t). \tag{1.5}$$

Consider the ideal control objective [see (1.4a)]

$$y(t) = w(t). \tag{1.6}$$

and further two cases, when the disturbance $v(t)$ is not zero [$v(t) \neq 0$] and it is zero [$v(t) = 0$].

a) $v(t) = 0$

From equation (1.5) for the control objective (1.6) we get

$$K_P = \frac{1}{k_1}. \tag{1.7}$$

It holds

$$\begin{aligned} &y(t) = K_P(k_1 \pm \Delta k_1 w(t) \;\Rightarrow \\ &y(t) = \left(1 \pm \frac{\Delta k_1}{k_1}\right) w(t). \end{aligned} \tag{1.8}$$

We can see that the relative changes of the plant gain $\pm\Delta k_1/k_1$ fully come out in the output variable $y(t)$.

For example, for the plant gain changes ±50 %, i.e. $\Delta k_1/k_1 = \pm 0.5$, on the basis of (1.8) we get

$$y(t) = (1 \pm 0.5) w(t).$$

b) $v(t) \neq 0$

For the open-loop controller gain K_P (1.7) and the relative change of plant gain $\Delta k_1/k_1$ we obtain

$$y(t) = \left(1 \pm \frac{\Delta k_1}{k_1}\right) w(t) + v(t). \tag{1.9}$$

We can see that in this case the disturbance variable $v(t)$ fully comes out in the output variable $y(t)$.

For example, for the same plant gain changes like in the previous case, i.e. $\Delta k_1/k_1 = \pm 0.5$ we get

$$y(t) = (1 \pm 0.5) w(t) + v(t).$$

It is clear that the open-loop control (open-loop control system) can be used only in these cases when we perfectly know the plant behaviour and disturbances do not act on the plant or their influence is negligible.

Example 1.2

It is necessary to analyse closed-loop control (the closed-loop control system) in Fig. 1.5, where K_P is the controller gain, k_1 – the plant gain. It is assumed that the plant gain k_1 may change by $\pm\, \Delta k_1$.

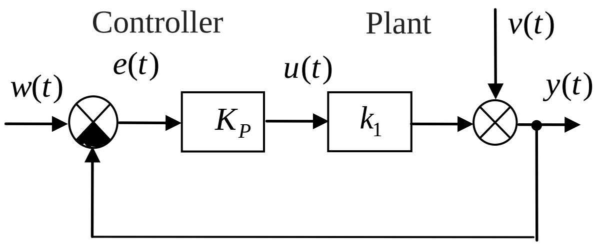

Fig. 1.5 Simple closed-loop control system – Example 1.2

Solution:

For the closed-loop control system the relations hold

$$\left.\begin{aligned} y(t) &= K_P k_1 e(t) + v(t) \\ e(t) &= w(t) - y(t) \end{aligned}\right\} \Rightarrow$$

$$y(t) = \frac{K_P k_1}{1 + K_P k_1} w(t) + \frac{1}{1 + K_P k_1} v(t). \tag{1.10}$$

In this case we can consider the plant gain changes $\pm\, \Delta k_1$ and the disturbance $v(t)$ acting, i.e. we can write

$$y(t) = \frac{K_P (k_1 \pm \Delta k_1)}{1 + K_P (k_1 \pm \Delta k_1)} w(t) + \frac{1}{1 + K_P (k_1 \pm \Delta k_1)} v(t) \Rightarrow$$

$$y(t) = \frac{1}{\frac{1}{K_P k_1\left(1 \pm \frac{\Delta k_1}{k_1}\right)} + 1} w(t) + \frac{1}{1 + K_P k_1\left(1 \pm \frac{\Delta k_1}{k_1}\right)} v(t) . \tag{1.11}$$

It is obvious that from (1.11) for

$$K_P \to \infty \quad \text{or} \quad K_P k_1 \to \infty \tag{1.12}$$

we obtain

$$y(t) \to w(t) .$$

We can see that for sufficiently high controller gain K_P or the product $K_P k_1$ the control objective (1.4a) will hold.

For example, for $K_P k_1 = 100$ and the plant gain changes ±50 %, i.e. $\Delta k_P/k_P = \pm 0.5$ we get

$$y(t) = \frac{1}{\frac{1}{100(1 \pm 0.5)} + 1} w(t) + \frac{1}{1 + 100(1 \pm 0.5)} v(t) \;\Rightarrow$$

$$y(t) = \left(0.9901 {}^{+0.0033}_{-0.0097}\right) w(t) + \left(0.0099 {}^{-0.0033}_{+0.0097}\right) v(t) .$$

In this case the plant gain $k_1$changes ±50 % cause the change of the controlled variable $y(t)$ less than 2 % and the disturbance variable $v(t)$ is supressed on a value less than 2 % of the original size.

From the above mentioned it is obvious that the closed-loop control (the closed-loop control system) is able to ensure high control performance for both functions, i.e. the tracking problem and regulatory problem as well.

Example 1.3

There is a closed-loop control system in Fig. 1.6, where two disturbance variables $v(t)$ and $v_1(t)$ act on the nonlinear plant which is described by the relation

$$y(t) = f[u(t) + v(t)] + v_1(t) . \tag{1.13}$$

It is necessary to find out the behaviour of this control system for $K_P \to \infty$.

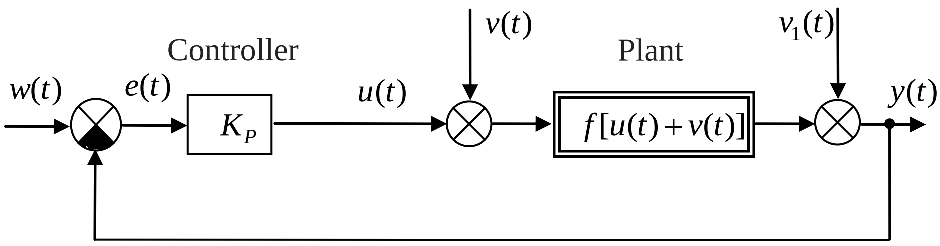

Fig. 1.6 Closed-loop control system with nonlinear plant – Example 1.3

Solution:

For the control system in Fig. 1.6 we can write

$$\left.\begin{array}{l} e(t) = w(t) - y(t) \\ e(t) = \dfrac{u(t)}{K_P} \end{array}\right\} \Rightarrow$$

$$y(t) = w(t) - \frac{u(t)}{K_P}\,. \tag{1.14}$$

On the basis of (1.13) we can determine $u(t)$, i.e.

$$f[u(t) + v(t)] = y(t) - v_1(t) \ \Rightarrow$$

$$u(t) + v(t) = f^{-1}[y(t) - v_1(t)] \ \Rightarrow$$

$$u(t) = f^{-1}[y(t) - v_1(t)] - v(t)\,. \tag{1.15}$$

After substituting (1.15) in (1.14) we get

$$y(t) = w(t) - \frac{f^{-1}[y(t) - v_1(t)] - v(t)}{K_P}\,. \tag{1.16}$$

It is obvious that for $K_P \to \infty$ we obtain

$$y(t) \to w(t)\,.$$

We can see that for the sufficiently high controller gain K_P on the basis of the closed-loop control (feedback control) it is possible to fulfil the control objective (1.4a) for the nonlinear plant and for two mutually independent disturbance variables.

2 MATHEMATICAL MODELS OF DYNAMICAL SYSTEMS

2.1 General mathematical models

For the design and study of the properties of systems we use their **mathematical models**. It is very advantageous because experimentation with real systems may be substituted by experimentation with their mathematical models, i.e. by **simulation**. It enables considerable reductions in cost and risk of damage to the real system. It is also important for essentially accelerating the whole process. New nontraditional solutions often arise.

In automatic control theory in the time domain, mathematical models have forms which are algebraic, transcendental, differential, partial differential, integral, difference, summation equations and their combinations. The mathematical model can be obtained by identification using an analytical or experimental method, if necessary by a combination of them. For example, a mathematical model can be obtained analytically and its parameters can be refined experimentally. Sometimes term identification means finding a mathematical model using an experimental method. We will only deal with such mathematical models that can be expressed in the forms of the t-invariant (stationary) ordinary differential equations, which describe real systems with lumped parameters.

When evaluating a mathematical model and the simulation results we must always remember that ***every mathematical model is only an approximation of the real system***.

Since even a very complex MIMO (**m**ulti-**i**nput **m**ulti-**o**utput) system is formed by combining SISO (**s**ingle-**i**nput **s**ingle-**o**utput) systems, main attention will be paid to SISO systems.

Consider the **SISO system** which is described by the generally nonlinear differential equation

$$g[y^{(n)}(t),\ldots,\dot{y}(t),y(t),u^{(m)}(t),\ldots,\dot{u}(t),u(t)]=0\,. \tag{2.1a}$$

$$\left.\begin{aligned}\dot{y}(t)&=\frac{\mathrm{d}y(t)}{\mathrm{d}t},\ y^{(i)}(t)=\frac{\mathrm{d}^i y(t)}{\mathrm{d}t^i};\ i=2,3,\ldots,n,\\ \dot{u}(t)&=\frac{\mathrm{d}u(t)}{\mathrm{d}t},\ u^{(j)}(t)=\frac{\mathrm{d}^j u(t)}{\mathrm{d}t^j};\ j=2,3,\ldots,m,\end{aligned}\right\} \tag{2.1b}$$

with initial conditions

$$\left.\begin{aligned}y(0)&=y_0,\dot{y}(0)=\dot{y}_0,\ldots,y^{(n-1)}(0)=y_0^{(n-1)},\\ u(0)&=u_0,\dot{u}(0)=\dot{u}_0,\ldots,u^{(m-1)}(0)=u_0^{(m-1)},\end{aligned}\right\} \tag{2.1c}$$

where $u(t)$ is the **input variable** (signal) = **input**, $y(t)$ – the **output variable** (signal) = **output**, g – the generally nonlinear function, n – the **system order**.

If the inequality

$$n>m \tag{2.2}$$

holds, then the mathematical model satisfies a **strong physical realizability condition**.

In case

$$n = m \tag{2.3}$$

it satisfies only a **weak** physical realizability condition.

For

$$n < m \tag{2.4}$$

the mathematical model is **not physically realizable** and therefore it does not express the behaviour of the real system.

The mathematical model (2.1a), in which the derivatives appear (2.1b), describes the **dynamic** (dynamical) **system** (it has a memory).

From the differential equation (2.1a) for

$$\lim_{t\to\infty} y^{(i)}(t) = 0;\ i = 1,2,\ldots,n,$$
$$\lim_{t\to\infty} u^{(j)}(t) = 0;\ j = 1,2,\ldots,m$$

it is possible to obtain the equation (if it exists)

$$y = f(u), \tag{2.5}$$

where

$$\left.\begin{aligned} y &= \lim_{t\to\infty} y(t), \\ u &= \lim_{t\to\infty} u(t). \end{aligned}\right\} \tag{2.6}$$

The equation (2.5) expresses the **static characteristic** of the given dynamic system (2.1), see e.g. Fig. 2.1.

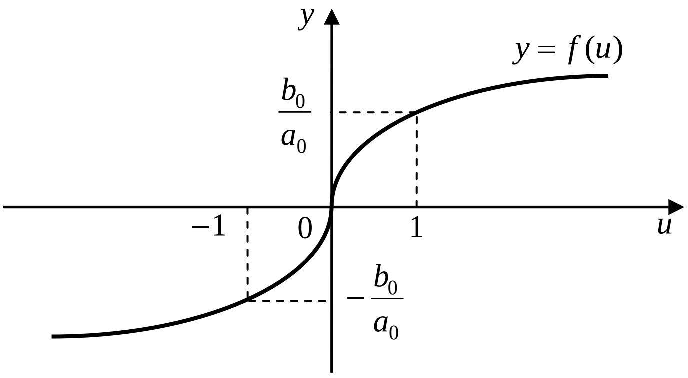

Fig. 2.1 Nonlinear static characteristic – Example 2.1

A static characteristic describes the dependency between output y and input u variables in a **steady-state**.

If derivatives do not appear in Equation (2.1a), i.e.,

$$g[y(t),u(t)] = 0 \quad \text{or} \quad g(y,u) = 0, \tag{2.7}$$

then it is the mathematical model of the **static system** (it has not a memory).

State space mathematical models of a dynamic system are very important. They are used for describing SISO systems and first of all MIMO systems.

The state space model of the SISO dynamic system has the form

$$\dot{\boldsymbol{x}}(t) = \boldsymbol{g}[\boldsymbol{x}(t), u(t)], \ \ \boldsymbol{x}(0) = \boldsymbol{x}_0 \quad \text{– \textbf{state equation}} \tag{2.8a}$$

$$y(t) = h[\boldsymbol{x}(t), u(t)] \quad \text{– \textbf{output equation}} \tag{2.8b}$$

$$\boldsymbol{x} = \begin{bmatrix} x_1 \\ x_2 \\ \vdots \\ x_n \end{bmatrix} = [x_1, x_2, ..., x_n]^T,$$

$$\boldsymbol{g} = \begin{bmatrix} g_1 \\ g_2 \\ \vdots \\ g_n \end{bmatrix} = [g_1, g_2, ..., g_n]^T,$$

where $\boldsymbol{x}(t)$ is the **state vector** (state) of the dimension n, $\boldsymbol{g}$ – the generally nonlinear function of the dimension n, h – the generally nonlinear function, T – the transposition symbol.

We often omit the independent variable time t in order to simplify a description.

The components $x_1, x_2, \ldots, x_n$ of the state $\boldsymbol{x}$ express the inner variables. Knowledge of them is very important for **state space control** (see Chapter 7).

The system order n is given by the number of state variables. If in the output equation the input $u(t)$ does not appear then the given dynamic system (2.8) is strongly physically realizable. In other cases, it is only weakly physically realizable.

The static characteristic (if it exists) from the state space model can be obtained for $t \to \infty \Rightarrow \dot{\boldsymbol{x}}(t) \to \boldsymbol{0}$ and by the elimination of the state variables (see example 2.1).

Example 2.1

The nonlinear dynamic system is described by the differential equation of the second order

$$a_2 \frac{\mathrm{d}^2 y(t)}{\mathrm{d}t^2} + a_1 \frac{\mathrm{d}\, y(t)}{\mathrm{d}t} + a_0 y(t) = b_0 \operatorname{sign}[u(t)]\sqrt{|u(t)|}\,, \tag{2.9}$$

with initial conditions $y(0) = y_0$ a $\dot{y}(0) = \dot{y}_0$.

It is necessary to:

a) determine the physically realizability,

b) determine and plot the static characteristic,

c) express the mathematical model (2.9) in the form of the state space model.

Solution:

a) Therefore $n = 2 > m = 0$ [in the right side of the differential equation there does not appear the derivative of $u(t)$], the given dynamic system is strongly physically realizable.

b) In the steady-state for $t \to \infty$ the derivatives in the equation (2.9) are zeros, and therefore in accordance with (2.6) we can write

$$a_0 y(t) = b_0 \operatorname{sign}(u)\sqrt{|u|} \;\Rightarrow$$
$$y = \frac{b_0}{a_0} \operatorname{sign}(u)\sqrt{|u|}$$

The obtained static characteristic is shown in Fig. 2.1.

c) If we choose the state variables, e.g.

$$x_1 = y,$$
$$x_2 = \dot{x}_1 = \dot{y},$$

then after substitution in the equation (2.9) and modification we get

$$\dot{x}_1 = x_2, \qquad\qquad x_1(0) = y_0,$$
$$\dot{x}_2 = -\frac{a_0}{a_2}x_1 - \frac{a_1}{a_2}x_2 + \frac{b_0}{a_2}\operatorname{sign}(u)\sqrt{|u|}, \qquad x_2(0) = \dot{y}_0.$$

The static characteristic can be obtained for the steady-state, i.e. $t \to \infty \Rightarrow$ $\dot{x}_1(t) \to 0$, $\dot{x}_2(t) \to 0$ and after elimination of the state variables

$$\left.\begin{aligned} 0 &= x_2 \\ 0 &= -\frac{a_0}{a_2}x_1 - \frac{a_1}{a_2}x_2 + \frac{b_0}{a_2}\operatorname{sign}(u)\sqrt{|u|} \\ y &= x_1 \end{aligned}\right\} \Rightarrow$$

$$y = \frac{b_0}{a_2}\operatorname{sign}(u)\sqrt{|u|}\,.$$

2.2 Linear dynamic systems

Linear mathematical models create a very important group of mathematical models of dynamic systems. These mathematical models must satisfy the condition of the linearity which consists of two partial properties: **additivity** and **homogeneity**.

Additivity

$$\left.\begin{aligned} u_1 &\to \text{system} \to y_1 \\ u_2 &\to \text{system} \to y_2 \end{aligned}\right\} \Rightarrow u_1 + u_2 \to \text{system} \to y_1 + y_2\,. \tag{2.10a}$$

Homogeneity:

$$u \to \text{system} \to y \Rightarrow au \to \text{system} \to ay\,. \tag{2.10b}$$

These partial properties may be joined

$$\left.\begin{aligned} u_1 &\to \text{system} \to y_1 \\ u_2 &\to \text{system} \to y_2 \end{aligned}\right\} \Rightarrow a_1u_1 + a_2u_2 \to \text{system} \to a_1y_1 + a_2y_2\,, \tag{2.11}$$

where a, a_1, a_2 are any constants; $u(t)$, $u_1(t)$ and $u_2(t)$ – the input variables (inputs); $y(t)$, $y_1(t)$ and $y_2(t)$ – the output variables (outputs).

The linearity of a dynamic system has such a property when the weighting sum of output variables corresponds to the weighting sum of input variables.

A very important property of linear dynamic systems is: ***every local property they have is at the same time their global property***.

Example 2.2

The static system is described by the linear algebraic equation

$$y(t) = k_1 u(t) + y_0 , \tag{2.12}$$

where k_1 and y_0 are constants.

Is it necessary to verify whether the mathematical model (2.12) is linear?

Solution:

We choose, e.g. $u_1(t) = 2$ and $u_2(t) = 4t$.

After substitution in (2.12) we obtain

$$\left.\begin{array}{l} u_1(t) = 2 \ldots \ \ y_1(t) = 2k_1 + y_0 \\ u_2(t) = 4t \ldots y_2(t) = 4k_1 t + y_0 \end{array}\right\} \Rightarrow y_1(t) + y_2(t) = 2k_1(1+2t) + 2y_0 ,$$

$$\begin{aligned} u(t) &= u_1(t) + u_2(t) = 2(1+2t) \ldots y = 2k_1(1+2t) + y_0 \neq y_1(t) + y_2(t) = \\ &= 2k_1(1+2t) + 2y_0 . \end{aligned}$$

We can see that for $y_0 \neq 0$ the mathematical model (2.12) from the point of view of the linearity definition (2.10) or (2.11) is not linear. The mathematical model (2.12) of a static system will be linear only for $y_0 = 0$, see Fig. 2.2.

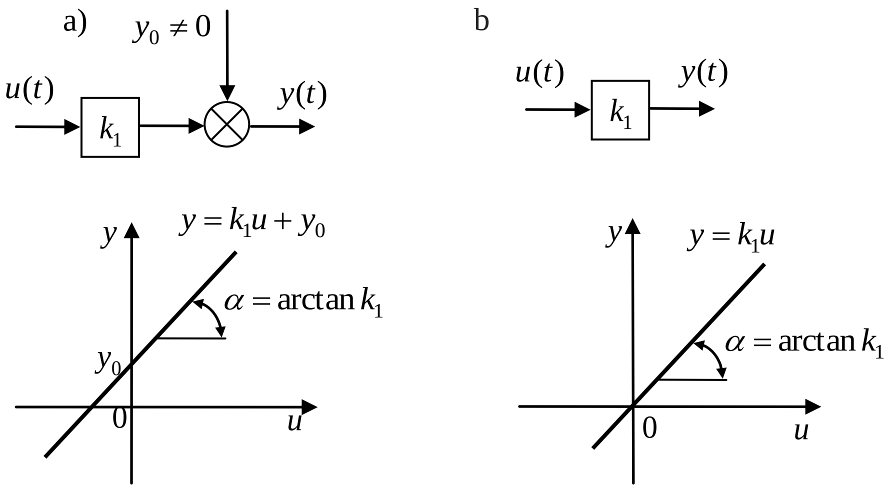

Fig. 2.2 Mathematical model of a static system: a) nonlinear, b) linear – Example 2.2

From the above it is clear that the static characteristic of linear systems (if it exists) must always pass through the origin of coordinates.

Example 2.3

The dynamic system (integrator) is described by the linear differential equation

$$\frac{\mathrm{d}\,y(t)}{\mathrm{d}t} = k_1 u(t),\ y(0) = y_0 \tag{2.13}$$

or the equivalent integral equation

$$y(t) = k_1 \int_0^t u(\tau)\,\mathrm{d}\tau + y_0 . \tag{2.14}$$

It is necessary to verify the linearity of the given mathematical model.

Solution:

We choose the same inputs as in Example 2.2 and we obtain

$$\left.\begin{array}{l} u_1(t) = 2 \ldots\ y_1(t) = 2k_1 t + y_0 \\ u_2(t) = 4t \ldots y_2(t) = 2k_1 t^2 + y_0 \end{array}\right\} \Rightarrow y_1(t) + y_2(t) = 2k_1 t(1+t) + 2y_0 ,$$

$$\begin{aligned} & u(t) = u_1(t) + u_2(t) = 2(1+2t) \ldots y = 2k_1 t(1+t) + y_0 \neq y_1(t) + y_2(t) = \\ & = 2k_1 t(1+t) + 2y_0 . \end{aligned}$$

Again we can see that the mathematical model (2.13) or (2.14) for $y_0 \neq 0$ does not satisfy the condition of the linearity (Fig. 2.3).

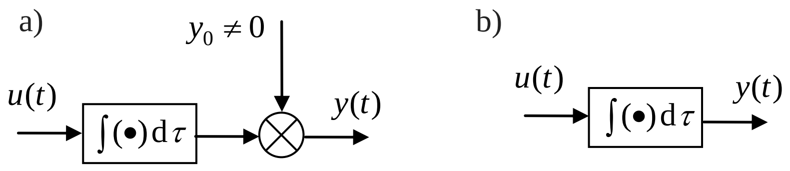

Fig. 2.3 Mathematical model of integrator: a) nonlinear, b) linear – Example 2.3

This particular conclusion can be generalized. ***For linear mathematical models we must always consider zero initial conditions***. Otherwise, we cannot work with them as with mathematical models satisfying the conditions of linearity.

3 MATHEMATICAL MODELS OF LINEAR DYNAMIC SYSTEMS

3.1 Basic linear mathematical models

The SISO linear dynamic system in the time domain is very often described by a linear differential equation with constant coefficients (we will consider only such systems)

$$a_n y^{(n)}(t) + \cdots + a_1 \dot{y}(t) + a_0 y(t) = b_m u^{(m)}(t) + \cdots + b_1 \dot{u}(t) + b_0 u(t) \tag{3.1a}$$

with the initial condition

$$\left.\begin{aligned} y(0) = y_0, \dot{y}(0) = \dot{y}_0, \ldots, y^{(n-1)}(0) = y_0^{(n-1)} \\ u(0) = u_0, \dot{u}(0) = \dot{u}_0, \ldots, u^{(m-1)}(0) = u_0^{(m-1)} \end{aligned}\right\} \tag{3.1b}$$

The conditions of physical realizability are given by the relations (2.2) − (2.4).

Applying the Laplace transform (see Appendix A) to the differential equation of the n-th order (3.1a) with initial conditions (3.1b) we obtain the algebraic equation of the n-th degree

$$(a_n s^n + \cdots + a_1 s + a_0) Y(s) - L(s) = (b_m s^m + \cdots + b_1 s + b_0) U(s) - R(s)$$

and from it we can determine the output variable transform

$$Y(s) = \underbrace{\underbrace{\frac{M(s)}{N(s)} U(s)}_{\substack{\text{Transform of response} \\ \text{on input}}} + \underbrace{\frac{L(s) - R(s)}{N(s)}}_{\substack{\text{Transform of response} \\ \text{on initial conditions}}}}_{\text{Transform of solution of differential equation}}, \tag{3.2}$$

$$M(s) = b_m s^m + \cdots + b_1 s + b_0 = b_m (s - s_1^0)(s - s_2^0) \ldots (s - s_m^0), \tag{3.3}$$

$$N(s) = a_n s^n + \cdots + a_1 s + a_0 = a_n (s - s_1)(s - s_2) \ldots (s - s_n), \tag{3.4}$$

where $Y(s)$ is the transform of the output variable $y(t)$, $U(s)$ – the transform of the input variable $u(t)$, $L(s)$ – the polynomial of the max degree $n – 1$ which is determined by the initial conditions of the left side of the differential equation, $R(s)$ – the polynomial of the max degree $m – 1$ which is determined by the initial conditions of the right side of the differential equation, $M(s)$ – the polynomial of the degree m which is determined by the coefficients of the right side of the differential equation, $N(s)$ – the **characteristic polynomial** of the degree n which is determined by the coefficients of the left side of the differential equation, s – the **complex variable** (dimension time^{-1}) [s^{-1}].

Since differential equation (3.1) is the mathematical model of the dynamic system it is obvious that the polynomial $N(s)$ is also at the same time the characteristic polynomial of this dynamic system.

Using the inverse Laplace transform (see Appendix A) on the transform of the solution (3.2) we obtain the original of the solution

$$y(t) = \mathrm{L}^{-1}\{Y(s)\}. \tag{3.5}$$

It is very advantageous to use appropriate Laplace transform tables. The tables are suitable for automatic control theory and are given in Appendix A.

From the relation (3.2) it follows that the relation can be used as the linear mathematical model of the given linear dynamic system if the transform of the response at the initial conditions is zero (i.e. the initial conditions are zero), see the conditions of the linearity (2.10) or (2.11). In this case we can write

$$Y(s) = \frac{M(s)}{N(s)} U(s) = G(s)U(s)\,, \tag{3.6}$$

$$\begin{aligned} G(s) &= \frac{Y(s)}{U(s)} = \frac{M(s)}{N(s)} = \\ &= \frac{b_m s^m + \cdots + b_1 s + b_0}{a_n s^n + \cdots + a_1 s + a_0} = \frac{b_m (s - s_1^0)(s - s_2^0)\ldots(s - s_m^0)}{a_n (s - s_1)(s - s_2)\ldots(s - s_n)}\,, \end{aligned} \tag{3.7}$$

where $G(s)$ is the **transfer function**, s_i – the **poles** of the linear dynamic system = the roots of the characteristic polynomial $N(s)$, s_j^0 – the **zeros** of the linear dynamic system = the roots of the polynomial $M(s)$. The difference $n - m$ is called the **relative degree** of the given system.

The transfer function $G(s)$ ***is given by the ratio of the transform of the output variable*** $Y(s)$ ***and of the transform of the input variable*** $U(s)$ ***for zero initial conditions***. It can be obtained directly from the differential equation (3.1a), because the transforms of the derivatives of the output $y(t)$ and the input $u(t)$ variables for zero initial conditions are given by the simple formulas

$$\left.\begin{aligned} \mathrm{L}\left\{y^{(i)}(t)\right\} &= s^i Y(s); \quad i = 1,2,\ldots,n, \\ \mathrm{L}\left\{u^{(j)}(t)\right\} &= s^j U(s); \quad j = 1,2,\ldots,m. \end{aligned}\right\} \tag{3.8}$$

The great advantage of the transfer function $G(s)$ is the fact that it allows to express the properties of the linear dynamic system in the complex variable domain by a block as in Fig. 3.1.

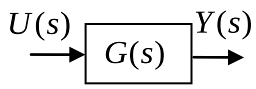

Fig. 3.1 Block diagram of the dynamic system

As it will be shown, it is very simple and effective to work with such blocks.

We can get the static characteristic of the linear dynamic system (if it exists) from the differential equation (3.1a) for

$$\left.\begin{aligned} \lim_{t\to\infty} y^{(i)}(t) &= 0; \quad i = 1,2,\ldots,n, \\ \lim_{t\to\infty} u^{(j)}(t) &= 0; \quad j = 1,2,\ldots,m, \end{aligned}\right\} \tag{3.9}$$

i.e.

$$y = k_1 u\,, \tag{3.10a}$$

$$k_1 = \frac{b_0}{a_0},\ a_0 \neq 0\,, \tag{3.10b}$$

where k_1 is the system (plant) gain.

From comparison (3.7), (3.9) and (3.10) a very important relationship between the time t and the complex variable s follows

$$t \to \infty \iff s \to 0\,. \tag{3.11}$$

It is clear that on the basis of the relation (3.11) we get the equation of the static characteristic (3.10) from the transfer function (3.7), and therefore it is possible to write

$$y = [\lim_{s\to 0} G(s)]u,\ a_0 \neq 0\,. \tag{3.12}$$

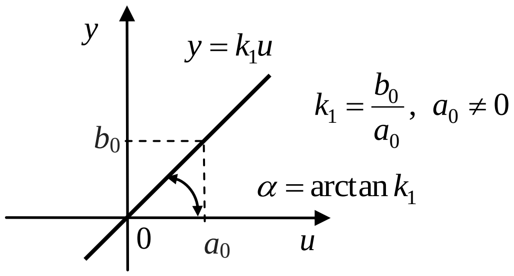

Fig. 3.2 Static characteristic of linear dynamic system

The static characteristic of the linear dynamic system is a straight line which always crosses through the origin of the coordinates (Fig. 3.2).

By substituting complex frequency jω for the complex variable s in the transfer function (3.7) we obtain the **frequency transfer function**

$$G(\mathrm{j}\omega) = G(s)\big|_{s=\mathrm{j}\omega} = \frac{b_m(\mathrm{j}\omega)^m + \cdots + b_1\,\mathrm{j}\omega + b_0}{a_n(\mathrm{j}\omega)^n + \cdots + a_1\,\mathrm{j}\omega + a_0} = A(\omega)\,\mathrm{e}^{\mathrm{j}\varphi(\omega)}\,, \tag{3.13}$$

$$A(\omega) = \operatorname{mod} G(\mathrm{j}\omega) = |G(\mathrm{j}\omega)|\,, \tag{3.14}$$

$$\varphi(\omega) = \arg G(\mathrm{j}\omega)\,, \tag{3.15}$$

where $A(\omega)$ is the **modulus** (amplitude, magnitude) of the frequency transfer function, $\varphi(\omega)$ – the **argument** or **phase** of the frequency transfer function, ω – the **angular frequency** (pulsation) (dimension time^{-1}) [s^{-1}].

In order to distinguish angular frequency (T – the period, f – the frequency)

$$\omega = \frac{2\pi}{T}\,, \tag{3.16}$$

from „ordinary“ frequency

$$f = \frac{1}{T} \tag{3.17}$$

with the unit [Hz] and the dimension [s^{-1}] for the angular frequency the notation [rad s^{-1}] is used.

The mapping of the frequency transfer function $G(\mathrm{j}\omega)$ for $\omega = 0$ to $\omega = \infty$ in the complex plane is called the **frequency response** (polar plot) (Fig. 3.3).

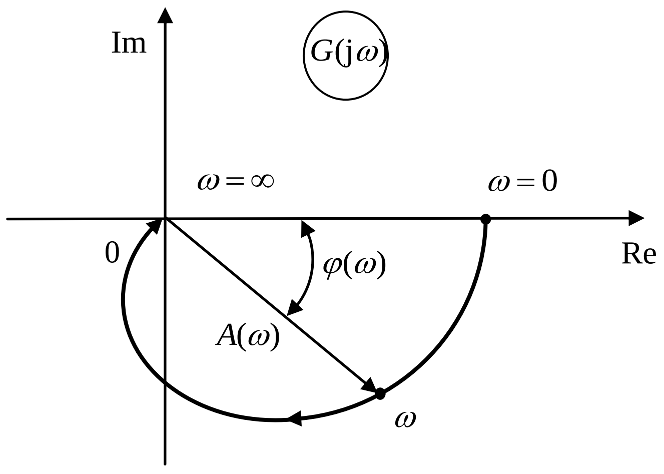

Fig. 3.3 Frequency response

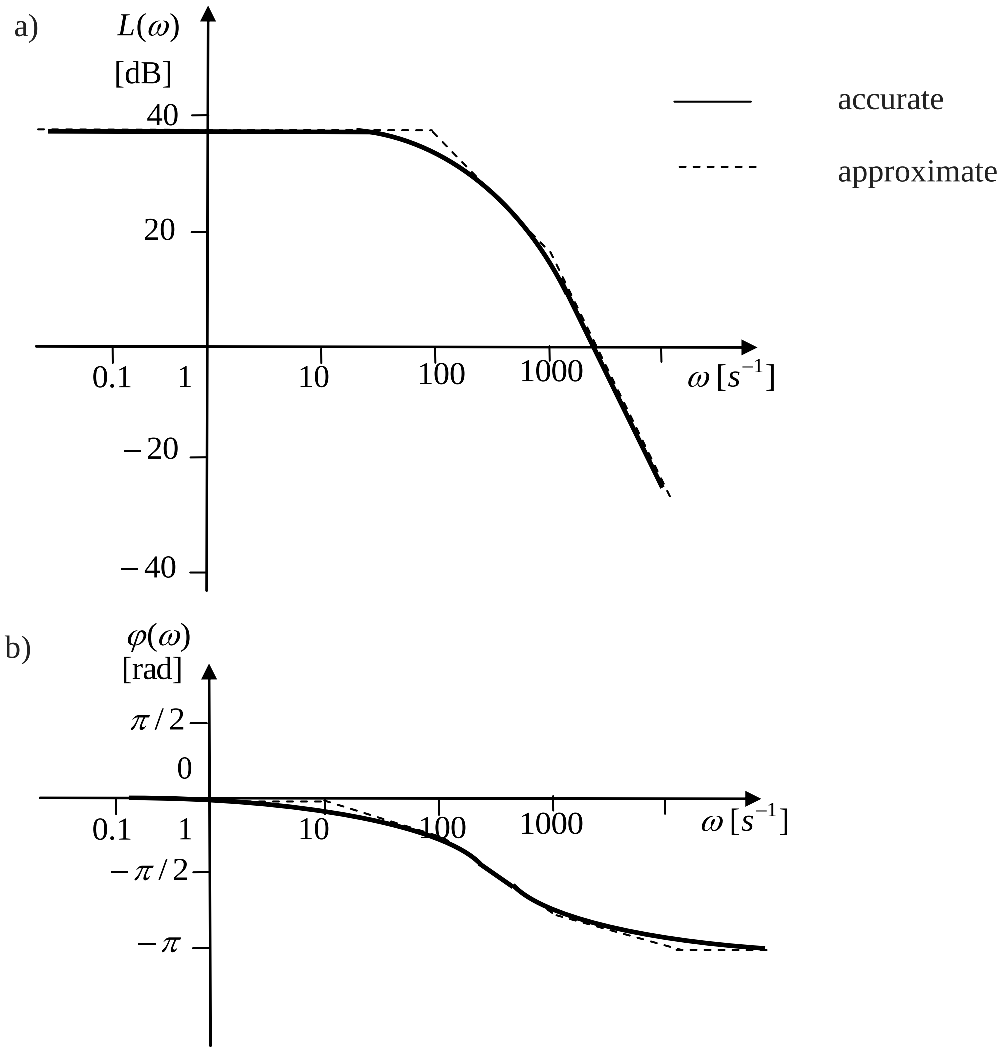

Fig. 3.4 Logarithmic frequency responses: a) Bode magnitude plot, b) Bode phase plot

Logarithmic frequency responses (Bode frequency responses) are most commonly used, see Fig. 3.4. In this case the **Bode magnitude plot**

$$L(\omega) = 20 \log A(\omega) \tag{3.18}$$

and the **Bode phase plot** $\varphi(\omega)$ are represented separately. The frequency axis has a logarithmic scale and the logarithmic modulus $L(\omega)$ is given in dB (decibels). For the Bode plots approximations are used on the basis of straight and asymptotic lines.

The frequency transfer function $G(\mathrm{j}\omega)$ expresses for each value of the angular frequency ω the amplitude (modulus, magnitude) $A(\omega)$ and the phase (argument) $\varphi(\omega)$ of the steady-state sinusoidal response $y(t)$ caused by the sinusoidal input $u(t)$ with the unit amplitude.

That means the ***frequency response can be obtained experimentally*** (Fig. 3.5). It has great significance especially for fast systems.

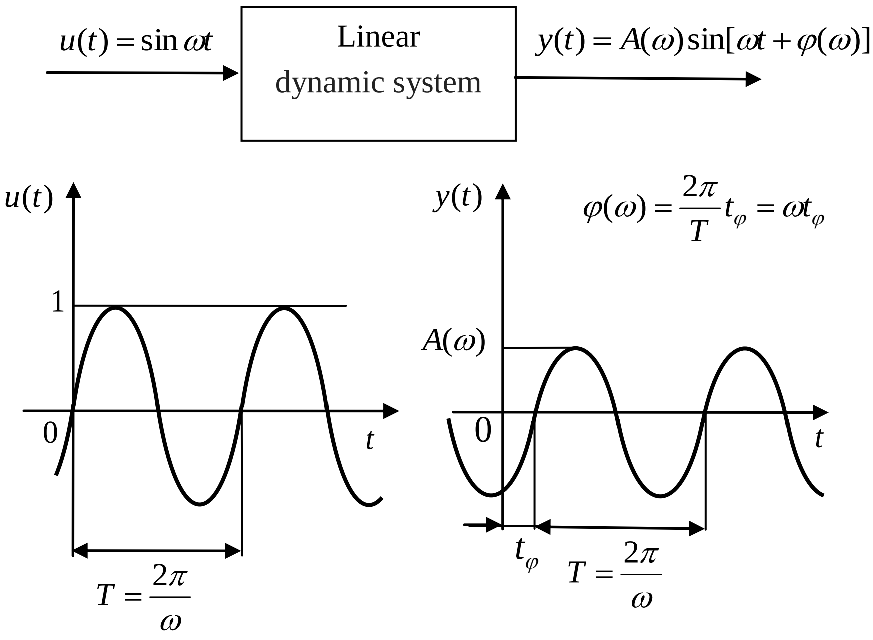

Fig. 3.5 Interpretation of frequency response

The conditions of the physical realizability are given by the relations (2.2) – (2.4). It is obvious that every real dynamic system cannot transfer a signal with an infinitely high angular frequency, therefore for strongly physically realizable dynamic systems there must hold

$$\left.\begin{aligned} \lim_{\omega\to\infty} G(\mathrm{j}\omega) &= 0 \\ \lim_{\omega\to\infty} A(\omega) &= 0 \\ \lim_{\omega\to\infty} L(\omega) &= -\infty \end{aligned}\right\} \Leftrightarrow \; n > m\,. \tag{3.19}$$

From the frequency transfer function (3.13) we can very easily get the equation of the static characteristic (if it exists) because for the steady-state $\omega = 0$ therefore it must hold

$$y = [\lim_{\omega\to 0} G(\mathrm{j}\omega)]u\,, \quad a_0 \neq 0\,. \tag{3.20}$$

It follows from (3.11) for $s = \mathrm{j}\omega$

$$t \to \infty \;\Leftrightarrow\; \omega \to 0\,. \tag{3.21}$$

It is clear that between the time t and the angular frequency ω the dual relationship holds (Fig. 3.6)

$$t \to 0 \;\Leftrightarrow\; \omega \to \infty\,. \tag{3.22}$$

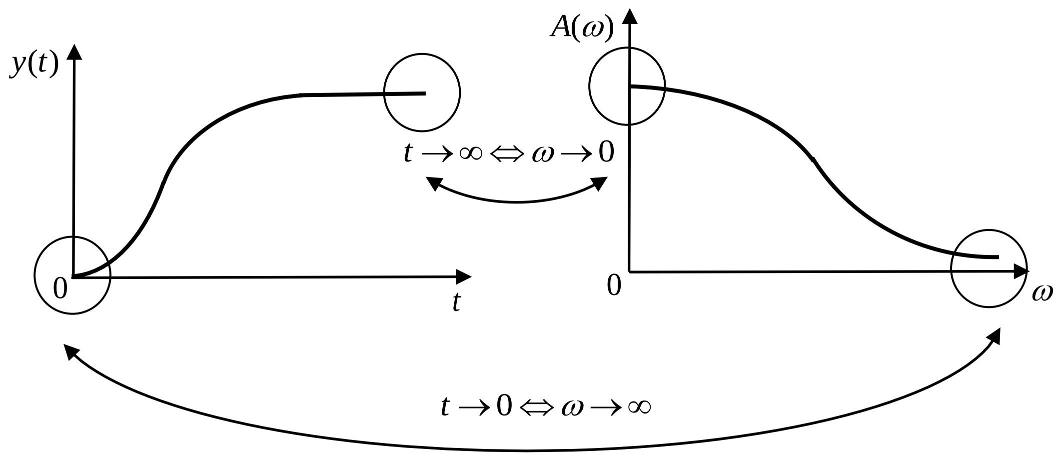

Fig. 3.6 Relationship between the time t and the angular frequency ω

From the relations (3.21), (3.22) and Fig. 3.6 it follows that the properties of the linear dynamic system for low angular frequencies decide about its properties in long periods, i.e. in the steady-states and vice versa. Similarly its properties for high angular frequencies decide about its properties for the initial time response, i.e. about the rise time of the time response (about the transient state) and vice versa.

Properties of linear dynamic systems with zero initial conditions can be expressed by time responses caused by the well-defined courses of an input variable.

In automatic control theory, there are two basic courses of input variable $u(t)$, they are the unit **Dirac impulse** $\delta(t)$ and unit **Heaviside step** $\eta(t)$, see Appendix A.

The **impulse response** $g(t)$ describes the response of the linear dynamic system on the input variable in the form of the Dirac impulse $\delta(t)$ for zero initial condition, see Fig. 3.7.

In accordance with the relation (3.6) we can write

$$Y(s) = G(s)U(s) \tag{3.23}$$

and for

$$u(t) = \delta(t) \,\hat{=}\, U(s) = 1$$

we get

$$y(t) = g(t) = \mathrm{L}^{-1}\{G(s)\}\,. \tag{3.24}$$

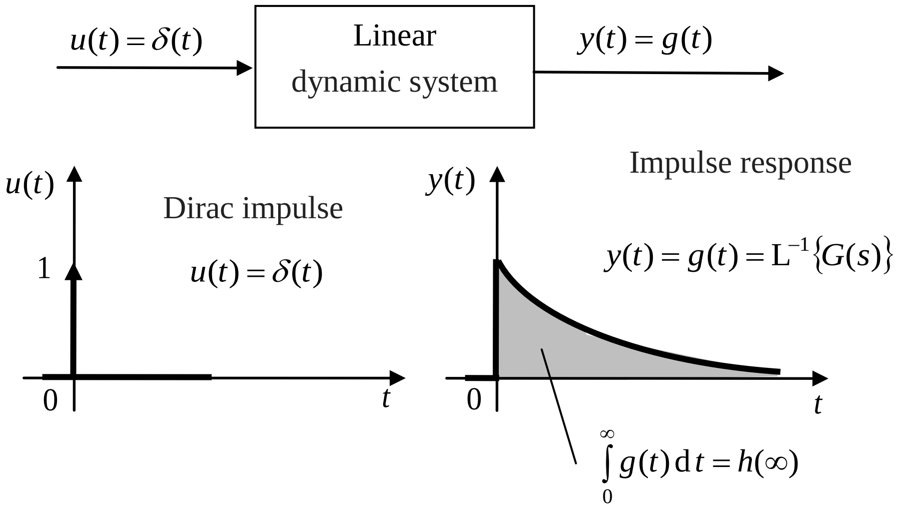

Fig. 3.7 Impulse response of the linear dynamic system

In the linear dynamic system a derivative or an integrating of the input variable $u(t)$ corresponds to a derivative or an integrating of the output variable $y(t)$.

We will use these properties for the determination of the static characteristic of the linear dynamic system on the basis of its impulse response $g(t)$. Since the static characteristic of the linear dynamic system is a straight line crossing through the origin of the coordinates it is enough to determine its one non-zero point. We can write

$$u = u(\infty) = \lim_{t\to\infty}\int_0^t \delta(\tau)\,\mathrm{d}\tau = 1,$$

$$y = y(\infty) = \lim_{t\to\infty}\int_0^t g(\tau)\,\mathrm{d}\tau\,.$$

From this we can easily get the equation of the static characteristic (if it exists)

$$y = [\lim_{t\to\infty}\int_0^t g(\tau)\,\mathrm{d}\tau]u\,. \qquad (3.25)$$

The strong condition of the physical realizability has the form

$$|g(0)| < \infty\,. \qquad (3.26)$$

If $g(0)$ contains the Dirac impulse $\delta(t)$, then the given linear dynamic system is only weakly physically realizable.

The **step response** $h(t)$ describes the response of the linear dynamic system on the input variable in the form of the Heaviside step $\eta(t)$ for zero initial condition, see Fig. 3.8.

On the basis of the relation (3.23) for

$$u(t) = \eta(t) \,\hat{=}\, U(s) = \frac{1}{s}$$

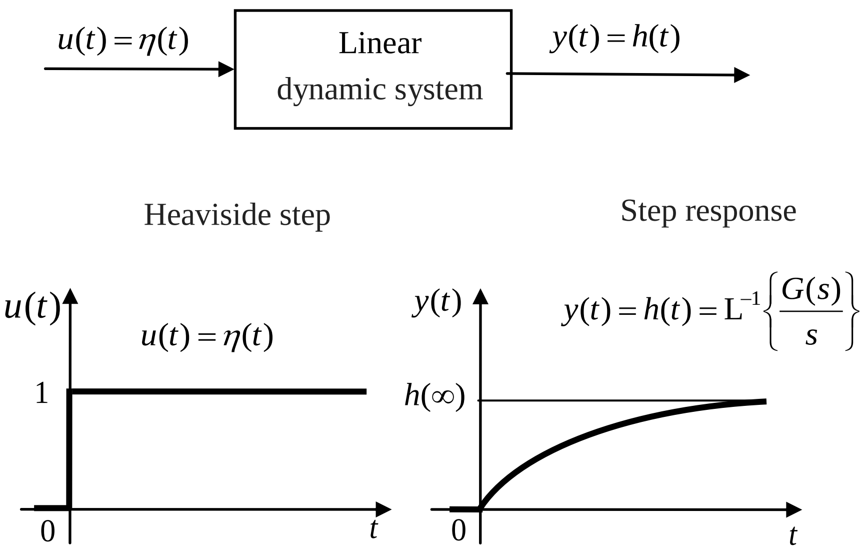

Fig. 3.8 Step response of the linear dynamic system

we get

$$y(t) = h(t) = \mathrm{L}^{-1}\left\{\frac{G(s)}{s}\right\}. \tag{3.27}$$

From the step response $h(t)$ the equation of the static characteristic may be very easily obtained (if it exists) because the relations hold

$$u = u(\infty) = \eta(\infty) = 1,$$

$$y = y(\infty) = h(\infty),$$

i.e.

$$y = [\lim_{t\to\infty} h(t)]u\,. \tag{3.28}$$

The strong condition of the physical realizability has the form

$$h(0) = 0 \tag{3.29}$$

and the weak condition

$$0 < |h(0)| < \infty\,. \tag{3.30}$$

It is useful to apply the **generalized derivative** which is defined by the relations (Fig. 3.9)

$$\left.\begin{aligned} \dot{x}(t) &= \dot{x}_{or}(t) + \sum_{i=1}^{p} h_i \delta(t - t_i), \\ h_i &= \lim_{t\to t_{i+}} x(t) - \lim_{t\to t_{i-}} x(t), \end{aligned}\right\} \tag{3.31}$$

where t_i are the points of discontinuity with the jumps h_i, $\dot{x}_{or}(t)$ − the ordinary derivative determined between the points of discontinuity.

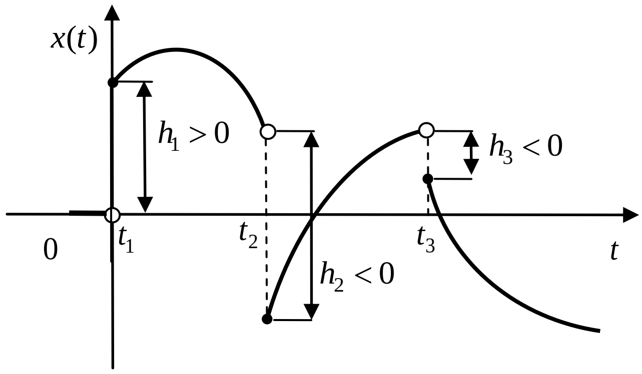

Fig. 3.9 Function $x(t)$ with points of discontinuity

By means of the generalized derivative it is possible to express the relationship between the Dirac impulse and the Heaviside step

$$\delta(t) = \frac{\mathrm{d}\eta(t)}{\mathrm{d}t} \;\Leftrightarrow\; \eta(t) = \int_0^t \delta(\tau)d\tau \tag{3.32}$$

and between the impulse and step responses

$$g(t) = \frac{\mathrm{d}h(t)}{\mathrm{d}t} \;\Leftrightarrow\; h(t) = \int_0^t g(\tau)d\tau\,, \tag{3.33}$$

$$G(s) = sH(s) \;\Leftrightarrow\; H(s) = \frac{G(s)}{s}\,. \tag{3.34}$$

From all mathematical models of the linear dynamic systems the state space model is the most general

$$\dot{\boldsymbol{x}}(t) = \boldsymbol{A}\boldsymbol{x}(t) + \boldsymbol{b}u(t), \quad \boldsymbol{x}(0) = \boldsymbol{x}_0 \quad - \text{state equation} \tag{3.35a}$$

$$y(t) = \boldsymbol{c}^T\boldsymbol{x}(t) + du(t) \qquad - \text{output equation} \tag{3.35b}$$

where $\boldsymbol{A}$ is the square system (dynamics) matrix of the order n [($n\times n$)], $\boldsymbol{b}$ – the vector of the input of the dimension n, $\boldsymbol{c}$ – the vector of the output of the dimension n, d – the transfer constant, T – the transposition symbol.

The block diagram of the state space model of the linear dynamic system (3.35) is in Fig. 3.10.

For $d = 0$ the state space model (3.35) satisfies the strong condition of the physical realizability and for $d \neq 0$ satisfies only the weak condition of physical realizability.

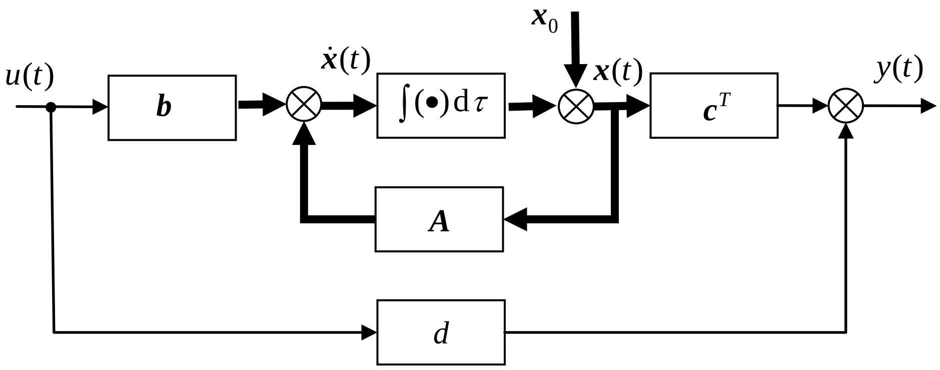

Fig. 3.10 Block diagram of the state space model of the linear dynamic system

If the state space model (3.35) satisfies the **controllability condition**

$$\boldsymbol{Q}_{co}(\boldsymbol{A},\boldsymbol{b}) = [\boldsymbol{b}, \boldsymbol{A}\boldsymbol{b}, \dots, \boldsymbol{A}^{n-1}\boldsymbol{b}], \quad \det \boldsymbol{Q}_{co}[\boldsymbol{A},\boldsymbol{b}] \neq 0 \tag{3.36}$$

and the **observability condition**

$$\boldsymbol{Q}_{ob}(\boldsymbol{A},\boldsymbol{c}) = [\boldsymbol{c}, \boldsymbol{A}^T\boldsymbol{c}, \dots, (\boldsymbol{A}^T)^{n-1}\boldsymbol{c}]^T, \quad \det \boldsymbol{Q}_{ob}[\boldsymbol{A},\boldsymbol{c}^T] \neq 0, \tag{3.37}$$

then for zero initial conditions [$\boldsymbol{x}(0) = \boldsymbol{x}_0 = \boldsymbol{0}$] we can get the transfer function on the basis of the Laplace transform

$$\left.\begin{aligned} s\boldsymbol{X}(s) &= \boldsymbol{A}\boldsymbol{X}(s) + \boldsymbol{b}U(s) \\ Y(s) &= \boldsymbol{c}^T\boldsymbol{X}(s) + dU(s) \end{aligned}\right\} \Rightarrow$$

$$G(s) = \frac{Y(s)}{U(s)} = \boldsymbol{c}^T(s\boldsymbol{I} - \boldsymbol{A})^{-1}\boldsymbol{b} + d\,, \tag{3.38}$$

where det is the determinant, $\boldsymbol{I}$ – the unit matrix, $\boldsymbol{Q}_{co}$ – the **controllability matrix** of order n [$(n\times n)$], $\boldsymbol{Q}_{ob}$ – the **observability matrix** of order n [$(n\times n)$].

From the transfer function (3.38) on the basis of (3.12) we can obtain the equation of the static characteristic (if it exists)

$$y = \lim_{s\to 0}[\boldsymbol{c}^T(s\boldsymbol{I} - \boldsymbol{A})^{-1}\boldsymbol{b} + d]u\,. \tag{3.39}$$

It is preferable for getting the transfer function to use the relation

$$G(s) = \frac{Y(s)}{U(s)} = \frac{\det(s\boldsymbol{I} - \boldsymbol{A} + \boldsymbol{b}\boldsymbol{c}^T) - \det(s\boldsymbol{I} - \boldsymbol{A})}{\det(s\boldsymbol{I} - \boldsymbol{A})} + d\,, \tag{3.40}$$

which does not demand the inversion of the functional matrix.

The controllability condition (3.36) expresses a very important property of the given linear dynamic system consisting in fact that there is such an input variable (control) $u(t)$ which can transfer the system from any initial state to any other state in a finite time.

The observability condition (3.37) expresses the fact that on the basis of the courses of the input variable (control) $u(t)$ and the output variable $y(t)$ at the given time interval it is possible to determine state $\boldsymbol{x}(t)$ in any time from this interval.

Transfer function (3.38) or (3.39) are determined on the basis of the state space model (3.35) uniquely. In contrast to the transfer function

$$G(s)=\frac{Y(s)}{U(s)}=\frac{b'_m s^m+\ldots+b'_1 s+b'_0}{a'_n s^n+\ldots+a'_1 s+a'_0} \tag{3.41a}$$

the state space model can have many (theoretically infinitely many) different forms. For example, for $n = m$ the transfer function (3.41a) can be written down in the form

$$G(s)=\frac{Y(s)}{U(s)}=\frac{b'_n}{a'_n}+\frac{b_{n-1}s^{n-1}+\ldots+b_1 s+b_0}{s^n+a_{n-1}s^{n-1}+\ldots+a_1 s+a_0}=$$

$$=d+\frac{b_{n-1}s^{n-1}+\ldots+b_1 s+b_0}{N(s)}\,. \tag{3.41b}$$

From such a modified transfer function as (3.41b) we can directly express the state space model (3.35) in the **canonical controller form**, where

$$\left.\begin{aligned}
&\boldsymbol{A}_c=\begin{bmatrix} 0 & 1 & 0 & \ldots & 0\\ 0 & 0 & 1 & \ldots & 0\\ \ldots & \ldots & \ldots & \ldots & \ldots\\ 0 & 0 & 0 & \ldots & 1\\ -a_0 & -a_1 & -a_2 & \ldots & -a_{n-1}\end{bmatrix},\ \boldsymbol{b}_c=\begin{bmatrix}0\\0\\ \vdots\\0\\1\end{bmatrix},\\
&\boldsymbol{c}_c^T=[b_0,b_1,\ldots,b_{n-1}],\ d=\frac{b'_n}{a'_n}.
\end{aligned}\right\} \tag{3.42}$$

The modified transfer function (3.41b) was obtained from the transfer function (3.41a) by dividing the nominator by the denominator and the residue by the coefficient a'_n.

The coefficients a_i and b_i can be obtained directly on the basis of the formulas

$$\left.\begin{aligned}
a_i&=\frac{a'_i}{a'_n}\\
b_i&=\frac{1}{a'_n}\left(b'_i-a'_i\frac{b'_n}{a'_n}\right)
\end{aligned}\right\}\ i=0,1,\ldots,n\,. \tag{3.43}$$

For the state space model in the canonical controller form (3.42) the dual **canonical observer form** exists

$$\left.\begin{aligned}
&\dot{\boldsymbol{x}}_c(t)=\boldsymbol{A}_c\boldsymbol{x}_c(t)+\boldsymbol{b}_c u(t), && \dot{\boldsymbol{x}}_o(t)=\boldsymbol{A}_o\boldsymbol{x}_o(t)+\boldsymbol{b}_o u(t),\\
&y(t)=\boldsymbol{c}_c^T\boldsymbol{x}_c(t)+du(t), && y(t)=\boldsymbol{c}_o^T\boldsymbol{x}_o(t)+du(t),
\end{aligned}\right\} \tag{3.44}$$

canonical controller form   canonical observer form

where

$$\left.\begin{aligned}
\boldsymbol{A}_o&=\boldsymbol{A}_c^T &&\Leftrightarrow&& \boldsymbol{A}_c=\boldsymbol{A}_o^T,\\
\boldsymbol{b}_o&=\boldsymbol{c}_c &&\Leftrightarrow&& \boldsymbol{b}_c=\boldsymbol{c}_o,\\
\boldsymbol{c}_o^T&=\boldsymbol{b}_c^T &&\Leftrightarrow&& \boldsymbol{c}_c^T=\boldsymbol{b}_o^T.
\end{aligned}\right\} \tag{3.45}$$

Transfer constant d remains the same in all forms of the state space models.

Both matrices $\boldsymbol{A}_c$ and $\boldsymbol{A}_o = \boldsymbol{A}_c^T$ in both state space models (3.44) have the **Frobenius canonical form** characterized in that the first or the last row, or the first or the last column contains the negative coefficients of the characteristic polynomial $N(s)$ for $a_n = 1$. Their characteristic polynomials are the same

$$\begin{aligned} N(s) &= \det(s\boldsymbol{I} - \boldsymbol{A}) = \det(s\boldsymbol{I} - \boldsymbol{A}_c) = \det(s\boldsymbol{I} - \boldsymbol{A}_o) = \\ &= s^n + a_{n-1}s^{n-1} + \ldots + a_1 s + a_0 = (s - s_1)(s - s_2)\cdots(s - s_n), \end{aligned} \tag{3.46}$$

where s_i are the **eigenvalues** which are the same for matrices $\boldsymbol{A}$, $\boldsymbol{A}_c$ and $\boldsymbol{A}_o = \boldsymbol{A}_c^T$.

From a comparison of the denominators in the transfer functions (3.40) and (3.41) and the polynomial (3.46) it follows that the roots of the characteristic polynomials are the eigenvalues of the matrices $\boldsymbol{A}$, $\boldsymbol{A}_c$ and $\boldsymbol{A}_o$, and therefore they are also the poles of the linear dynamic system.

We can obtain the canonical state space models (3.44) from the general state space model (3.35) on the basis of the transformation matrices $\boldsymbol{T}_c$ and $\boldsymbol{T}_o$

$$\boldsymbol{T}_c = \boldsymbol{Q}_{co}(\boldsymbol{A}, \boldsymbol{b})\boldsymbol{Q}\,, \tag{3.47}$$

$$\boldsymbol{T}_o^{-1} = \boldsymbol{Q}\boldsymbol{Q}_{co}(\boldsymbol{A}, \boldsymbol{c}^T)\,, \tag{3.48}$$

where the matrix

$$\boldsymbol{Q} = \begin{bmatrix} a_1 & a_2 & \ldots & a_{n-1} & 1 \\ a_2 & a_3 & \ldots & 1 & 0 \\ \ldots & \ldots & \ldots & \ldots & \ldots \\ a_{n-1} & 1 & \ldots & 0 & 0 \\ 1 & 0 & \ldots & 0 & 0 \end{bmatrix} \tag{3.49}$$

is made up from the coefficients of the characteristic polynomial $N(s)$ for $a_n = 1$, except the coefficient a_0, see also relation (3.41b). Then we can write

canonical controller form

$$\begin{aligned} &\boldsymbol{x}_c = \boldsymbol{T}_c^{-1}\boldsymbol{x}, \\ &\boldsymbol{A}_c = \boldsymbol{T}_c^{-1}\boldsymbol{A}\boldsymbol{T}_c,\ \boldsymbol{b}_c = \boldsymbol{T}_c^{-1}\boldsymbol{b} = [0,0,\ldots,1]^T,\ \boldsymbol{c}_c^T = \boldsymbol{c}^T\boldsymbol{T}_c = [b_0, b_1, \ldots, b_{n-1}], \end{aligned} \tag{3.50}$$

canonical observer form

$$\begin{aligned} &\boldsymbol{x}_o = \boldsymbol{T}_o^{-1}\boldsymbol{x}, \\ &\boldsymbol{A}_o = \boldsymbol{T}_o^{-1}\boldsymbol{A}\boldsymbol{T}_o,\ \boldsymbol{b}_o = \boldsymbol{T}_o^{-1}\boldsymbol{b} = [b_0, b_1, \ldots, b_{n-1}]^T,\ \boldsymbol{c}_o^T = \boldsymbol{c}^T\boldsymbol{T}_o = [0,0,\ldots,1]. \end{aligned} \tag{3.51}$$

Vectors $\boldsymbol{b}_o$ and $\boldsymbol{c}_c$ are created by the coefficients b_i of the nominator in the relation (3.41) and they can be determined directly on the basis of the formulas (3.43).

From the above mentioned mathematical models the state space model is the most general. Assuming controllability and observability [see relations (3.36) and (3.37)] and, of course, zero initial conditions, all these mathematical models of the linear dynamical systems, i.e., linear differential equations, transfer functions, frequency transfer functions, impulse responses, step responses and linear state space models are equivalent and mutually transferable.

For this reason, for the analysis and synthesis of control systems there should always be used such a mathematical model that is the most suitable for a given purpose.

3.2 Classification of linear dynamic systems

Linear dynamic systems can be classified according to various criteria. In this text the classification of linear dynamic systems is done on the basis of their properties for $t \to \infty$, or for $\omega \to 0$ [see (3.21)].

Linear dynamic systems can be classified on **proportional**, **derivative** and **integrating** systems (Fig. 3.11).

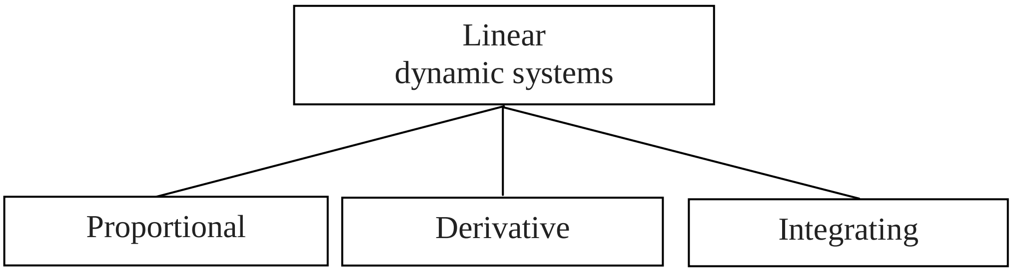

Fig. 3.11 Basic classification of linear dynamic systems

For proportional, derivative and integral linear dynamic systems the static characteristics (Fig. 3.12a), the step responses for $t \to \infty$ (Fig. 3.12b), the frequency responses for $\omega \to 0$ (Fig. 3.12c) and the Bode magnitude plots for $\omega \to 0$ (Fig. 3.12d) are shown in Figure 3.12.

Proportional systems

The general transfer function of a proportional system of the n-th order with time delay ($T_d > 0$) has the form

$$G(s) = \frac{Y(s)}{U(s)} = \frac{b_m s^m + \cdots + b_1 s + b_0}{a_n s^n + \cdots + a_1 s + a_0} \mathrm{e}^{-T_d s}, \; a_0 > 0, \; b_0 \neq 0, \; T_d \geq 0, \tag{3.52}$$

where T_d is **time delay** (dead time), n – the system order.

The polynomial $a_n s^n + \ldots + a_1 s + a_0$ has all roots in the left half plane of the complex plane s [this assumption holds also in relations (3.57) and (3.58)]. The general properties of proportional systems in the time and the frequency domains are shown in Fig. 3.12 (on the left).

The transfer function of the time delay is represented by the transcendental function

$$\mathrm{e}^{-T_d s} . \tag{3.53}$$

It is often approximated by the algebraic functions, e.g.

$$\mathrm{e}^{-T_d s} = \frac{1}{\mathrm{e}^{T_d s}} \approx \frac{1}{T_d s + 1}, \tag{3.54}$$

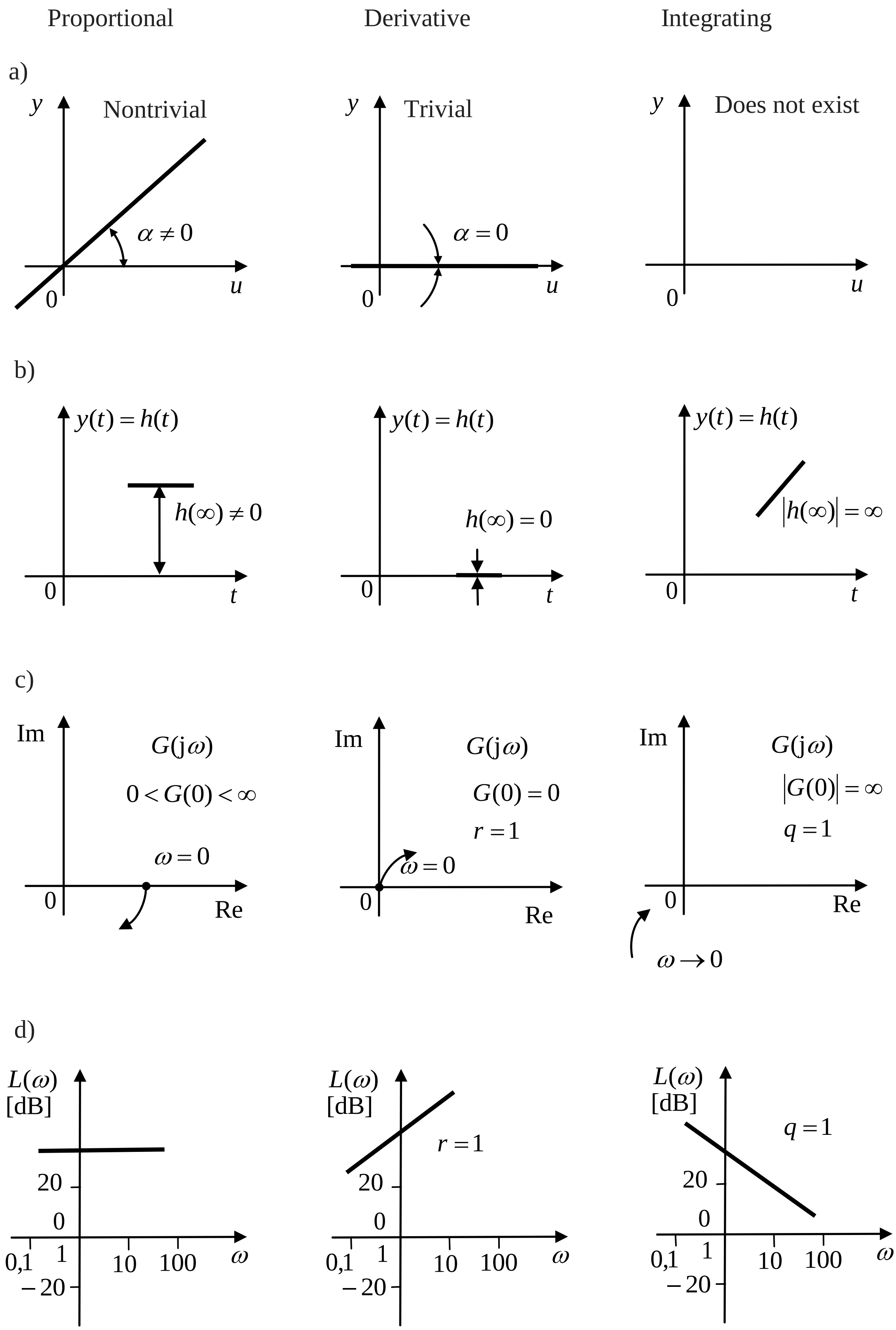

Fig. 3.12 Linear dynamic systems: a) static characteristics, b) step responses, c) frequency responses, d) Bode magnitude plots

$$\mathrm{e}^{-T_d s} = \frac{\mathrm{e}^{-\frac{T_d}{2}s}}{\mathrm{e}^{\frac{T_d}{2}s}} \approx \frac{1-\dfrac{T_d}{2}s}{1+\dfrac{T_d}{2}s}. \tag{3.55}$$

For approximation

$$\mathrm{e}^{\pm x} \approx 1 \pm x \tag{3.56}$$

Taylor's expansion was used.

The approximation of the time delay (3.55) is also called the Padé expansion of the first order.

The time delay (3.53) in the time domain makes for shifting on the right of the time response without any changes to its shape (Fig. 3.13a).

In the frequency domain the time delay (3.53) does not affect a modulus. It increases a negative phase therefore the frequency response creates the endless spiral around the origin (Fig. 3.13b).

a)

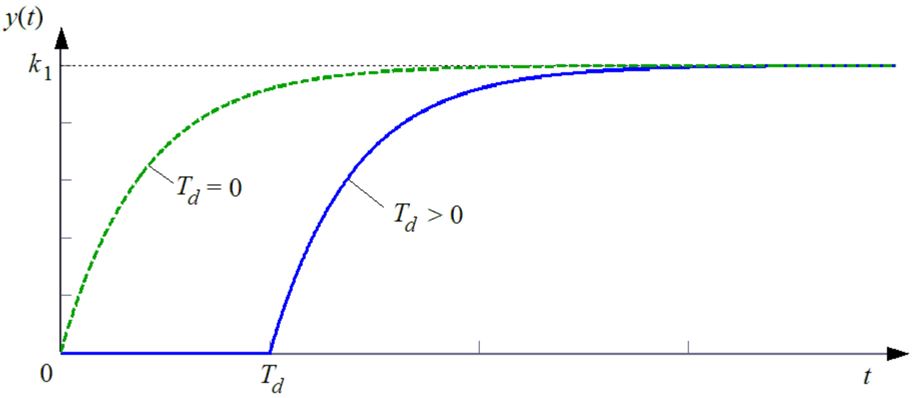

b)

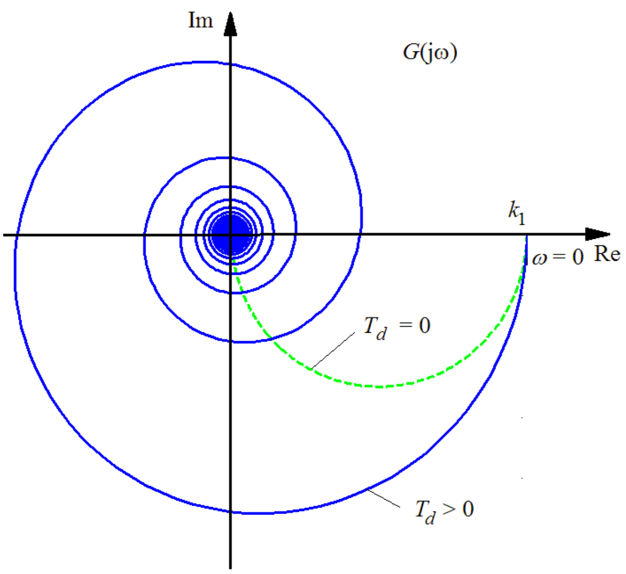

Fig. 3.13 Influence of time delay on: a) time response, b) frequency response

Derivative systems

The general transfer function of a derivative system of the r-th order with time delay ($T_d > 0$) has the form

$$G(s)=\frac{Y(s)}{U(s)}=\frac{s^r(b_m s^m+\cdots+b_1 s+b_0)}{a_n s^n+\cdots+a_1 s+a_0}\,\mathrm{e}^{-T_d s},\qquad a_0>0,\ b_0\neq 0,\ \ r\geq 1,\ T_d\geq 0. \tag{3.57}$$

The general properties of derivative systems in the time and frequency domains are shown in Fig. 3.12 (in the middle).

Integrating systems

The general transfer function of an integrating system of the q-th order with time delay ($T_d > 0$) has the form

$$G(s)=\frac{Y(s)}{U(s)}=\frac{b_m s^m+\cdots+b_1 s+b_0}{s^q(a_n s^n+\cdots+a_1 s+a_0)}\,\mathrm{e}^{-T_d s},\qquad a_0>0,\ b_0\neq 0,\ \ q\geq 1,\ T_d\geq 0. \tag{3.58}$$

The total order of the integrating system (3.58) is $n + q$.

The general properties of integrating systems in the time and frequency domains are shown in Fig. 3.12 (on the right).

Example 3.1

A mathematical model of the linear dynamic system has the form of the linear differential equation with constant coefficients

$$T_1\frac{\mathrm{d}\,y(t)}{\mathrm{d}t}+y(t)=k_1u(t-T_d)\,, \tag{3.59}$$

where T_1 is the time constant [s], T_d – the time delay [s], k_1 – the system gain [-].

It is necessary to express the given mathematical model in the forms of the transfer function, the frequency transfer function, the impulse response, the step response and the state space model. On the basis of all models it is necessary to determine the physical realizability and the static characteristic.

Solution:

Differential equation

The mathematical model is already in the form of the linear differential equations.

It shows that $n = 1 > m = 0$, i.e. the relative degree is equal to one, and therefore the dynamic system is strongly physically realizable.

From the differential equation (3.59) for $t \to \infty$ we can get the equation of the static characteristic [see (3.2)]

$$y=k_1u\,. \tag{3.60}$$

Transfer function

By means of the Laplace transform for zero initial condition from the differential equation (3.59) we get [see (3.8)]

$$T_1 sY(s) + Y(s) = k_1 U(s)\mathrm{e}^{-T_d s} \;\Rightarrow$$

$$G(s) = \frac{Y(s)}{U(s)} = \frac{k_1}{T_1 s + 1}\mathrm{e}^{-T_d s} \;. \tag{3.61}$$

Because $n = 1 > m = 0$, the given linear dynamic system is strongly physically realizable.

The static characteristic can be obtained on the basis of (3.12)

$$y = [\lim_{s \to 0} G(s)]u \;\Rightarrow\; y = k_1 u \,.$$

Frequency transfer function

The frequency transfer function can be easily obtained [see (3.13)]

$$G(\mathrm{j}\omega) = G(s)\big|_{s=\mathrm{j}\omega} = \frac{k_1}{1 + \mathrm{j}T_1\omega} = \mathrm{e}^{-\mathrm{j}T_d\omega} = A(\omega)\,\mathrm{e}^{\mathrm{j}\varphi(\omega)} \,, \tag{3.62a}$$

$$A(\omega) = \operatorname{mod} G(\mathrm{j}\omega), \;\; \varphi(\omega) = \arg G(\mathrm{j}\omega) \,. \tag{3.62b}$$

We divide the frequency transfer function (3.62) into two parts

$$G(\mathrm{j}\omega) = G_1(\mathrm{j}\omega)G_2(\mathrm{j}\omega) = A_1(\omega)A_2(\omega)\,\mathrm{e}^{\mathrm{j}[\varphi_1(\omega)+\varphi_2(\omega)]} \,, \tag{3.63}$$

$$G_1(\mathrm{j}\omega) = \frac{k_1}{1 + \mathrm{j}T_1\omega} \;\Rightarrow$$

$$A_1(\omega) = \operatorname{mod} G_1(\mathrm{j}\omega) = \operatorname{mod}\frac{k_1}{1 + \mathrm{j}T_1\omega} = \frac{k_1}{\sqrt{1 + (T_1\omega)^2}} \,, \tag{3.64a}$$

$$\varphi_1(\omega) = \arg G_1(\mathrm{j}\omega) = \arg\frac{k_1}{1 + \mathrm{j}T_1\omega} = -\operatorname{arctg} T_1\omega \,, \tag{3.64b}$$

$$G_2(\mathrm{j}\omega) = \mathrm{e}^{-\mathrm{j}T_d\omega} \;\Rightarrow$$

$$A_2(\omega) = \operatorname{mod} G_2(\mathrm{j}\omega) = \operatorname{mod}\, \mathrm{e}^{-\mathrm{j}T_d\omega} = 1 \,, \tag{3.65a}$$

$$\varphi_2(\omega) = \arg G_2(\mathrm{j}\omega) = \arg\, \mathrm{e}^{-\mathrm{j}T_d\omega} = -T_d\omega \,. \tag{3.65b}$$

Relations (3.64) and (3.65) were obtained on the basis of known formulas for complex numbers

$$\operatorname{mod}\frac{1}{a + \mathrm{j}b} = \frac{1}{\operatorname{mod}(a + \mathrm{j}b)} = \frac{1}{\sqrt{a^2 + b^2}} \,, \tag{3.66a}$$

$$\arg\frac{1}{a + \mathrm{j}b} = -\arg(a + \mathrm{j}b) = -\arctan\frac{b}{a} \tag{3.66b}$$

and the Euler formula

$$\mathrm{e}^{-\mathrm{j}x} = \cos x - \mathrm{j}\sin x \,. \tag{3.67}$$

Then for frequency transfer function (3.62) the relations hold

$$A(\omega) = A_1(\omega)A_2(\omega) = \frac{k_1}{\sqrt{1+(T_1\omega)^2}}\,, \tag{3.68a}$$

$$\varphi(\omega) = \varphi_1(\omega) + \varphi_2(\omega) = -\arctan T_1\omega - T_d\omega\,. \tag{3.68b}$$

From the relations (3.64), (3.65) and (3.68) it follows that the time delay has no effect on the modulus (the modulus of the time delay is equal to one), but significantly increases the negative phase.

Just an endless growth of a negative phase causes the creation of the endless spiral at the frequency response, see Fig. 3.13b.

Impulse response

The impulse response $g(t)$ is the original of the transfer function $G(s)$. Since the transfer function (3.61) contains the time delay, it is suitable to write it down in the form (similarly to the frequency transfer function)

$$\left.\begin{aligned} &G(s) = G_1(s)G_2(s),\\ &G_1(s) = \frac{k_1}{T_1 s+1},\ \ G_2(s) = \mathrm{e}^{-T_d s} \end{aligned}\right\} \tag{3.69}$$

and to find the impulse response $g_1(t)$, i.e. the original of the transfer function $G_1(s)$ which do not contain the time delay (see Appendix A)

$$g_1(t) = \mathrm{L}^{-1}\{G_1(s)\} = \mathrm{L}^{-1}\left\{\frac{k_1}{T_1 s+1}\right\} = \frac{k_1}{T_1}\mathrm{e}^{-\frac{t}{T_1}}\,. \tag{3.70}$$

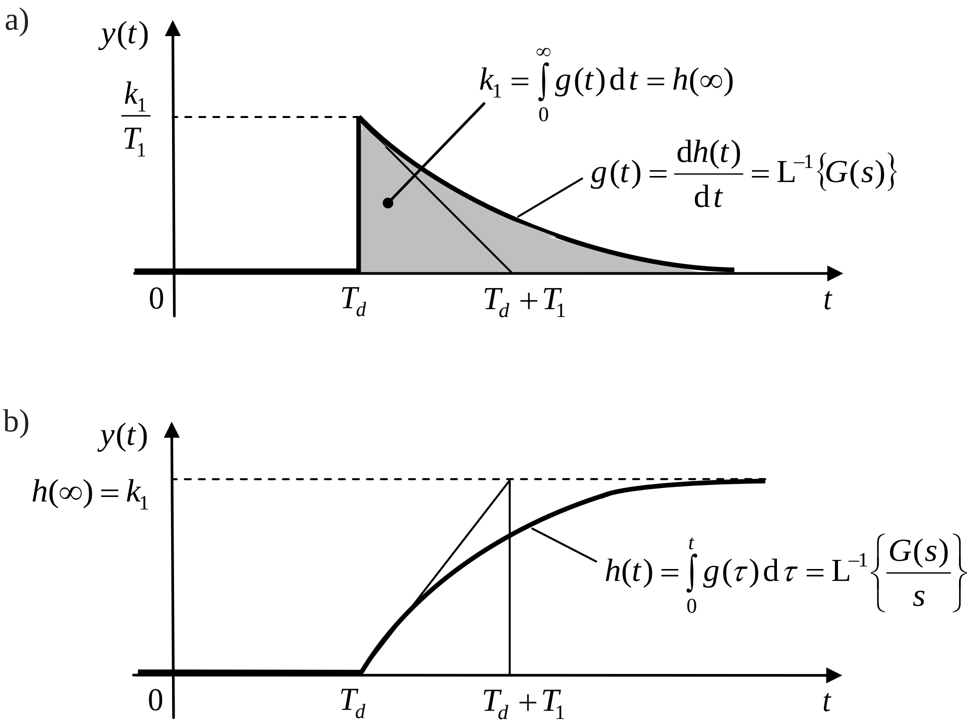

Fig. 3.14 Time responses: a) impulse, b) step – Example 3.1

The resulting impulse response will be delayed by T_d, and therefore we can write (Fig. 3.14a)

$$g(t) = \frac{k_1}{T_1} \mathrm{e}^{-\frac{t-T_d}{T_1}} \eta(t - T_d)\,. \tag{3.71}$$

We must use the delayed Heaviside step $\eta(t - T_d)$, because it ensures

$$g(t) = 0 \quad \text{for} \quad t < T_d\,. \tag{3.72}$$

At time $t = T_d$, i.e. at the beginning of the input $u(t)$ acting at impulse response $g(t)$ does not contain the Dirac impulse $\delta(t - T_d)$, and therefore the linear dynamic system is strongly physically realizable (Fig. 3.14a).

The static characteristic can be determined on the basis of the relation (3.25). In accordance with (3.25) we can write

$$\lim_{t\to\infty} \int_0^t g(\tau)\,\mathrm{d}\tau = \frac{k_1}{T_1} \int_0^\infty \mathrm{e}^{-\frac{t-T_d}{T_1}} \eta(t - T_d)\,\mathrm{d}t =$$

$$= \frac{k_1}{T_1} \int_{T_d}^\infty \mathrm{e}^{-\frac{t-T_d}{T_1}} \mathrm{d}t = \frac{k_1}{T_1} \int_0^\infty \mathrm{e}^{-\frac{\tau}{T_1}} \mathrm{d}\tau = \left[-k_1 \mathrm{e}^{-\frac{\tau}{T_1}} \right]_0^\infty = k_1$$

$$\Rightarrow \; y = k_1 u.$$

Step response

Similarly for the impulse response we use the relations (3.69) and in accordance with the formula (3.27) for part of the transfer function without time delay and we get

$$h_1(t) = \mathrm{L}^{-1}\left\{ \frac{G_1(s)}{s} \right\} = \mathrm{L}^{-1}\left\{ \frac{k_1}{s(T_1 s + 1)} \right\} = k_1 \left(1 - \mathrm{e}^{-\frac{t}{T_1}} \right). \tag{3.73}$$

The resulting step response $h(t)$ will be delayed by T_d, and therefore we can write (Figs 3.13a and 3.14b)

$$h(t) = k_1 \left(1 - \mathrm{e}^{-\frac{t-T_d}{T_1}} \right) \eta(t - T_d)\,. \tag{3.74}$$

The delayed Heaviside step $\eta(t - T_d)$ ensures

$$h(t) = 0 \quad \text{for} \quad t < T_d\,. \tag{3.75}$$

At time $t = T_d$, i.e. at the beginning of the input $u(t)$ acting the step response $h(t)$ equals zero and therefore the linear dynamic system is strongly physically realizable.

For determining the static characteristic the relation (3.28) is used

$$\lim_{t\to\infty} h(t) = \lim_{t\to\infty} \left[k_1 \left(1 - \mathrm{e}^{-\frac{t-T_d}{T_1}} \right) \eta(t - T_d) \right] = k_1 \; \Rightarrow$$

$$y = k_1 u.$$

We easily make sure that the relation (Fig. 3.14) holds

$$g(t) = \frac{\mathrm{d}h(t)}{\mathrm{d}t} \quad \Leftrightarrow \quad h(t) = \int_0^t g(\tau) d\tau \,.$$

State space model

Since the linear differential equation (3.59) is very simple, e.g for $x(t) = y(t)$ we can directly write

$$\left.\begin{aligned} \dot{x}(t) &= -\frac{1}{T_1}x(t) + \frac{k_1}{T_1}u(t - T_d) && - \text{state equation} \\ y(t) &= x(t) && - \text{output equation} \end{aligned}\right\} \tag{3.76}$$

where $x(t)$ is the state.

It is obvious that the form (3.76) is only one of many possible equivalent forms of a state space model.

For the state space model (3.76) $d = 0$, and therefore the linear dynamic system is strongly physically realizable.

The static characteristic can be obtained on the basis of the state space model (3.76)

$$t \to \infty \;\Rightarrow\; \dot{x}(t) \to 0 \;\Rightarrow$$

$$\left.\begin{aligned} 0 &= -\frac{1}{T_1}x + \frac{k_1}{T_1}u \\ y &= x \end{aligned}\right\} \Rightarrow y = k_1 u \,.$$

It is evident from all the above mentioned mathematical models that it is the proportional system of the first order with a time delay (see Fig. 12.3).

For this system the following abbreviations are often used: FOPTD system (**f**irst **o**rder **p**lus **t**ime **d**elay system), FOPDT system (**f**irst **o**rder **p**lus **d**ead **t**ime system) and FOLPD system (**f**irst **o**rder **l**ag **p**lus time **d**elay system).

The FOPTD system is very important for automatic control theory because it is very often used for the approximation of nonoscillatory plants of high order.

Example 3.2

It is necessary to express a resistance, an inductance and a capacitance in the form of impedance transforms and transfer functions (Fig. 3.15). In Fig. 3.15 there are: $u(t)$ – the voltage [V], $i(t)$ – the current [A], R – the resistance [Ω], L – the inductance [H], C – the capacitance [F].

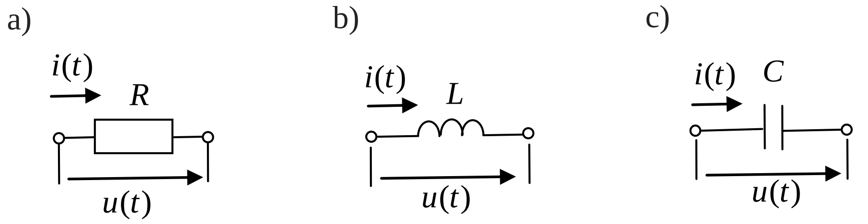

Fig. 3.15 – Passive electrical elements: a) resistor, b) inductor, c) capacitor

Solution:

In order to determine the impedance transform $Z(s)$ we use the generalized Ohm's Law

$$I(s) = \frac{U(s)}{Z(s)} \;\Rightarrow$$

$$Z(s) = \frac{U(s)}{I(s)}, \tag{3.77}$$

where $U(s)$ is the voltage transform, $I(s)$ – the current transform.

The transfer function of the passive electrical element with the impedance transform $Z(s)$ depends on if the input is the current $I(s)$ or the voltage $U(s)$, see Fig. 3.16.

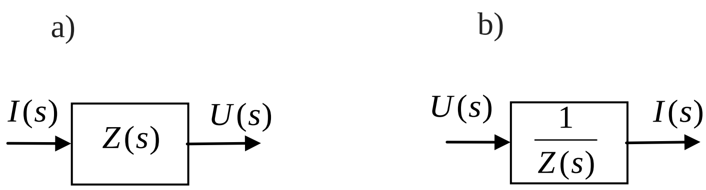

Fig. 3.16 Transfer function of the passive electrical element: a) input = current, b) input = voltage

a) Resistor

For a resistor with the resistance R it holds

$$u(t) = Ri(t)\,.$$

Using the Laplace transform we get

$$U(s) = RI(s) \;\Rightarrow$$

$$Z(s) = \frac{U(s)}{I(s)} = R. \tag{3.78}$$

The resistor with the resistance R has the property of the ideal proportional system for current or voltage inputs (Fig. 3.17a).

b) Inductor

For an inductor with the inductance L it holds

$$u(t) = L\frac{\mathrm{d}i(t)}{\mathrm{d}t} \;\Leftrightarrow\; i(t) = \frac{1}{L}\int_0^t u(\tau)\,\mathrm{d}\tau\,.$$

Applying the Laplace transform with the zero initial condition we get

$$U(s) = LsI(s) \;\Rightarrow$$

$$Z(s) = \frac{U(s)}{I(s)} = Ls. \tag{3.79}$$

The inductor with the inductance L has the property of the ideal derivative system for the current input and the property of the ideal integrating system for the voltage input (Fig. 3.17b).

c) Capacitor

For a capacitor with capacitance C it holds

$$u(t) = \frac{1}{C}\int_0^t i(\tau)\,\mathrm{d}\tau \;\Leftrightarrow\; i(t) = C\frac{\mathrm{d}u(t)}{\mathrm{d}t}\ .$$

Applying the Laplace transform with the zero initial condition we get

$$U(s) = \frac{1}{Cs}I(s) \;\Rightarrow$$

$$Z(s) = \frac{U(s)}{I(s)} = \frac{1}{Cs}. \qquad (3.80)$$

The capacitor with capacitance C has the property of the ideal system for the current input and the property of the ideal derivative system for the voltage input (Fig. 3.17c).

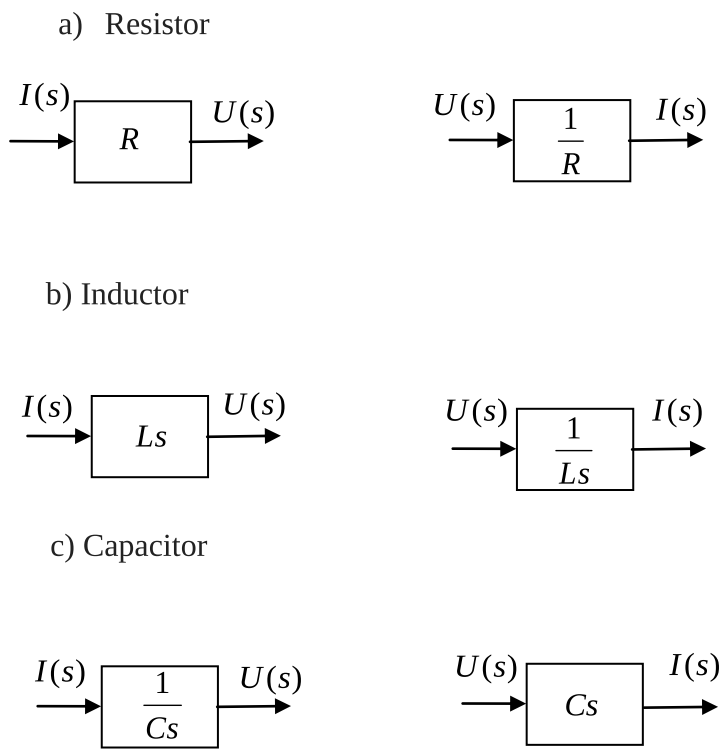

Fig. 3.17 Transfer functions of passive electrical elements: a) resistor, b) inductor, c) capacitor

3.3 Block diagram algebra

Block diagrams have been used in the previous chapters. Now we show that the block diagrams representing complex systems can be easily simplified by using **block diagram algebra**.

The system (subsystem, element, etc.) is expressed in block diagrams by the block containing its transfer function. Addition and subtraction (comparison) of the variables (signals) are expressed by the summing node and variables (signals) branching is expressed by the information node (Fig. 3.18).

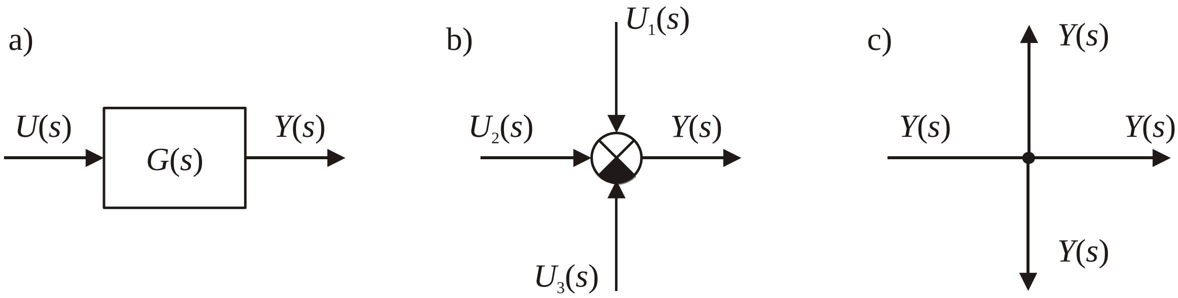

$$Y(s) = G(s)U(s) \qquad\qquad Y(s) = U_1(s) + U_2(s) - U_3(s)$$

Fig. 3.18 Representation: a) linear dynamic system by block, b) addition and subtraction by the summing node, c) branching by the information node

The filled segment of the summation node or minus sign means subtraction of the corresponding variable (signal). From the summation node only one variable can come out. For the reason of simplicity and clarity the independent variable *s* is not often explicitly written in transfer functions and transforms in the block diagrams.

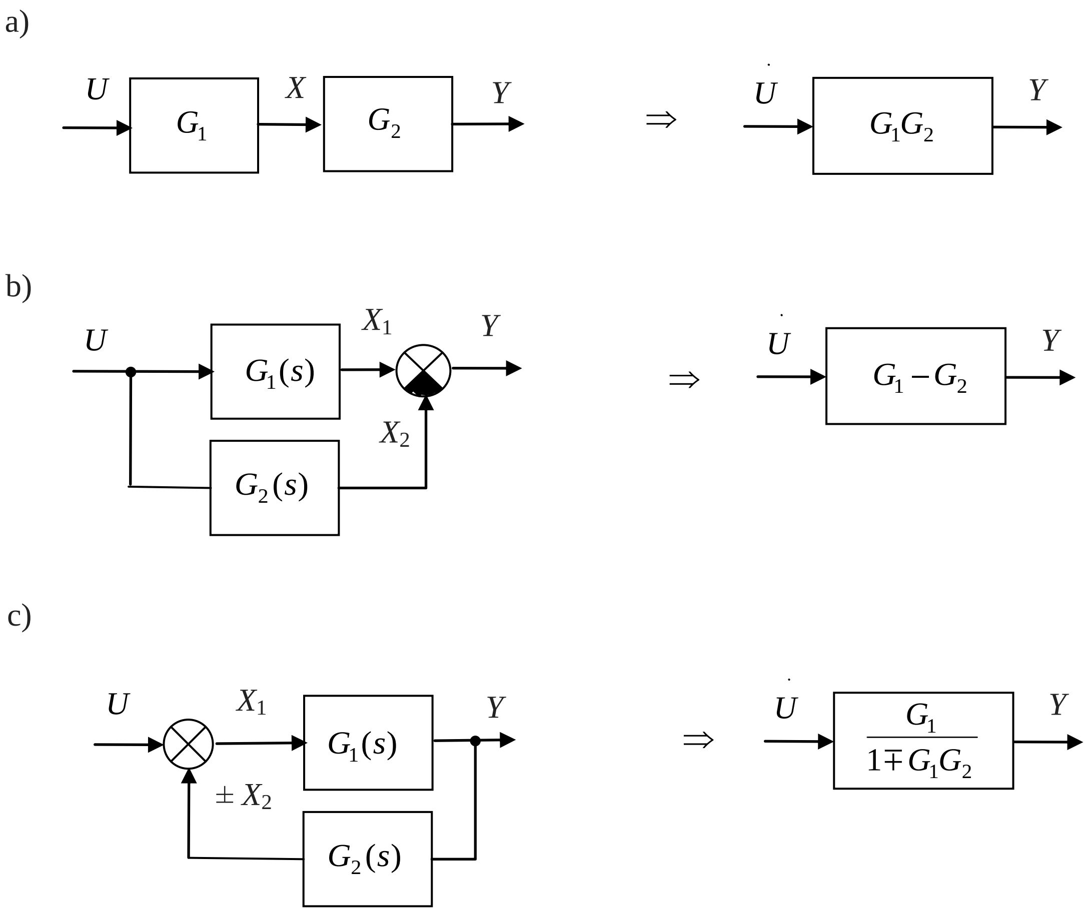

Fig. 3.19 Interconnection of blocks: a) serial, b) parallel, c) feedback

For the serial (cascade) interconnection in Fig. 3.19a it holds

$$\left.\begin{aligned} Y(s) &= G_2(s)X(s) \\ X(s) &= G_1(s)U(s) \end{aligned}\right\} \Rightarrow G(s) = \frac{Y(s)}{U(s)} = G_1(s)G_2(s) = G_2(s)G_1(s)\,. \tag{3.81}$$

For the serial interconnection of the blocks the resultant transfer function is the product of the particular transfer functions (it does not depend on the order).

For the parallel interconnection in Fig. 3.19b it holds

$$\left.\begin{aligned} Y(s) &= X_1(s) - X_2(s) \\ X_1(s) &= G_1(s)U(s) \\ X_2(s) &= G_2(s)U(s) \end{aligned}\right\} \Rightarrow G(s) = \frac{Y(s)}{U(s)} = G_1(s) - G_2(s)\,. \tag{3.82}$$

Tab. 3.1 Basic block diagram transformations

Moving an information node ahead of a block	
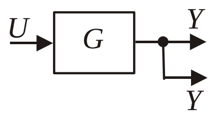	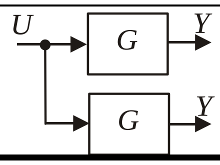
Moving an information node behind a block	
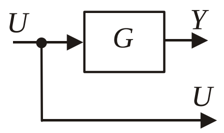	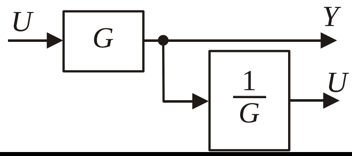
Moving a summing node behind a block	
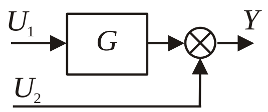	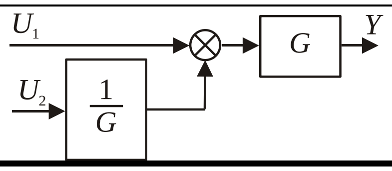
Moving a summing node ahead of a block	
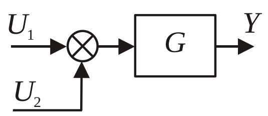	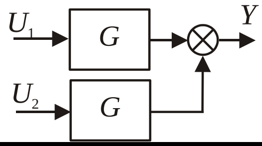
Moving a block from a parallel interconnection	
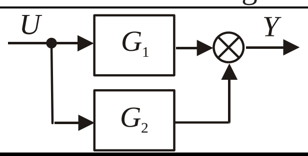	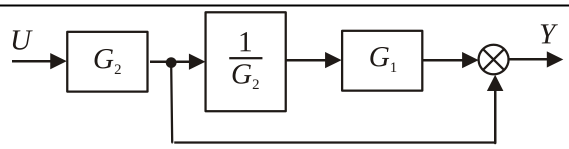
Moving a block from a feedback interconnection	
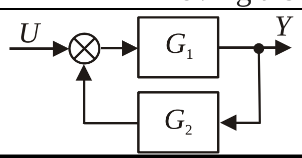	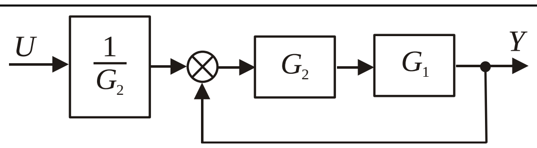

For the parallel interconnection of the blocks the resultant transfer function is the sum of the particular transfer functions taking into account the signs at the summing node.

For the feedback interconnection in Fig. 3.19c it holds

$$\left.\begin{aligned} Y(s) &= G_1(s)X_1(s) \\ X_1(s) &= U(s) \pm X_2(s) \\ X_2(s) &= G_2(s)Y(s) \end{aligned}\right\} \Rightarrow G(s) = \frac{Y(s)}{U(s)} = \frac{G_1(s)}{1 \mp G_1(s)G_2(s)}. \tag{3.83}$$

For the feedback interconnection the resultant transfer function is given by the transfer function in the forward path (branch) divided by the negative (in case of positive feedback), or the positive (in the case of negative feedback) product of the transfer functions in the forward and feedback paths (branches) increased by one. The transfer function of the path without the block (transfer function) is considered as a unit.

With knowledge of the three basic interconnections and simple modification of the block diagrams, which are shown in Tab. 3.1, we can easily simplify any even very complex block diagram.

If the block diagram contains multiple input and output variables, then for each output variable all the input variables are considered, the variables which are not considered are assumed equal to zero (they are not drawn). The resulting transfer functions for each input variable are given by the sum of the effects of the all input variables (it is based on the linearity). For reasons of clarity, the resulting transfer function often uses a subscript, the first letter indicates the input variable and the second letter indicates the output variable (sometimes the opposite order is used).

Example 3.3

The simple electrical circuit with the passive electrical elements with the impedance transforms $Z_1(s)$ and $Z_2(s)$ is shown in Fig. 3.20. It is necessary to determine its transfer function assuming that the voltage $u_1(t)$ [V] is the input and the voltage $u_2(t)$ [V] is the output.

Solution:

We determine the transfer function of the electrical circuit in Fig. 3.20a in three ways.

a) Classical approach

Since for both impedances the current $i(t)$ is the same, therefore we can write

$$\left.\begin{aligned} Z_1(s)I(s) &= U_1(s) - U_2(s) \\ Z_2(s)I(s) &= U_2(s) \end{aligned}\right\} \Rightarrow \frac{Z_1(s)}{Z_2(s)} + 1 = \frac{1}{G(s)} \Rightarrow$$

$$G(s) = \frac{U_2(s)}{U_1(s)} = \frac{Z_2(s)}{Z_1(s) + Z_2(s)}. \tag{3.84}$$

b) Voltage divider

The circuit in Fig. 3.20a can be regarded as a voltage divider in Fig. 3.20b. For a voltage divider it holds

$$\frac{U_2(s)}{U_1(s)} = \frac{Z_2(s)}{Z_1(s)+Z_2(s)}.$$

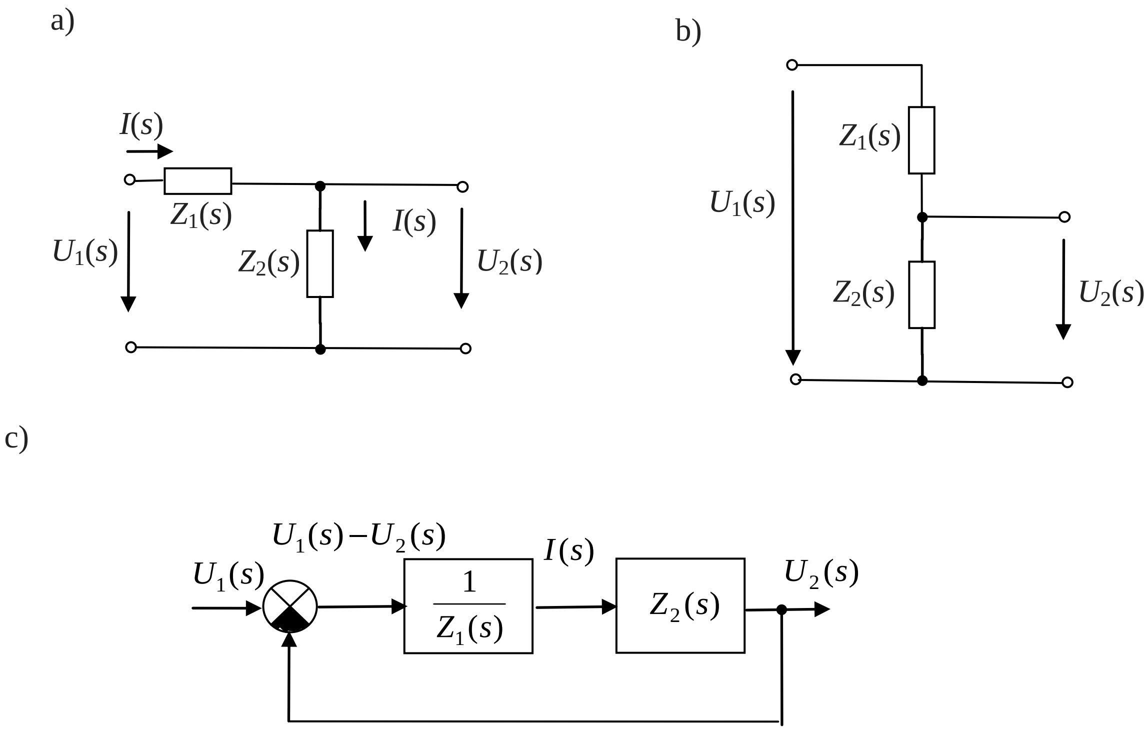

Fig. 3.20 Simple electrical circuit with passive elements: a) scheme, b) voltage divider, c) feedback circuit – Example 3.3

c) Feedback circuit

The electrical circuit in Fig. 3.20a can also be considered as the feedback circuit in Fig. 3.20c. In accordance with the relations (3.81) and (3.83) we can directly write

$$G(s) = \frac{U_2(s)}{U_1(s)} = \frac{\dfrac{Z_2(s)}{Z_1(s)}}{1+\dfrac{Z_2(s)}{Z_1(s)}} = \frac{Z_2(s)}{Z_1(s)+Z_2(s)}.$$

Example 3.4

An operational amplifier (op-amp) is a very important active element that has wide application in mechatronics. In electronics and electrical engineering it is available as an integrated circuit. It is an amplifier with a high gain (theoretically infinitely high) and a large input resistance (theoretically infinitely large), which works with negative feedback (Fig. 3.21). By the appropriate choice of the feedback impedance $Z_2(s)$ and the impedance $Z_1(s)$ in the input the operational amplifier can realize various dynamic properties. The power supply for operational amplifiers is not drawn and its simplified scheme is used (Fig. 3.21b).

It is necessary to derive the transfer function of the operational amplifier.

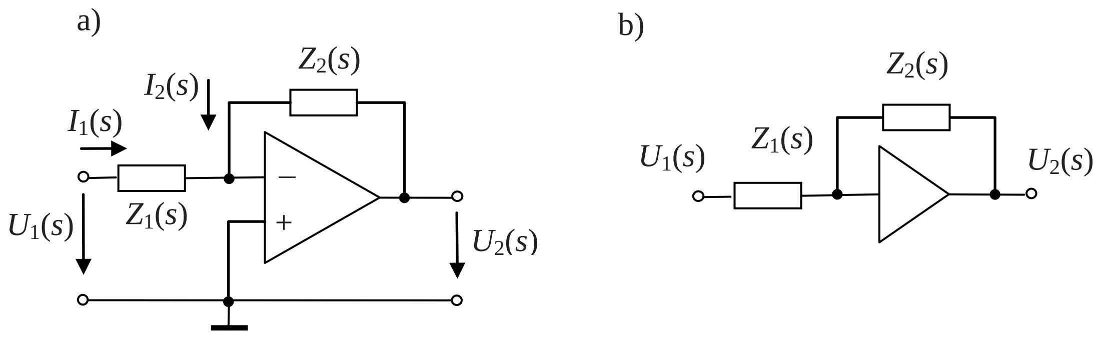

Fig. 3.21 Operational amplifier: a) scheme, b) simplified scheme – Example 3.4

Solution:

Since the amplification and the input resistance of the operational amplifier are very high, it is obvious that any current cannot flow in it, i.e. it must hold

$$I_1(s) + I_2(s) = 0 \;\Rightarrow\; \frac{U_1(s)}{Z_1(s)} + \frac{U_2(s)}{Z_2(s)} = 0 \;\Rightarrow$$

$$G(s) = \frac{U_2(s)}{U_1(s)} = -\frac{Z_2(s)}{Z_1(s)}. \tag{3.85}$$

Example 3.5

For all circuits with the operational amplifier in Fig. 3.22 it is necessary to determine their transfer functions.

Solution:

For a determination of the transfer functions of the electrical circuits with an operational amplifier in Fig. 3.22 we will use the derived formula (3.85) in Example 3.4, i.e.

$$G(s) = \frac{U_2(s)}{U_1(s)} = -\frac{Z_2(s)}{Z_1(s)}.$$

Assuming that the resistance is in [Ω] and the capacitance is in [F], the product of the resistance and capacitance is in [s].

a)

$$G(s) = \frac{U_2(s)}{U_1(s)} = -\frac{R_2}{R_1}. \tag{3.86}$$

It is the ideal proportional system (ideal amplifier) – P.

b)

$$G(s) = \frac{U_2(s)}{U_1(s)} = -\frac{R}{\frac{1}{Cs}} = -RCs. \tag{3.87}$$

It is the ideal derivative system – D.

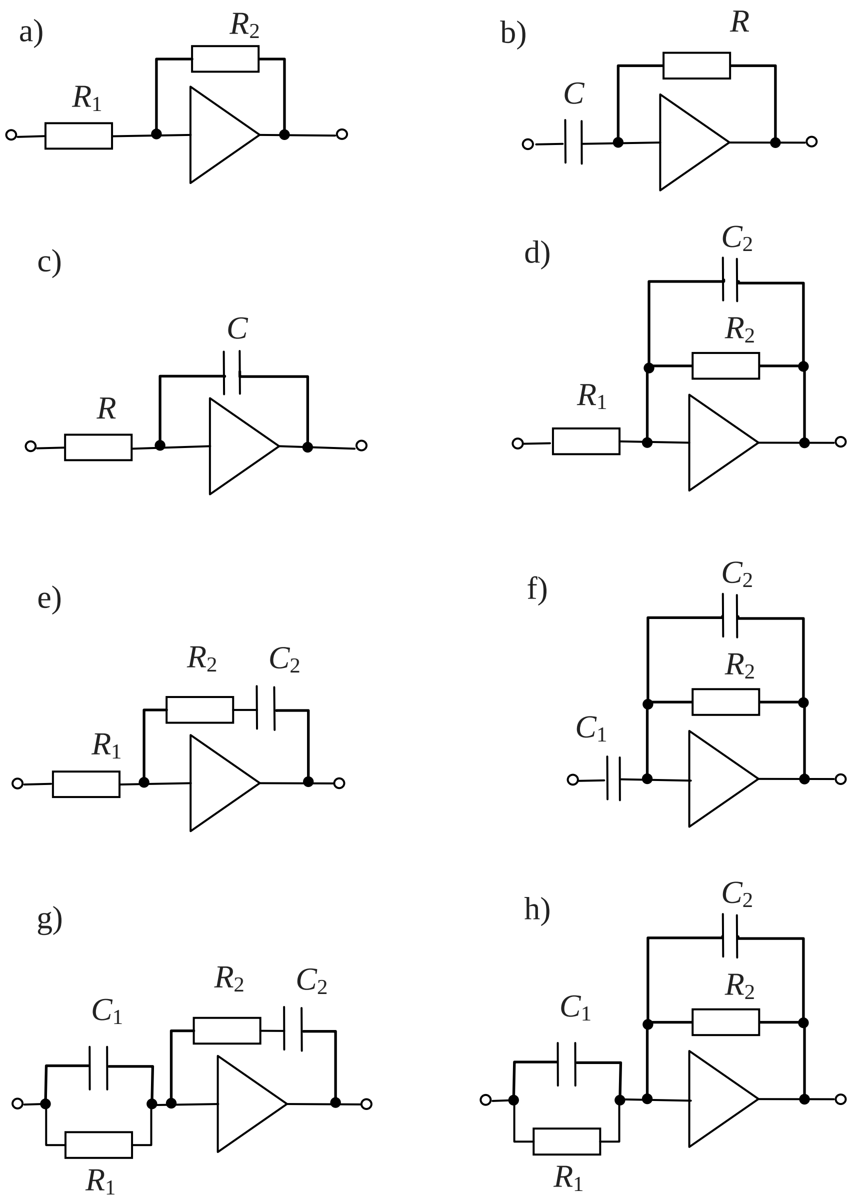

Fig. 3.22 Electrical circuits with an operational amplifier – Example 3.5

c)

$$G(s)=\frac{U_2(s)}{U_1(s)}=-\frac{\frac{1}{Cs}}{R}=-\frac{1}{RCs}\,. \tag{3.88}$$

It is the ideal integrating system – I.

d)

$$G(s)=\frac{U_2(s)}{U_1(s)}=-\frac{\dfrac{\dfrac{R_2}{C_2s}}{R_2+\dfrac{1}{C_2s}}}{R_1}=-\frac{R_2}{R_1}\frac{1}{R_2C_2s+1}\,. \tag{3.89}$$

It is the proportional system of the first order

e)

$$G(s)=\frac{U_2(s)}{U_1(s)}=-\frac{R_2+\dfrac{1}{C_2s}}{R_1}=-\frac{R_2C_2s+1}{R_1C_2s}\,. \tag{3.90}$$

This electrical circuit with the operational amplifier realizes the **PI controller** (for more details see Section 5.1).

f)

$$G(s)=\frac{U_2(s)}{U_1(s)}=-\frac{\dfrac{\dfrac{R_2}{C_2s}}{R_2+\dfrac{1}{C_2s}}}{\dfrac{1}{C_1s}}=-\frac{R_2C_1s}{R_2C_2s+1}\,. \tag{3.91}$$

It is the derivative system of the first order (the real derivative system).

g)

$$G(s)=\frac{U_2(s)}{U_1(s)}=-\frac{R_2+\dfrac{1}{C_2s}}{\dfrac{\dfrac{R_1}{C_1s}}{R_1+\dfrac{1}{C_1s}}}=-\frac{(R_1C_1s+1)(R_2C_2s+1)}{R_1C_2s}\,. \tag{3.92}$$

This electrical circuit with the operational amplifier realizes the **PID controller with interaction** (for more details see Section 5.1).

h)

$$G(s)=\frac{U_2(s)}{U_1(s)}=-\frac{\dfrac{\dfrac{R_2}{C_2s}}{R_2+\dfrac{1}{C_2s}}}{\dfrac{\dfrac{R_1}{C_1s}}{R_1+\dfrac{1}{C_1s}}}=-\frac{R_2}{R_1}\frac{R_1C_1s+1}{R_2C_2s+1}\,. \tag{3.93}$$

This electrical circuit with the operational amplifier realizes the **lead-lag compensator**. It improves an undesirable frequency response.

Example 3.6

It is necessary to derive a mathematical model of a DC motor with a constant separate excitation (furthermore, we will use “DC motor”) in Fig. 3.23, where means: J_m – the total moment of inertia reduced in the motor shaft [kg m^2], $i_a(t)$ – the armature current [A], $u_a(t)$ – the armature voltage [V], R_a - the total resistance of the armature circuit [Ω], L_a – the total inductance of the armature circuit [H], b_m – the coefficient of viscous friction [N m s rad^{-1}], $m(t)$ - the motor torque [N m], $m_l(t)$ – the load torque [N m], $\alpha(t)$ – the angle of the motor shaft [rad], $\omega(t)$ – the angular velocity of the motor shaft [rad s^{-1}], c_m – the motor constant [N m A^{-1}], c_e – the motor constant [V s rad^{-1}], $u_e(t)$ – the induced voltage [V], Φ – the constant magnetic flux of the excitation [Wb].

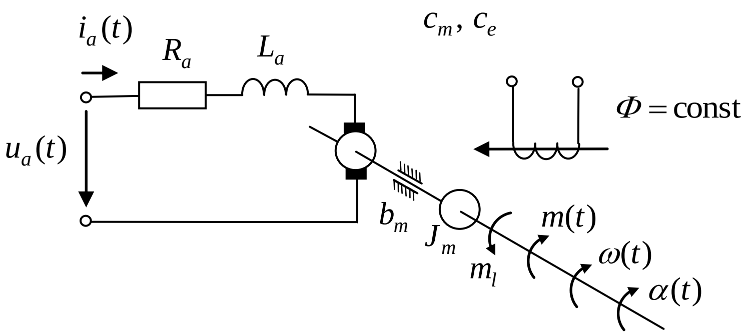

Fig. 3.23 Simplified scheme of the DC motor – Example 3.6

Solution:

In accordance with Fig. 3.23 we can write [3, 16, 21]:

$$\left.\begin{aligned} \frac{\mathrm{d}\alpha(t)}{\mathrm{d}t} &= \omega(t), \\ J_m \frac{\mathrm{d}\omega(t)}{\mathrm{d}t} + b_m\omega(t) &= m(t) - m_l(t), \\ m(t) &= c_m i_a(t), \\ L_a \frac{\mathrm{d}i_a(t)}{\mathrm{d}t} + R_a i_a(t) &= u_a(t) - u_e(t), \\ u_e(t) &= c_e\omega(t). \end{aligned}\right\} \tag{3.94}$$

Applying the Laplace transform with zero initial conditions and after modification we get

$$A(s) = \frac{1}{s}\Omega(s),$$
$$\Omega(s) = \frac{1}{J_m s + b_m}[M(s) - M_l(s)],$$
$$M(s) = c_m I_a(s),$$
$$I_a(s) = \frac{1}{L_a s + R_a}[U_a(s) - U_e(s)],$$
$$U_e(s) = c_e \Omega(s).$$

Now we can easily make up a block diagram corresponding to the above equations (Fig. 3.24).

On the basis of the block diagram in Fig. 3.24 we can easily obtain the transfer functions:

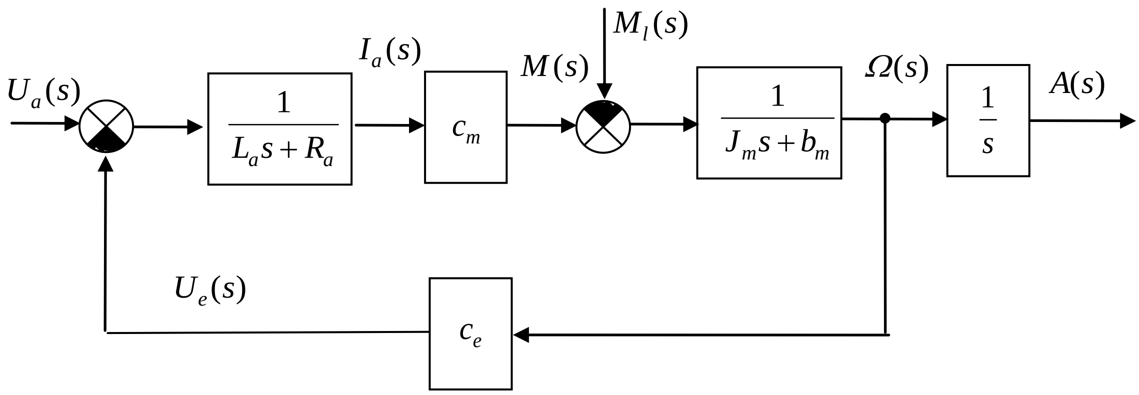

Fig. 3.24 Bock diagram of DC motor – Example 3.6

Angular velocity of the motor shaft

$$\frac{\Omega(s)}{U_a(s)} = \frac{c_m}{(J_m s + b_m)(L_a s + R_a) + c_e c_m}, \tag{3.95}$$

$$\frac{\Omega(s)}{M_l(s)} = -\frac{L_a s + R_a}{(J_m s + b_m)(L_a s + R_a) + c_e c_m}. \tag{3.96}$$

Angle of the motor shaft

$$\frac{A(s)}{U_a(s)} = \frac{c_m}{s[(J_m s + b_m)(L_a s + R_a) + c_e c_m]}, \tag{3.97}$$

$$\frac{A(s)}{M_l(s)} = -\frac{L_a s + R_a}{s[(J_m s + b_m)(L_a s + R_a) + c_e c_m]}. \tag{3.98}$$

For powers in steady-state equality holds

$$u_e i_a = m\omega \;\Rightarrow\; c_e \omega i_a = c_m i_a \omega \;\Rightarrow\; c_e = c_m. \tag{3.99}$$

The state space model of the DC motor can be easily obtained from the equations (3.94)

$$\left.\begin{aligned}
\frac{\mathrm{d}\alpha(t)}{\mathrm{d}t} &= \omega(t), \\
\frac{\mathrm{d}\omega(t)}{\mathrm{d}t} &= -\frac{b_m}{J_m}\omega(t) + \frac{c_m}{J_m} i_a(t) - \frac{1}{J_m} m_l(t), \\
\frac{\mathrm{d}i_\mathrm{a}(t)}{\mathrm{d}t} &= -\frac{c_e}{L_a}\omega(t) - \frac{R_a}{L_a} i_a(t) + \frac{1}{L_a} u_a(t).
\end{aligned}\right\} \tag{3.100}$$

The equations (3.100) can be written down in the matrix form

$$\begin{bmatrix} \frac{\mathrm{d}\alpha(t)}{\mathrm{d}t} \\ \frac{\mathrm{d}\omega(t)}{\mathrm{d}t} \\ \frac{\mathrm{d}i_\mathrm{a}(t)}{\mathrm{d}t} \end{bmatrix} = \begin{bmatrix} 0 & 1 & 0 \\ 0 & -\frac{b_m}{J_m} & \frac{c_m}{J_m} \\ 0 & -\frac{c_e}{L_a} & -\frac{R_a}{L_a} \end{bmatrix} \begin{bmatrix} \alpha(t) \\ \omega(t) \\ i_a(t) \end{bmatrix} + \begin{bmatrix} 0 \\ 0 \\ \frac{1}{L_a} \end{bmatrix} u_a(t) - \begin{bmatrix} 0 \\ \frac{1}{J_m} \\ 0 \end{bmatrix} m_l(t) \tag{3.101}$$

4 MATHEMATICAL MODEL SIMPLIFICATION

4.1 Linearization

Linear dynamical systems are in principle the idealization of real dynamic systems. The real world is nonlinear, and therefore, if we want to use linear models, we have to agree to various simplifying assumptions. One of the most important assumptions is that the system operates in the "close" neighbourhood of the **operating point**. In this neighbourhood the mathematical model of the dynamic system can be considered as linear.

Assume that a nonlinear dynamical system is described by the differential equation (2.1a)

$$g[y^{(n)}(t),\ldots,\dot{y}(t),y(t),u^{(m)}(t),\ldots,\dot{u}(t),u(t)]=0\,.$$

Using the Taylor expansion and we will consider only linear terms due to increments and we get

$$\left.\frac{\partial g}{\partial y^{(n)}}\right|_0 \Delta y^{(n)}(t)+\cdots+\left.\frac{\partial g}{\partial \dot{y}}\right|_0 \Delta\dot{y}(t)+\left.\frac{\partial g}{\partial y}\right|_0 \Delta y(t)+$$
$$+\left.\frac{\partial g}{\partial u^{(m)}}\right|_0 \Delta u^{(m)}(t)+\cdots+\left.\frac{\partial g}{\partial \dot{u}}\right|_0 \Delta\dot{u}(t)+\left.\frac{\partial g}{\partial u}\right|_0 \Delta u(t)=0\,.$$

After modification we obtain the **linearized differential equation**

$$a_n\Delta y^{(n)}(t)+\cdots+a_1\Delta\dot{y}(t)+a_0\Delta y(t)=b_m\Delta u^{(m)}(t)+\cdots+b_1\Delta\dot{u}(t)+b_0\Delta u(t)\,, \tag{4.1}$$

where

$$\left.\begin{aligned} a_i&=\left.\frac{\partial g}{\partial y^{(i)}}\right|_0,\ \Delta y^{(i)}(t)=y^{(i)}(t),\ i=1,2,\ldots,n,\\ a_0&=\left.\frac{\partial g}{\partial y}\right|_0,\ \Delta y(t)=y(t)-y_0,\end{aligned}\right\} \tag{4.2}$$

$$\left.\begin{aligned} b_j&=-\left.\frac{\partial g}{\partial u^{(j)}}\right|_0,\ \Delta u^{(j)}(t)=u^{(j)}(t),\ j=1,2,\ldots,m,\\ b_0&=-\left.\frac{\partial g}{\partial u}\right|_0,\ \Delta u(t)=u(t)-u_0.\end{aligned}\right\} \tag{4.3}$$

The partial derivatives in equations (4.2) and (4.3) should be calculated for the operating point (u_0, y_0) which lies on the static characteristics [see (2.5)]

$$y=f(u)\,,$$

i.e.

$$y_0=f(u_0)\,. \tag{4.4}$$

The linearized static characteristic has the form

$$\Delta y(t)=k_1\Delta u(t)\ \text{ or }\ \Delta y=k_1\Delta u\,, \tag{4.5}$$

where the coefficient k_1 can be determined on the basis of the relations (4.2) and (4.3)

$$k_1 = -\left.\frac{\dfrac{\partial g}{\partial u}}{\dfrac{\partial g}{\partial y}}\right|_0 = \left.\frac{\mathrm{d}\,f}{\mathrm{d}\,u}\right|_0 = \frac{b_0}{a_0},\; a_0 \neq 0\,. \tag{4.6}$$

The geometric interpretation of the **linearization** of the nonlinear static characteristic is shown in Fig. 4.1. We can see that it is a tangent line at the operating point to the original nonlinear static characteristics.

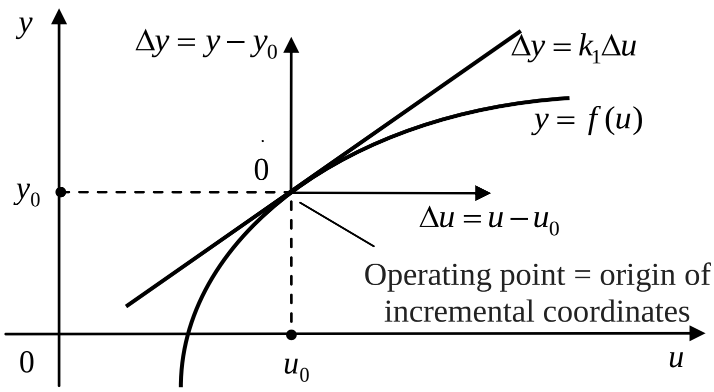

Fig. 4.1 Geometric interpretation of linearization of nonlinear static characteristic

From comparison of the equations (4.1) and (3.1a) it follows that they have the same form, but the input and output variables are represented by their increments and coefficients (4.2) and (4.3) depend on the operating point (u_0, y_0).

After linearization the linearized static characteristic (4.5) must pass through the origin of the **incremental coordinates** (Fig. 4.1).

The output variable can be approximately expressed by the relation

$$\hat{y}(t) = y_0 + \Delta y(t)\,, \tag{4.7}$$

where $\hat{y}(t)$ is the output variable obtained from the linearized mathematical model.

Now consider the mathematical model of the nonlinear static system with one output variable y and m input variables $u_1, u_2, \ldots, u_m$.

$$y = f(u_1, u_2, \ldots, u_m)\,. \tag{4.8}$$

As in the previous case, we use the Taylor expansion and the linearized mathematical model is determined by the tangent hyperplane

$$\Delta y(t) = \sum_{j=1}^{m} k_j \Delta u_j\,, \tag{4.9a}$$

$$k_j = \left.\frac{\partial f}{\partial u_j}\right|_0,\quad j = 1,2,\ldots,m\,. \tag{4.9b}$$

When the mathematical model of nonlinear dynamic systems is in the state space representation (2.8)

$$\dot{\boldsymbol{x}}(t) = \boldsymbol{g}[\boldsymbol{x}(t), u(t)],$$

$$y(t) = h[\boldsymbol{x}(t), u(t)],$$

then the linearization proceeds similarly. The Taylor expansion is used and the linear terms with respect to increments are considered only, i.e.

$$\left.\begin{aligned} \Delta\dot{\boldsymbol{x}}(t) &= \boldsymbol{A}\Delta\boldsymbol{x}(t) + \boldsymbol{b}\Delta u(t), \\ \Delta y(t) &= \boldsymbol{c}^T \Delta\boldsymbol{x}(t) + d\Delta u(t), \end{aligned}\right\} \tag{4.10a}$$

where

$$\left.\begin{aligned} &\Delta\dot{\boldsymbol{x}}(t) = \dot{\boldsymbol{x}}(t), && \Delta\boldsymbol{x}(t) = \boldsymbol{x}(t) - \boldsymbol{x}_0, \\ &\Delta u(t) = u(t) - u_0, && \Delta y(t) = y(t) - y_0, \\ &\boldsymbol{A} = \left.\frac{\partial \boldsymbol{g}}{\partial \boldsymbol{x}}\right|_0, && \boldsymbol{b} = \left.\frac{\partial \boldsymbol{g}}{\partial u}\right|_0, \\ &\boldsymbol{c} = \left.\frac{\partial h}{\partial \boldsymbol{x}}\right|_0, && d = \left.\frac{\partial h}{\partial u}\right|_0. \end{aligned}\right\} \tag{4.10b}$$

In all cases it is assumed that the partial derivatives (4.2), (4.3), (4.9b) and (4.10) exist and are continuous.

The transition from the incremental variables to the absolute variables is given by relations

$$\left.\begin{aligned} \hat{y}(t) &= y_0 + \Delta y(t), \\ u(t) &= u_0 + \Delta u(t). \end{aligned}\right\} \tag{4.11}$$

Throughout the whole text, if not expressed otherwise, all transfer functions are considered at the operating point, i.e. it is worked with incremental variables, although it is not explicitly stated and variables are not referred to as incremental.

Example 4.1

It is necessary to derive a simplified mathematical model of the hydraulic double acting linear motor with the spool control valve (the valve for continuous flow control) and to perform the linearization (Fig. 4.2). It is assumed that the compressibility of the hydraulic fluid is negligible, the pressure loss in the source pipelines and the leakage are negligible as well. The control valve is described by the nonlinear equation of the static characteristic in the form (p_z = const.)

$$q(t) = q[z_1(t), p_z - p(t)]. \tag{4.12}$$

In Fig. 4.2 it means: m – the total mass (piston + piston rod + load) [kg], $z_1(t)$ – the input spool displacement [m], $z_2(t)$ – the output piston displacement [m], $p(t)$ – the pressure in the working space [Pa], p_z – the source pressure [Pa], A – the area of the piston (the same for both sides) [m^2], b – the coefficient of viscous friction [kg s^{-1}], $q(t)$ – the volumetric flow rate [m^3 s^{-1}], $f(t)$ – the external force [N].

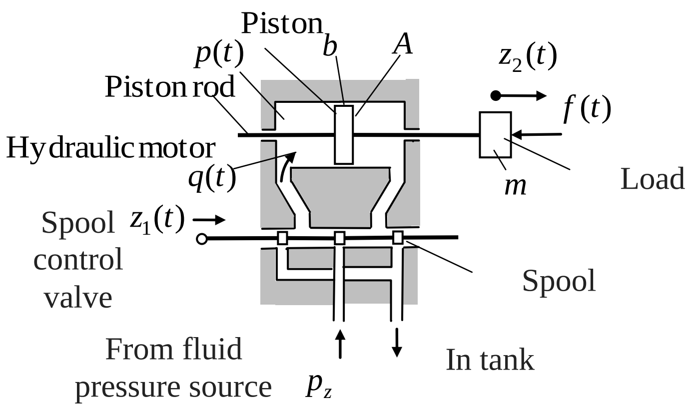

Fig. 4.2 Simplified scheme of hydraulic double acting linear motor with spool control valve – Example 4.1

Solution:

Under the above simplifying assumptions, we can write [3, 16]:

force balance

$$m\frac{\mathrm{d}^2 z_2(t)}{\mathrm{d}t^2}+b\frac{\mathrm{d}z_2(t)}{\mathrm{d}t}=Ap(t)-f(t), \tag{4.13}$$

volumetric flow rate balance

$$A\frac{\mathrm{d}z_2(t)}{\mathrm{d}t}=q(t), \tag{4.14}$$

control valve static characteristic

$$q(t)=q[z_1(t), p_z-p(t)].$$

The position of the piston rod $z_2(t)$ corresponding to the middle position of the piston is the operating point, we mark it as z_{20}.

Because for the increment of the output displacement the equality

$$\Delta z_2(t)=z_2(t)-z_{20}, \tag{4.15}$$

holds, we can write

$$\frac{\mathrm{d}\Delta z_2(t)}{\mathrm{d}t}=\frac{\mathrm{d}z_2(t)}{\mathrm{d}t},\quad \frac{\mathrm{d}^2\Delta z_2(t)}{\mathrm{d}t^2}=\frac{\mathrm{d}^2 z_2(t)}{\mathrm{d}t^2}. \tag{4.16}$$

The linearized equations (4.12) − (4.14) will have the forms

$$m\frac{\mathrm{d}^2\Delta z_2(t)}{\mathrm{d}t^2}+b\frac{\mathrm{d}\Delta z_2(t)}{\mathrm{d}t}=A\Delta p(t)-\Delta f(t), \tag{4.17}$$

$$A\frac{\mathrm{d}z_2(t)}{\mathrm{d}t}=\Delta q(t), \tag{4.18}$$

$$\Delta q(t)=k_{z_1}\Delta z_1(t)-k_p\Delta p(t). \tag{4.19}$$

$$k_{z_1} = \left.\frac{\partial q}{\partial z_1}\right|_0, \; k_p = -\left.\frac{\partial q}{\partial p}\right|_0, \tag{4.20}$$

$$q_0 = q(z_{10}, p_z - p_0), \tag{4.21}$$

$$\left.\begin{aligned} &\Delta z_1(t) = z_1(t) - z_{10}, \;\; \Delta q(t) = q(t) - q_0, \\ &\Delta f(t) = f(t) - f_0, \quad \Delta p(t) = p(t) - p_0, \end{aligned}\right\} \tag{4.22}$$

where the quantity z_{10}, z_{20}, p_0, q_0, f_0 correspond to the operating point or nominal values.

The partial derivative (4.20) must be computed for the operating point.

Assuming zero initial conditions we use the Laplace transform on the equations and after modification we get.

$$\Delta Z_2(s) = \frac{A}{ms^2 + bs}\Delta P(s) - \frac{1}{ms^2 + bs}\Delta F,$$

$$\Delta Q(s) = As\Delta Z_2(s),$$

$$\Delta P(s) = \frac{1}{k_p}[k_{z_1}\Delta Z_1(s) - \Delta Q(s)].$$

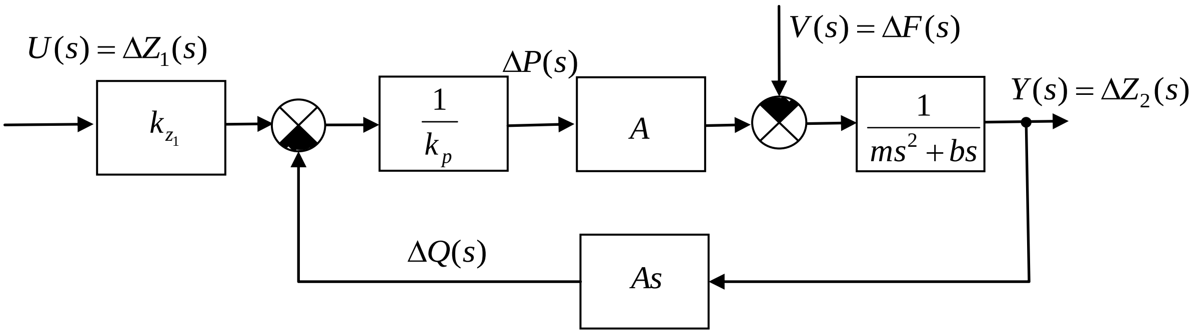

Fig. 4.3 Block diagram of the linearized hydraulic double acting linear motor with spool control valve – Example 4.1

Based on the block diagram, we can easily determine the transfer functions

$$G_{uy}(s) = \frac{Y(s)}{U(s)} = \frac{\Delta Z_2(s)}{\Delta Z_1(s)} = \frac{\dfrac{Ak_{z_1}}{bk_p + A^2}}{s\left(\dfrac{mk_p}{bk_p + A^2}s + 1\right)} = \frac{k_1}{s(T_1 s + 1)}, \tag{4.23}$$

$$G_{vy}(s) = \frac{Y(s)}{V(s)} = \frac{\Delta Z_2(s)}{\Delta F(s)} = -\frac{\dfrac{k_p}{bk_p + A^2}}{s\left(\dfrac{mk_p}{bk_p + A^2}s + 1\right)} = -\frac{k_2}{s(T_1 s + 1)}, \tag{4.24}$$

$$T_1 = \frac{mk_p}{bk_p + A^2}, \ k_1 = \frac{Ak_{z_1}}{bk_p + A^2}, \ k_2 = \frac{k_p}{bk_p + A^2}, \tag{4.25}$$

where T_1 is the time constant [s], k_1 – the gain for the input spool displacement [s^{-1}], k_2 – the external force gain [N^{-1} m s^{-1}].

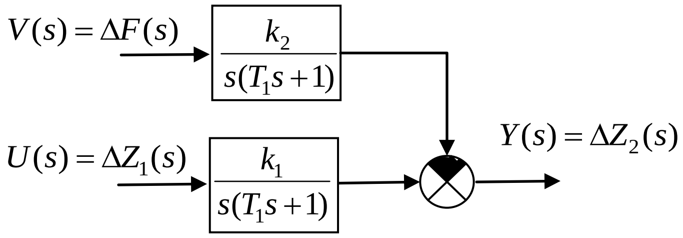

Fig. 4.4 Simplified block diagram of the linearized hydraulic double acting linear motor with spool control valve – Example 4.1

On the basis of the transfer functions (4.23) and (4.24) the linearized hydraulic linear motor with the control valve can be expressed by a very simple block diagram (Fig. 4.4).

If the pressure $p(t)$ is constant, then $k_p = 0$ [see (4.20)] and the substantial simplification of both transfer functions (4.23) and (4.24) takes place

$$G_{uy}(s) = \frac{Y(s)}{U(s)} = \frac{\Delta Z_2(s)}{\Delta Z_1(s)} = \frac{k_{z_1}}{As}, \tag{4.26}$$

$$G_{vy}(s) = \frac{Y(s)}{V(s)} = \frac{\Delta Z_2(s)}{\Delta F(s)} = 0, \tag{4.27}$$

where k_{z1} is the gain [m^3 s].

The transfer function (4.26) is the simplest mathematical model of the hydraulic linear motor with the control valve.

4.2 Plant transfer function modification

Mathematical models obtained in an analytical or experimental way are often too complex. They are mostly mathematical models of controlled systems, i.e. plants or processes. If a plant´s mathematical model has the form of a transfer function, then it is possible to simplify it on the basis of its step response or directly by the simple modification (conversion) of its transfer function.

Plant transfer function modification on the basis of step response

Suppose we can obtain by simulation the plant step response, then it is possible to use one of the following procedures. All of these procedures can be also used for simple experimental identification, assuming that the courses of the step responses are properly made up (by filtering, smoothing, etc.). We work with incremental variables, i.e., all courses begin at the origin of the coordinates. It is assumed that the time constants satisfy the condition

$$T_i \geq T_{i+1}, \quad i = 1,2,\dots, \tag{4.28}$$

i.e. the time constant with lower subscript has greater or equal value than the time constant with the higher subscript.

The modification of the plant transfer function consists in plotting the step response and the subsequent determination of its transfer function in the desired form.

If the plant is nonoscillatory proportional and has the step response $h_P(t)$ similar to Fig. 4.5a, the simplest way to identify its transfer function is to determine the substitute time delay $T_u = T_{d1}$ and the substitute time constant $T_n = T_1$ on the basis of Fig. 4.5a.

$$G_P(s) = \frac{k_1}{T_1 s + 1} \mathrm{e}^{-T_{d1}s}, \tag{4.29}$$

where T_1 is the time constant, T_{d1} – the time delay, k_1 – the plant gain.

This is the transfer function of the FOPTD (**f**irst **o**rder **p**lus **t**ime **d**elay) plant.

In this way the determined transfer function is very rough. It is used for the preliminary controller tuning by the Ziegler – Nichols step response method (see Section 6.2) [2 – 4, 10, 21 – 24, 26, 29, 31].

a) b)

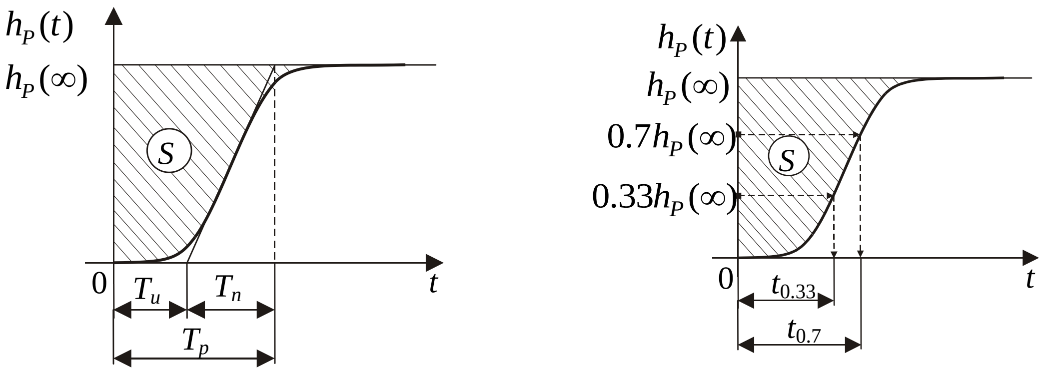

Fig. 4.5 Plant transfer function determination on the basis of: a) substitute time delay $T_u = T_{d1}$ and substitute time constant $T_n = T_1$, b) times $t_{0.33}$ and $t_{0.7}$

Considerably the better way for determination of the transfer function in the form (4.29) is using the times $t_{0.33}$ and $t_{0.7}$ in accordance with Fig. 4.5b and the following formulas [22, 26, 29]

$$\begin{aligned} T_1 &\doteq 1.245(t_{0.7} - t_{0.33}) \approx 1.25(t_{0.7} - t_{0.33}), \\ T_{d1} &\doteq 1.498 t_{0.33} - 0.498 t_{0.7} \approx 1.5 t_{0.33} - 0.5 t_{0.7}. \end{aligned} \tag{4.30}$$

These relations are analytically determined. For the normalized step response it can be written (Fig. 4.6)

$$\frac{h_P(t)}{h_P(\infty)} = (1 - \mathrm{e}^{-(t - T_{d1})/T_1})\eta(t - T_{d1}).$$

The delayed Heaviside step $\eta(t - T_{d1})$ ensures $h_P(t) = 0$ for $t < T_{d1}$.

For values A and B the equations

$$A = 1 - \mathrm{e}^{-(t_A - T_{d1})/T_1},$$

$$B = 1 - \mathrm{e}^{-(t_B - T_{d1})/T_1}$$

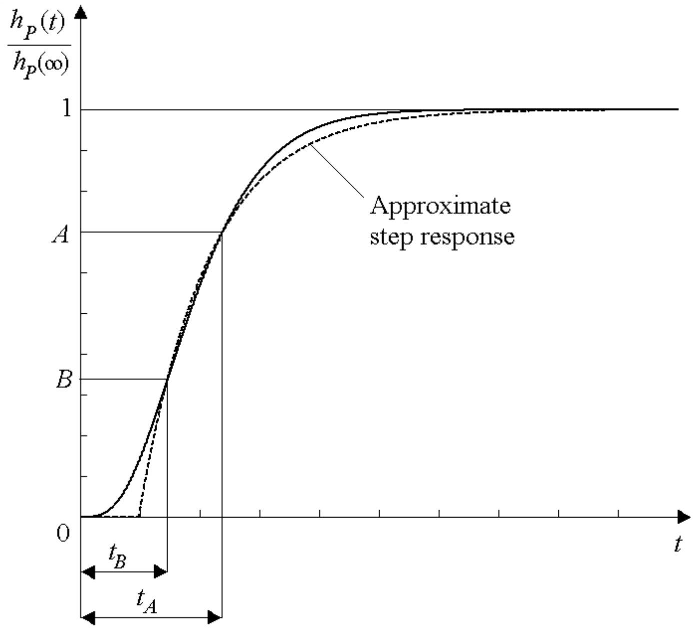

Fig. 4.6 Plant transfer function determination on the basis of times t_A and t_B

hold, from which the desired formulas are obtained

$$T_1 = \frac{1}{\ln(1-A) - \ln(1-B)}(t_B - t_A),$$

$$T_{d1} = \frac{1}{\ln(1-A) - \ln(1-B)}[t_B \ln(1-A) - t_A \ln(1-B)].$$

It is obvious that the values A and B of the normalized step response should be chosen so they are approximately equal to 1/3 and 2/3, and so that the numerical coefficients in resultant formulas are easy to remember.

For instance for A = 0.33 and B = 0.7 there is obtained (4.30).

Similarly for A = 0.28 and B = 0.63 there is obtained

$$\begin{aligned} T_1 &\doteq 1.502(t_{0.63} - t_{0.28}) \approx 1.5(t_{0.63} - t_{0.28}), \\ T_{d1} &\doteq 1.493 t_{0.28} - 0.493 t_{0.63} \approx 1.5 t_{0.28} - 0.5 t_{0.63}. \end{aligned} \tag{4.31}$$

On the basis of the times $t_{0.33}$ and $t_{0.7}$ it is possible to obtain the transfer function of the nonoscillatory SOPTD (**s**econd **o**rder system **p**lus **t**ime **d**elay) plant [22, 26, 29]:

$$G_P(s) = \frac{k_1}{(T_2 s + 1)^2} \mathrm{e}^{-T_{d2} s}, \tag{4.32}$$

where

$$\begin{aligned} T_2 &\doteq 0.794(t_{0.7} - t_{0.33}), \\ T_{d2} &\doteq 1.937 t_{0.33} - 0.937 t_{0.7}. \end{aligned} \tag{4.33}$$

The complementary area S over the step response can be used for approximate verification (Fig. 4.5)

$$T_1 + T_{d1} \approx \frac{S}{h_P(\infty)}, \qquad 2T_2 + T_{d2} \approx \frac{S}{h_P(\infty)}. \tag{4.34}$$

The formulas (4.33) were obtained numerically from the correspondences of the original step response and the approximate step response in the values $h_P(0) = 0$, $h_P(t_{0.33}) = 0.33h_P(\infty)$, $h_P(t_{0.7}) = 0.7h_P(\infty)$ and $h_P(\infty)$ [22, 26, 29].

Very good approximation of the step response course of the nonoscillatory SOPTD plant can be obtained for the transfer function with two different time constants

$$G_P(s) = \frac{k_1}{(T_1 s + 1)(T_2 s + 1)} \mathrm{e}^{-T_{d2}s} , \tag{4.35}$$

where

$$\begin{aligned} &T_1 = \frac{1}{2}\left(D_2 + \sqrt{D_2^2 - 4D_1^2}\right), \qquad T_2 = \frac{1}{2}\left(D_2 - \sqrt{D_2^2 - 4D_1^2}\right), \\ &T_{d2} = 1.937t_{0.33} - 0.937t_{0.7}, \\ &D_1 = 0.794(t_{0.7} - t_{0.33}),\ D_2 = \frac{S}{h_P(\infty)} - T_{d2}. \end{aligned} \tag{4.36}$$

The inequality $D_2 > 2D_1$ must hold, otherwise the transfer function (4.32) must be used.

For fast mutual conversion of the plant transfer functions Tab. 4.1 and the diagram (4.37) can be used [22, 26, 29].

$$\begin{array}{ccc} & \dfrac{1}{(T_i s + 1)^i}\mathrm{e}^{-T_{di}s} & \\ \swarrow & & \searrow \\ \dfrac{1}{T_1 s + 1}\mathrm{e}^{-T_{d1}s} & \longleftrightarrow & \dfrac{1}{(T_2 s + 1)^2}\mathrm{e}^{-T_{d2}s} \end{array} \tag{4.37}$$

Tab. 4.1 Table for fast transfer function conversion in accordance with the diagram (4.37)

$\dfrac{1}{(T_i s+1)^i}\mathrm{e}^{-T_{di}s}$	i	1	2	3	4	5	6
$\dfrac{1}{T_1 s+1}\mathrm{e}^{-T_{d1}s}$	$\dfrac{T_1}{T_i}$	1	1.568	1.980	2.320	2.615	2.881
	$\dfrac{T_{d1}-T_{di}}{T_i}$	0	0.552	1.232	1.969	2.741	3.537
$\dfrac{1}{(T_2 s+1)^2}\mathrm{e}^{-T_{d2}s}$	$\dfrac{T_2}{T_i}$	0.638	1	1.263	1.480	1.668	1.838
	$\dfrac{T_{d2}-T_{di}}{T_i}$	* –0.352	0	0.535	1.153	1.821	2.523

* Applicable for $T_{d1} > 0.352T_1$.

Tab. 4.1 was obtained numerically on condition that the values $h_P(0)$, $h_P(t_{0.33})$, $h_P(t_{0.7})$ and $h_P(\infty)$ of the original and the conversed step responses are the same.

For approximate identification of the IFOPD (**i**ntegral plus **f**irst **o**rder **p**lus time **d**elay) plant with the transfer function

$$G_P(s) = \frac{k_1}{s(T_1 s + 1)} \mathrm{e}^{-T_{d1} s} \tag{4.38}$$

it is possible to use its step response (Fig. 4.7), where the time delay is approximately estimated. If the input step is not a unit, i.e. $\Delta u(t) \neq \eta(t)$, but $\Delta u(t) = \Delta u \eta(t)$, then it is necessary to consider the value in brackets.

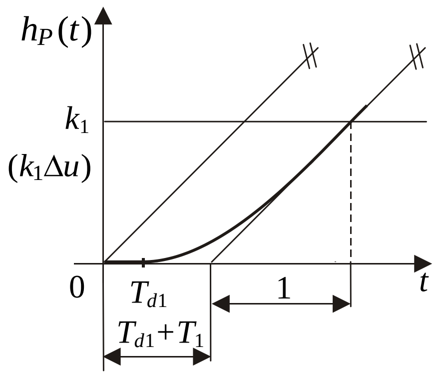

Fig. 4.7 Integrating plant transfer function determination

Direct transfer function modification

The simplest direct transfer function modification (conversion) is based on the equality of complementary areas over original and conversed plant step responses.

Nonoscillatory proportional plants

a)

$$\begin{gathered} \frac{k_1}{(T_1 s + 1)\prod_{i=2}^{n}(T_i s + 1)} \approx \frac{k_1}{(T_1 s + 1)(T_\Sigma s + 1)}, \\ T_\Sigma = \sum_{i=2}^{n} T_i,\ T_1 >> T_i,\ i = 2, 3, \ldots, n. \end{gathered} \tag{4.39}$$

b)

$$\begin{gathered} \frac{k_1}{(T_1 s + 1)\prod_{i=2}^{n}(T_i s + 1)} \approx \frac{k_1}{(T_1 s + 1)} \mathrm{e}^{-T_d s}, \\ T_d = \sum_{i=2}^{n} T_i,\ T_1 >> T_i,\ i = 2, 3, \ldots, n. \end{gathered} \tag{4.40}$$

c)

$$\frac{k_1}{(T_1s+1)(T_2s+1)\prod_{i=3}^{n}(T_is+1)} \approx \frac{k_1}{(T_1s+1)(T_2s+1)}\mathrm{e}^{-T_ds},$$
$$T_d = \sum_{i=3}^{n} T_i,\ \ T_1 \ge T_2 >> T_i,\ \ i = 3,4,\ldots,n. \tag{4.41}$$

d)

$$\frac{k_1}{(T_0^2s^2+2\xi_0T_0s+1)\prod_{i=1}^{n}(T_is+1)} \approx \frac{k_1}{T_0^2s^2+2\xi_0T_0s+1}\mathrm{e}^{-T_ds},$$
$$T_d = \sum_{i=1}^{n} T_i,\ \ T_0 >> T_i,\ \ i = 1,2,\ldots,n. \tag{4.42}$$

Nonoscillatory integrating plants

a) $$\frac{k_1}{s\prod_{i=1}^{n}(T_is+1)} \approx \frac{k_1}{s(T_\Sigma s+1)},\qquad T_\Sigma = \sum_{i=1}^{n} T_i\ , \tag{4.43}$$

b) $$\frac{k_1}{s\prod_{i=1}^{n}(T_is+1)} \approx \frac{k_1}{s}\mathrm{e}^{-T_ds},\qquad T_d = \sum_{i=1}^{n} T_i\ , \tag{4.44}$$

c)

$$\frac{k_1}{s(T_1s+1)\prod_{i=2}^{n}(T_is+1)} \approx \frac{k_1}{s(T_1s+1)}\mathrm{e}^{-T_ds},$$
$$T_d = \sum_{i=2}^{n} T_i,\ \ T_1 >> T_i,\ \ i = 2,3,\ldots,n. \tag{4.45}$$

It is advantageous to use a combination of the substitute summary time constant T_Σ and the substitute time delay T_d, see the "half rule" below.

If in the numerator of the plant transfer function the binomials

$$1 \pm \tau_i s\ , \tag{4.46}$$

stand up, then each binomial can be substituted by the term

$$\mathrm{e}^{\pm\tau_i s} \tag{4.47}$$

on the assumption that the resulting time delay will be positive.

The fact that in the above simple modifications the equality of the complementary areas over the origin and the modified plant step responses hold can be easily shown. They are considered the plant transfer functions

$$G_P(s) = \frac{1}{\prod_{i=1}^{n}(T_is+1)} \approx \frac{1}{T_\Sigma s+1} = G_1(s)\ , \tag{4.48}$$

$$G_P(s) = \frac{1}{\prod_{i=1}^{n}(T_i s + 1)} \approx \mathrm{e}^{-T_d s} = G_2(s)\,, \tag{4.49}$$

$$T_\Sigma = T_d = \sum_{i=1}^{n} T_i\,. \tag{4.50}$$

It is obvious that it holds (see Appendix A)

$$\int_0^\infty x(t)\,\mathrm{d}t = \lim_{s\to 0} X(s)\,, \tag{4.51}$$

where $X(s)$ is the Laplace transform of the time function $x(t)$

$$X(s) = \int_0^\infty x(t)\,\mathrm{e}^{-st}\,\mathrm{d}t\,.$$

Therefore, for the complementary area over the step response $h_p\,(t)$ it can be written

$$\int_0^\infty [1 - h_P(t)]\,\mathrm{d}t = \lim_{s\to 0}\left[\frac{1}{s} - \frac{1}{s\prod_{i=1}^{n}(T_i s + 1)}\right] = \lim_{s\to 0}\frac{\prod_{i=1}^{n}(T_i s + 1) - 1}{s\prod_{i=1}^{n}(T_i s + 1)} =$$

$$= \lim_{s\to 0}\frac{\left(\prod_{i=1}^{n} T_i\right)s^{n-1} + \ldots + \sum_{i=1}^{n} T_i}{\prod_{i=1}^{n}(T_i s + 1)} = \sum_{i=1}^{n} T_i\,. \tag{4.52}$$

For the transfer function $G_1(s)$ the complementary area over the step response $h_1(t)$ can be obtained on the basis of the last relation

$$\int_0^\infty [1 - h_1(t)]\,\mathrm{d}t = T_\Sigma\,.$$

For the transfer function $G_2(s)$ the complementary area over the step response $h_2(t)$ can be obtained on the basis of the relation

$$\int_0^\infty [1 - h_2(t)]\,\mathrm{d}t = \int_0^\infty [1 - \eta(t - T_d)]\,\mathrm{d}t = T_d\,.$$

Geometric interpretation of the substitute summary time constant T_Σ and the substitute time delay T_d is shown in Fig. 4.8.

The substitute step responses $h_1(t)$ and $h_2(t)$ crosses the original step response $h_P(t)$ at such a point, so that areas S_1 and S_2 above and below the corresponding substitute step response are the same.

The empirical method using the "**half rule**" is very simple and effective at the same time [20].

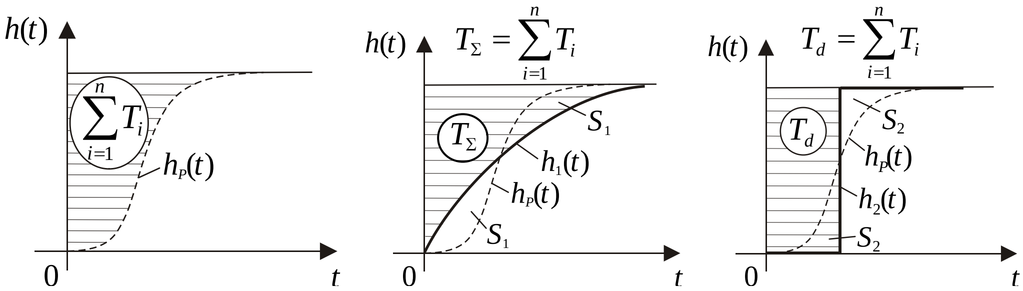

Fig. 4.8 Geometric interpretation of substitute summary time constant $T_\sum$ and substitute time delay T_d

Assuming that the plant transfer function has the form with unstable zeros

$$G_P(s) = \frac{\prod_j (1-\tau_{j0}s)}{\prod_i (T_{i0}s+1)} \mathrm{e}^{-T_{d0}s}, \tag{4.53}$$

$$T_{i0} \geq T_{i+1,0}, \; \tau_{j0} \geq 0, \; T_{d0} \geq 0,$$

then on the basis of the " half rule" for the substitute plant transfer function (4.29) we get

$$T_1 = T_{10} + \frac{T_{20}}{2}, \qquad T_{d1} = T_{d0} + \frac{T_{20}}{2} + \sum_{i \geq 3} T_{i0} + \sum_j \tau_{j0}, \tag{4.54}$$

or for the substitute plant transfer function (4.35)

$$T_1 = T_{10}, \quad T_2 = T_{20} + \frac{T_{30}}{2}, \qquad T_{d2} = T_{d0} + \frac{T_{30}}{2} + \sum_{i \geq 4} T_{i0} + \sum_j \tau_{j0}. \tag{4.55}$$

It is obvious, that the equalities

$$\sum_i T_{i0} + \sum_j \tau_{j0} + T_{d0} = T_1 + T_{d1} = T_1 + T_2 + T_{d2}, \tag{4.56}$$

hold, i.e. the "half rule" conserves the equality of the complementary areas over the substitute plant step responses and the original plant step response. In these areas it suitably divides between a time constant and a time delay or among two time constants and a time delay.

In the case when plant transfer functions have stable zeros the use of the procedure based on times $t_{0.33}$ and $t_{0.7}$ is preferable and at the same time it is more accurate.

Example 4.2

The plant transfer function is

$$G_P(s) = \frac{2}{(6s+1)^4}. \tag{4.57}$$

It is necessary to modify it in the forms (4.29) and (4.32) on the basis of the diagram (4.37) and Tab. 4.1 as well as the “half rule” (the time constant is in min).

Solution:

In accordance with scheme (4.37) and Tab. 4.1 we can write: $k_1 = 2$, $T_4 = 6$, $T_{d4} = 0$.

a) The transfer function (4.29)

$$\frac{T_1}{T_4} = 2.320 \Rightarrow T_1 = 2.32T_4 = 13.92 \doteq 13.9 \text{ min},$$

$$\frac{T_{d1} - T_{d4}}{T_4} = 1.969 \Rightarrow T_{d1} = 1.969T_4 = 11.814 \doteq 11.8 \text{ min}$$

$$G_P(s) = \frac{2}{(6s+1)^4} \approx \frac{2}{13.9s+1} e^{-11.8s}. \tag{4.58}$$

b) The transfer function (4.32)

$$\frac{T_2}{T_4} = 1.480 \Rightarrow T_2 = 1.48T_4 = 8.88 \doteq 8.9 \text{ min},$$

$$\frac{T_{d2} - T_{d4}}{T_4} = 1.153 \Rightarrow T_{d2} = 1.153T_4 = 6.918 \doteq 6.9 \text{ min}$$

$$G_P(s) = \frac{2}{(6s+1)^4} \approx \frac{2}{(8.9s+1)^2} e^{-6.9s}. \tag{4.59}$$

A comparison of the step response obtained from the transfer function (4.57) with the step responses obtained on the basis of the modified transfer functions (4.58) and (4.59) is shown in Fig. 4.9.

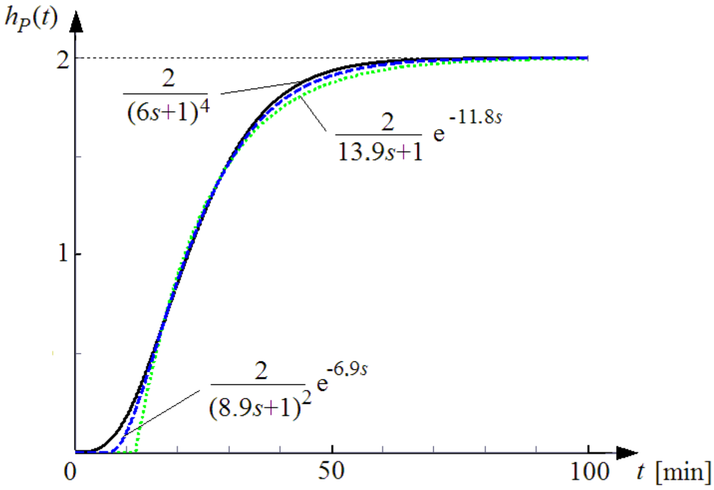

Fig. 4.9 Comparison of step responses (Tab. 4.1) – Example 4.2

Now for comparison we simplify the transfer function (4.57) using the "half rule".

For the "half rule" we can write: $T_{10} = T_{20} = T_{30} = T_{40} = 6$, $T_{d0} = 0$.

a) The transfer function (4.29)

In accordance with the relation (4.54) we get

$$T_1 = T_{10} + \frac{T_{20}}{2} = 9 \text{ min}, \; T_{d1} = T_{d0} + \frac{T_{20}}{2} + T_{30} + T_{40} = 15 \text{ min},$$

$$G_P(s) = \frac{2}{(6s+1)^4} \approx \frac{2}{9s+1} e^{-15s}. \qquad (4.60)$$

b) The transfer function (4.35)

In accordance with the relation (4.55) we get

$$T_1 = T_{10} = 6 \text{ min}, \; T_2 = T_{20} + \frac{T_{30}}{2} = 9 \text{ min}, \; T_{d2} = T_{d0} + \frac{T_{30}}{2} + T_{40} = 9 \text{ min},$$

$$G_P(s) = \frac{2}{(6s+1)^4} \approx \frac{2}{(9s+1)(6s+1)} e^{-9s}. \qquad (4.61)$$

A comparison of the step responses is shown in Figure 4.10.

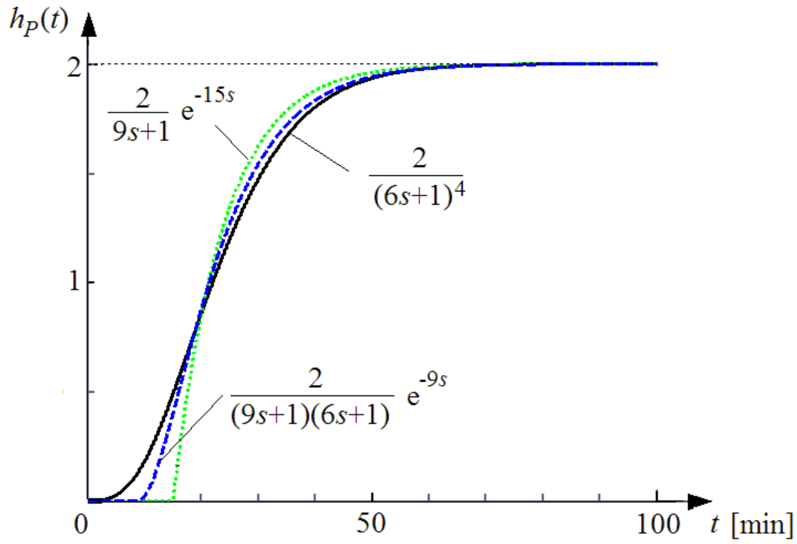

Fig. 4.10 Comparison of step responses ("half rule") – Example 4.2

Example 4.3

On the basis of the "half rule" the transfer function with the unstable zero

$$G_P(s) = \frac{1-s}{(5s+1)(2s+1)^2} e^{-3s} \qquad (4.62)$$

must be modified in the forms (4.29) and (4.35). The time constants and the time delay are in seconds.

Solution:

For the transfer function (4.62) we can write: $T_{10} = 5$, $T_{20} = T_{30} = 2$, $\tau_{10} = 1$, $T_{d0} = 3$.

a) The transfer function (4.29)

In accordance with the relation (4.54) we can directly write

$$T_1 = T_{10} + \frac{T_{20}}{2} = 6\ \text{s},\ T_{d1} = T_{d0} + \frac{T_{20}}{2} + T_{30} + \tau_{10} = 7\ \text{s},$$

$$G_P(s) = \frac{1-s}{(5s+1)(2s+1)^2}\text{e}^{-3s} \approx \frac{1}{6s+1}\text{e}^{-7s}. \tag{4.63}$$

b) The transfer function (4.35)

Similarly as in the previous case, in accordance with (4.55) we can write

$$T_1 = T_{10} = 5\ \text{s},\ T_2 = T_{20} + \frac{T_{30}}{2} = 3\ \text{s},\ T_{d_2} = T_{d0} + \frac{T_{30}}{2} + \tau_{10} = 5\ \text{s},$$

$$G_P(s) = \frac{1-s}{(5s+1)(2s+1)^2}\text{e}^{-3s} \approx \frac{1}{(5s+1)(3s+1)}\text{e}^{-5s}. \tag{4.64}$$

A comparison of the step responses is shown in Fig. 4.11.

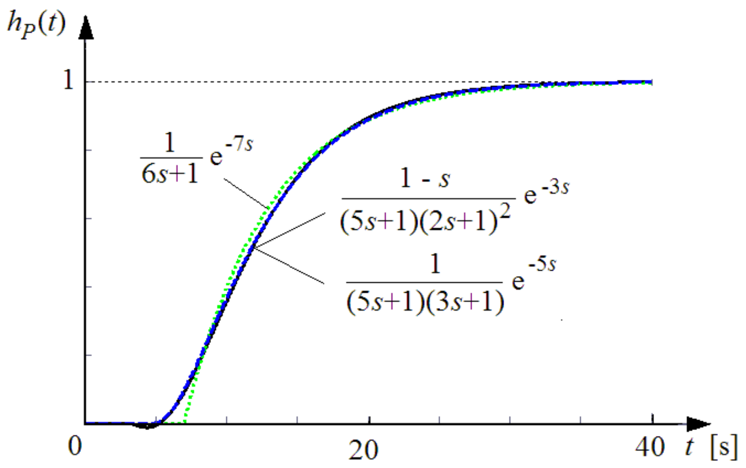

Fig. 4.11 Comparison of step responses – Example 4.3

5 CLOSED-LOOP CONTROL SYSTEMS

5.1 Controllers

We will mostly deal with the closed-loop control system (further we will use mostly the control system) in Fig. 5.1 (see also Fig. 1.3), where the $G_C(s)$ is the controller transfer function, $G_P(s)$ – the plant (process) transfer function, $W(s)$ – the transform of the desired variable $w(t)$, $E(s)$ – the transform of the control error $e(t)$, $U(s)$ – the transform of the manipulated variable $u(t)$, $Y(s)$ – the transform of the controlled (process) variable $y(t)$, $V(s)$ and $V_1(s)$ – the transforms of the disturbance variables $v(t)$ and $v_1(t)$.

For reasons of simplicity we will very often omit the word "transform", because it will be clear from the text whether the transform or the original of the corresponding variable is concerned.

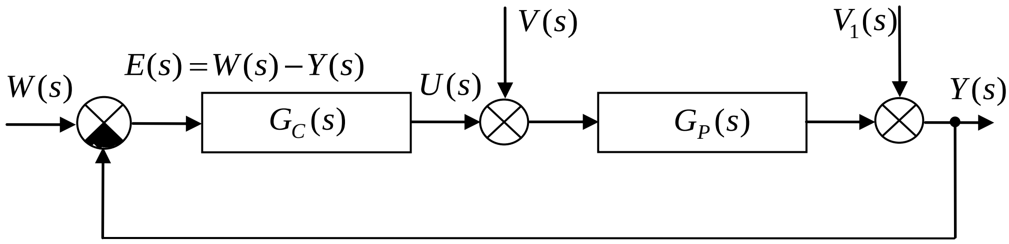

Fig. 5.1 Block diagram of the control system

If the disturbance variables cannot be measured or otherwise specified more precisely, it is appropriate to aggregate them into a single disturbance variable and place it in the least favourable position in the control system. In the case of the integrating plant it is its input and, if the plant is proportional it is its output.

As it was already mentioned in Chapter 1 the control objective can be expressed in two equivalent forms, see the relations (1.4). For the control system in Fig. 5.1 we can write:

a) The control objective in the form

$$y(t) \to w(t) \;\hat{=}\; Y(s) \to W(s). \qquad (5.1)$$

According to Fig. 5.1 and the linearity principle we can write

$$Y(s) = G_{wy}(s)W(s) + G_{vy}(s)V(s) + G_{v_1y}(s)V_1(s), \qquad (5.2)$$

where

$$G_{wy}(s) = \frac{G_C(s)G_P(s)}{1 + G_C(s)G_P(s)} \qquad (5.3)$$

is the **(closed-loop) control system transfer function**,

$$G_{vy}(s) = \frac{G_P(s)}{1 + G_C(s)G_P(s)} = [1 - G_{wy}(s)]G_P(s) \qquad (5.4)$$

and

$$G_{v_1y}(s) = \frac{1}{1 + G_C(s)G_P(s)} = 1 - G_{wy}(s) \tag{5.5}$$

are the **disturbance transfer functions** for the disturbance variables $V(s)$ and $V_1(s)$.

For fulfilling the control objective (5.1) for any desired variable $W(s)$ and any disturbance variables $V(s)$ and $V_1(s)$ these conditions must hold

$$G_{wy}(s) \to 1, \tag{5.6}$$

$$G_{vy}(s) \to 0, \tag{5.7}$$

$$G_{v_1y}(s) \to 0. \tag{5.8}$$

The first condition for the control system transfer function (5.6) expresses the controller function consisting in the tracking of the desired variable $W(s)$ by the controlled variable $Y(s)$, it is the servo problem. The other two conditions (5.7) and (5.8) represent the controller function consisting in rejecting disturbance variables $V(s)$ and $V_1(s)$, it is a regulatory problem [this applies in particular to disturbances $V(s)$].

From (5.4) and (5.5) it follows, when the condition (5.6) for the control system transfer function will hold, then at the same time the conditions (5.7) and (5.8) for disturbance transfer functions will hold.

b) The control objective in the form

$$e(t) \to 0 \ \hat{=}\ E(s) \to 0. \tag{5.9}$$

According to Fig. 5.1 and the linearity principle we can write

$$E(s) = G_{we}(s)W(s) + G_{ve}(s)V(s) + G_{v_1e}(s)V_1(s), \tag{5.10}$$

where

$$G_{we}(s) = \frac{1}{1 + G_C(s)G_P(s)} = 1 - G_{wy}(s) \tag{5.11}$$

is the desired variable-to-the control error transfer function or the error control system transfer function,

$$G_{ve}(s) = -\frac{G_P(s)}{1 + G_C(s)G_P(s)} = -[1 - G_{wy}(s)]G_P(s) \tag{5.12}$$

and

$$G_{v_1e}(s) = -\frac{1}{1 + G_C(s)G_P(s)} = -[1 - G_{wy}(s)] \tag{5.13}$$

are the disturbance variable-to-the control error transfer functions for the disturbance variables $V(s)$ and $V_1(s)$.

The transfer functions (5.3) – (5.5) and (5.11) – (5.13) are the **basic transfer functions** of the given control system. ***The first or the second triad of the transfer functions describes the control system uniquely***.

For fulfilling the control objective (5.9) for any desired variable $W(s)$ and any disturbance variables $V(s)$ and $V_1(s)$ these conditions must hold

$$G_{we}(s) \to 0, \tag{5.14}$$

$$G_{ve}(s) \to 0, \tag{5.15}$$

$$G_{v_1 e}(s) \to 0. \tag{5.16}$$

Similarly as in the previous case the first condition for the desired variable-to-the control error transfer function (5.14) expresses the controller function consisting in the tracking of the desired variable $W(s)$ by the controlled variable $Y(s)$ (the servo problem). The other two conditions (5.15) and (5.16) represent the controller function consisting in rejecting the disturbance variables $V(s)$ and $V_1(s)$ (the regulatory problem).

From (5.11) – (5.13) it also follows, when the condition (5.6) for the control system transfer function will hold, then at the same time the conditions (5.14) – (5.16) will hold.

We see that both control objective formulations (5.1) and (5.9) are equivalent to each other and it is obvious that if the condition (5.6) for the control system transfer function will hold, all conditions, i.e. (5.7), (5.8) and (5.14) – (5.16) will hold too.

Therefore, we will further deal mainly with the control objective (5.1) and main attention will be paid to the control system transfer function (5.3).

The control system frequency transfer function has the form

$$G_{wy}(\mathrm{j}\omega) = G_{wy}(s)\big|_{s=\mathrm{j}\omega} = \frac{G_C(\mathrm{j}\omega)G_P(\mathrm{j}\omega)}{1+G_C(\mathrm{j}\omega)G_P(\mathrm{j}\omega)} = \frac{1}{\dfrac{1}{G_C(\mathrm{j}\omega)G_P(\mathrm{j}\omega)}+1} \tag{5.17}$$

and it is obvious that the relations hold

$$\left.\begin{matrix} |G_C(\mathrm{j}\omega)| \to \infty \\ G_P(\mathrm{j}\omega) \neq 0 \end{matrix}\right\} \Rightarrow G_{wy}(\mathrm{j}\omega) \to 1 \Rightarrow G_{wy}(s) \to 1, \tag{5.18}$$

or

$$|G_C(\mathrm{j}\omega)G_P(\mathrm{j}\omega)| \to \infty \Rightarrow G_{wy}(\mathrm{j}\omega) \to 1 \Rightarrow G_{wy}(s) \to 1. \tag{5.19}$$

From relation (5.18) it follows that if a sufficiently high value of the modulus of the frequency controller transfer function will be ensured

$$A_C(\omega) = \operatorname{mod} G_C(\mathrm{j}\omega) = |G_C(\mathrm{j}\omega)|, \tag{5.20}$$

then conditions (5.6) and (5.8) will be held with sufficient accuracy and for the nonsingular $G_P(s)$ the condition (5.7) will be held as well.

If the plant properties given by the plant transfer function $G_P(s)$ will be known, then it is easier to ensure a sufficiently high value of the modulus of the frequency open-loop control system transfer function

$$A_o(\omega) = \operatorname{mod} G_o(\mathrm{j}\omega) = |G_o(\mathrm{j}\omega)| = |G_C(\mathrm{j}\omega)G_P(\mathrm{j}\omega)|, \tag{5.21}$$

see relations (5.19).

High values of the modules $A_C(\omega)$ or $A_o(\omega)$ must be ensured in the operating range of angular frequencies while ensuring stability and the required control process performance. This can be achieved by an appropriately selected controller and its subsequent proper tuning.

Industrial controllers are available in different versions and modifications, and therefore the basic structures and modifications of the commonly used conventional controllers will be presented [2 – 6, 9 – 11, 13 – 17, 19 – 31].

Analog (continuous) conventional controllers are implemented as a combination of three basic components (terms): **proportional** – **P**, **integral** – **I** and **derivative** – **D**. The controller which consists of all three components is called the **proportional plus integral plus derivative controller** or for short the **PID controller** and its properties in the time domain can be described by the relation

$$\begin{aligned} u(t) &= \underbrace{K_P e(t)}_{P} + \underbrace{K_I \int_0^t e(\tau)\,\mathrm{d}\tau}_{I} + \underbrace{K_D \frac{\mathrm{d}e(t)}{\mathrm{d}t}}_{D} = \\ &= K_P\left[e(t) + \frac{1}{T_I}\int_0^t e(\tau)\,\mathrm{d}\tau + T_D\frac{\mathrm{d}e(t)}{\mathrm{d}t}\right], \end{aligned} \tag{5.22}$$

where K_P, K_I and K_D are the **proportional**, **integral** and **derivative component weights**, K_P – the **controller gain** (the proportional component weight), T_I and T_D – the **integral** and **derivative time constants**.

Some industrial controllers instead of the gain K_P use the inverse value

$$pp = \frac{100}{k_P}\,[\%] \tag{5.23}$$

called the **proportional band**.

The parameters K_P, K_I and K_D, or K_P, T_I and T_D are the **controller adjustable parameters**. The task of controller tuning is to ensure the required control performance process by selecting the appropriate values of the controller adjustable parameters for the given plant.

Among the controller adjustable parameters the conversion relations hold

$$K_I = \frac{K_P}{T_I}, \qquad K_D = K_P T_D, \tag{5.24}$$

or

$$T_I = \frac{K_P}{K_I}, \qquad T_D = \frac{K_D}{K_P}. \tag{5.25}$$

Since the proportional component weight K_P is identical to controller gain K_P, and also in its name, the controller gain is often used.

Using the Laplace transform and assuming zero initial conditions from relation (5.22) the PID controller transfer function is obtained

$$G_C(s) = \frac{U(s)}{E(s)} = K_P + \frac{K_I}{s} + K_D s = K_P\left(1 + \frac{1}{T_I s} + T_D s\right). \tag{5.26}$$

Fig. 5.2 shows the modules of the components P, I and D of the PID controller. From Fig. 5.2 it follows that the integral component (I) provides a high modulus of the frequency PID controller transfer function at low angular frequencies and especially at steady state (ω = 0), the derivative component (D) at high angular frequencies and the proportional component (P) over the entire operating range of angular frequencies, but especially for middle angular frequencies. Just by using the appropriate choice of components P, I and D, i.e., by the appropriate choice of values of controller adjustable parameters K_P, K_I and K_D, or K_P, T_I and T_D there can be achieved a high modulus of the frequency controller transfer function (5.20) or the modulus of the frequency open-loop control system transfer function (5.21), and thus fulfilment of the conditions (5.18) or (5.19).

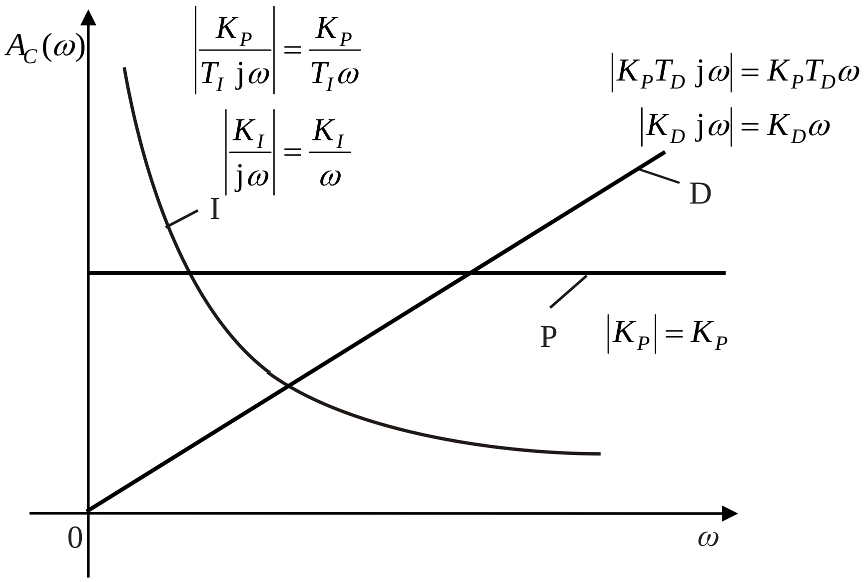

Fig. 5.2 Courses of component modules of PID controller

Tab. 5.1 Transfer functions of conventional controllers

	Type	**Transfer function** $G_C(s)$
1	P	K_P
2	I	$\frac{1}{T_I s}$
3	PI	$K_P\left(1+\frac{1}{T_I s}\right)$
4	PD	$K_P(1+T_D s)$
5	PID	$K_P\left(1+\frac{1}{T_I s}+T_D s\right)$
6	PID_i	$K_P'\left(1+\frac{1}{T_I' s}\right)(1+T_D' s)$

In practice, simpler controllers are used (relations with time constants are considered only): the P (proportional) controller, the I (integral) controller, the PI (proportional plus integral) controller and the PD (proportional plus derivative) controller. The transfer functions of conventional controllers are transparently brought out in Tab. 5.1 (the rows 1 – 5). A controller with just a derivative component cannot be used because it reacts only at the time change of $e(t)$, i.e. $\dot{e}(t)$, therefore it causes disconnection of the control loop in the steady state.

A block diagram of the PID controllers with the transfer function (5.26) is shown in Fig. 5.3a, which shows that it has a parallel structure. For such type of PID controller all the adjustable parameters can be set independently, and therefore controllers with a parallel structure are also called PID controllers **without interaction** (non-interacting).

a)

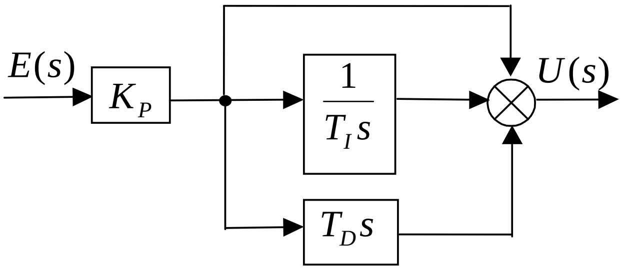

b)

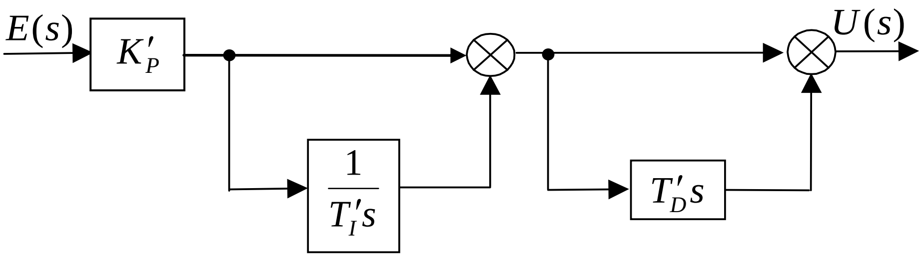

Fig. 5.3 Block diagram of PID controller with structure: a) parallel (without interaction), b) serial (with interaction)

Sometimes the form (5.26) with weights is only considered as a **parallel form** of the PID controller and the form with time constants (Fig. 5.3a) is often called the **standard form** according to ISA (The **I**nternational **S**ociety of **A**utomation, formerly the **I**nstrument **S**ociety of **A**merica).

A PID controller can be also realized on the basis of the **serial** (cascade) structure (see Fig. 5.3b). Its transfer function has the form

$$G_C(s) = \underbrace{K'_P\left(1+\frac{1}{T'_I s}\right)}_{\text{PI}}\underbrace{(1+T'_D s)}_{\text{PD}} = K'_P\,\frac{(T'_I s+1)(T'_D s+1)}{T'_I s}, \tag{5.27}$$

which can be rewritten on the parallel structure (5.26)

$$G_C(s) = \underbrace{K'_P \frac{T'_I + T'_D}{T'_I}}_{K_P}(1 + \underbrace{\frac{1}{T'_I + T'_D}}_{\frac{1}{T_I}} \frac{1}{s} + \underbrace{\frac{T'_I T'_D}{T'_I + T'_D}}_{T_D} s) . \tag{5.28}$$

From equation (5.28) it is obvious that when the values of the integral time T'_I or derivative time T'_D are changed then all adjustable parameters K_P T_I and T_D corresponding to the parallel (standard) structure change their values, i.e. there is an interaction between the adjustable parameters. Therefore the PID controller with a serial structure is also called the PID controller **with interaction** (interacting) and is referred to as the $\mathrm{PID_i}$ controller (see Tab. 5.1, row 6).

Among the adjustable parameters of the parallel and the serial structure the simple conversion relations hold [2, 26, 29]:

$$K_P = K'_P i, \qquad T_I = T'_I i, \qquad T_D = \frac{T'_D}{i}, \qquad i = 1 + \frac{T'_D}{T'_I}, \tag{5.29}$$

$$K'_P = K_P \beta, \qquad T'_I = T_I \beta, \qquad T'_D = \frac{T_D}{\beta}, \qquad \beta = \frac{1}{2} + \sqrt{\frac{1}{4} - \frac{T_D}{T_I}} . \tag{5.30}$$

The coefficient i is also called the **interaction factor**. The values of the adjustable parameters K_P, T_I and T_D of the PID controller (without interaction) are the effective values, since most controller tuning methods assume the standard parallel structure of the PID controller (Fig. 5.3a), and therefore the values of the adjustable parameters K'_P, T'_I and T'_D of the $\mathrm{PID_i}$ controller (with interaction) should be converted into the effective values on the basis of the relations (5.29), i.e. on the K_P, T_I and T_D.

For the PID controller with a serial structure, i.e. for the $\mathrm{PID_i}$ controller the restriction

$$\frac{T_D}{T_I} \le \frac{1}{4}, \tag{5.31}$$

exists which is not however essential [see formula for β (5.30)].

The serial structure of the $\mathrm{PID_i}$ controller has its advantages. It simply can be realized, e.g. as a serial interconnection of the PI and the PD controllers, see Fig. 5.3b and relation (5.27). Its production is also cheaper. Realization of the $\mathrm{PID_i}$ controller on the basis of the operational amplifier is shown in Example 3.5. For $T'_D = T_D = 0$ parallel and serial structures are equivalent to the PI controller.

From a theoretical point of view the derivative component has a positive stabilizing effect on the control process. From a practical point of view, however the derivative component has a very unpleasant property, which consists of amplifying a high frequency noise (see Fig. 5.2), and quick changes. For instance if the derivative component of the PD or PID controllers

$$K_D \frac{\mathrm{d}e(t)}{\mathrm{d}t} = K_P T_D \frac{\mathrm{d}e(t)}{\mathrm{d}t} \tag{5.32}$$

processes the control error $e(t)$, which contains harmonic noise with the amplitude a_S and the angular frequency ω_S, i.e. [2]

$$e(t) + a_S \sin \omega_S t\,,$$

then the derivative component (5.32) output is

$$K_P T_D [\frac{\mathrm{d}e(t)}{\mathrm{d}t} + a_S \omega_S \cos \omega_S t]\,, \qquad (5.33)$$

where $\frac{\mathrm{d}e(t)}{\mathrm{d}t}$ is the useful part of the derivative component and $a_S \omega_S \cos \omega_S t$ is the parasite part of the derivative component.

From the relation (5.33) it follows that for higher angular frequencies ω_S the parasite part will dominate over the useful part and the derivative component output can cause an incorrect controller function and even in the whole control system. This is why the ideal derivative operation is practically unusable. An **internal filter** of the derivative component with the transfer function

$$\frac{1}{\frac{T_D}{N}s+1} = \frac{1}{\alpha T_D s + 1}, \qquad \alpha = \frac{1}{N}\,, \qquad (5.34)$$

is used, where $N = 5 \div 20$ or $\alpha = 0.05 \div 0.2$ [2, 17, 22, 24 – 26, 29].

The task of the internal filter is to attenuate the parasite noise, which the controlled variable $y(t)$ mainly contains. When the values of $\alpha \le 0.1$, then the internal filter does not fundamentally affect the final properties of a controller, and it is not therefore usually considered during controller tuning. In industrial controllers the internal filter (5.34) is usually preset to $\alpha = 0.1$ ($N = 10$) [2, 4, 22, 29].

The transfer function of the PID controller with the internal filter has the form

$$G_C(s) = K_P \left(1 + \frac{1}{T_I s} + \frac{T_D s}{\alpha T_D s + 1} \right). \qquad (5.35)$$

Conventional controllers given in Tab. 5.1, even with internal filter (5.35), allow such tuning which ensures the desired control process performance only from the point of view of the desired variable $w(t)$ and the disturbance variable $v_1(t)$ acting on the plant output.

If disturbance variable $v(t)$ is acting on the plant input, a compromise tuning is usually used. Problems arise when the plant has an integral character, then a compromise tuning is not possible [22, 25, 29, 30]. In this case, it is appropriate to use the controller with two degrees of freedom (2DOF controllers).

For instance properties of the ideal 2DOF PID controller are described in what is called the ISA form (Fig. 5.4) [2, 22, 29]

$$U(s) = K_P \left\{ bW(s) - Y(s) + \frac{1}{T_I s}[W(s) - Y(s)] + T_D s[cW(s) - Y(s)] \right\}, \qquad (5.36)$$

where b is the set-point weight for proportional component, c – the set-point weight for derivative component.

Both weights can change in the range from 0 to 1. For $b = c = 1$ the relation (5.36) expresses the equation of the conventional PID controller (the 1DOF PID controller), see the relation (5.26).

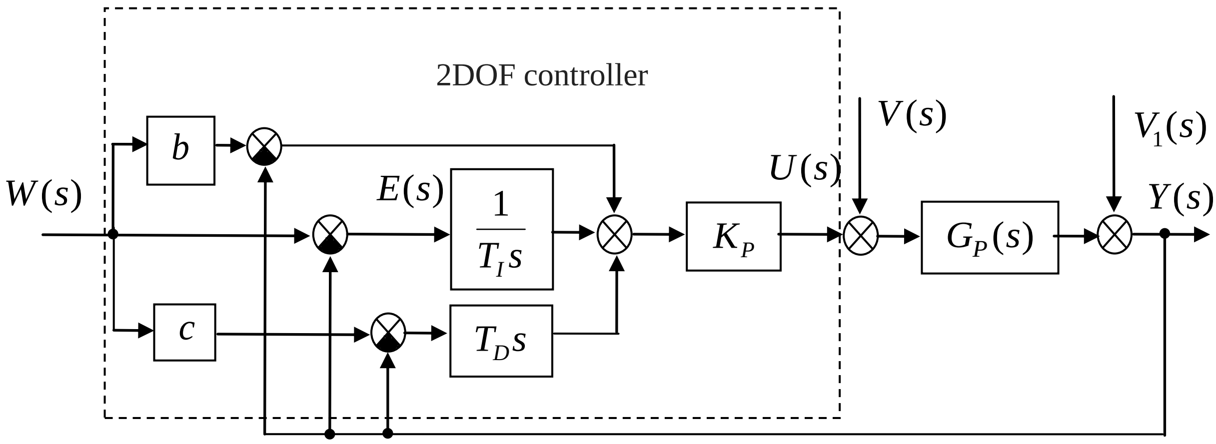

Fig. 5.4 Block diagram of the 2DOF PID controller corresponding to relation (5.36)

The relation (5.36) can be rewritten in the form

$$U(s) = G_F(s)G_C(s)W(s) - G_C(s)Y(s), \tag{5.37}$$

$$G_F(s) = \frac{cT_I T_D s^2 + bT_I s + 1}{T_I T_D s^2 + T_I s + 1}, \tag{5.38}$$

$$G_C(s) = K_P \frac{T_I T_D s^2 + T_I s + 1}{T_I s} = K_P \left(1 + \frac{1}{T_I s} + T_D s\right), \tag{5.39}$$

where $G_F(s)$ is the input filter transfer function, $G_C(s)$ – the conventional (1DOF) PID controller transfer function.

The block diagram in Fig. 5.5 corresponds to the relation (5.37).

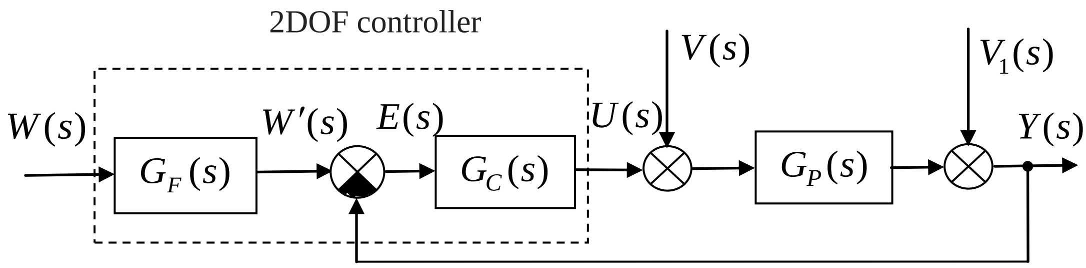

Fig. 5.5 Block diagram of 2DOF PID controller corresponding to relation (5.37)

From Fig. 5.5 it is clear, that the PID controller with the transfer function $G_C(s)$ [(5.39)] is tuned with regard to quickly attenuate the negative influence of the disturbance variable $v(t)$ (the regulatory problem) and by the appropriate choice of weights b and c the input filter with the transfer function $G_F(s)$ is tuned [(5.38)] from the point of view of the changes of the desired variable $w(t)$ (the servo problem). For $b = c = 1 \Rightarrow G_F(s) = 1$ and the control system in Fig. 5.5 there are the properties of a control system with a conventional PID controller, i.e. with a controller with one degree of freedom (1DOF).

When using a controller with an integral component and with the **manipulated variable limiting** (i.e. in the presence of **saturation**), a very unpleasant phenomenon appears – the so-called **windup (**the ongoing integration). Fig. 5.6 explains it.

Since the transforms of variables and the originals of variables stand out at the same time in Fig. 5.6, all variables are thereby represented by small letters without specifying independent variables.

Precaution against the windup is called **antiwindup** and it can be realized as shown in Fig. 5.6a. Fig. 5.6b shows that when $u_1(t)$ exceeds the value of $u(t) = u_m$, a negative feedback takes effect (Fig. 5.6a) and the input of the integrator is reduced with the value $a[u_1(t) - u(t)]$ and it causes a drop in the growth of the output value of the integrator $u_1(t)$. The courses $u_1(t)$ and $u(t)$ in Fig. 5.6b show that the implementation of the antiwindup caused the significant reduction windup delay T_d^w. The windup delay T_d^w is the main reason of a prolonged overshoot in the control system, and thereby a deterioration of control process performance. The value of a (Fig. 5.6a) must be sufficiently large, as is apparent from Fig. 5.6b.

a)

b)

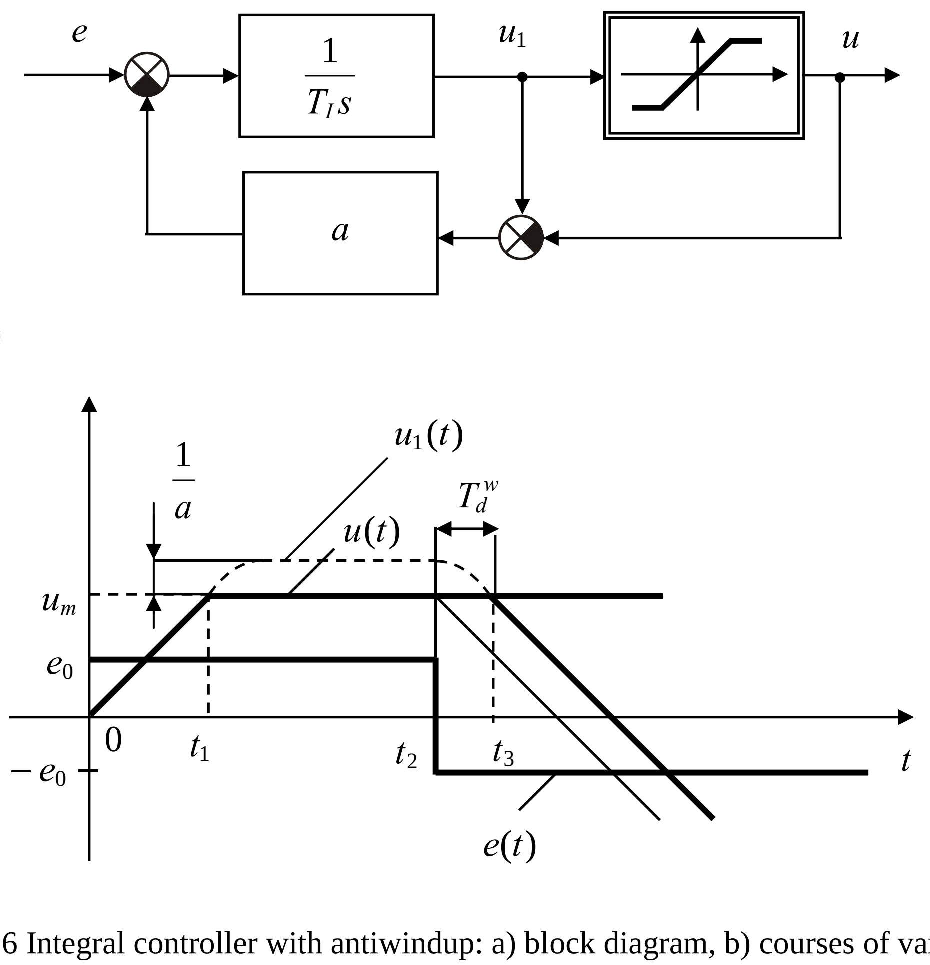

Fig. 5.6 Integral controller with antiwindup: a) block diagram, b) courses of variables

The realization of the PI controller with the antiwindup is shown in Fig. 5.7.

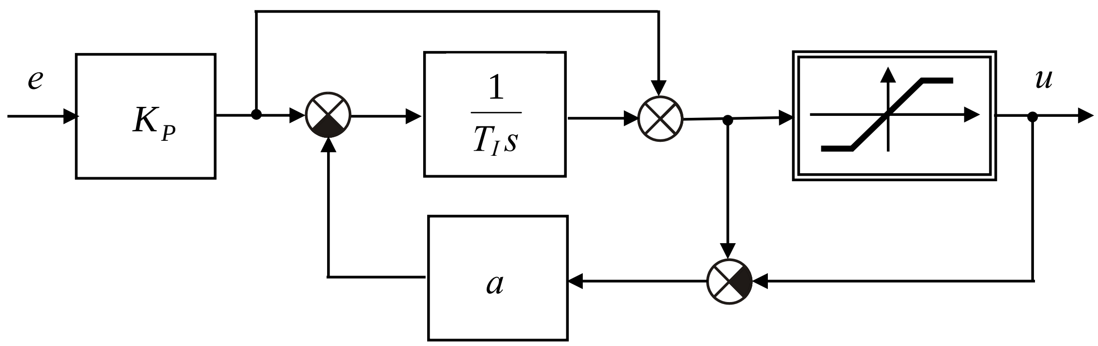

Fig. 5.7 Realization of the PI controller with antiwindup

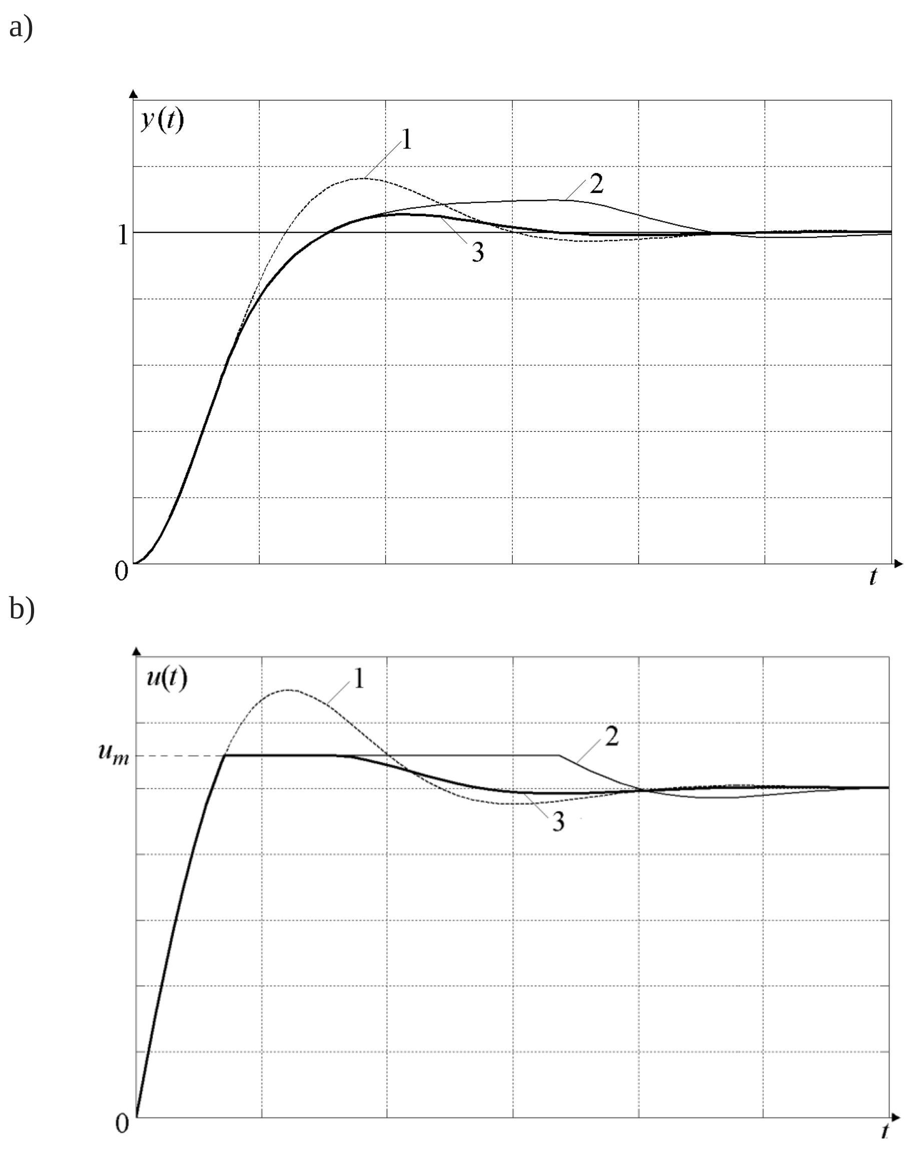

Fig. 5.8 Courses of controlled variable a) and manipulated variable b) in a control system with I controller: 1 – linear, 2 – with saturation and without antiwindup, 3 – with saturation and with antiwindup

The courses of controlled variable and manipulated variable in the control system with the I controller are shown in Fig. 5.8 for three cases. The first case – without the saturation (the linear control system) – course 1, the second case – with the saturation and without the antiwindup (the nonlinear control system) – course 2, the third case – with the saturation and with the antiwindup (the nonlinear control system) – course 3. From Fig. 5.8 it is clear that manipulated variable limiting causes a slow response. Manipulated variable limiting usually has a stabilizing effect, but if an antiwindup is not used, the control process performance is significantly reduced.

The ongoing integration – the windup acts primarily in analog controllers. In digital controllers the antiwindup is simply dealt with by stopping the integration (summation) at saturation.

5.2 Stability

The stability of the linear control system is its ability to stabilize all variables at finite values if the input values are fix ed at finite values. The input variables in the control system are the desired variable $w(t)$, and any disturbance variable, often aggregated into a single disturbance variable $v(t)$ or $v_1(t)$.

It is obvious that the following stability definition is equivalent. ***The linear control system is stable if the output is always bounded for any bounded input***. It is called BIBO stability (**b**ounded-**i**nput **b**ounded-**o**utput).

From both stability definitions it follows that stability is a characteristic property of the control system, which does not depend on inputs or outputs (it does not hold for nonlinear control systems).

Since the control system (Fig. 5.1) is fully described by the equation

$$Y(s) = G_{wy}(s)W(s) + G_{vy}(s)V(s) + G_{v_1y}(s)V_1(s) \tag{5.40a}$$

or

$$E(s) = G_{we}(s)W(s) + G_{ve}(s)V(s) + G_{v_1e}(s)V_1(s), \tag{5.40b}$$

it is clear that the stability must be given by a term which figures in all basic control system transfer functions $G_{wy}(s)$, $G_{vy}(s)$ and $G_{v1y}(s)$ or $G_{we}(s)$, $G_{ve}(s)$ and $G_{v1e}(s)$. From the basic control system transfer functions (5.3) – (5.5) and (5.11) – (5.13) it follows that this term is their denominator

$$1 + G_C(s)G_P(s) = 1 + G_o(s) = 1 + \frac{M_o(s)}{N_o(s)} = \frac{N_o(s) + M_o(s)}{N_o(s)} = \frac{N(s)}{N_o(s)}, \tag{5.41}$$

where $G_o(s)$ is the open-loop control system transfer function (it is generally given by the product of all transfer functions in the loop), $N_o(s)$ – the characteristic polynomial of the open-loop control system (the denominator of the open-loop control system transfer function), $M_o(s)$ – the polynomial in the nominator of the open-loop control system transfer function.

The polynomial

$$N(s) = N_o(s) + M_o(s) \tag{5.42}$$

is called the **characteristic polynomial** of the control system and after its equating to zero the **characteristic equation** of the control system

$$N(s) = 0 \tag{5.43}$$

is obtained.

The characteristic polynomial (5.42) figures in the denominator of each basic control system transfer function after its arrangement, and therefore it is at the same time the characteristic polynomial of the differential equation describing the control system.

We show that a necessary and sufficient condition for the stability of the linear control system is that the roots s_1, s_2, ..., s_n of its characteristic polynomial (or its characteristic equation)

$$N(s) = a_n s^n + \ldots + a_1 s + a_0 = a_n (s - s_1)(s - s_2)\ldots(s - s_n) \tag{5.44}$$

have negative real parts, i.e. (see Fig. 5.9)

$$\operatorname{Re} s_i < 0, \qquad \text{for} \qquad i = 1, 2, \ldots, n. \tag{5.45}$$

The negativity condition (5.45) ***for the real parts of the roots of the characteristic polynomial of the control system*** (5.42) ***or, equivalently, for the real parts of the roots of the characteristic equation of the control system*** (5.43) ***is a necessary and sufficient condition for the*** (***asymptotic***) ***stability of the control system***.

Since the concept of stability of the nonlinear control system has a somewhat different meaning, it is necessary, if there could be a misunderstanding, when the necessary and sufficient conditions for stability of the linear control systems hold to use a more precise concept of "asymptotic" stability.

It should be noted that complex roots (poles) always come in complex conjugate pairs (i.e. in the symmetry in the real axis in the complex plane s).

It should also be noted that the roots s_1, s_2, ..., s_n are at the same time the poles of the basic control system transfer functions (i.e. the poles of the control system). This does not apply to the zeros of the basic control system transfer functions. The poles of the control system are determined for their dynamic properties.

Now we will show how the necessary and sufficient condition for stability of the control system (5.45) can be obtained.

Consider any basic control system transfer function, e.g. the control system transfer function

$$G_{wy}(s) = \frac{M(s)}{N(s)} \tag{5.46}$$

and the desired variable transform

$$W(s) = \frac{M_w(s)}{N_w(s)}, \tag{5.47}$$

where $M(s)$, $M_w(s)$ and $N_w(s)$ are the polynomials and $N(s)$ is the characteristic polynomial of the control system.

Assuming that the characteristic polynomial of the control system $N(s)$ has the simple roots s_1, s_2, ..., s_n and the polynomial $N_w(s)$ has the simple roots $s_1^w, s_2^w, \ldots, s_p^w$

[p is the degree of the polynomial $N_w(s)$], the controlled variable transform – the response transform

$$Y(s) = G_{wy}(s)W(s) = \frac{M(s)}{N(s)}\frac{M_w(s)}{N_w(s)} \tag{5.48}$$

can be written as the sum of partial fractions (see Appendix A)

$$Y(s) = \underbrace{\sum_{i=1}^{n}\frac{A_i}{s-s_i}}_{Y_T(s)} + \underbrace{\sum_{j=1}^{p}\frac{B_j}{s-s_j^w}}_{Y_S(s)} = Y_T(s) + Y_S(s)\,, \tag{5.49}$$

where $Y_T(s)$ is the transform of the transient response part, $Y_S(s)$ the transform of the steady response part.

The original of the controlled variable $y(t)$ can be obtained from (5.49) on the basis of the Laplace transform

$$y(t) = y_T(t) + y_S(t) = \sum_{i=1}^{n} A_i\,\mathrm{e}^{s_i t} + \sum_{j=1}^{p} B_j\,\mathrm{e}^{s_j^w t}\,. \tag{5.50}$$

The constants A_i and B_j in the relations (5.49) and (5.50) generally depend on the form of the control system transfer function $G_{wy}(s)$ and the desired variable $W(s)$, see (5.46) and (5.47).

The course of the transient response part of the controlled variable $y_T(t)$ depends on the roots of the characteristic polynomial of the control system, i.e. of its poles and it is given by relation

$$y_T(t) = \sum_{i=1}^{n} A_i\,\mathrm{e}^{s_i t}\,. \tag{5.51}$$

The course of the steady response part of the controlled variable

$$y_S(t) = \sum_{j=1}^{p} B_j\,\mathrm{e}^{s_j^w t} \tag{5.52}$$

is given by the course of the desired variable $w(t)$.

Here, the steady course means the given general time function, e.g. $y_S(t) = Bt$, $y_S(t) = B\sin\omega t$, etc. contrary to the steady (idle) state, e.g. $y_S(t) = y_S = \text{const.}$

From relation (5.50) it follows that for the bounded input variable – the desired variable $w(t)$ ($\operatorname{Re} s_j^w < 0$ for $j = 1, 2,..., p$) the output variable – the controlled variable $y(t)$ will be bounded if and only if its transient response part $y_T(t)$ will be bounded, i.e. if the condition (5.45) will hold. Therefore for a stable control system the transient response part must vanish for an increasing time t, i.e.

$$\lim_{t\to\infty} y_T(t) = 0\,, \tag{5.53}$$

hence for $t \to \infty$ it holds

$$y(t) \to y_S(t)\,. \tag{5.54}$$

The last relation shows that the control system stability is its ability to stabilize the output – the controlled variable $y(t) \to y_S(t)$ at the steady-state input – the desired variable $w(t) \to w_S(t)$.

For the control system from the control objective $y(t) \to w(t)$ the obvious requirement follows $y_S(t) \to w_S(t)$.

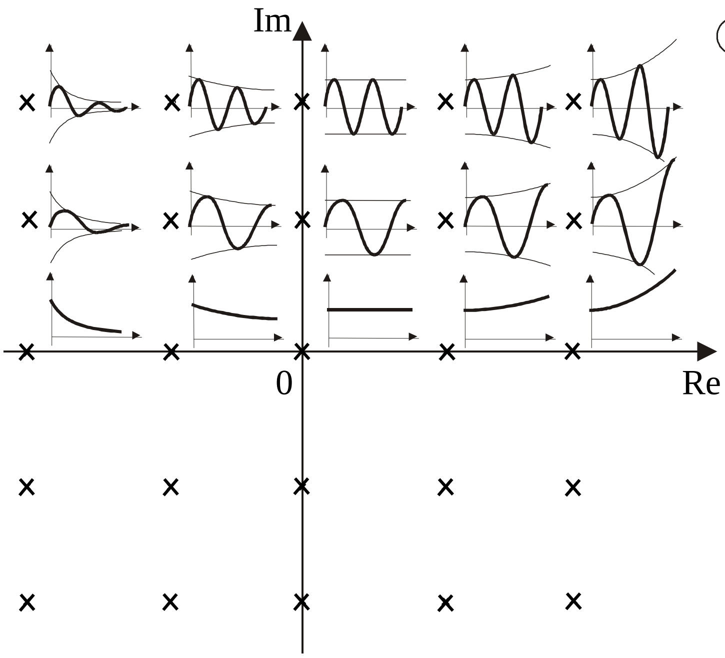

Fig. 5.9 Influence of control system pole placement on the course of transient response

It is obvious that all conclusions will also apply for the multiple roots of the polynomials $N(s)$ and $N_w(s)$ in equation (5.48), because adding negligibly small numbers to multiple roots changes them at simple roots and the small change cannot significantly affect the properties of the control system.

The influence of control system pole placement on courses of transient responses is shown in Fig. 5.9. It should be noted that the oscillatory response is caused by the complex conjugate pair of poles.

For a control system with a time delay the open-loop transfer function has the form [compare with (5.41)]

$$G_o(s) = \frac{M_o(s)}{N_o(s)} \mathrm{e}^{-T_d s}, \tag{5.55}$$

from which the **characteristic quasipolynomial** of the control system can be obtained [compare with (5.42)]

$$N(s) = N_o(s) + M_o(s)\mathrm{e}^{-T_d s}. \tag{5.56}$$

The characteristic quasipolynomial (5.56) has an infinite number of roots, i.e. the control system with a time delay has an infinite number of poles. Therefore verifying the fulfilment of the necessary and sufficient condition for stability (5.45) by direct calculation is unrealistic.

The stability of the control system is a necessary condition for its proper operation. For stability verification a wide variety of criteria is used, which allow to check the fulfilment of inequality (5.45) without the labourously calculating the roots of the characteristic polynomial or quasipolynomial of the control system $N(s)$.

Three stability criteria will be introduced without derivation: Hurwitz, Mikhailov and Nyquist.

Hurwitz stability criterion

The Hurwitz stability criterion is an algebraic criterion, and therefore it is not suitable for control systems with a time delay (the exponential function is not an algebraic function). However, it can be used for approximately verifying stability when the time delay is represented by an approximation in the form of a rational function, e.g. (3.54) or (3.55).

The Hurwitz stability criterion can be formulated in the form:

„The linear control system with the characteristic polynomial

$$N(s) = a_n s^n + \ldots + a_1 s + a_0$$

is (asymptotically) stable [i.e. the inequalities (5.45) hold] if and only if, when:

a) all coefficients a_0, a_1,..., a_n exist and are positive (it is the **Stodola necessary stability condition**, it was formulated by a Slovak technician A. Stodola)

b) the main corner minors (subdeterminants) of the Hurwitz matrix

$$\boldsymbol{H} = \begin{bmatrix} a_{n-1} & a_{n-3} & a_{n-5} & \ldots & 0 \\ a_n & a_{n-2} & a_{n-4} & \ldots & 0 \\ 0 & a_{n-1} & a_{n-3} & \ldots & 0 \\ \ldots & \ldots & \ldots & \ldots & \ldots \\ 0 & 0 & 0 & \ldots & a_0 \end{bmatrix}, \tag{5.57}$$

$$H_1 = a_{n-1}, \; H_2 = \begin{vmatrix} a_{n-1} & a_{n-3} \\ a_n & a_{n-2} \end{vmatrix}, \; \ldots, \; H_n = |\boldsymbol{H}|$$

are positive.“

Since the equalities $H_1 = a_{n-1}$, $H_n = a_0 H_{n-1}$ hold, it is enough to check only the positiveness of H_2, H_3, ..., H_{n-1}. The zero value of one of Hurwitz minors indicates the stability boundary. For instance, if $a_0 = 0$, then one pole is zero (it is the origin of the coordinates in the complex plane s). This case characterizes the **nonoscillating stability boundary**. If $H_{n-1} = 0$, then the two poles are imaginary (the poles are on an imaginary axis in symmetry by the origin in complex plane s). This case characterizes the **oscillating stability boundary**, see Fig. 5.9

If the Stodola necessary stability condition holds, then the simplified **Lineard-Chipart stability criterion** can be used, which consists only in checking the positiveness of all odd or all even Hurwitz minors.

The disadvantage of the Hurwitz stability criterion is its computational complexity for $n \geq 5$.

Mikhailov stability criterion

The Mikhailov criterion is a frequency stability criterion with a very wide field of use. Here it will be shown as a simple formulation suitable for control systems without a time delay.

The Mikhailov stability criterion is based on the characteristic polynomial of the control system $N(s)$ from which after substituting $s = \mathrm{j}\omega$ the **Mikhailov function** is obtained

$$N(\mathrm{j}\omega) = N(s)\big|_{s=\mathrm{j}\omega} = N_P(\omega) + \mathrm{j}N_Q(\omega)\,, \tag{5.58}$$

where

$$N_P(\omega) = \mathrm{Re}\,N(\mathrm{j}\omega) = a_0 - a_2\omega^2 + a_4\omega^4 - \ldots \tag{5.59a}$$

is the real part and

$$N_Q(\omega) = \mathrm{Im}\,N(\mathrm{j}\omega) = a_1\omega - a_3\omega^3 + a_5\omega^5 - \ldots \tag{5.59b}$$

is the imaginary part of the Mikhailov function.

Its plot is called the **Mikhailov hodograph** (curve, characteristic).

Now the Mikhailov stability criterion can be formulated in the form:

"The linear control system is (asymptotically) stable if and only if its Michailov hodograph $N(\mathrm{j}\omega)$ for $0 \le \omega \le \infty$ begins on the positive real axis and successively passes through n quadrants in a positive direction (counter-clockwise)."

This formulation can be written for a change of the Mikhailov function argument

$$\Delta \underset{0\le\omega\le\infty}{\arg} N(\mathrm{j}\omega) = n\frac{\pi}{2}\,, \tag{5.60}$$

where n is the control system characteristic polynomial $N(s)$ degree.

The courses of the Mikhailov hodographs for stable control systems are shown in Fig 5.10a and for unstable control systems in Fig. 5.10b.

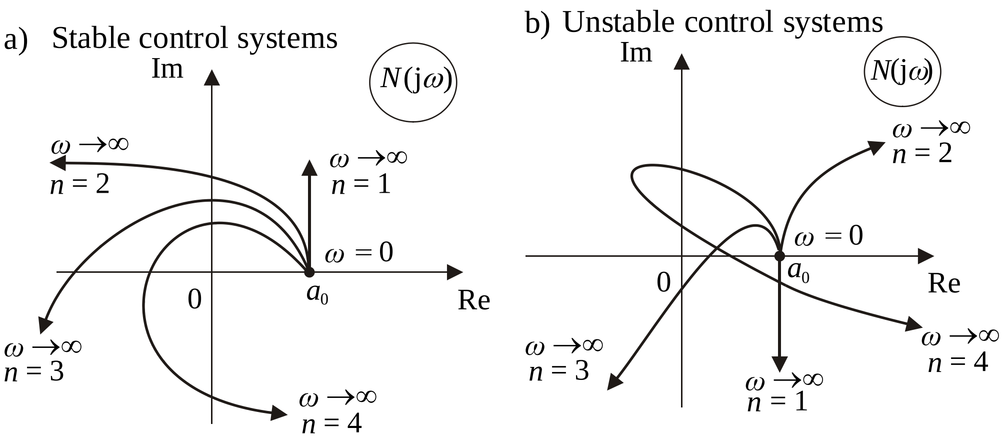

Fig. 5.10 Courses of Mikhailov hodographs for control systems:
a) stable, b) unstable

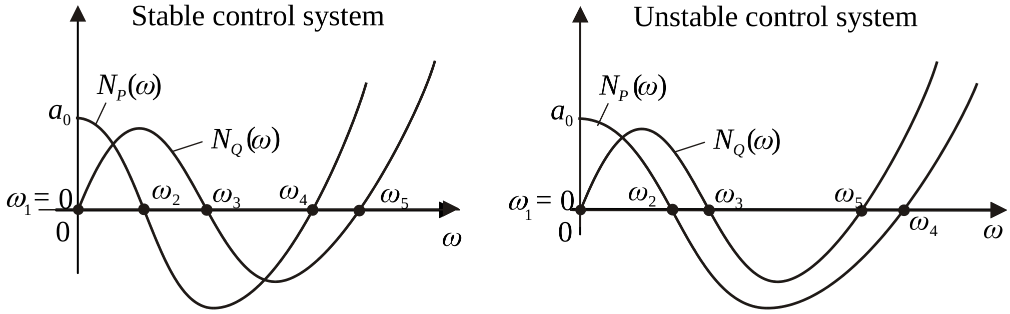

Fig. 5.11 Courses of real part $N_P(\omega)$ and imaginary part $N_Q(\omega)$ of the Mikhailov hodograph for n = 5 for control system: a) stable, b) unstable

From the courses of the Mikhailov hodographs for stable control systems in Fig. 5.10a it follows that for $0 \le \omega \le \infty$ the imaginary part $N_Q(\omega)$ and the real part $N_P(\omega)$ of the Mikhailov hodograph are successively equal to zero [the imaginary part $N_Q(\omega)$ when passing through the real axis and the real part $N_P(\omega)$ when passing through the imaginary axis], hence the Mikhailov stability criterion can be formulated in an equivalent form (Fig. 5.11):

"The linear control system is (asymptotically) stable if and only if $N_P(0) = a_0 > 0$ and if for $0 \le \omega \le \infty$ roots of $N_Q(\omega)$ and $N_P(\omega)$ alternate with each other."

The advantage of this formulation is that it can be written analytically:

$$\left.\begin{aligned} N_P(\omega)\big|_{\omega=0} &= N_P(0) > 0, \quad \left.\frac{\mathrm{d}N_P(\omega)}{\mathrm{d}\omega}\right|_{\omega=0} = \frac{\mathrm{d}N_P(0)}{\mathrm{d}\omega} \le 0, \\ N_Q(\omega)\big|_{\omega=0} &= N_Q(0) = 0, \quad \left.\frac{\mathrm{d}N_Q(\omega)}{\mathrm{d}\omega}\right|_{\omega=0} = \frac{\mathrm{d}N_Q(0)}{\mathrm{d}\omega} > 0 \end{aligned}\right\} \tag{5.61}$$

$$\left.\begin{aligned} &N_Q(\omega) = 0 \;\Rightarrow\; \omega_1 = 0 < \omega_3 < \omega_5 < \ldots \\ &N_P(0) = a_0 > 0,\; N_P(\omega) = 0 \;\Rightarrow\; \omega_2 < \omega_4 < \ldots \end{aligned}\right\} \Rightarrow \omega_1 = 0 < \omega_2 < \omega_3 < \omega_4 < \ldots \tag{5.62}$$

It is clear that the number of roots ω_i is equal to the control system characteristic polynomial $N(s)$ degree n.

If the control system is on the nonoscillating stability boundary than $N_P(0) = a_0 = 0$ and the Mikhailov hodograph begins from the origin of coordinates. On the other hand, if $N_P(0) = a_0 > 0$ and the Mikhailov hodograph passes through the origin of coordinates, then it is on the oscillating stability boundary, see Fig. 5.12. In this case, the real part $N_P(\omega)$ and the imaginary part $N_Q(\omega)$ are zero at the same time. This property of the Mikhailov hodograph (function) can be advantageously used for the analytical determination of the **ultimate** (critical) **angular frequency** ω_c and other ultimate parameters, which most frequently is the **ultimate controller gain** K_{Pc} or the **ultimate integral time** T_{Ic}.

These ultimate parameters cause the control system to be on the stability boundary, i.e. in the critical state between stability and instability. In this case, just a slight change of these parameters causes that the control system will be stable or unstable. For this reason, when verifying control system stability on the basis of various approximations the results must be always accepted very carefully.

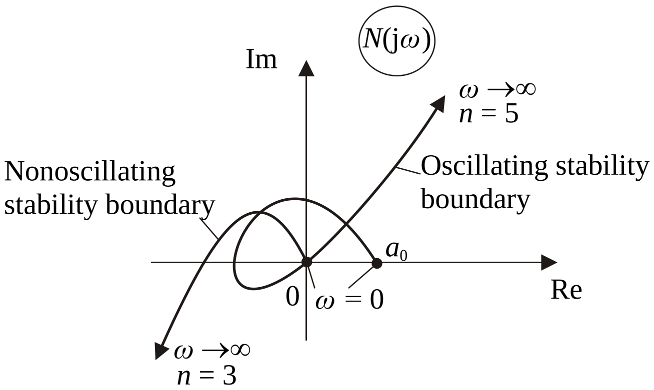

Fig. 5.12 Courses of Mikhailov hodographs for the control system on the stability boundary

The geometric formulation of the Mikhailov stability criterion is appropriate in this case, when the characteristic polynomial coefficients are specified numerically, otherwise it is always preferable to have an analytical formulation.

The Mikhailov stability criterion in the above two formulations may also be used for the approximate stability verification of control systems with a time delay, assuming that the time delay is approximated by a rational function, e.g. (3.54) or (3.55).

Nyquist stability criterion

The Nyquist stability criterion is the frequency criterion, and unlike the Hurwitz and Mikhailov criteria it is based on the properties of the open-loop of the control system and it is suitable for control systems with a time delay. It may even be extended to some nonlinear control systems.

The control system in Fig. 5.13 is considered. It is clear that when oscillation arises with a constant amplitude and a constant angular frequency on the stability boundary [$W(s) = V(s) = 0$] it is necessary that oscillation in the feedback path must be the same as oscillation in the forward path but with a negative sign, see Fig. 5.13. It can be expressed with the transfer functions

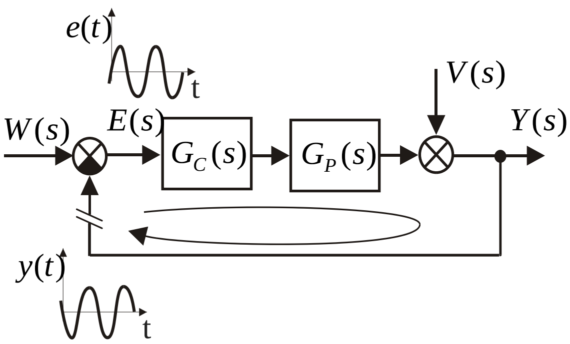

Fig. 5.13 Control system on the stability boundary

$$G_o(s) = -1 \;\Rightarrow\; G_o(\mathrm{j}\omega_c) = -1, \tag{5.63}$$

where $G_o(s) = G_C(s)G_P(s)$ is the open-loop (control system) transfer function (it is generally given by the product of all transfer functions in the loop), ω_c – the ultimate angular frequency.

It is obvious that the open loop is stable (otherwise the occurrence and duration of the constant oscillation in the control loop is not possible).

For the control system in Fig. 5.13 the relation (5.63) expresses the condition for the oscillating stability boundary. This condition can be obtained on the basis of the same denominators of the basic transfer functions [e.g. see (5.3) – (5.5) and (5.11) – (5.13)], where the term $1 + G_o(s)$ appears. It is clear that the critical state occurs when that term is equal to zero, which corresponds to (5.63).

The relation (5.63) expresses the fact that if the linear control system is on the oscillating stability boundary, then the frequency response of the stable open control loop passes through the point -1 on the negative real half-axis.

The point -1 on the negative real half-axis is called the **critical point** and the open-loop frequency response is called the **Nyquist plot**.

Now we can formulate the Nyquist stability criterion:

"The linear control system is (asymptotically) stable if and only if when the frequency response of the stable open-loop control system, i.e. the Nyquist plot $G_o(\mathrm{j}\omega)$ for $0 \leq \omega \leq \infty$ does not surround the critical point (–1 + j0) on the negative half-axis."

The main cases of the Nyquist plots $G_o(\mathrm{j}\omega)$ for a stable open-loop and $q = 0$ due to the critical point (–1 + j0) are shown in Fig. 5.14. ***The integrating elements in the forward and feedback path (i.e. in the loop) from the point of view of the Nyquist stability criterion are not considered as unstable*** (they are in fact neutral elements). Their number is denoted by the letter q and it is called the **control system type**. In this case, when there is a decision on whether the Nyquist plot surrounds or does not surround the critical point (–1 + j0), it is necessary to connect this plot with a positive real half-axis by a circle of an infinitely large radius (shown dashed), see Fig. 5.15.

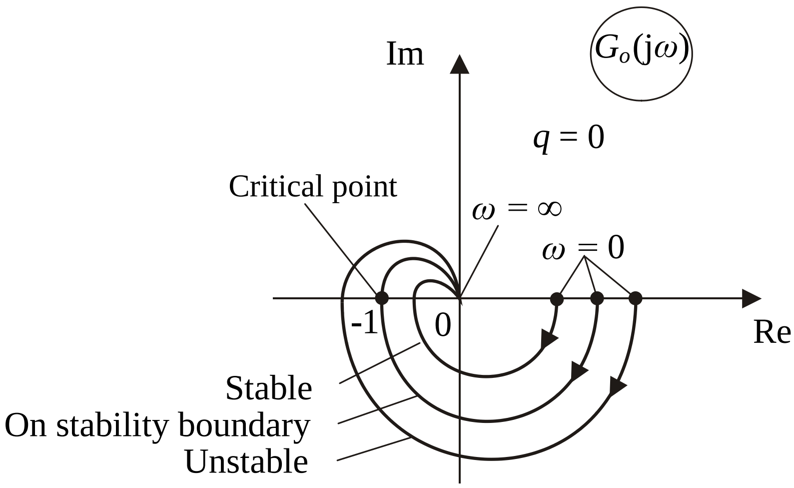

Fig. 5.14 Nyquist plots $G_o(\mathrm{j}\omega)$ for the stable open-loop and $q = 0$

If the Nyquist plot $G_o(\mathrm{j}\omega)$ for $q = 2$ has the course as in Fig. 5.15, then **conditional stability** occurs, because decreasing or increasing the value $A_o(\omega)$ for the phase $-\pi$ may cause instability of the control system.

The geometric form of the Nyquist stability criterion has been formulated above. The analytical form can be very useful too. It is necessary to introduce the **gain crossover angular frequency** ω_g, which is defined by the equality (Fig. 5.16)

$$A_o(\omega_g) = 1 \tag{5.64}$$

and the **phase crossover angular frequency** ω_p, which is defined by the equality (Fig. 5.16)

$$\varphi_o(\omega_p) = -\pi \, . \tag{5.65}$$

The angular frequency ω_p can be also determined from the relation

$$\mathrm{Im} G_o(\mathrm{j}\omega_p) = 0 \, . \tag{5.66}$$

For the oscillating stability boundary the relation holds

$$\omega_c = \omega_g = \omega_p \, . \tag{5.67}$$

Now the Nyquist stability criterion can be written analytically in some of the forms:

$$G_o(\mathrm{j}\omega_p) = \mathrm{Re} G_o(\mathrm{j}\omega_p) > -1 \, , \tag{5.68}$$

$$A_o(\omega_p) < 1 \, , \tag{5.69}$$

$$\varphi_o(\omega_g) > -\pi \, . \tag{5.70}$$

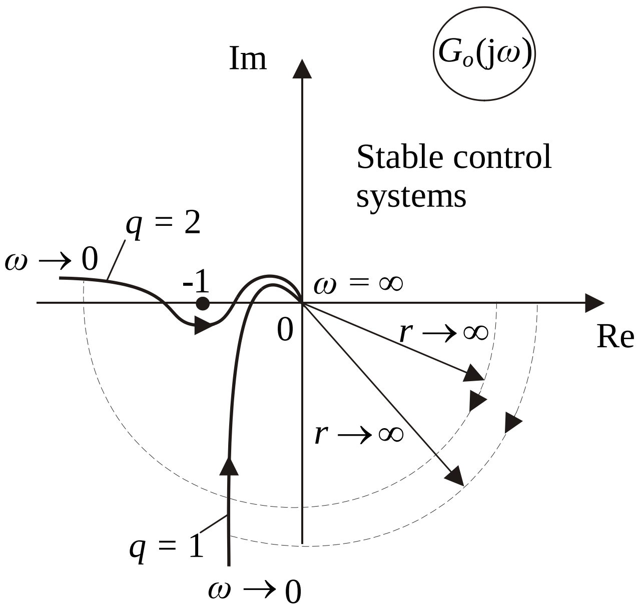

Fig. 5.15 Nyquist plots $G_o(\mathrm{j}\omega)$ for stable open-loop and pro $q = 1$ and $q = 2$

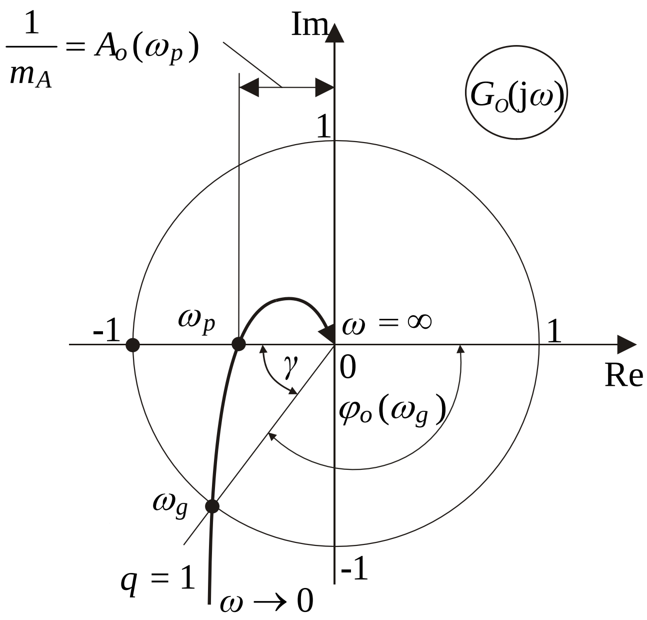

Fig. 5.16 Gain margin m_A and phase margin γ

It is obvious that the simple analytical formulation of the Nyquist stability criterion (5.68) – (5.70) applies to unconditionally stable control systems. For conditionally stable control systems it can be easily extended.

Very important indices can be defined on the basis of the angular frequencies ω_g and ω_p (Fig. 5.16):

the **gain margin**

$$m_A = \frac{1}{A_o(\omega_p)} \tag{5.71}$$

and the **phase margin**

$$\gamma = \pi + \varphi_o(\omega_g)\,. \tag{5.72}$$

The gain margin m_A expresses how many times the value of $A_o(\omega_p)$ can be increased (how many times the open-loop gain k_o can be increased) in order for the control system to reach the stability boundary. Similarly, the phase margin γ expresses how much the phase $\varphi_o(\omega_g)$ (in the absolute value) can be increased in order for the control system to reach the stability boundary.

Since the controller integral component brings into the open-loop of the control system a negative phase, i.e. it reduces the phase margin γ, therefore the ***controller integral component destabilizes*** (it deteriorates a stability) ***the control system***. In contrast, the controller derivative component brings into the open-loop of the control system a positive phase, i.e. it increases the phase margin γ, therefore the ***controller derivative component stabilizes*** (it improves a stability) ***the control system*** (of course for a suitable filtration).

As regards the controller proportional component, which is expressed by the controller gain K_P, it is clear that by increasing the controller gain K_P, the open-loop gain k_o increases and thus reduces the gain margin m_A, therefore the ***controller***

proportional component destabilizes the control system. Conditionally stable control systems are an exception.

The time delay is extremely dangerous for the stability of the control system. Its frequency transfer function has the form

$$G(\mathrm{j}\omega) = \mathrm{e}^{-T_d \mathrm{j}\omega} = A(\omega)\mathrm{e}^{\mathrm{j}\varphi(\omega)}, \tag{5.73a)}$$

$$A(\omega) = 1, \tag{5.73b}$$

$$\varphi(\omega) = -T_d\omega. \tag{5.73c}$$

From relations (5.73) it is obvious that the time delay does not change the modulus [see (5.73b)], but it linearly increases the negative phase by increasing angular frequency [see (5.73c)], i.e. it reduces the phase margin γ. Therefore, the ***time delay always significantly destabilizes the control system.***

The given formulations of the Nyquist stability criterion applies only to stable open-loop control system, and therefore it is necessary at first to check the stability of the open-loop control system and then to proceed to the verification of closed-loop control system stability.

The Nyquist stability criterion for unstable control systems can be formulated in the form:

"The linear control system is (asymptotically) stable if and only if when the Nyquist plot $G_o(\mathrm{j}\omega)$ of the unstable open-loop control system with p unstable poles surrounds the critical point $(-1 + \mathrm{j}0)$ in the positive direction (counter-clockwise) $p/2$ times (i.e. $p\pi$)."

Example 5.1

The characteristic polynomial of the control system has the form

$$N(s) = a_2 s^2 + a_1 s + a_0 .$$

On the basis of the Hurwitz stability criterion it is necessary to determine the conditions for the coefficients a_0, a_1 and a_2, which ensure the stability of the control system.

Solution:

a) From the necessary Stodola condition it follows: $a_0 > 0$, $a_1 > 0$, $a_2 > 0$.

b) The Hurwitz matrix for $n = 2$ has the form

$$\boldsymbol{H} = \begin{bmatrix} a_1 & 0 \\ a_2 & a_0 \end{bmatrix}.$$

Because the Hurwitz minor $H_{n-1} = a_1 > 0$, it is obvious that for the characteristic polynomial of the second degree the Stodola condition for the existence and nonnegativity of the coefficients $a_0 > 0$, $a_1 > 0$ and $a_2 > 0$ is a necessary and a sufficient condition for the (asymptotic) stability of the control system.

Example 5.2

For the control system in Fig. 5.17 on the basis of the Hurwitz stability criterion it is necessary to mark out the stable region in an adjustable controller parameter plane (K_P,T_I), ($k_1 > 0$, $T_1 > 0$).

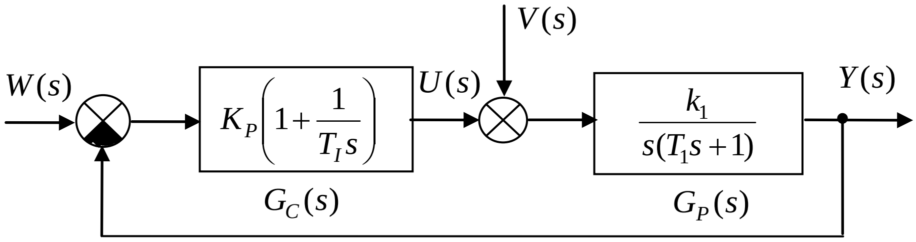

Fig. 5.17 Block diagram of the control system – Example 5.2

Solution:

In accordance with Fig. 5.17 the open-loop control system transfer function is given by the relation

$$G_o(s) = G_C(s)G_P(s) = \frac{K_P k_1 (T_I s + 1)}{T_I s^2 (T_1 s + 1)} = \frac{M_o(s)}{N_o(s)}.$$

The characteristic polynomial of the control system has the form

$$N(s) = N_o(s) + M_o(s) = T_I T_1 s^3 + T_I s^2 + K_P k_1 T_I s + K_P k_1.$$

a) From the Stodola necessary condition it follows:

$$K_P > 0, \quad T_I > 0.$$

b) The Hurwitz matrix for n = 3 has the form

$$\boldsymbol{H} = \left[\begin{array}{cc:c} T_I & K_P k_1 & 0 \\ T_I T_1 & K_P k_1 T_I & 0 \\ \hdashline 0 & T_I & K_P k_1 \end{array}\right].$$

It is enough to verify the positivity of the Hurwitz minor

$$H_2 = \begin{vmatrix} T_I & K_P k_1 \\ T_I T_1 & K_P k_1 T_I \end{vmatrix} = K_P k_1 T_I (T_I - T_1) > 0 \;\Rightarrow\; T_I > T_1.$$

The stable region in the adjustable controller parameter plane (K_P,T_I) determines the last inequality $T_I > T_1$ and the condition $K_P > 0$. The equality $K_P = 0$ determines the nonoscillating stability boundary and the oscillating stability boundary is given by the equality $T_I = \mathrm{T}_1$ (Fig. 5.18).

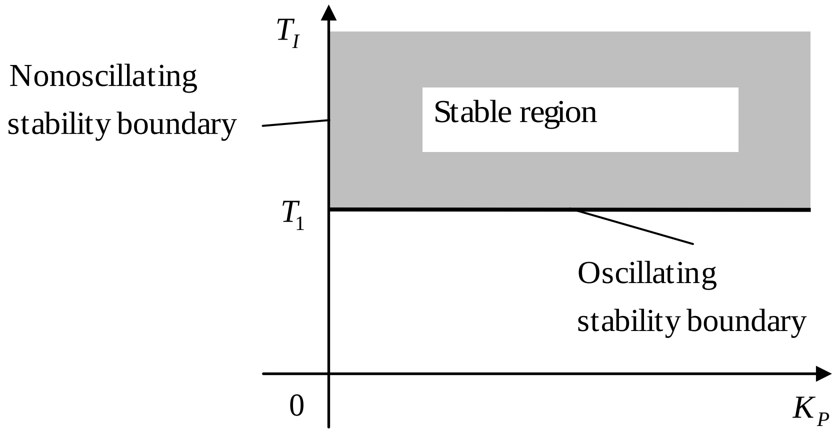

Fig. 5.18 Stable region for control system in Fig. 5.17 – Example 5.2

Example 5.3

For the control system in Fig. 5.17 (Example 5.2) on the basis of the Mikhailov stability criterion it is necessary to mark out the stable region in an adjustable controller parameter plane (K_P,T_I), ($k_1 > 0$, $T_1 > 0$).

Solution:

The characteristic polynomial $N(s)$ was already determined in Example 5.2

$$N(s) = T_I T_1 s^3 + T_I s^2 + K_P k_1 T_I s + K_P k_1 .$$

and therefore the Mikhailov function has the form

$$N(\mathrm{j}\omega) = N(s)\big|_{s=\mathrm{j}\omega} = T_I T_1 (\mathrm{j}\omega)^3 + T_I (\mathrm{j}\omega)^2 + K_P k_1 T_I \,\mathrm{j}\omega + K_P k_1 =$$
$$= N_P(\omega) + \mathrm{j} N_Q(\omega),$$
$$N_P(\omega) = K_P k_1 - T_I \omega^2,$$
$$N_Q(\omega) = T_I (K_P k_1 - T_1 \omega^2)\omega.$$

In accordance with the analytical formulation of the Mikhailov stability criterion (5.62) we can write

$$T_I (K_P k_1 - T_1 \omega^2)\omega = 0 \;\Rightarrow\; \omega_1 = 0,\; \omega_3 = \sqrt{\frac{K_P k_1}{T_1}},$$
$$K_P k_1 - T_I \omega^2 = 0 \;\Rightarrow\; \omega_2 = \sqrt{\frac{K_P k_1}{T_I}}.$$

For the roots of the imaginary part $N_Q(\omega)$ and real part $N_P(\omega)$ of the Mikhailov function the inequalities

$$\omega_1 = 0 < \omega_2 = \sqrt{\frac{K_P k_1}{T_I}} < \omega_3 = \sqrt{\frac{K_P k_1}{T_1}},$$

must hold. From these inequalities there is obtained

$$\sqrt{\frac{K_P k_1}{T_I}} < \sqrt{\frac{K_P k_1}{T_1}} \;\Rightarrow\; T_I > T_1 .$$

This inequality together with the Stodola necessary condition of the nonnegativity of the coefficients of the characteristic polynomial $N(s)$, i.e. $K_P > 0$ and $T_I > 0$ give us the same stable region as in Example 5.2 (Fig. 5.18).

Example 5.4

On the basis of the Nyquist stability criterion for the control system with the time delay in Fig. 5.19 it is necessary to determine the integral time T_I, which ensures the (asymptotic) stability ($k_1 > 0$).

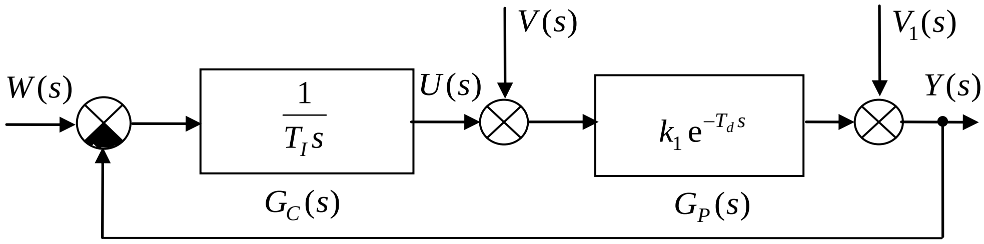

Fig. 5.19 Block diagram of the control system – Example 5.4

Solution:

In accordance with Fig. 5.19 the open-loop control system transfer function has the form

$$G_o(s) = G_C(s) G_P(s) = \frac{k_1}{T_I s} \mathrm{e}^{-T_d s} .$$

The open-loop control system contains one integrating element (the controller), and therefore it can be considered as stable.

The frequency open-loop control system transfer function is given by the relation

$$G_o(\mathrm{j}\omega) = G_o(s)\big|_{s=\mathrm{j}\omega} = \frac{k_1}{T_I\,\mathrm{j}\omega} \mathrm{e}^{-T_d\,\mathrm{j}\omega} = -\mathrm{j}\frac{k_1}{T_I \omega} \mathrm{e}^{-\mathrm{j}T_d\omega} = \frac{k_1}{T_I\omega} \mathrm{e}^{-\mathrm{j}\left(T_d\omega + \frac{\pi}{2}\right)} =$$
$$= A_o(\omega)\,\mathrm{e}^{\mathrm{j}\varphi_o(\omega)},$$

where

$$A_o(\omega) = \frac{k_1}{T_I \omega}, \quad \varphi_o(\omega) = -\left(T_d\omega + \frac{\pi}{2}\right).$$

For rewriting the above relation the property

$$\frac{1}{\mathrm{j}} = -\mathrm{j} = \mathrm{e}^{-\mathrm{j}\frac{\pi}{2}}$$

was used.

In order for the stability of the control system it must hold [see (5.69) and (5.65)]

$$\left.\begin{aligned} A_o(\omega_p) < 1 \;&\Rightarrow\; \frac{k_1}{T_I \omega_p} < 1 \\ \varphi_o(\omega_p) = -\pi \;&\Rightarrow\; -\left(T_d \omega_p + \frac{\pi}{2}\right) = -\pi \end{aligned}\right\} \Rightarrow \quad \begin{aligned} \omega_p &= \frac{\pi}{2T_d}, \\ T_I &> \frac{2k_1 T_d}{\pi}. \end{aligned}$$

For

$$T_I = \frac{2k_1 T_d}{\pi}$$

the oscillating stability boundary is obtained, for which relation $\omega_p = \omega_g = \omega_c$ holds (Fig. 5.20).

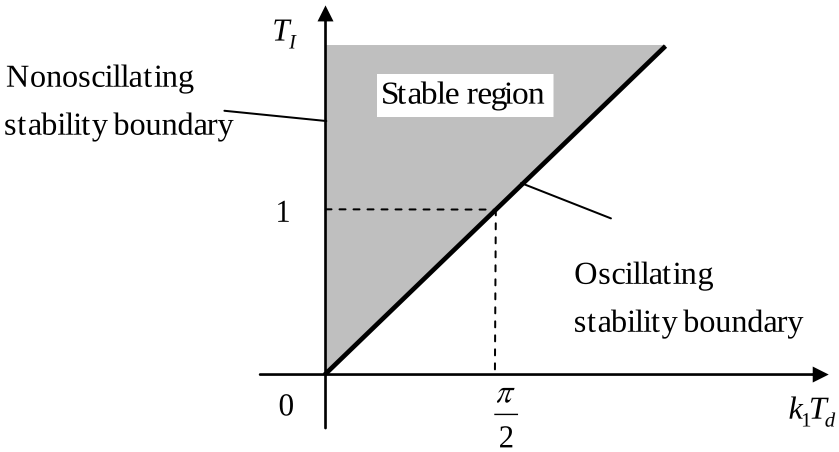

Fig. 5.20 Stable region for the control system in Fig. 5.19 – Example 5.4

Example 5.5

The two transfer functions are given

$$G_1(s) = \frac{Y(s)}{U(s)} = \frac{s+1}{s+1}$$

and

$$G_2(s) = \frac{Y(s)}{U(s)} = \frac{s-1}{s-1}.$$

It is necessary to analyze the ideal and the real reduction (cancellation) of the binomials in these transfer functions.

Solution:

In control theory we usually use the word **cancellation** or **compensation** instead of the word reduction.

In the case of the transfer function $G_1(s)$ the stable pole $s_1 = -1$ cancels the stable zero $s_1^0 = -1$ (the roots of the numerator = zeros, the roots of the denominator = poles). In the case of the transfer function $G_2(s)$ the unstable pole $s_1 = 1$ cancels the unstable zero $s_1^0 = 1$.

a) The ideal cancellation

$$G_1(s)=\frac{Y(s)}{U(s)}=\frac{s+1}{s+1}=1,$$
$$h_1(t)=\mathrm{L}^{-1}\left\{\frac{1}{s}G_1(s)\right\}=\mathrm{L}^{-1}\left\{\frac{1}{s}\right\}=\eta(t)=1.$$

$$G_2(s)=\frac{Y(s)}{U(s)}=\frac{s-1}{s-1}=1,$$
$$h_2(t)=\mathrm{L}^{-1}\left\{\frac{1}{s}G_2(s)\right\}=\mathrm{L}^{-1}\left\{\frac{1}{s}\right\}=\eta(t)=1.$$

In the case of the ideal cancellation the same terms are reduced in the denominator and numerator, and therefore the step responses $h_1(t)$ and $h_2(t)$ are identical.

b) The real cancellation (ε – small number)

$$G_1(s)=\frac{Y(s)}{U(s)}=\frac{s+(1+\varepsilon)}{s+1}=\frac{s}{s+1}+\frac{1+\varepsilon}{s+1},$$
$$h_1(t)=\mathrm{L}^{-1}\left\{\frac{1}{s}G_1(s)\right\}=\mathrm{L}^{-1}\left\{\frac{1}{s+1}\right\}+\mathrm{L}^{-1}\left\{\frac{1+\varepsilon}{s(s+1)}\right\}=$$
$$=\mathrm{e}^{-t}+(1+\varepsilon)(1-\mathrm{e}^{-t})=1+\varepsilon-\varepsilon\mathrm{e}^{-t}.$$

$$\lim_{t\to\infty}h_1(t)=1+\varepsilon\,.$$

$$G_2(s)=\frac{Y(s)}{U(s)}=\frac{s-(1+\varepsilon)}{s-1}=\frac{s}{s-1}-\frac{1+\varepsilon}{s-1},$$
$$h_2(t)=\mathrm{L}^{-1}\left\{\frac{1}{s}G_2(s)\right\}=\mathrm{L}^{-1}\left\{\frac{1}{s-1}\right\}-\mathrm{L}^{-1}\left\{\frac{1+\varepsilon}{s(s-1)}\right\}=$$
$$=\mathrm{e}^{t}+(1+\varepsilon)(1-\mathrm{e}^{t})=1+\varepsilon-\varepsilon\mathrm{e}^{t},$$

$$\lim_{t\to\infty}\left|h_2(t)\right|=\infty\,.$$

For the real cancellation of the stable binomials the step response is slightly different from the step response for the ideal cancellation. The difference depends on the size and sign of the small number ε. In contrast, in the case of the real cancellation of the unstable binomials the step response is always unstable.

The unstable terms in the transfer functions must not be cancelled. The uncontrollable and unobservable modes arise for the cancellation of the unstable terms and it causes instability.

6 CLOSED-LOOP CONTROL SYNTHESIS

6.1 Control performance

The simplest way to a control performance assessment is on the basis of the step responses caused by input variables. In Chapter 5 it was said that by ensuring the suitable control system properties considering the desired variable $w(t)$, then the suitable properties generally will be ensured for the disturbance variables $v(t)$ and $v_1(t)$ too. For the 1DOF conventional controller and disturbance $v_1(t)$ which is applied to the plant output, that always holds.

Two exemplary control system step responses (servo responses, set-point responses) are shown in Fig. 6.1.

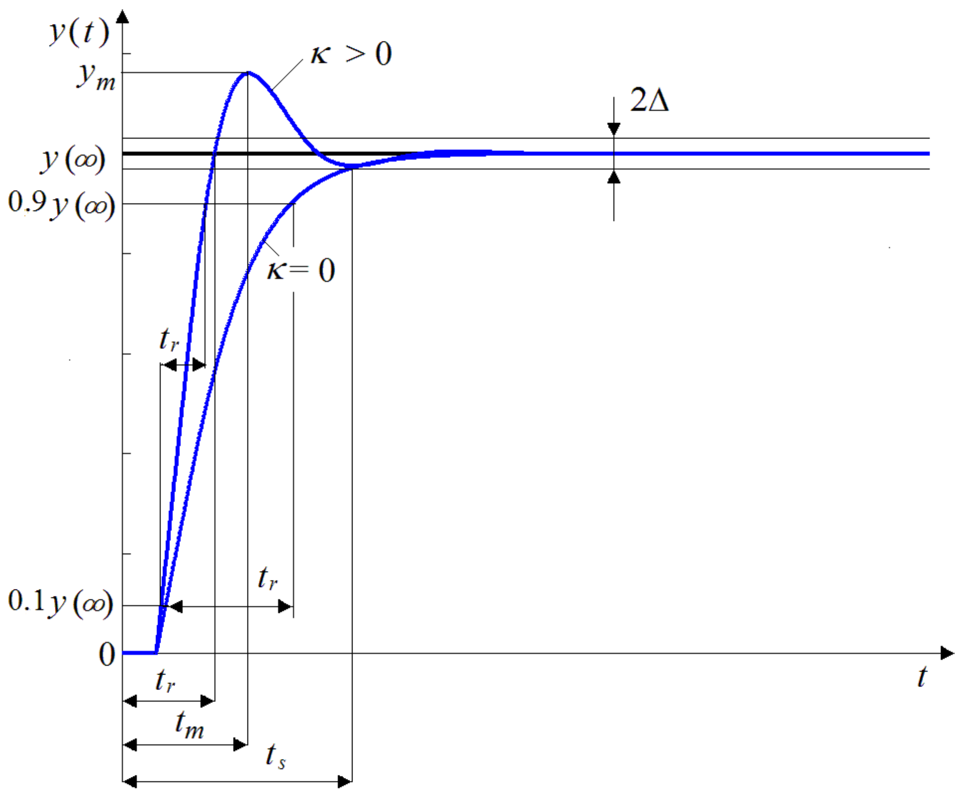

Fig. 6.1 Control system step responses with marked control performance indices

From a practical point of view, the most important performance indices are the **relative overshoot** κ and the **settling time** t_s (Fig. 6.1). The relative overshoot is defined by the relation

$$\kappa = \frac{y_m - y(\infty)}{y(\infty)}, \qquad y_m = y(t_m), \tag{6.1}$$

where y_m is the maximum value of the controlled variable (the first peak), t_m – the time of reaching the value y_m (the peak time), $y(\infty)$ – the steady-state value of the controlled variable.

The settling time t_s is given by the time, when the controlled variable $y(t)$ gets in the band with width 2Δ, i.e. $y(\infty) \pm \Delta$, where the **control tolerance** is given

$$\Delta = \delta\, y(\infty), \quad \delta = 0.01 \div 0.05 \qquad (1 \div 5)\ \%. \tag{6.2}$$

The relative control tolerance δ has most frequently the value 0.05 or 0.02.

For the settling time t_s the value of the relative control tolerance δ must be always given. If it is not specified, then it is assumed that $\delta = 0.05$ (5%).

The case $\kappa = 0$ corresponds to a nonoscillatory control process, which is required for processes where overshoot may cause undesirable effects (they are mainly thermal and chemical processes, but also the movements of assembly robots and manipulators, etc.).

For a nonoscillatory control process a minimum of the settling time t_s is often required. Such a control process is called the marginal nonoscillatory control process.

For $\kappa > 0$ the control process is oscillatory and it is faster than the nonoscillatory one. The rate of increase of the controlled variable $y(t)$ can be measured using the **rise time** t_r. It is the time at which the controlled variable $y(t)$ reaches the steady-state value $y(\infty)$. Most often the rise time t_r is defined as the time required for the response to go from 0.1 $y(\infty)$ to 0.9 $y(\infty)$. In this way the defined index of the rate of increase controlled variable $y(t)$ is applicable to both oscillatory and nonoscillatory control processes and even for processes with time delay.

The control process with the relative overshoot κ about 0.05 (5%) is acceptable for most plants and processes. If the minimum of the settling time t_s is at the same time ensured, then such control process is often regarded as “practically optimal”. It is widely used wherever small overshoot does not matter or is desirable, e.g. for pointer type measuring and recording instruments (in this case the small overshoot enables a faster interpolation of a pointer position).

Since the plant is always continuous, therefore, the control process performance is frequently assessed for the continuous (analog) control system.

The **integral criteria** are very suitable for a complex evaluation of the control process performance.

It is obvious that if the given integral criterion will be smaller, then the control performance will be higher. In order to not operate with the two variables $y(t)$ and $w(t)$, it is suitable to operate only with the control error $e(t) = w(t) - y(t)$ and it is assumed that $e(\infty) = 0$. If $e(\infty) \neq 0$, then in all relations for the integral criteria the term $e(t) - e(\infty)$ must be substitute in lieu $e(t)$.

Integral of error

$$I_{IE} = \int_0^\infty e(t)\,\mathrm{d}t\,. \tag{6.3a}$$

The integral of error I_{IE} (IE = **i**ntegral of **e**rror) is the simplest integral criterion.

It is not suitable for oscillatory processes, because $I_{IE} = 0$ for the control process on the oscillating stability boundary. Its best advantage is that it can be easily computed (see Appendix A)

$$I_{IE} = \lim_{s \to 0} E(s) = \lim_{s \to 0} \int_0^\infty e(t)\,\mathrm{e}^{-st}\,\mathrm{d}t = \int_0^\infty e(t)\,\mathrm{d}t\,. \tag{6.3b}$$

Integral of absolute error

$$I_{IAE} = \int_0^\infty |e(t)|\,\mathrm{d}t\,. \tag{6.3c}$$

The criterion of the absolute error I_{IAE} (IAE = **i**ntegral of **a**bsolute **e**rror) removes the disadvantages of the previous integral criterion I_{IE}, and therefore it is applicable to both the nonoscillatory and the oscillatory control processes. However, it has a very unpleasant behaviour consisting in the fact that in the points where $e(t)$ changes sign the derivative is not defined. Therefore the value of this criterion cannot be calculated analytically but only numerically or by simulations.

Integral of squared error

$$I_{ISE} = \int_0^\infty e^2(t)\,\mathrm{d}t\,. \tag{6.3d}$$

The criterion of the squared error I_{ISE} (ISE = **i**ntegral of **s**quared **e**rror) removes the disadvantages of the two previous integral criteria I_{IE} and I_{IAE}, because it is also applicable for the oscillatory control process and its value can be determined analytically [the course $e^2(t)$ is smooth], but the resulting control process is too oscillating. Its use is appropriate in those cases, when the desired variable $w(t)$ or the disturbance variable $v(t)$ have a random character.

ITAE criterion

$$I_{ITAE} = \int_0^\infty t|e(t)|\,\mathrm{d}t\,. \tag{6.3e}$$

The ITAE integral criterion I_{ITAE} (ITAE = **i**ntegral of **t**ime multiplied by **a**bsolute **e**rror) contains the time and the control error, and therefore it simultaneously minimizes both the error and the settling time t_s. It is a very popular integral criterion, although in the case of oscillatory courses its value can be determined only numerically or by simulation.

The most important integral criteria were briefly described. The values of the controller adjustable parameters can be determined by their minimization, which is often done by simulation.

The **steady-state errors** are the important control performance index. These errors can be caused by the input standard testing signals, which have the forms: the step input, the ramp input (it is the integral of the step input) and the parabolic input (it is the integral of the ramp input).

The overall control error is given by (5.10)

$$E(s) = E_w(s) + E_v(s) + E_{v_1}(s)\,,$$

where

$$E_w(s) = G_{we}(s)W(s),\;\; E_v(s) = G_{ve}(s)V(s),\;\; E_{v_1}(s) = G_{v_1e}(s)V_1(s)\,,$$

are partial control errors caused by the corresponding input variables.

Because the equality

$$G_{we}(s) = -G_{v_1 e}(s),$$

holds [see (5.11) and (5.13)] it is worth considering only the control errors caused by the desired variable $w(t)$ and the disturbance variable $v(t)$ in the plant input.

The standard testing signals are:

the step input

$$w(t) = w_0 \eta(t) \mathrel{\hat{=}} W(s) = \frac{w_0}{s}, \quad v(t) = v_0 \eta(t) \mathrel{\hat{=}} V(s) = \frac{v_0}{s}, \tag{6.4}$$

the ramp input

$$w(t) = w_1 t \eta(t) \mathrel{\hat{=}} W(s) = \frac{w_1}{s^2}, \quad v(t) = v_1 t \eta(t) \mathrel{\hat{=}} V(s) = \frac{v_1}{s^2}, \tag{6.5}$$

the parabolic input

$$w(t) = \frac{1}{2} w_2 t^2 \eta(t) \mathrel{\hat{=}} W(s) = \frac{w_2}{s^3}, \quad v(t) = \frac{1}{2} v_2 t^2 \eta(t) \mathrel{\hat{=}} V(s) = \frac{v_2}{s^3}. \tag{6.6}$$

On the basis of the final value theorem it is possible to compute the steady-state control errors

$$e_w(\infty) = \lim_{t \to \infty} e_w(t) = \lim_{s \to 0} sE_w(s), \;\; e_v(\infty) = \lim_{t \to \infty} e_v(t) = \lim_{s \to 0} sE_v(s). \tag{6.7}$$

From the frequency control system transfer function (5.17) the modulus (magnitude) or logarithmic modulus can be obtained

$$A_{wy}(\omega) = \operatorname{mod} G_{wy}(\mathrm{j}\omega) = \left| G_{wy}(\mathrm{j}\omega) \right| \;\text{ or }\; L_{wy}(\omega) = 20 \log A_{wy}(\omega). \tag{6.8}$$

The typical course of the control system magnitude response $A_{wy}(\omega)$ is shown in Fig. 6.2. From Fig. 6.2 some of the control performance indices can be obtained: $A_{wy}(\omega_R)$ – the **peak resonance** (the resonant magnitude), ω_R – the **resonant angular frequency**, ω_b – the **cut-off angular frequency**.

For the well-tuned control system it is recommended that the relations

$$A_{wy}(\omega_R) \le 1.1 \div \mathbf{1.5} \quad \text{or } L_{wy}(\omega_R) \le (0.8 \div \mathbf{3.5}) \text{ dB}. \tag{6.9}$$

would hold [2, 4, 9, 10, 22, 29].

A too high value of the peak resonance gives a high oscillation and significant overshoots.

The cut-off angular frequency ω_b determines the width of the control system operating bandwidth, i.e. the range of operating angular frequencies. The higher value enables the control system to better process higher angular frequencies. Its value is given by a decrease of the modulus $A_{wy}(\omega)$ [$L_{wy}(\omega)$] on the value $\frac{1}{\sqrt{2}} A_{wy}(0) \doteq 0.707 A_{wy}(0)$ [$L_{wy}(0) - 3$ dB] and for the big peak resonance $A_{wy}(\omega_R)$ by an increase the modulus $A_{wy}(\omega)$ [$L_{wy}(\omega)$] on the value $\sqrt{2} A_{wy}(0) \doteq 1.414 A_{wy}(0)$ [$L_{wy}(0) + 3$ dB].

From the magnitude response $A_{wy}(\omega)$ the control system type q can be determined, because the relations hold

$$A_{wy}(0)=1 \quad \text{or} \quad L_{wy}(0)=0 \quad \Rightarrow \quad q \geq 1, \tag{6.10}$$

$$A_{wy}(0)<1 \quad \text{or} \quad L_{wy}(0)<0 \quad \Rightarrow \quad q=0. \tag{6.11}$$

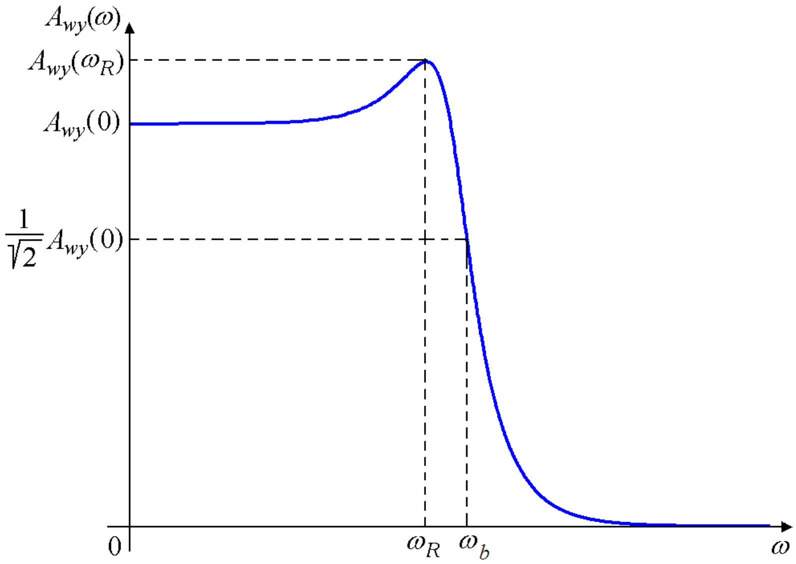

Fig. 6.2 Control system magnitude response

The control system type q can be determined on the basis of the frequency response of the open-loop control system (the Nyquist plot) $G_o(\mathrm{j}\omega)$ for $\omega \to 0$, see. Figs 5.15 and 5.16.

The gain crossover angular frequency ω_g and the phase crossover angular frequency ω_p are given by the relations [see (5.64) and (5.65)]

$$A_o(\omega_g)=1 \tag{6.12}$$

$$\varphi_o(\omega_p)=-\pi\ , \tag{6.13}$$

where

$$A_o(\omega)=\operatorname{mod} G_o(\mathrm{j}\omega)=|G_o(\mathrm{j}\omega)| \tag{6.14}$$

is the modulus of the frequency response of the open-loop control system and

$$\varphi_o(\omega)=\arg G_o(\mathrm{j}\omega) \tag{6.15}$$

is the phase of the frequency response of the open-loop control system.

For the oscillating stability boundary the equalities hold [see (5.67)]

$$\omega_c=\omega_g=\omega_p\,, \tag{6.16}$$

where ω_c is the ultimate angular frequency.

From the Nyquist plot very important control performance indices can be determined, like the gain margin m_A and the phase margin γ (see Figs 5.15 and 5.16). For common control systems the following values are recommended

$$m_A = \mathbf{2} \div 5 \quad \text{or } m_L = 20\log m_A = (\mathbf{6} \div 14)\ \text{dB}, \tag{6.17}$$

$$\gamma = \mathbf{30}° \div 60° \ \left(\frac{\boldsymbol{\pi}}{\mathbf{6}} \div \frac{\pi}{3}\right). \tag{6.18}$$

The bold values should not be in any case exceeded [2, 4, 9, 10, 13, 22, 24, 29].

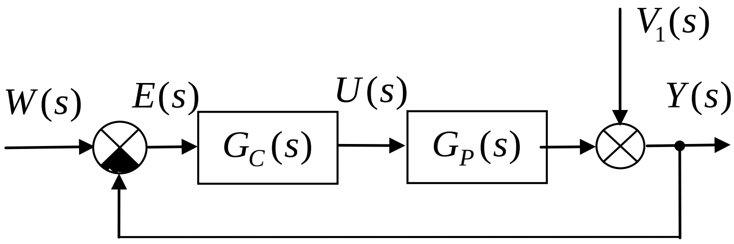

Fig. 6.3 Block diagram of the control system

The frequency transfer functions $G_{wy}(\mathrm{j}\omega)$ and $G_{v_1y}(\mathrm{j}\omega)$ [see Fig. 6.3 and relations (5.3), (5.5)] have for the automatic control theory essential importance and therefore they are also written by special symbols $T(\mathrm{j}\omega)$ and $S(\mathrm{j}\omega)$ and they have special names. From equation (5.5) it follows

$$G_{wy}(\mathrm{j}\omega) + G_{v_1y}(\mathrm{j}\omega) = 1 \ \Leftrightarrow \ T(\mathrm{j}\omega) + S(\mathrm{j}\omega) = 1. \tag{6.19}$$

The function $S(\mathrm{j}\omega)$ is called the **sensitivity function** and the function $T(\mathrm{j}\omega)$ the **complementary sensitivity function**.

The name of the sensitivity function $S(\mathrm{j}\omega)$ follows from the following considerations (Fig. 6.3).

From the relation

$$Y(\mathrm{j}\omega) = G_{wy}(\mathrm{j}\omega)W(\mathrm{j}\omega) = \frac{G_C(\mathrm{j}\omega)G_P(\mathrm{j}\omega)}{1 + G_C(\mathrm{j}\omega)G_P(\mathrm{j}\omega)}W(\mathrm{j}\omega) \tag{6.20}$$

for $W(\mathrm{j}\omega)$ = constant we get

$$\frac{\mathrm{d}Y(\mathrm{j}\omega)}{Y(\mathrm{j}\omega)} = \frac{\mathrm{d}G_{wy}(\mathrm{j}\omega)}{G_{wy}(\mathrm{j}\omega)}, \tag{6.21}$$

i.e. the relative change of the controlled variable (its transform) is equal to the relative change of the control system properties (its transfer function). Similarly, from (6.20) the relationship is derived

$$\frac{\mathrm{d}G_{wy}(\mathrm{j}\omega)}{G_{wy}(\mathrm{j}\omega)} = \frac{1}{1 + G_C(\mathrm{j}\omega)G_P(\mathrm{j}\omega)}\left[\frac{\mathrm{d}G_C(\mathrm{j}\omega)}{G_C(\mathrm{j}\omega)} + \frac{\mathrm{d}G_P(\mathrm{j}\omega)}{G_P(\mathrm{j}\omega)}\right],$$

or

$$\frac{\mathrm{d}Y(\mathrm{j}\omega)}{Y(\mathrm{j}\omega)} = \frac{\mathrm{d}G_{wy}(\mathrm{j}\omega)}{G_{wy}(\mathrm{j}\omega)} = S(\mathrm{j}\omega)\left[\frac{\mathrm{d}G_C(\mathrm{j}\omega)}{G_C(\mathrm{j}\omega)} + \frac{\mathrm{d}G_P(\mathrm{j}\omega)}{G_P(\mathrm{j}\omega)}\right], \tag{6.22}$$

which expresses the influence of the relative changes in the properties of the controller (its transfer function) and the plant (its transfer function) on the relative change of the control system properties (its transfer function), and thus on the relative change of the controlled variable (its transform). From relation (6.22) it is clear that this influence expresses just the sensitivity function $S(\mathrm{j}\omega)$. For its lower value the lower influence of the relative changes of the controller and the plant properties will be on the relative change of the control system properties, and hence the relative change of the controlled variable.

The sensitivity function $S(\mathrm{j}\omega)$ therefore expresses the sensitivity of the control system to very small mostly unspecified changes of the control system elements.

A typical course of the sensitivity function modulus $|S(\mathrm{j}\omega)| = \operatorname{mod} S(\mathrm{j}\omega)$ is shown in Fig. 6.4. The scale of the angular frequency ω is usually logarithmic.

The **maximum value of the sensitivity function modulus**

$$M_S = \max_{0\le\omega<\infty} |S(\mathrm{j}\omega)| = \max_{0\le\omega<\infty} \left| \frac{1}{1+G_C(\mathrm{j}\omega)G_P(\mathrm{j}\omega)} \right| \tag{6.23}$$

has a very important interpretation.

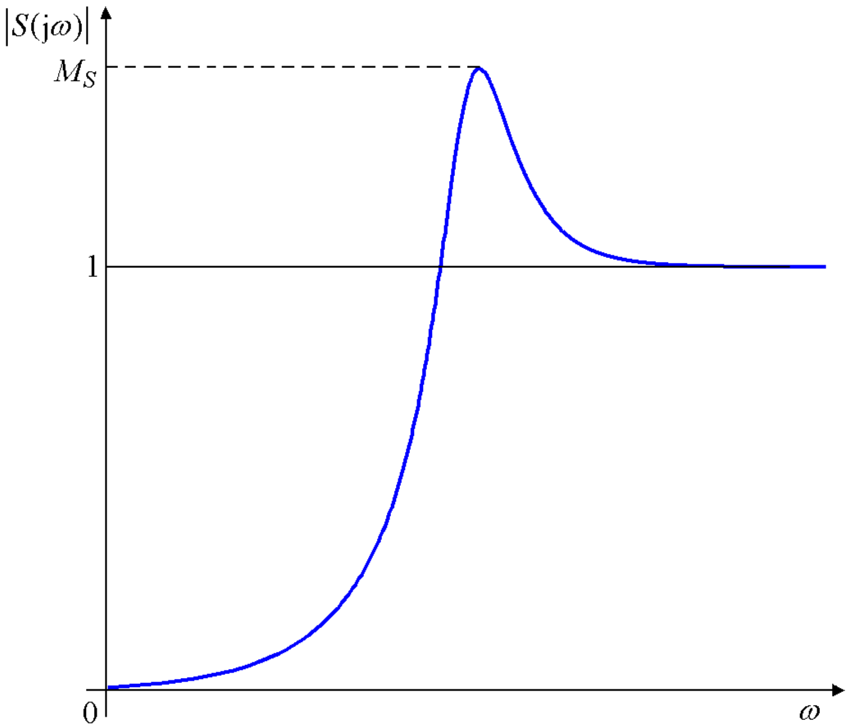

Fig. 6.4 Course of sensitivity function modulus

The inverted value of the maximum of the sensitivity function modulus $1/M_S$ is exactly the shortest distance of the Nyquist plot $G_o(\mathrm{j}\omega)$ to the critical point (–1 + j0), see Fig. 6.5.

The value M_S for a well-tuned control system should not be greater than 2 and it ought be in the range [2, 13, 22, 29]

$$1.4 \le M_S \le \mathbf{2}\,. \tag{6.24}$$

The maximum of the sensitivity function modulus M_S can be used to estimate the gain and the phase margin, because the inequalities hold

$$m_A > \frac{M_S}{M_S - 1}, \tag{6.25}$$

$$\gamma > 2\arcsin\frac{1}{2M_S}. \tag{6.26}$$

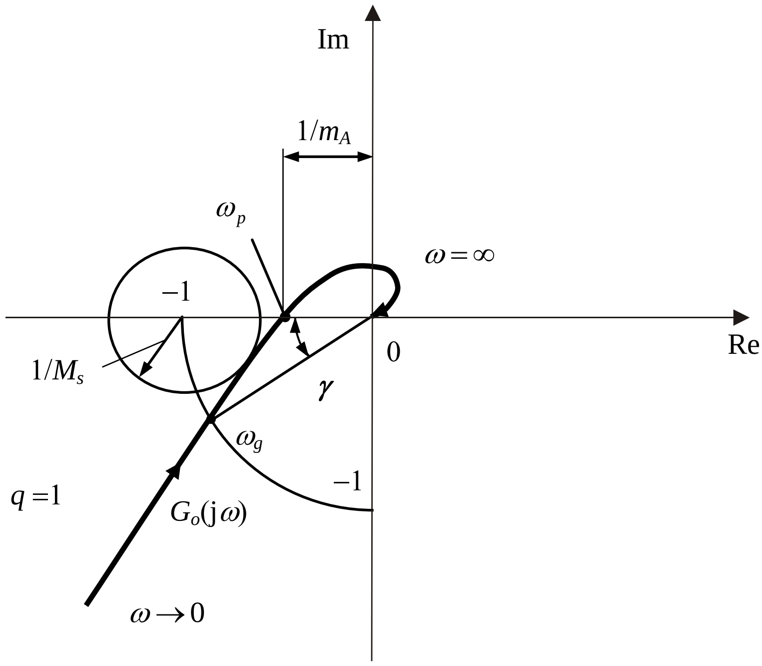

Fig. 6.5 Geometrical interpretation of the maximum of sensitivity function modulus M_S

The maximum of the sensitivity function modulus M_S is a complex control performance index, because from the relations (6.25) and (6.26) it follows that for $M_S \leq 2$ the gain margin $m_A \geq 2$ and the phase margin $\gamma > 29$ will be ensured. Similarly for $M_S \leq 1.4$ the inequalities $m_A \geq 3.5$ and $\gamma > 42°$ hold. The opposite statement is not valid, i.e. the values m_A and γ do not guarantee the corresponding value M_S [2, 13].

Another great advantage of the maximum of the sensitivity function modulus M_S is that it can be used to express the slopes of the **sector nonlinearity** (Fig 6.6)

$$\alpha = \frac{M_S}{M_S + 1} \leq \frac{f(u_1)}{u_1} \leq \frac{M_S}{M_S - 1} = \beta, \tag{6.27}$$

in which the control system with nonlinearity (Fig. 6.7) is asymptotically stable [2, 13].

Nonlinearities or a time-varying gain often appears in real control systems. These cases can be described by the sector nonlinearity

$$u_2 = f(u_1), \quad f(0) = 0,$$

which crosses through the origin and it is defined by the lines of the slopes α and β (Fig. 6.6)

$$0 < \alpha u_1 \leq f(u_1) \leq \beta u_1 \;\Rightarrow\; 0 < \alpha \leq \frac{f(u_1)}{u_1} \leq \beta. \tag{6.28}$$

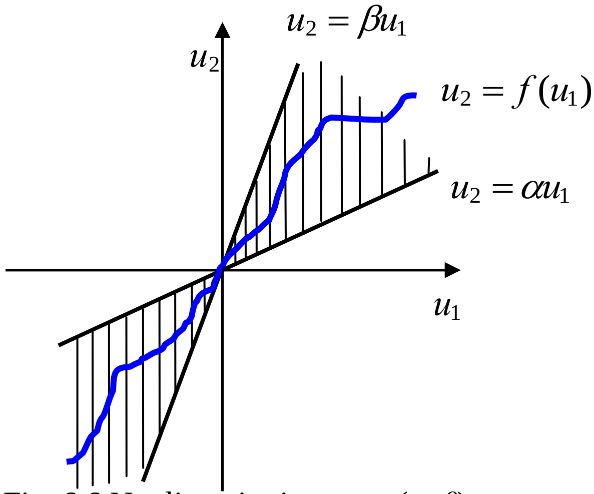

Fig. 6.6 Nonlinearity in sector (α, β)

The actuator is nonlinear in the majority of cases, see Fig. 6.7a. For the purpose of stability verifying the block diagram in Fig. 6.7a can be modified in the block diagram in Fig. 6.7b.

a)

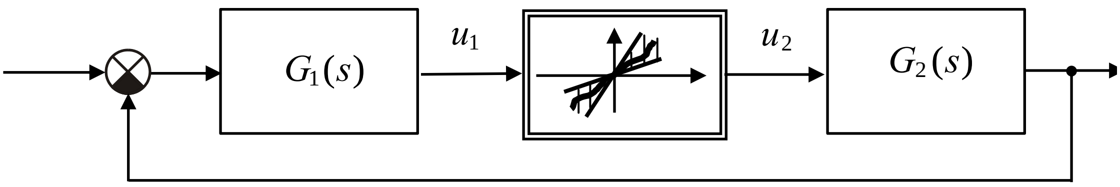

b)

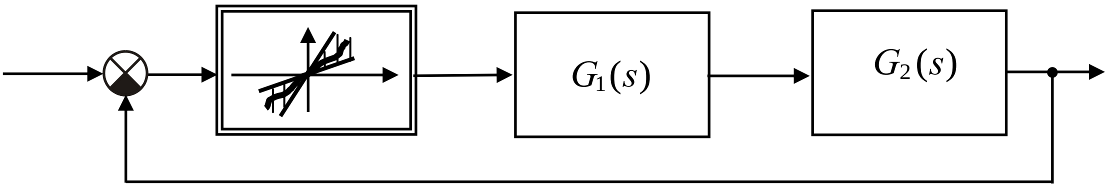

Fig. 6.7 Control system with segment nonlinearity: a) original, b) modified

The stability of the control system with the sector nonlinearity may be verified on the basis of the **circle stability criterion**: "The control system with the nonlinearity in the sector (α, β) is asymptotically stable if the frequency response (the polar plot) of the stable linear part with the transfer function

$$G(s) = G_1(s)G_2(s) \tag{6.29}$$

passes on the right side of the circle which crosses through the points $-\dfrac{1}{\alpha}$, $-\dfrac{1}{\beta}$ and which has the centre on the negative half-axis (Fig. 6.8) [13].

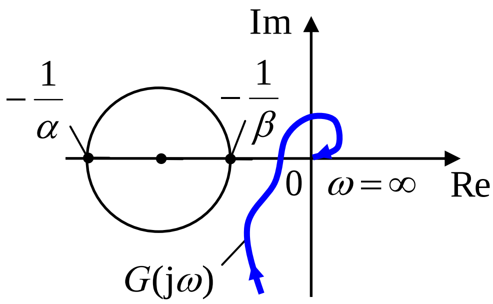

Fig. 6.8 Geometrical interpretation of circle stability criterion

It is obvious that for $\alpha = \beta > 0$ and $G_o(s) = \alpha G(s)$ the circle stability criterion converts into the Nyquist stability criterion for the stable open-loop control systems.

For instance on the basis of (6.27) for $M_S = 2$ the slopes $\alpha = 0.67$ and $\beta = 2$ of the sector nonlinearity can be obtained, similarly for $M_S = 1.4$ the slopes $\alpha = 0.58$ and $\beta = 3.5$ can be obtained.

With the sensitivity or the insensitivity of the control system to very small changes in the properties of its elements there is a very close relation to the **robustness** of the control system, which is its ability to hold the control objective for the larger, mostly quantitatively defined, changes of the properties mostly of the plant (or other control system elements) and for some decrease of the control performance, but always ensuring its stability. For instance the maximum of the sensitivity function modulus M_S determines the sector (α, β) for the nonlinearity or time-varying gain that does not cause loss of the stability, i.e. the M_S expresses in a certain way the robustness of the control system for the sector nonlinearity or the time-varying gain in the sector (α, β).

6.2 Controller tuning

At present, there are a huge number of different controller tuning methods [1 – 11, 13 – 15, 17, 19 – 31]. Only some selected controller tuning methods will be described here, which are based on closed-loop control system properties (Paragraphs 6.2.1 – 6.2.4) and on the knowledge of the plant mathematical model (Paragraphs 6.2.5 – 6.2.10).

6.2.1 Ziegler-Nichols closed-loop method

The ZN (**Z**iegler-**N**ichols) closed-loop method (the ZN ultimate parameter method) comes from the real control system for shutting down the integral ($T_I \to \infty$) and the derivative ($T_D \to 0$) components and the oscillatory stability boundary caused by the controller gain K_P [2, 4, 17, 22, 29, 31].

For the oscillating stability boundary the ultimate (critical) period T_c and the ultimate (critical) controller gain K_{Pc} are determined from any control system variable (see Fig. 6.9) and from the controller. It is obvious that the ultimate gain K_{Pc} is determined iteratively.

The values of the adjustable parameters for the selected controller are calculated on the basis of Tab. 6.1

For the P controller the gain margin $m_A = 2$.

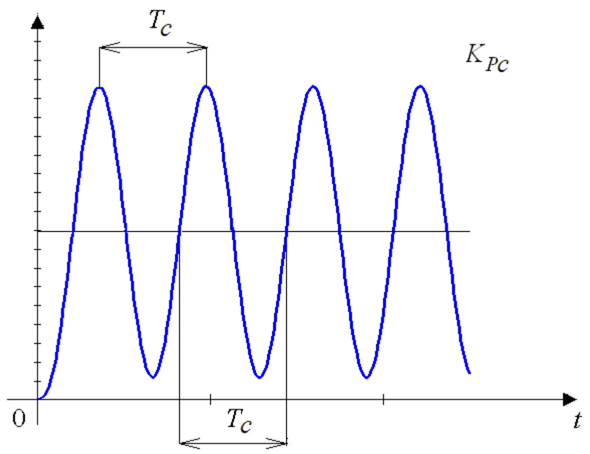

Fig. 6.9 Determination of ultimate period T_c

The destabilizing influence of the integral component in the PI controller is expressed by decrease of K_P^* in comparison with the P controller and the stabilizing influence of the derivative component (with an appropriate filtration) in the standard PID controller is expressed by increase of K_P^* (compare with Tab. 6.4). The ratio $T_D^*/T_I^* = 1/4$.

Tab. 6.1 Controller adjustable parameters for the Ziegler-Nichols closed-loop method (ZN closed-loop method)

Controller	K_P^*	T_I^*	T_D^*
P	$0.5K_{Pc}$	–	–
PI	$0.45K_{Pc}$	$\frac{T_c}{1.2} \doteq 0.83T_c$	–
PID	$0.6K_{Pc}$	$0.5T_c$	$0.125T_c$

The ZN closed-loop method is also applicable for the I controllers. In this case, the control system is brought up on the oscillating stability boundary by decreasing the integral time T_I. When the oscillating stability boundary occurs then the ultimate integral time T_{Ic} is determined and for the tuning the value

$$T_I^* = 2T_{Ic} \tag{6.30}$$

is used.

Even in this case, the gain margin $m_A = 2$.

We choose

$$T_I^* = (4-6)T_{Ic} \tag{6.31}$$

if the nonoscillatory control process is required. In this case the gain margin is $m_A = 4 - 6$ [22, 29].

The ZN closed-loop method is particularly advantageous because it does not assume any knowledge of the plant properties and it is operating with the real plant and the controller. Its major disadvantage is that it must bring the control system to the oscillating stability boundary, i.e. the control system must oscillate, which could cause the plant damage or its nonlinear properties can arise.

Its other disadvantage is that it is too aggressive, which follows from the requirement of the quarter-decay ratio, see Fig. 6.10. After controller tuning by the ZN closed-loop method the real overshoot is from 10 % to 60 %, at an average for the various plants around 25 %. The controller tuning by the ZN closed-loop method is suitable for a stabilizing control in the case when disturbance variable $v(t)$ influences the plant input.

Procedure:

1. All connections of the control system and the functionality of all its elements must be checked.
2. The desired variable (set-point) value $w(t)$ is set and in the manual mode $y(t) \approx w(t)$ is set too, the integral component ($T_I \to \infty$) and the derivative component ($T_D \to 0$) are shut down, the controller gain K_P is decreased and the controller is switched to the automatic mode.
3. The controller gain K_P is subsequently increased as for a small change of the desired variable $w(t)$ the stable oscillation arises which corresponds to the oscillating stability boundary.
4. From the periodic course of any control system variable the ultimate period T_c and from the P controller settings – the ultimate gain K_{Pc} are determined.
5. For the chosen controller on the basis of Tab. 6.1 (Tab. 6.2 – Tyreus-Lyuben) the values of the adjustable parameters are determined.

6.2.2 Tyreus-Lyuben method

The procedure for controller tuning by this method is the same as for the ZN closed-loop method. The values of the adjustable parameters are determined on the basis of Tab. 6.2 [2, 17, 22, 29]. From a comparison of the Tabs 6.1 and 6.2 it follows that the TLM (**T**yreus-**L**yuben **m**ethod) is very conservative.

Tab. 6.2 Controller adjustable parameters for the Tyreus-Lyuben method (LTM)

Controller	K_P^*	T_I^*	T_D^*
PI	$0.31K_{Pc}$	$2.2T_c$	–
PID	$0.45K_{Pc}$	$2.2T_c$	$\frac{T_c}{6.3} \doteq 0.16T_c$

6.2.3 Quarter-decay method

The QDM (**q**uarter-**d**ecay **m**ethod) is a modification of the ZN closed-loop method. In contrast to it this method does not assume control system oscillation on the stability boundary and therefore it operates in the linear region and it can be used for more plants [22, 29].

Tab. 6.3 Controller adjustable parameters for the quarter-decay method (QDM)

Controller	K_P^*	T_I^*	T_D^*
P	$K_{P1/4}$	–	–
PI	$0.9K_{P1/4}$	$T_{1/4}$	–
PID	$1.2K_{P1/4}$	$0.6T_{1/4}$	$0.15T_{1/4}$

Procedure:

1. and 2. The same steps like for the ZN closed-loop method.

3. The controller gain K_P is subsequently increased until the step response $y(t)$ caused by the desired variable $w(t)$ has such a course that the ratio of two consecutive amplitudes is equal to 1/4, see Fig. 6.10.

4. The time $T_{1/4}$ is determined from the step response $y(t)$ and the controller gain $K_{P1/4}$ is read from the P controller.

5. For the chosen controller on the basis of Tab. 6.3 the values of its adjustable parameters are determined.

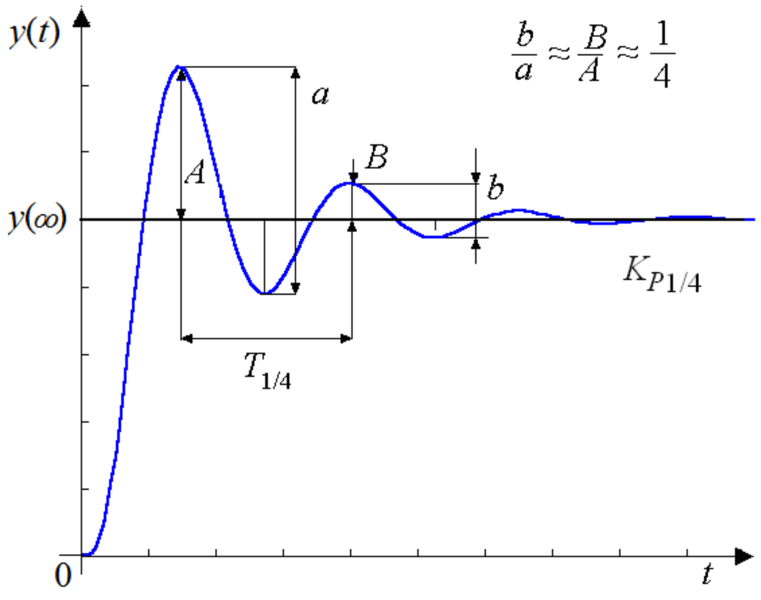

Fig. 6.10 Control system tuning by the quarter-decay method (QDM)

6.2.4 Good gain method

The GGM (**g**ood **g**ain **m**ethod) is similar to the ZN closed-loop method and is described in [6, 29].

Procedure:

1. and 2. The same steps like for the ZN closed-loop method.

3. The controller gain K_P is subsequently increased until the step response $y(t)$, caused by the desired variable $w(t)$, has the course with the overshoot and the

observable undershoot (Fig. 6.11). This course corresponds to the controller gain K_{PGG}. The step of the desired variable $w(t)$ does not cause a nonlinear behaviour, i.e. especially a saturation.

4. The integral time is set to the value

$$T_I^* = 1.5T_{ou} \tag{6.32}$$

and the controller gain is set to the value

$$K_P^* = 0.8K_{PGG}. \tag{6.33}$$

The time T_{ou} is determined in accordance with Fig. 6.11.

5. In case of using the derivative component the derivative time is set to the value

$$T_D^* = 0.25T_I^*. \tag{6.34}$$

When the noise appears or the manipulated variable $u(t)$ is too active, then the use of the derivative component is not suitable and it must be shut down.

6. The final desired course of the controlled variable $y(t)$ is obtained by fine tuning of the controller gain K_P, or the integral time constant T_I.

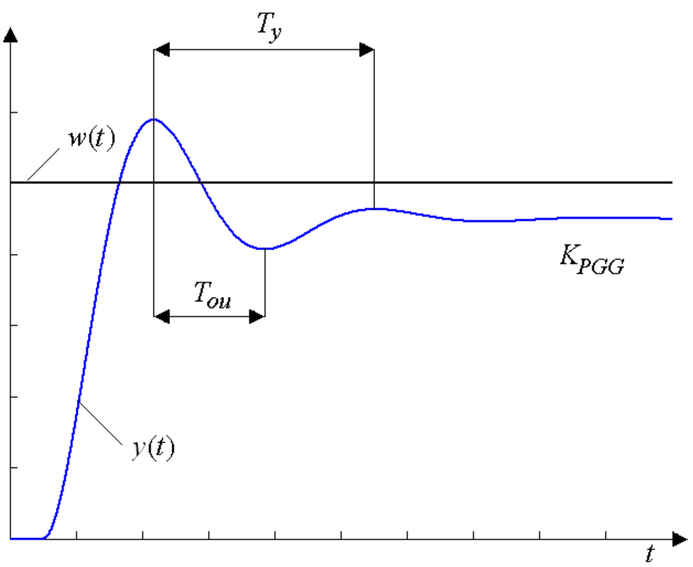

Fig. 6.11 Control system tuning by the good gain method (GGM)

A certain advantage of the GGM is that for the slightly oscillating course the first undershoot can be determined better than the second overshoot.

The GGM is based on the following considerations [6].

It is assumed that the closed-loop control system has the properties that can be expressed by the transfer function

$$G_{wy}(s) = \frac{1}{T_w^2 s^2 + 2\xi_w T_w s + 1}. \tag{6.35}$$

The relative damping ξ_w = 0.6 causes the relative overshoot $\kappa \approx 0.1$ (10 %) and the small observable undershoot. The period of the damped oscillation is

$$T_{GG} = \frac{2\pi T_w}{\sqrt{1-\xi_w^2}} = \frac{2\pi T_w}{0.8} = 2T_{ou}\,.$$

The control system with the transfer function (6.35) will be on the oscillating stability boundary for $\xi_w = 0$ with the ultimate period

$$T_c = 2\pi T_w\,.$$

The relation between the time T_{ou} of a damped oscillation for the GGM and the ultimate period T_c of the undamped oscillations is

$$T_c = 0.8T_{GG} = 1.6T_{ou}\,.$$

For the ZN closed-loop method the relation

$$T_I = \frac{T_c}{1.2} = \frac{1.6T_{ou}}{1.2} = 1.33T_{ou}$$

holds (see Tab. 6.1).

Because the controller tuning by the ZN closed-loop method is too aggressive, therefore the value

$$T_I^* = 1.5T_{ou}$$

is chosen.

For the ZN closed-loop method the PI controller gain K_P^* is a 0.9 multiple of the P controller gain K_P^*. Since the integral component destabilizes the control system, the controller gain K_{PGG} should therefore be decreased, i.e.

$$K_P^* = 0.8K_{PGG}\,.$$

It is obvious that the above mentioned GGM is only applicable to plants which can oscillate with the P controller in accordance with Fig. 6.11.

Example 6.1

For the plant with the transfer function

$$G_P(s) = \frac{1.5}{(4s+1)^3}$$

it is necessary to tune suitable controllers by the (the time constant is in seconds):

a) ZN closed-loop method,

b) TLM,

c) QDM,

d) GGM.

Solution:

a) The experimental ZN closed-loop method

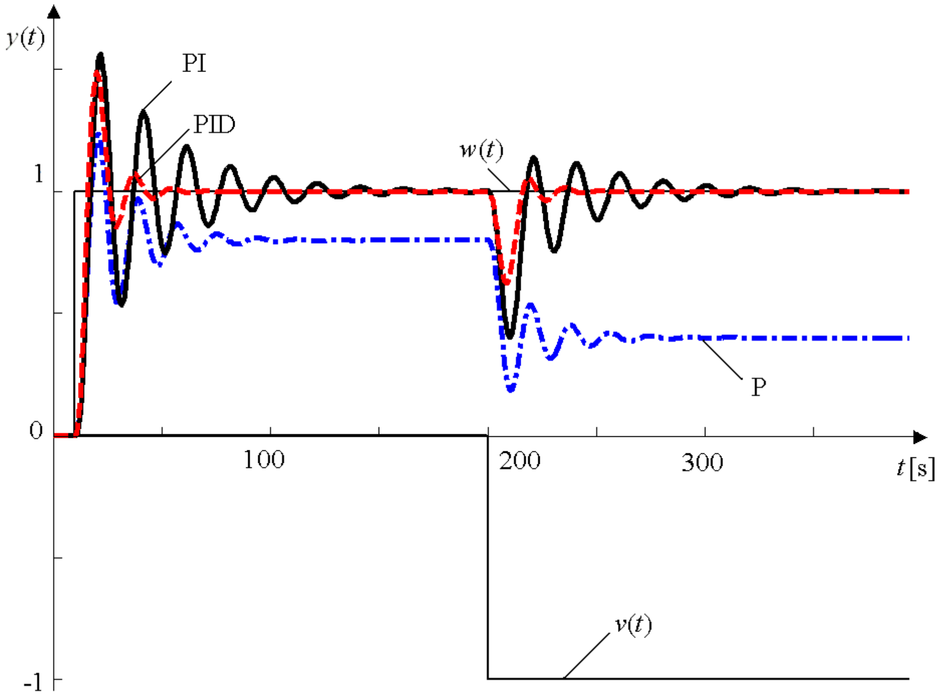

Fig. 6.12 Responses for the control system tuned by the ZN closed-loop method – Example 6.1

After shutting down the integral and the derivative components the controller gain K_P was subsequently increased until for a small change of the desired variable $w(t)$ the oscillating stability boundary was obtained. From the P controller the ultimate gain $K_{Pc} = 5.3$ was read and from the periodic course the ultimate period $T_c = 14.5$ s was obtained. On the basis of Tab. 6.1 the values of the adjustable parameters for chosen controllers were calculated:

P: $K_P^* = 0.5K_{Pc} = 2.65$;

PI: $K_P^* = 0.45K_{Pc} = 2.39$; $T_I^* = 0.83T_c = 12.04\,\text{s}$;

PID: $K_P^* = 0.6K_{Pc} = 3.18$; $T_I^* = 0.5T_c = 7.25\,\text{s}$; $T_D^* = 0.125T_c = 1.81\,\text{s}$.

The responses $y(t)$ for the control system with different controllers tuned by the ZN closed-loop method are shown in Fig. 6.12.

b) The experimental TLM

For the ultimate parameters $K_{Pc} = 5.3$ and $T_c = 14.5$ s obtained in the previous point a) on the basis of Tab. 6.2 the values of the adjustable parameters for chosen controllers were calculated:

PI: $K_P^* = 0.31K_{Pc} = 1.64$; $T_I^* = 2.2T_c = 31.9\,\text{s}$;

PID: $K_P^* = 0.45K_{Pc} = 2.39$; $T_I^* = 2.2T_c = 31.9\,\text{s}$; $T_D^* = 0.16T_c = 2.32\,\text{s}$.

The responses $y(t)$ for the control system with different controllers tuned by the TLM are shown in Fig. 6.13.

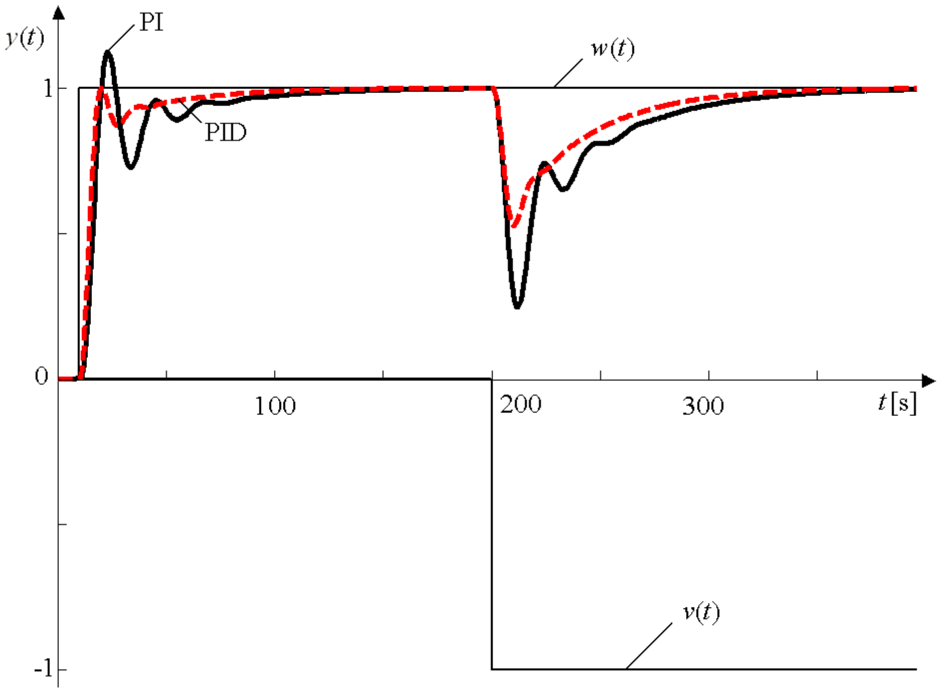

Fig. 6.13 Responses for the control system tuned by TLM – Example 6.1

c) The experimental QDM

After shutting down the integral and the derivative components the controller gain K_P was subsequently increased until the step response $y(t)$ caused by the desired variable $w(t)$ had the course with the ratio $B/A \approx 1/4$ (Fig. 6.10). From the P controller the gain $K_{P1/4} = 1.9$ was read and from the step response $y(t)$ the time $T_{1/4} = 20.5$ s was obtained. On the basis of Tab. 6.3 the values of the adjustable parameters for chosen controllers were calculated:

P: $K_P^* = K_{P1/4} = 1.9$;

PI: $K_P^* = 0.9K_{P1/4} = 1.71$; $T_I^* = T_{1/4} = 20.5$;

PID: $K_P^* = 1.2K_{P1/4} = 2.28$; $T_I^* = 0.6T_{1/4} = 12.3\,\mathrm{s}$; $T_D^* = 0.15T_{1/4} = 3.08\,\mathrm{s}$.

The responses $y(t)$ for the control system with different controllers tuned by the QDM are shown in Fig. 6.14.

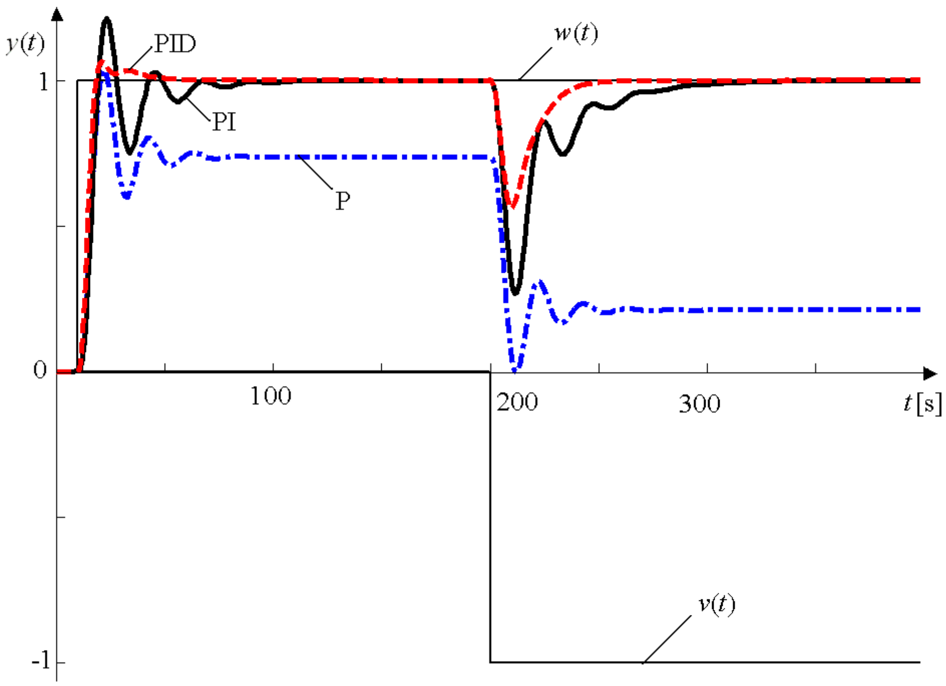

Fig. 6.14 Responses for the control system tuned by QDM – Example 6.1

d) The GGM

After shutting down the integral and the derivative components the controller gain K_P was subsequently increased until the step response $y(t)$ caused by the desired variable $w(t)$ had the course with the overshoot and the observable undershoot in accordance with Fig. 6.11. From the P controller the gain $K_{PGG} = 1.5$ was read and from the step response $y(t)$ the time $T_{ou} = 11.6$ s was obtained. The values of the adjustable parameters were determined on the basis of relations (6.32) – (6.34):

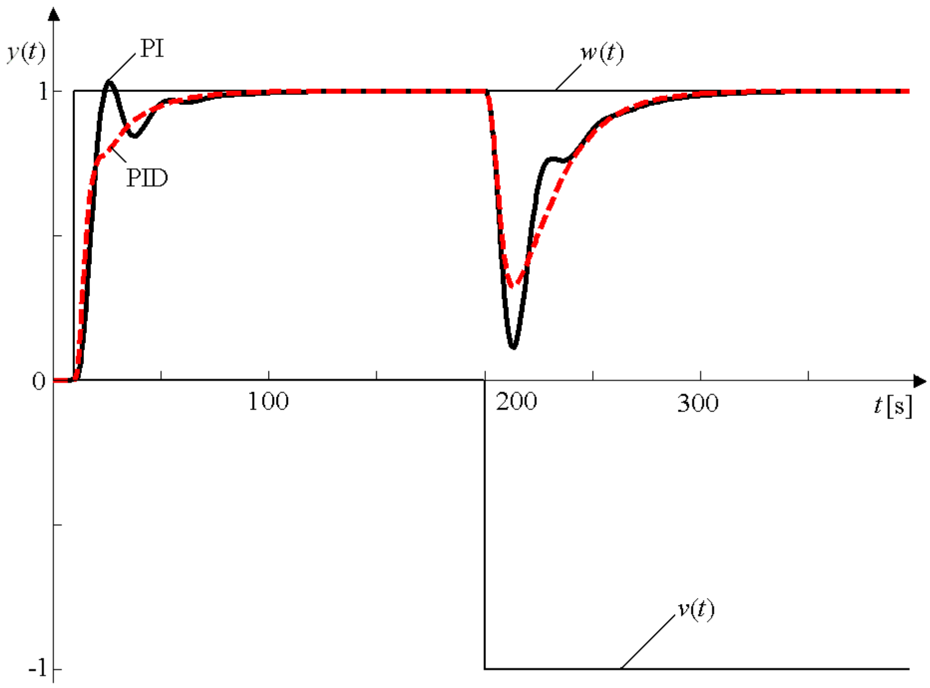

Fig. 6.15 Responses for the control system tuned by GGM – Example 6.1

PI: $K_P^* = 0.8K_{PGG} = 1.2$; $T_I^* = 1.5T_{ou} = 17.6\,\text{s}$;

PID: $K_P^* = 0.8K_{PGG} = 1.2$; $T_I^* = 1.5T_{ou} = 17.6\,\text{s}$; $T_D^* = 0.25T_I^* = 4.4\,\text{s}$.

The responses $y(t)$ for the control system with different controllers tuned by the GGM are shown in Fig. 6.15.

Although on the basis of one plant the described experimental controller tuning methods cannot be objectively assessed, it is clear that the ZN closed-loop method gives an oscillating control process with large overshoots – the tuning is too aggressive. It generally does not ensure the stability. The TLM is less aggressive than the ZN closed-loop method. The great disadvantage of both methods is that they need to bring the control system on the oscillating stability boundary, which is not allowed for most real control systems. Due to great steady-state control errors the P controller is unusable in this case.

The remaining experimental methods are very simple and they give in most cases practically acceptable results.

6.2.5 Ziegler-Nichols open-loop method

The ZN open-loop method (the ZN step response method) is based on the nonoscillatory step response of the proportional plant. From the plant step response the (substitute) time delay T_u, the (substitute) time constant T_n and the plant gain k_1 are determined in accordance with Fig. 4.5a.

The values of the adjustable parameters for the selected controllers are given in Tab. 6.4 [2, 22, 29, 31].

Similarly like for the ZN closed-loop method the destabilizing influence of the integral component in the PI controller is expressed by a decrease of K_P^* in comparison with the P controller and the stabilizing influence of the derivative component (with an appropriate filtration) in the standard PID controller is expressed by an increase of K_P^* (compare with Tab. 6.1). The ratio T_D^*/T_I^* = 1/4.

From Tabs 6.4 and 6.1 it follows that both ZN methods for the P controller ensure the gain margin m_A = 2, that means the double increase of the controller gain K_P^* brings the control system on the oscillating stability boundary.

Tab. 6.4 Controller adjustable parameters for the Ziegler-Nichols open-loop method (ZN open-loop method)

Controller	K_P^*	T_I^*	T_D^*
P	$\dfrac{T_n}{k_1 T_u}$	–	–
PI	$0.9\dfrac{T_n}{k_1 T_u}$	$3.33T_u$	–
PID	$1.2\dfrac{T_n}{k_1 T_u}$	$2T_u$	$0.5T_u$

The ZN open-loop method is generally more aggressive than the ZN closed-loop method [2].

Procedure:

1. From the plant step response the time delay T_u, the time constant T_n and the plant gain k_1 are determined (see Section 4.2, Fig. 4.5a).
2. On the basis of Tab. 6.4 the values of the adjustable parameters for chosen controllers are calculated.

Example 6.2

From the plant step response with the transfer function (see Example 6.1)

$$G_P(s) = \frac{1.5}{(4s+1)^3}$$

its parameters were obtained by the experimental identification: T_u = 3.2 s, T_n = 14.8 s and k_1 = 1.5.

It is necessary to tune the P, PI and PID controllers by the ZN open-loop method.

Solution:

On the basis of Tab. 6.4 we can write:

$$\text{P:}\ \ K_P^* = \frac{T_n}{k_1 T_u} \doteq 3.08\,;$$

$$\text{PI:}\ \ K_P^* = 0.9\frac{T_n}{k_1 T_u} \doteq 2.78\,; \quad T_I^* = 3.33 T_u \doteq 10.66 \ \text{s};$$

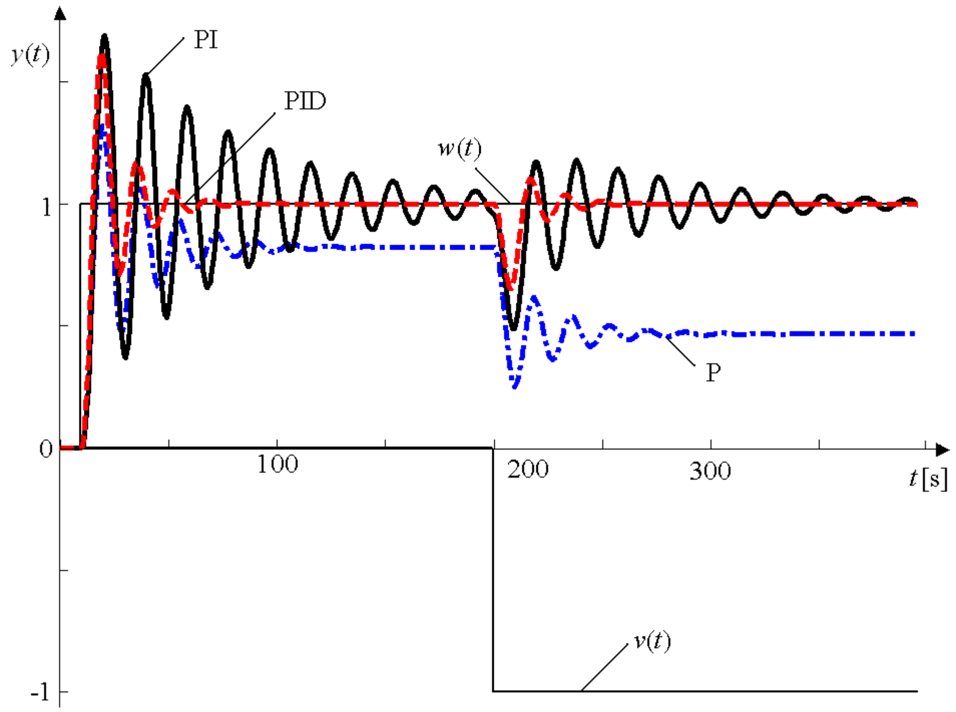

Fig. 6.16 Responses for control system tuned by the ZN open-loop method – Example 6.2

$$\text{PID: } K_P^* = 1.2\frac{T_n}{k_1 T_u} \doteq 3.08; \quad T_I^* = 2T_u = 6.4\,\text{s}; \quad T_D^* = 0.5T_u = 1.6\,\text{s}.$$

The responses $y(t)$ for the control system with different controllers tuned by the ZN open-loop method are shown in Fig. 6.16. We can see that the ZN open-loop method is really more aggressive than the ZN closed-loop method (compare with Fig. 6.12). The P controller is unusable in this case too.

6.2.6 „Universal“ experimental method

From the many existing experimental controller tuning methods the very simple and in most practical cases effective method, here called the UEM ("**u**niversal" **e**xperimental **m**ethod) is given below. It was developed in the former USSR [4, 9]. It is suitable for systems with transfer functions (Tabs 6.5 and 6.6)

$$G_P(s) = \frac{k_1}{T_1 s + 1} \mathrm{e}^{-T_d s} \tag{6.36}$$

and

$$G_P(s) = \frac{k_1}{s} \mathrm{e}^{-T_d s}. \tag{6.37}$$

The UEM is quite similar to the Chien-Hrones-Reswick method [2].

The UEM enables conventional controller tuning both from the point of view of the desired variable $w(t)$ (servo problem) and the disturbance variable $v(t)$ (regulatory problem) which acts on the plant input for three control performance indices (criteria): the fastest response without overshoot, the fastest response with relative overshoot κ = 0.2 (20 %) and the minimum of the integral of the squared error (ISE). Here the control process with the maximum relative overshoot from 0.02 (2 %) to 0.05 (5 %) is considered as the fastest response without overshoot.

Procedure:

1. The plant transfer function must be converted on one form (6.36) or (6.37) on the basis of the methods described in Section 4.2.
2. According to the control performance requirements the suitable controller, the kind of control process (without the overshoot, with the overshoot 20 %, minimum of ISE) and the purpose (the servo or regulatory problem) are chosen and then on the basis of Tab. 6.5 for the plant transfer function (6.36) or Tab. 6.6 for the plant transfer function (6.37) the values of the controller adjustable parameters are computed.

Example 6.3

For the plant with transfer function (see Examples 6.1 and 6.2)

$$G_P(s) = \frac{1.5}{(4s+1)^3}$$

it is necessary to tune the PI controller (the time constant is in seconds).

Tab. 6.5 Controller adjustable parameters for the "universal" experimental method (UEM)

$\frac{k_1}{T_1 s+1}\mathrm{e}^{-T_d s}$		Control process				
		Fastest response without overshoot		Fastest response with overshoot 20 %		Minimum of ISE
Controller		Tuning from the point of view				
		Desired variable *w*	Disturbance variable *v*	Desired variable *w*	Disturbance variable *v*	Disturbance variable *v*
P	K_P^*	$0.3\frac{T_1}{k_1T_d}$	$0.3\frac{T_1}{k_1T_d}$	$0.7\frac{T_1}{k_1T_d}$	$0.7\frac{T_1}{k_1T_d}$	–
PI	K_P^*	$0.35\frac{T_1}{k_1T_d}$	$0.6\frac{T_1}{k_1T_d}$	$0.6\frac{T_1}{k_1T_d}$	$0.7\frac{T_1}{k_1T_d}$	$\frac{T_1}{k_1T_d}$
	T_I^*	$1.17T_1$	$0.8T_d+0.5T_1$	T_1	$T_d+0.3T_1$	$T_d+0.35T_1$
PID	K_P^*	$0.6\frac{T_1}{k_1T_d}$	$0.95\frac{T_1}{k_1T_d}$	$0.95\frac{T_1}{k_1T_d}$	$1.2\frac{T_1}{k_1T_d}$	$1.4\frac{T_1}{k_1T_d}$
	T_I^*	T_1	$2.4T_d$	$1.36T_1$	$2T_d$	$1.3T_d$
	T_D^*	$0.5T_d$	$0.4T_d$	$0.64T_d$	$0.4T_d$	$0.5T_d$

Tab. 6.6 Controller adjustable parameters for the "universal" experimental method (UEM)

$\frac{k_1}{s}\mathrm{e}^{-T_d s}$		Control process				
		Fastest response without overshoot		Fastest response with overshoot 20 %		Minimum of ISE
Controller		Tuning from the point of view				
		Desired variable *w*	Disturbance variable *v*	Desired variable *w*	Disturbance variable *v*	Disturbance variable *v*
P	K_P^*	$0.37\frac{1}{k_1T_d}$	$0.37\frac{1}{k_1T_d}$	$0.7\frac{1}{k_1T_d}$	$0.7\frac{1}{k_1T_d}$	–
PI	K_P^*	$0.37\frac{1}{k_1T_d}$	$0.46\frac{1}{k_1T_d}$	$0.7\frac{1}{k_1T_d}$	$0.7\frac{1}{k_1T_d}$	$\frac{1}{k_1T_d}$
	T_I^*	∞	$5.75T_d$	∞	$3T_d$	$4.3T_d$
PID	K_P^*	$0.65\frac{1}{k_1T_d}$	$0.65\frac{1}{k_1T_d}$	$1.1\frac{1}{k_1T_d}$	$1.1\frac{1}{k_1T_d}$	$1.36\frac{1}{k_1T_d}$
	T_I^*	∞	$5T_d$	∞	$2T_d$	$1.6T_d$
	T_D^*	$0.4T_d$	$0.23T_d$	$0.53T_d$	$0.37T_d$	$0.5T_d$

Solution:

The plant transfer function $G_P(s)$ has not the desired form (6.36), and therefore in accordance with the scheme (4.37) and Tab. 4.1 we can write ($i = 3$, $k_1 = 2$, $T_3 = 4$ s, $T_{d3} = 0$ s):

$$\frac{T_1}{T_3} = 1.980 \qquad \Rightarrow \qquad T_1 = 1.98 \cdot 4 = 7.92\,\text{s};$$

$$\frac{T_{d1} - T_{d3}}{T_3} = 1.232 \quad \Rightarrow \quad T_{d1} = 1.232 \cdot 4 + 0 \doteq 4.93\,\text{s};$$

$$G_P(s) = \frac{1.5}{(4s+1)^3} \approx \frac{k_1}{T_1 s + 1}\mathrm{e}^{-T_{d1}s} = \frac{1.5}{7.92s+1}\mathrm{e}^{-4.93s}.$$

The PI controller tuning from the point of view of the desired variable $w(t)$ (Tab. 6.5):

a) without overshoot (0 %)

$$K_P^* = 0.35\frac{T_1}{k_1 T_{d1}} \doteq 0.37; \quad T_I^* = 1.17T_1 \doteq 9.27\,\text{s};$$

b) with overshoot 0.2 (20 %)

$$K_P^* = 0.6\frac{T_1}{k_1 T_{d1}} \doteq 0.64; \quad T_I^* = T_1 = 7.92\,\text{s};$$

The PI controller tuning from the point of view of the disturbance variable $v(t)$ which acts on the plant input (Tab. 6.5):

a) without overshoot (0 %)

$$K_P^* = 0.6\frac{T_1}{k_1 T_{d1}} \doteq 0.64; \quad T_I^* = 0.8T_{d1} + 0.5T_1 \doteq 7.90\,\text{s};$$

b) with overshoot 0.2 (20 %)

$$K_P^* = 0.7\frac{T_1}{k_1 T_{d1}} \doteq 0.75; \quad T_I^* = T_{d1} + 0.3T_1 \doteq 7.31\text{s};$$

c) minimum of ISE

$$K_P^* = \frac{T_1}{k_1 T_{d1}} \doteq 1.07; \quad T_I^* = T_{d1} + 0.35T_1 \doteq 7.70\,\text{s}.$$

The responses of the control system with the PI controller tuned by the UEM from point of view of the desired variable $w(t)$ are shown in Fig. 6.17a and from point of view of the disturbance variable $v(t)$ which acts on the plant input are shown in Fig. 6.17b.

From both figures it is evident that the UEM gives acceptable results even for a very rough approximation of the plant transfer function.

Example 6.4

It is necessary to tune the PI controller by the UEM for the integrating plant with the transfer function

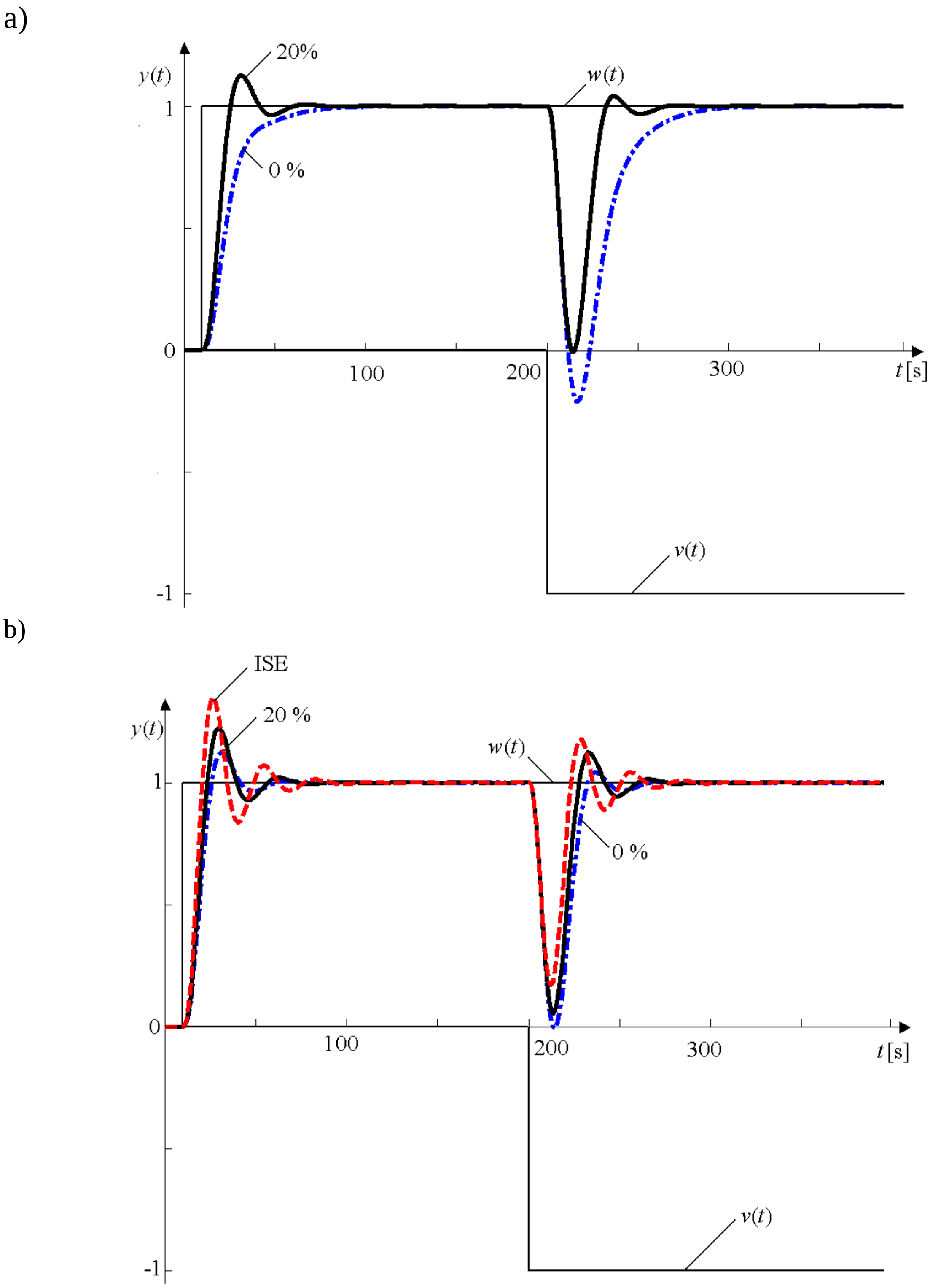

Fig. 6.17 Responses of the control system with the PI controller tuned by the UEM from the point of view: a) desired variable $w(t)$, b) disturbance variable $v(t)$ – Example 6.3

$$G_P(s) = \frac{0.05}{s(s+1)} e^{-4s} .$$

The time constant and the time delay are in seconds.

Solution:

The plant transfer function must be converted to the form (6.37). In accordance with the relation (4.44) for T_1 = 1 s and T_{d1} = 4 s we can write:

$$T_d = T_{d1} + T_1 = 5 \text{ s};$$

$$G_P(s) = \frac{0.05}{s(s+1)} \mathrm{e}^{-4s} \approx \frac{0.05}{s} \mathrm{e}^{-5s} .$$

The PI controller tuning from the point of view of the desired variable $w(t)$ (Tab. 6.6):

a) without overshoot (0 %)

$$K_P^* = 0.37 \frac{1}{k_1 T_d} \doteq 1.48; \quad T_I^* = \infty;$$

b) with overshoot 0.2 (20 %)

$$K_P^* = 0.7 \frac{1}{k_1 T_d} = 2.8; \quad T_I^* = \infty .$$

The PI controller tuning from the point of view of the disturbance variable $v(t)$ which acts on the plant input (Tab. 6.6):

a) without overshoot (0 %)

$$K_P^* = 0.46 \frac{1}{k_1 T_d} \doteq 1.84; \quad T_I^* = 5.75 T_d = 28.75 \,\text{s};$$

b) with overshoot 0.2 (20 %)

$$K_P^* = 0.7 \frac{1}{k_1 T_d} = 2.8; \quad T_I^* = 3T_d = 15 \,\text{s};$$

c) minimum of ISE

$$K_P^* = \frac{1}{k_1 T_d} = 4, \quad T_I^* = 4.3 T_d = 21.5 \,\text{s}.$$

The responses of the control system with the PI controller tuned by the UEM are shown in Fig. 6.18. From Figure 6.18a it follows that regulatory responses are unacceptable. It is caused by a shut down of the integral component ($T_I^* = \infty$) of the PI controller, which converts to the P regulator. Servo responses for integrating plants and for a conventional controller with an integrating component always contain very big overshoots which cannot be removed by any tuning [29, 30]. In our case see Fig. 6.18b. The unacceptable overshoots can be supressed by the use of a suitable input filter or a 2DOF controller.

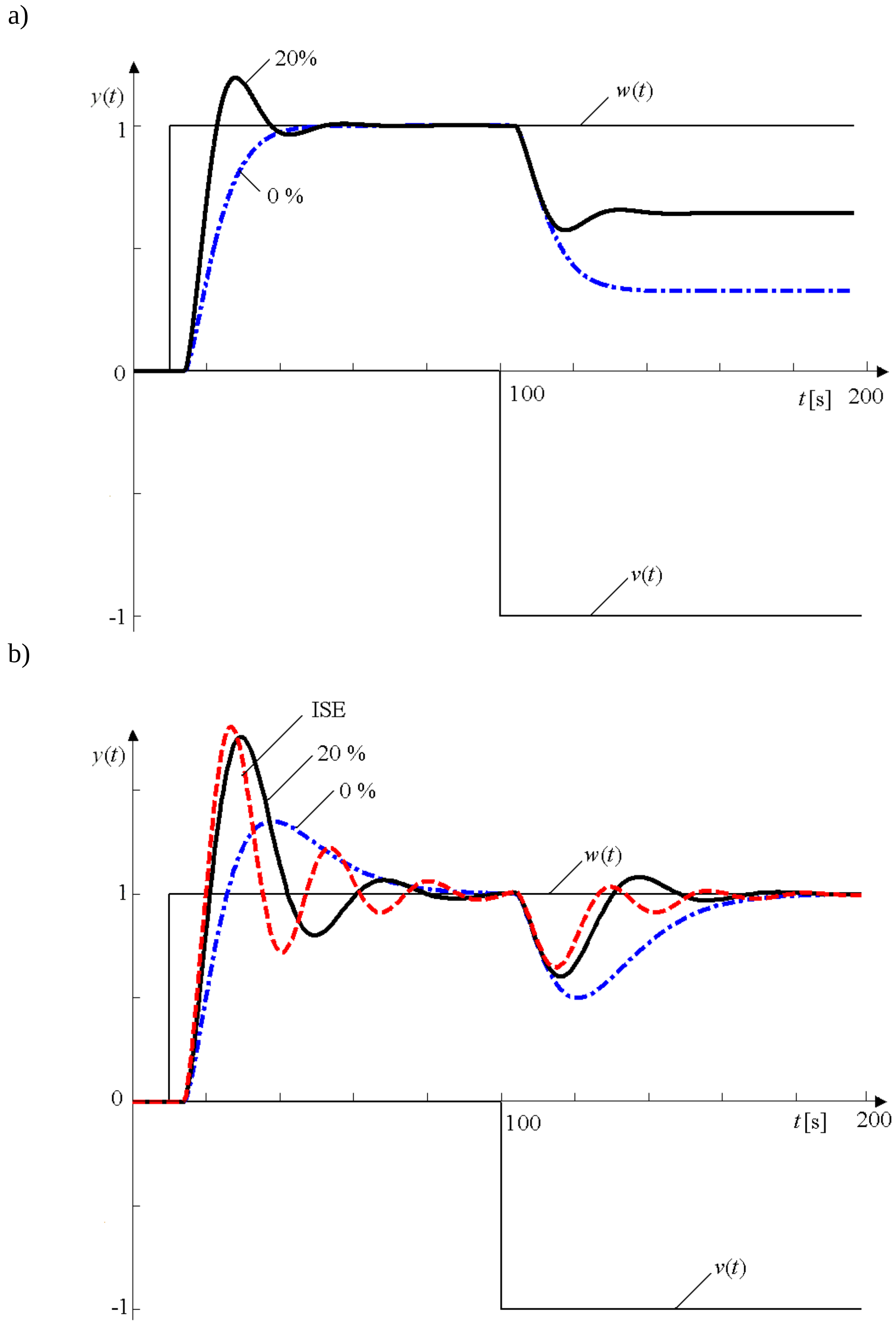

Fig. 6.18 Responses of the control system with the PI controller tuned by the UEM from the point of view: a) desired variable $w(t)$, b) disturbance variable $v(t)$ – Example 6.4

6.2.7 SIMC method

The SIMC method belongs among simple but effective controller tuning methods [20]. It is based on the internal model control – IMC (**i**nternal **m**odel **c**ontrol), and therefore its author suggests shortening the SIMC interpret as "Simple Control" or

"Skogestad IMC". Although the SIMC method is based on the IMC method for the controller design uses the formula for the direct synthesis (e.g. see Fig. 6.3)

$$G_C(s) = \frac{1}{G_P(s)} \frac{G_{wy}(s)}{1 - G_{wy}(s)}, \tag{6.38}$$

where

$$G_P(s) = G_P'(s) \mathrm{e}^{-T_d s} \tag{6.39}$$

is the plant transfer function and

$$G_{wy}(s) = \frac{1}{T_w s + 1} \mathrm{e}^{-T_d s} \tag{6.40}$$

is the desired control system transfer function and T_w is the time constant of the closed-loop control system.

After substitution (6.39) and (6.40) in (6.38) the controller transfer function

$$G_C(s) = \frac{1}{G_P'(s)} \frac{1}{T_w s + 1 - \mathrm{e}^{-T_d s}} \tag{6.41}$$

is obtained.

By the use of the approximation

$$\mathrm{e}^{-T_d s} \approx 1 - T_d s \tag{6.42}$$

the simplified controller transfer function

$$G_C(s) = \frac{1}{G_P'(s)} \frac{1}{(T_w + T_d)s} \tag{6.43}$$

is obtained.

The controller design procedure will be shown for the plant with the transfer function

$$G_P(s) = \frac{k_1}{(T_1 s + 1)(T_2 s + 1)} \mathrm{e}^{-T_d s}, \quad T_1 \geq T_2. \tag{6.44}$$

It is obvious that

$$G_P'(s) = \frac{k_1}{(T_1 s + 1)(T_2 s + 1)},$$

and therefore after its substitution in (6.43) the controller transfer function

$$G_C(s) = \frac{(T_1 s + 1)(T_2 s + 1)}{k_1 (T_w + T_d)s} = K_P' \left(1 + \frac{1}{T_I' s}\right)(T_D' s + 1) \tag{6.45}$$

is obtained from which follows, that it is the $\mathrm{PID_i}$ controller [the PID controller with serial structure , see (5.27)], where

$$K_P' = \frac{T_1}{k_1 (T_w + T_d)}, \quad T_I' = T_1, \quad T_D' = T_2. \tag{6.46}$$

Tab. 6.7 Controller adjustable parameters for the SIMC method [29]

Plant		Controller			
		Type	$K_P^*(K_P'^*)$	$T_I^*(T_I'^*)$	$T_D^*(T_D'^*)$
1	$k_1\,\mathrm{e}^{-T_d s}$	I	–	$2k_1T_d$	–
2	$\dfrac{k_1}{T_1s+1}\mathrm{e}^{-T_d s}$	PI	$\dfrac{T_1}{2k_1T_d}$	$\min[T_1, 8T_d]$	–
3	$\dfrac{k_1}{(T_1s+1)(T_2s+1)}\mathrm{e}^{-T_d s}$, $T_1 \geq T_2$	PIDi	$\dfrac{T_1}{2k_1T_d}$	$\min[T_1, 8T_d]$	T_2
4*		PID	$\dfrac{T_1+T_2}{2k_1T_d}$	T_1+T_2	$\dfrac{T_1T_2}{T_1+T_2}$
5*			$\dfrac{T_1(T_2+8T_d)}{16k_1T_d^2}$	T_2+8T_d	$\dfrac{8T_2T_d}{T_2+8T_d}$
6	$\dfrac{k_1}{s}\mathrm{e}^{-T_d s}$	PI	$\dfrac{1}{2k_1T_d}$	$8T_d$	–
7	$\dfrac{k_1}{s(T_2s+1)}\mathrm{e}^{-T_d s}$	PIDi	$\dfrac{1}{2k_1T_d}$	$8T_d$	T_2
8		PID	$\dfrac{T_2+8T_d}{16k_1T_d^2}$	T_2+8T_d	$\dfrac{8T_2T_d}{T_2+8T_d}$
9	$\dfrac{k_1}{s^2}\mathrm{e}^{-T_d s}$	PIDi	$\dfrac{1}{16k_1T_d^2}$	$8T_d$	$8T_d$
10		PID	$\dfrac{1}{8k_1T_d^2}$	$16T_d$	$4T_d$

*The row 4 holds for $T_1 \leq 8T_d$, the row 5 for $T_1 > 8T_d$. The adjustable parameters $K_P'^*$, $T_I'^*$ and $T_D'^*$ hold for the PIDi controller (with a serial structure).

By choice of the time constant T_w we can obtain the differently fast responses, but simultaneously also the corresponding requirements on the control variable. It is obvious that for the more aggressive tuning the response will be faster, but at the same time greater demands will be on the control variable.

The time constant T_w is sometimes denoted as λ and then we speak about the λ-tuning.

The tuning on the basis of relations (6.46) gives a very good and fast servo response but in the case

$$T_1 >> T_d \tag{6.47}$$

a very slow regulatory response. Therefore Skogestad modifies the integral time

$$T_I' = \min\left[T_1,\ 4(T_w + T_d)\right]. \tag{6.48}$$

Skogestad recommends the further modification

$$T_w = T_d\,. \tag{6.49}$$

In this way row 3 in Tab. 6.7 was obtained.

The modifications (6.48) and (6.49) give a relatively fast regulatory response and simultaneously ensure a good robustness of the tuning [20], see Tab. 6.8.

The cases in rows 1, 2, 3 (for $T_1 \le 8T_d$) and 4 in Tab. 6.7 are the same as for the desired model method for the relative overshoot $\kappa \approx 0.05$ (5 %), see Paragraph 6.2.8.

Tab. 6.8 Basic control performance indices for the control system tuned by the SIMC method in accordance with Tab. 6.7

Control performance indices	Rows in Tab. 6.7	
	1, 2, 3 (for $T_1 \le 8T_d$) and 4	6, 7
M_S	1.59	1.70
m_A	3.14	2.96
m_L [dB]	9.94	9.43
γ [deg]	61.4	46.9
γ [rad]	1.07	0.82
$A_{wy}(\omega_R)$	1.00	1.30
$\omega_p T_d$	1.57	1.49
$\omega_g T_d$	0.50	0.51
$\Delta T_d / T_d$	2.14	1.59

For $T_1 \le 4(T_w + T_d)$ or $T_1 \le 8T_d$ the SIMC method is the compensation method because the numerator of the controller transfer function cancels the corresponding term in the denominator of the plant transfer function.

The basic control performance indices for the SIMC method (Tab. 6.7) are in Tab. 6.8 [20].

For rows 2, 3 (for $T_1 > 8T_d$) and 5 in Tab. 6.7 the values of the control performance indices lie between the values in the left and right columns whereas the right column is the limit case.

In the last row in Tab. 6.8 the **relative delay margin** is

$$\frac{\Delta T_d}{T_d} = \frac{\gamma}{\omega_g T_d}\,. \tag{6.50}$$

It expresses the relative time delay change which causes a loss of control system stability [13].

The values of the control performance indices in Tab. 6.8 are in the recommended limits [see relations (6.9), (6.17), (6.18) and (6.24)] and show a good robustness of the control system tuned by the SIMC method (Tab. 6.7).

The last two rows in the Tab. 6.7 are related to the integrating systems of the second order with a time delay for which a conventional controller tuning is a very difficult problem, because in this case the type of the control system is $q = 3$.

Procedure:

1. The plant transfer function is converted on the basis of any methods from Section 4.2 to a suitable form in accordance with Tab. 6.7. The form of the plant transfer function simultaneously determines the recommended controller.
2. For the recommended controller the values of its adjustable parameters are computed on the basis of Tab. 6.7.

Example 6.5

For the plant with the transfer function

$$G_P(s) = \frac{1}{(6s+1)(4s+1)(2s+1)} \mathrm{e}^{-3s}$$

it is necessary to tune the PI and PID controllers by the SIMC method (the time constants and the time delay are in seconds).

Solution:

In accordance with the "half rule" we can write ($T_{10} = 6$ s, $T_{20} = 4$ s, $T_{30} = 2$ s, $T_{d0} = 3$ s, $k_1 = 1$):

a) The transfer function (4.29) [see (4.54)]

$$T_1 = T_{10} + \frac{T_{20}}{2} = 8\,\mathrm{s}, \quad T_d = T_{d0} + \frac{T_{20}}{2} + T_{30} = 7\,\mathrm{s};$$

$$G_P(s) = \frac{1}{(6s+1)(4s+1)(2s+1)} \mathrm{e}^{-3s} \approx \frac{1}{8s+1} \mathrm{e}^{-7s}.$$

Since $T_1 < 8T_d$ on the basis of the row 2 in Tab. 6.7 there is obtained

$$K_P^* = 0.57; \quad T_I^* = 8\,\mathrm{s}.$$

b) The transfer function (4.35) [see (4.55)]

$$T_1 = T_{10} = 6\,\mathrm{s}, \quad T_2 = T_{20} + \frac{T_{30}}{2} = 5\,\mathrm{s}, \quad T_d = T_{d0} + \frac{T_{30}}{2} = 4\,\mathrm{s};$$

$$G_P(s) = \frac{1}{(6s+1)(4s+1)(2s+1)} \mathrm{e}^{-3s} \approx \frac{1}{(6s+1)(5s+1)} \mathrm{e}^{-4s}.$$

Since $T_1 < 8T_d$ on the basis of the row 4 in Tab. 6.7 there is obtained

$$K_P^* = 1.38; \quad T_I^* = 11\,\mathrm{s}; \quad T_D^* = 2.73\,\mathrm{s}.$$

The responses of the control system tuned by the SIMC method are shown in Fig. 6.19. It is evident that the SIMC method gives for very rough approximations of the plant transfer function results which can be successfully used in practice.

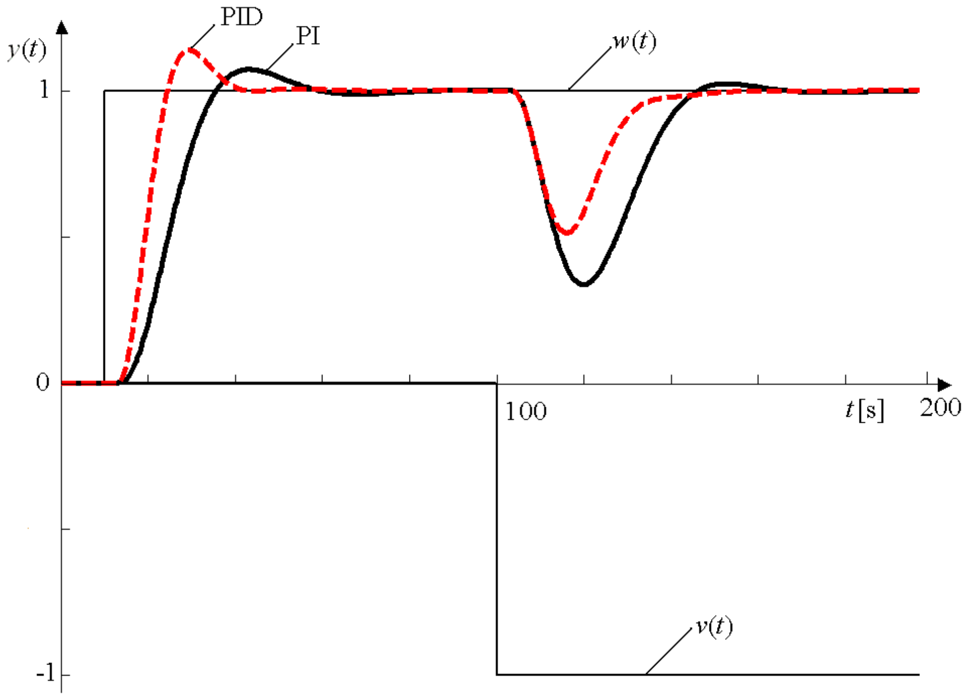

Fig. 6.19 Responses of the control system tuned by the SIMC method – Example 6.5

6.2.8 Desired model method

The DMM (**d**esired **m**odel **m**ethod), formerly also known as inverse dynamics method, was developed at the Faculty of Mechanical Engineering, Technical University of Ostrava [22, 29]. This method is very simple.

The DMM uses the formula for the direct synthesis (6.38)

$$G_C(s) = \frac{1}{G_P(s)} \frac{G_{wy}(s)}{1 - G_{wy}(s)}, \tag{6.51}$$

where

$$G_P(s) = G_P'(s) \mathrm{e}^{-T_d s} \tag{6.52}$$

is the plant transfer function and

$$G_{wy}(s) = \frac{k_o}{s + k_o \mathrm{e}^{-T_d s}} \mathrm{e}^{-T_d s} \tag{6.53}$$

is the desired control system transfer function and k_o is the open-loop gain.

The simple open-loop transfer function

$$G_o(s) = G_C(s) G_P(s) = \frac{k_o}{s} \mathrm{e}^{-T_d s} \tag{6.54}$$

corresponds to the desired control system transfer function (6.53).

After substitution (6.52) and (6.53) in (6.51) the transfer function of the designed controller

$$G_C(s) = \frac{k_o}{sG'_P(s)} \tag{6.55}$$

is obtained.

It is obvious that the same transfer function (6.55) will be obtained for (6.52) on the basis of the open-loop transfer function (6.54).

In order for the conventional controller transfer function to be obtained on the basis of the formula (6.55) the plant transfer function must have one of the forms in Tab. 6.9. If it is necessary to use a concrete controller then the plant transfer function must be converted to a corresponding form.

It is very important that the plant transfer functions in Tab. 6.9 in the part $G'_P(s)$ have not any unstable zeros and poles, and therefore the use of the formula (6.51) or (6.55) is fully correct.

For instance for a plant with transfer function

$$G_P(s) = \frac{k_1}{(T_1 s+1)(T_2 s+1)} \mathrm{e}^{-T_d s}, \ T_1 \geq T_2 \tag{6.56}$$

for [see (6.52)]

$$G'_P(s) = \frac{k_1}{(T_1 s+1)(T_2 s+1)}$$

after substitution in (6.55), the transfer function of the PID$_i$ controller gets

$$G_C(s) = \frac{k_o(T_1 s+1)(T_2 s+1)}{k_1 s} = K'_P \frac{(T'_I s+1)(T'_D s+1)}{T'_I s},$$

where

$$K'_P = \frac{k_o T_1}{k_1}, \quad T'^*_I = T_1, \quad T'^*_D = T_2 . \tag{6.57}$$

After using the conversion relations (5.29) the transfer function (5.26) of the conventional PID controller with adjustable parameters there will be obtained

$$K_P = \frac{k_o(T_1+T_2)}{k_1}, \quad T^*_I = T_1 + T_2, \quad T^*_D = \frac{T_1 T_2}{T_1+T_2} . \tag{6.58}$$

Similarly in this simple way we can get relations for the adjustable parameters of conventional controllers for all remaining rows in Tab. 6.9.

There remains to determine the appropriate open-loop gain k_o. The desired control system transfer function (6.53) in the form of the anisochronous mathematical model [32] has the advantage not only in its relative simplicity, but also in the fact that by changing the open-loop gain k_o different servo responses can be easily achieved, i.e. a different control performance can be obtained, see Fig. 6.20.

The open-loop gain k_o for the critical nonoscillatory control process and for the oscillatory control process on the oscillating stability boundary can be easily determined analytically assuming that the non-dominant poles and zeros of the control system have a negligible influence on its behaviour [22, 29].

From the characteristic quasipolynomial of the control system [see the denominator of the desired control system transfer function (6.53)]

$$N(s) = s\,\mathrm{e}^{T_d s} + k_o \tag{6.59}$$

the double real dominant pole s_2 and the corresponding open-loop gain k_o can be determined from the equations

$$\left.\begin{aligned} N(s) &= 0 \\ \frac{\mathrm{d}\,N(s)}{\mathrm{d}\,s} &= 0 \end{aligned}\right\} \Rightarrow \left.\begin{aligned} s\,\mathrm{e}^{T_d s} + k_o &= 0 \\ T_d s + 1 &= 0 \end{aligned}\right\} \Rightarrow \begin{aligned} s_2 &= -\frac{1}{T_d}, \\ k_o &= \frac{1}{\mathrm{e}\,T_d}. \end{aligned} \tag{6.60}$$

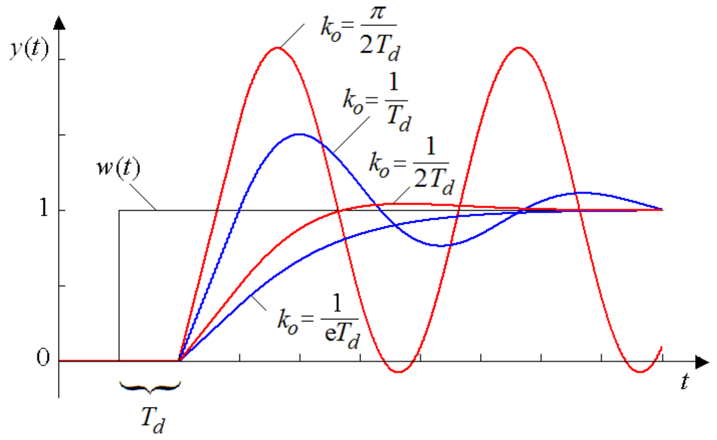

Fig. 6.20 Influence of the open-loop gain k_o on servo step responses

The open-loop gain k_o for the oscillating stability boundary (i.e. the ultimate open-loop gain) can be obtained for $s_{1,2} = \pm\,\mathrm{j}\omega_c$ from the characteristic equation

$$s\,\mathrm{e}^{T_d s} + k_o = 0 \tag{6.61}$$

as a main solution, i.e.

$$\pm\,\mathrm{j}\omega_c\,\mathrm{e}^{\pm \mathrm{j}\omega_c T_d} + k_o = 0 \;\Rightarrow\; \omega_c = \frac{\pi}{2T_d},\;\; k_o = \frac{\pi}{2T_d}. \tag{6.62}$$

For solving the complex equation (6.61) the Euler formula

$$\mathrm{e}^{\pm \mathrm{j}x} = \cos x \pm \mathrm{j}\sin x \tag{6.63}$$

was used.

From both relations (6.60) and (6.62) which express the open-loop gain k_o, the conclusion may be made, that it can be written in the form

$$k_o = \frac{1}{\beta T_d}, \tag{6.64}$$

where β is the coefficient depending on the relative overshoot κ [see Fig. 6.20 and relation (6.1)]

$$\begin{aligned} \kappa = 0 &\Rightarrow \beta = \mathrm{e}, \\ \kappa = 1 &\Rightarrow \beta = \frac{2}{\pi}. \end{aligned} \tag{6.65}$$

In order to determine the dependence of the coefficient β on the relative overshoot κ, it is necessary to compare the two dominant poles of the control system with transfer function (6.53) (see Fig. 6.21)

$$s_{1,2} = -\omega \operatorname{cotg} \varphi \pm \mathrm{j}\omega \tag{6.66}$$

with the corresponding pair of the poles of the control system with the transfer function (see Fig. 6.21)

$$G_{wy}(s) = \frac{\omega_w^2}{s^2 + 2\xi_w \omega_w s + \omega_w^2} \mathrm{e}^{-T_d s}, \tag{6.67}$$

where ξ_w and ω_w is the relative damping and the natural angular frequency of the control system.

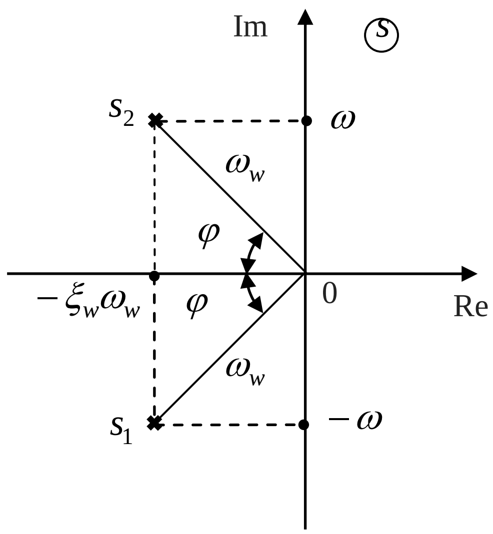

Fig. 6.21 Position of the dominant poles of a control system in complex plane *s*

After substitution of (6.66) in (6.61) and modification the complex equation

$$-\omega \operatorname{cotg} \varphi \pm \mathrm{j}\omega + k_o \mathrm{e}^{-T_d(-\omega \operatorname{cotg}\varphi \pm \mathrm{j}\omega)} = 0 \tag{6.68}$$

is obtained.

The complex equation (6.68) after considering the Euler formula (6.63) can be expressed in the form of two real equations

$$\begin{aligned} -\omega \operatorname{cotg} \varphi + k_o \mathrm{e}^{\omega T_d \operatorname{cotg}\varphi} \cos \omega T_d &= 0, \\ \omega - k_o \mathrm{e}^{\omega T_d \operatorname{cotg}\varphi} \sin \omega T_d &= 0, \end{aligned} \tag{6.69}$$

the main solution is

$$\omega = \frac{\varphi}{T_d},$$
$$k_o = \frac{\varphi}{T_d \sin\varphi} \mathrm{e}^{-\frac{\varphi}{\operatorname{tg}\varphi}}. \tag{6.70}$$

Tab. 6.9 Controller adjustable parameters for the desired model method (DMM)

Plant transfer function		Controller				
		Type	$K_P^*(K_P'^*)$		$T_I^*(T_I'^*)$	$T_D^*(T_D'^*)$
			$T_d = 0$	$T_d > 0$		
1	$\frac{k_1}{s}\mathrm{e}^{-T_d s}$	P	$\frac{1}{k_1 T_w}$	$\frac{1}{k_1 \beta T_d}$	–	–
2	$\frac{k_1}{T_1 s + 1}\mathrm{e}^{-T_d s}$	PI	$\frac{T_1}{k_1 T_w}$	$\frac{T_1}{k_1 \beta T_d}$	T_1	–
3	$\frac{k_1}{s(T_1 s + 1)}\mathrm{e}^{-T_d s}$	PD	$\frac{1}{k_1 T_w}$	$\frac{1}{k_1 \beta T_d}$	–	T_1
4	$\frac{k_1}{(T_1 s + 1)(T_2 s + 1)}\mathrm{e}^{-T_d s}$ $T_1 \ge T_2$	PIDi	$\frac{T_1}{k_1 T_w}$	$\frac{T_1}{k_1 \beta T_d}$	T_1	T_2
5		PID	$\frac{T_1 + T_2}{k_1 T_w}$	$\frac{T_1 + T_2}{k_1 \beta T_d}$	$T_1 + T_2$	$\frac{T_1 T_2}{T_1 + T_2}$
6	$\frac{k_1}{T_0^2 s^2 + 2\xi_0 T_0 s + 1}\mathrm{e}^{-T_d s}$ $0.5 < \xi_0 \le 1$	PID	$\frac{2\xi_0 T_0}{k_1 T_w}$	$\frac{2\xi_0 T_0}{k_1 \beta T_d}$	$2\xi_0 T_0$	$\frac{T_0}{2\xi_0}$

The adjustable parameters $K_P'^*$, $T_I'^*$ and $T_D'^*$ hold for the $\mathrm{PID_i}$ controller (with a serial structure).

The coefficient β is given by formula [see (6.64)]

$$\beta = \frac{\sin\varphi}{\varphi} \mathrm{e}^{\frac{\varphi}{\operatorname{tg}\varphi}}. \tag{6.71}$$

For instance it is obvious that for

$$\varphi = 0 \Rightarrow \beta = \mathrm{e} \Rightarrow k_o = \frac{1}{\mathrm{e} T_d}$$

and

$$\varphi = \frac{\pi}{2} \Rightarrow \beta = \frac{2}{\pi} \Rightarrow k_o = \frac{\pi}{2T_d},$$

the same results like (6.60) and (6.62) were obtained.

Since the angle φ (Fig. 6.21) for the control system with the transfer function (6.67) is given by the relative damping ξ_w, i.e.

$$\varphi = \arccos \xi_w \,, \tag{6.72}$$

therefore the desired servo step response can be obtained by the suitable choice of the relative damping ξ_w.

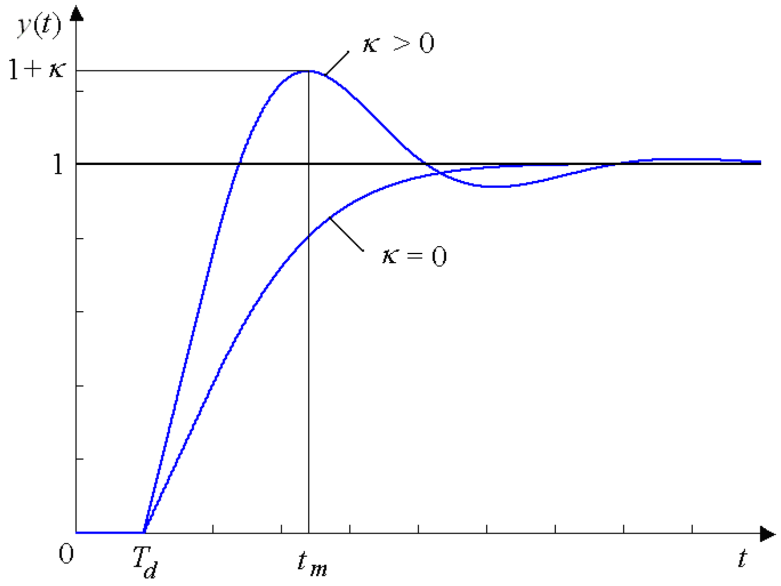

Fig. 6.22 Servo step responses of the control system

In practice the use of the relative overshoot κ is preferable instead of the relative damping ξ_w (Fig. 6.22). The relative overshoot κ can be determined from the step response obtained from the transfer function (6.67)

$$y(t) = \left\{1 - \frac{\omega_w}{\omega} \mathrm{e}^{-(t-T_d)\xi_w\omega_w} \sin\left[(t-T_d)\omega + \arcsin\frac{\omega}{\omega_w}\right]\right\}\eta(t-T_d)\,, \tag{6.73a}$$

$$\frac{\omega}{\omega_w} = \sqrt{1-\xi_w^2}\,, \tag{6.73b}$$

where $\eta(t)$ is the unit Heaviside step.

The maximum overshoot appears in time t_m, when the derivative of the step response (6.73) with respect time t (i.e. the impulse response)

$$\frac{\mathrm{d}\,y(t)}{\mathrm{d}\,t} = \left\{\frac{\omega_w^2}{\omega} \mathrm{e}^{-(t-T_d)\xi_w\omega_w} \sin[(t-T_d)\omega]\right\}\eta(t-T_d) \tag{6.74}$$

will be for $t > T_d$ for the first time equal to zero, i.e.

$$t_m = \frac{\pi}{\omega} + T_d\,. \tag{6.75}$$

After substitution (6.75) in (6.73) there is obtained

$$y(t_m) = 1 + \kappa = 1 + \mathrm{e}^{-\frac{\pi\xi_w}{\sqrt{1-\xi_w^2}}} \quad \Rightarrow$$

$$\Rightarrow\ \kappa = \mathrm{e}^{-\frac{\pi\xi_w}{\sqrt{1-\xi_w^2}}}\ \Rightarrow \tag{6.76}$$

$$\Rightarrow\ \xi_w = \frac{|\ln\kappa|}{\sqrt{\pi^2+\ln^2\kappa}}\,. \tag{6.77}$$

On the basis of the relations (6.77), (6.72), (6.71) and (6.64) the open-loop gain k_o and coefficient β can be determined for the given (desired) relative overshoot κ.

For the relative overshoot in the range $0 \le \kappa \le 0.5$ (0 – 50 %) the corresponding values ξ_w, φ [rad] and β were computed, see Tab. 6.10.

Tab. 6.10 Values of coefficients β' and β for given relative overshoot κ

κ	0	0.05	0.10	0.15	0.20	0.25	0.30	0.35	0.40	0.45	0.50
ξ_w	1	0.690	0.591	0.517	0.456	0.404	0.358	0.317	0.280	0.246	0.215
φ	0	0.809	0.938	1.028	1.097	1.155	1.205	1.248	1.287	1.322	1.354
β'	2.718	1.935	1.710	1.549	1.423	1.319	1.230	1.153	1.086	1.026	0.972
β	2.718	1.944	1.720	1.561	1.437	1.337	1.248	1.172	1.104	1.045	0.992

In Tab. 6.10 the values of β calculated on the basis of the relations (6.77), (6.72), (6.71) and (6.64) are marked as β', because they were obtained analytically by comparing the two poles of the control system (6.67) with the two dominant poles of the control system (6.53) neglecting its non-dominant poles [22, 29]. The experimentally corrected values are marked as β. The differences between the values of β' obtained analytically and the values of β corrected experimentally are not greater than 2 % and for the relative overshoot in the range $0 \le \kappa \le 0.2$ (0-20 %) are even less than 1 %.

For computation of the coefficient β the formula

$$\beta(\kappa) = 2.718 - 0.4547\kappa^{0.3432} \tag{6.78}$$

can be used, where κ is the relative overshoot in percentages [1].

The basic control performance indices were determined for the control system with conventional controllers tuned by the DMM, see Tab. 6.11.

From Tab. 6.11 it follows that for $0 \le \kappa \le 0.2$ (0-20 %) the tuning by the DMM satisfies all the recommended values of the most important control performance indices, see (6.9) (6.17) (6.18) and (6.24), so the MPM for $\kappa \le 0.2$ (20 %) guarantees a good control system robustness.

From a comparison of Tabs 6.9 – 6.11 for $\kappa = 0.05$ (5 %) with Tabs 6.7 and 6.8, it is clear that the DMM for the proportional plants is equivalent to the SIMC method for $T_1 \le 8T_d$ and $T_w = T_d$; the DMM exactly uses $\beta = 1.944$ and the SIMC method uses $\beta = 2$. For this reason, they are almost identical values of the basic control performance indices, compare Tab. 6.8 (the left column) with Tab. 6.11 for $\kappa = 0.05$.

The essential difference between these two methods lies in the choice of the desired control system transfer function. The SIMC method assumes that the desired control system transfer function for $T_w = T_d$ has the form [see (6.40)]

Tab. 6.11 Basic control performance indices for the control system tuned by the desired model method (DMM)

κ	0	0,05	0,1	0,15	0,2	0,25	0,3	0,35	0,4
M_S	1.394	1.615	1.737	1.859	1.987	2.123	2.282	2.458	2.665
m_A	4.27	3.05	2.70	2.45	2.26	2.10	1.96	1.84	1.73
m_L [dB]	12.609	9.686	8.627	7.783	7.082	6.444	5.845	5.296	4.761
γ [deg]	68.9	60.5	56.7	53.3	50.1	47.1	44.1	41.1	38.1
γ[rad]	1.20	1.06	0.99	0.93	0.88	0.82	0.77	0.72	0.67
$A_{wy}(\omega_R)$	1	1.002	1.056	1.142	1.247	1.367	1.512	1.678	1.876
$L_{wy}(\omega_R)$ [dB]	0	0.017	0.473	1.153	1.917	2.715	3.591	4.496	5.465
$\omega_p T_d$	$\frac{\pi}{2} \doteq 1.57$								
$\omega_g T_d$	0.37	0.51	0.58	0.64	0.70	0.75	0.80	0.85	0.91
$\Delta T_d/T_d$	3.27	2.05	1.70	1.45	1.26	1.10	0.96	0.84	0.73

$$G_{wy}(s) = \frac{1}{T_w s + 1} \mathrm{e}^{-T_d s}$$

and the DMM for (6.64) has the form [see (6.53)]

$$G_{wy}(s) = \frac{1}{\beta T_d s + \mathrm{e}^{-T_d s}} \mathrm{e}^{-T_d s} .$$

It is obvious that the SIMC method in its basic form, i.e. for $T_1 \leq 8T_d$ and $T_w = T_d$ can never ensure the properties of the control system expressed by the control system transfer function (6.40). In contrast, the DMM ensures the properties of the control system given by the transfer function (6.53) not only for the value of $\beta = 1.944$ (≈ 2), but also for other values of β in Tab. 6.10 with a high accuracy.

Tab. 6.9 can be extended for the ideal proportional plant with time delay

$$G_P(s) = k_1 \mathrm{e}^{-T_d s} \tag{6.79}$$

with recommended I controller

$$G_C(s) = \frac{1}{T_I s} \tag{6.80}$$

for

$$T_I^* = k_1 \beta T_d . \tag{6.81}$$

The DMM can be used for systems without a time delay, i.e. $T_d = 0$, but in this case, the desired control system transfer function is supposed in the simple form [compare with (6.53)]

$$G_{wy}(s) = \frac{1}{T_w s + 1} , \tag{6.82}$$

where T_w is the time constant of the closed-loop control system. The recommended controller transfer function can be obtained after substitution (6.82) in (6.51)

$$G_C(s) = \frac{1}{G_P(s)T_w s}. \tag{6.83}$$

For instance for the plant with the transfer function

$$G_P(s) = \frac{k_1}{(T_1 s + 1)(T_2 s + 1)}, \quad T_1 \geq T_2 \tag{6.84}$$

on the basis of the relation (6.83) the transfer function of the PID$_i$ controller

$$G_C(s) = \frac{(T_1 s + 1)(T_2 s + 1)}{k_1 T_w s} = K_P' \frac{(T_I' s + 1)(T_D' s + 1)}{T_I' s}$$

is obtained, where

$$K_P'^* = \frac{T_1}{k_1 T_w}, \quad T_I'^* = T_1, \quad T_D'^* = T_2, \tag{6.85}$$

or after use of the relation (5.29) the transfer function of the conventional PID controller is obtained [see (5.26)] with the adjustable parameters

$$K_P^* = \frac{T_1 + T_2}{k_1 T_w}, \quad T_I^* = T_1 + T_2, \quad T_D^* = \frac{T_1 T_2}{T_1 + T_2}. \tag{6.86}$$

The time constant T_w should be chosen with regard to the limitation of the manipulated variable $u(t)$ [the smaller $T_w \Rightarrow$ the greater demands on the manipulated variable $u(t)$] and the required settling time t_s. For instance, for the given relative control tolerance δ it holds [see Fig. 6.1]

$$\begin{aligned} &\delta = 0.05 \ (5\ \%) \ \Rightarrow \ t_s \approx 3T_w, \\ &\delta = 0.02 \ (2\ \%) \ \Rightarrow \ t_s \approx 4T_w. \end{aligned} \tag{6.87}$$

Example 6.6

For the plant with the transfer function

$$G_P(s) = \frac{2}{(6s+1)(4s+1)(2s+1)^2}$$

it is necessary to tune the PI and PID controllers by the DMM so that the relative overshoot will be about 10 % (time constants are in seconds).

Solution:

The plant transfer function does not correspond to the forms in Tab. 6.9, and therefore it is necessary to modify them so that they will be suitable for the PI and PID controllers, i.e. they must by converted to the forms in rows 2 and 4 (5) in Tab. 6.9.

In accordance with the “half rule” we can write: $k_1 = 2$, $T_{10} = 6$ s, $T_{20} = 4$ s, $T_{30} = T_{40} = 2$ s.

The transfer function (4.29) [see (4.54)]:

$$T_1 = T_{10} + \frac{T_{20}}{2} = 8\,\text{s}, \quad T_d = \frac{T_{20}}{2} + T_{30} + T_{40} = 6\,\text{s},$$

$$G_P(s) = \frac{2}{(6s+1)(4s+1)(2s+1)^2} \approx \frac{2}{8s+1} e^{-6s}.$$

On the basis of Tab. 6.9 (row 2) and Tab. 6.10 for $k_1 = 2$, $T_1 = 8$ s, $T_d = 6$ s and $\kappa = 0.1 \Rightarrow \beta = 1.720$ we can write

$$K_P^* = \frac{T_1}{k_1 \beta T_d} \doteq 0.39; \quad T_I^* = T_1 = 8\,\text{s}.$$

The transfer function (4.35) [see (4.55)]:

$$T_1 = T_{10} = 6\,\text{s}, \quad T_2 = T_{20} + \frac{T_{30}}{2} = 5\,\text{s}, \quad T_d = \frac{T_{30}}{2} + T_{40} = 3\,\text{s},$$

$$G_P(s) = \frac{2}{(6s+1)(4s+1)(2s+1)^2} \approx \frac{2}{(6s+1)(5s+1)} e^{-3s}.$$

On the basis of Tab. 6.9 (row 5) and Tab. 6.10 for $k_1 = 2$, $T_1 = 6$ s, $T_2 = 5$ s, $T_d = 3$ s and $\kappa = 0.1 \Rightarrow \beta = 1.720$ we can write

$$K_P^* = \frac{T_1 + T_2}{k_1 \beta T_d} \doteq 1.07; \quad T_I^* = T_1 + T_2 = 11\,\text{s}, \quad T_D^* = \frac{T_1 T_2}{T_1 + T_2} \doteq 2.73\,\text{s}.$$

The control system responses are shown in Fig. 6.23. It is obvious that even for the rough approximation of the plant transfer function the obtained responses reflect both the good applicability of the DMM and the “half rule”.

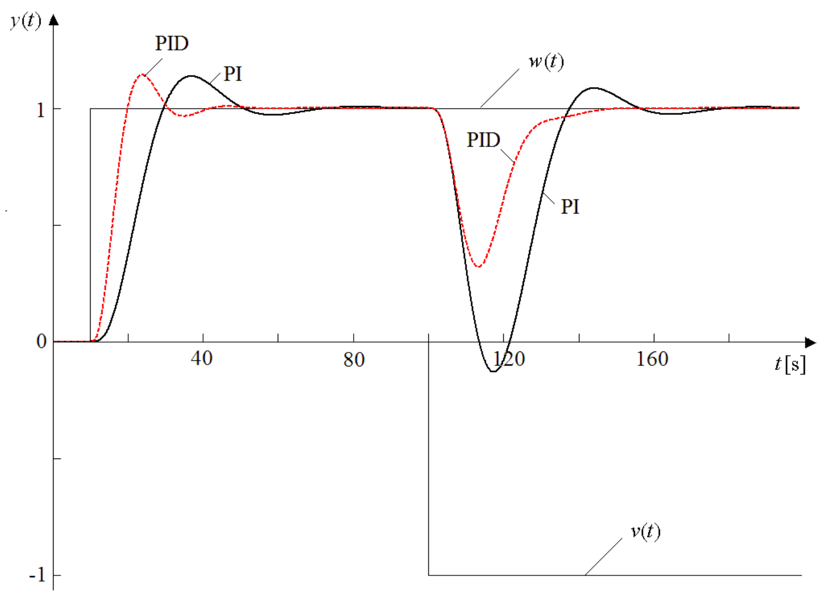

Fig. 6.23 Responses of the control system tuned by DMM – Example 6.6

Example 6.7

It is necessary to tune the PID controller by the DMM for the plant with the transfer function

$$G_P(s) = \frac{2}{(5s+1)(3s+1)} e^{-6s}$$

so as to the relative overshoot was $\kappa = 0$; 0.1 and 0.2 (time constants and time delay are in seconds).

Solution:

The plant transfer function has a suitable form for the PID controller (see Tab. 6.9, row 5) and therefore for $k_1 = 2$, $T_1 = 5$ s, $T_2 = 3$ s, $T_d = 6$ s on the basis of Tabs 6.9 and 6.10 we can directly write:

$$\kappa = 0 \;\Rightarrow\; \beta = 2.718 \;\Rightarrow\; K_P^* = \frac{T_1 + T_2}{k_1 \beta T_d} \doteq 0.25;$$

$$\kappa = 0.1 \;\Rightarrow\; \beta = 1.720 \;\Rightarrow\; K_P^* \doteq 0.39;$$

$$\kappa = 0.2 \;\Rightarrow\; \beta = 1.437 \;\Rightarrow\; K_P^* \doteq 0.46;$$

$$T_I^* = T_1 + T_2 = 8 \text{ s},\; T_D^* = \frac{T_1 T_2}{T_1 + T_2} \doteq 1.88 \text{ s}.$$

The responses of the control system are shown in Fig. 6.24. We can see that the resulting courses are very accurate.

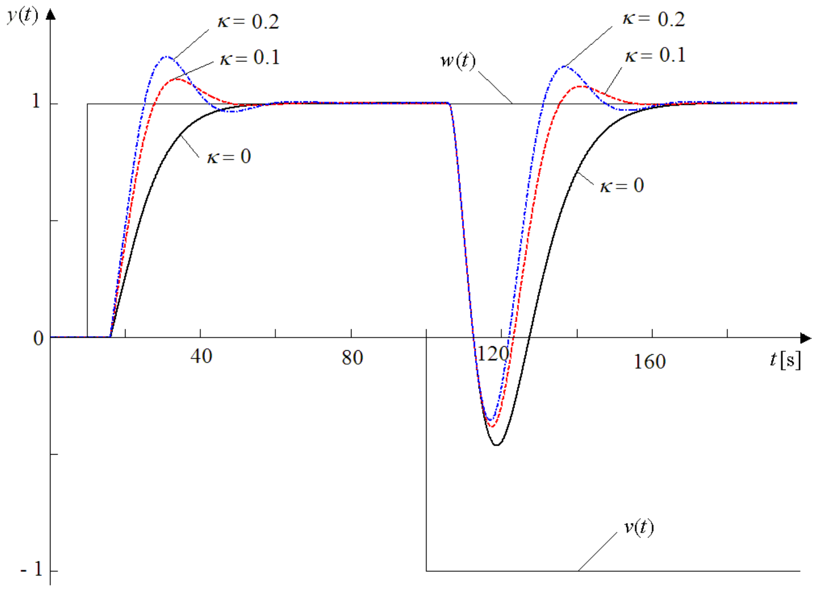

Fig. 6.24 Responses of the control system with the PID controller tuned by DMM – Example 6.7

6.2.9 Modulus optimum method

The MOM (**m**odulus **o**ptimum **m**ethod) belongs among analytical controller tuning methods. It is based on the requirement for the modulus of the frequency control system transfer function [7, 21, 22, 27, 29]

$$G_{wy}(s) \to 1 \Rightarrow G_{wy}(\mathrm{j}\omega) \to 1 \Rightarrow A_{wy}(\omega) \to 1.$$

It is assumed that the desired course of $A_{wy}(\omega)$ should be a monotonically decreasing function in accordance with Fig. 6.25.

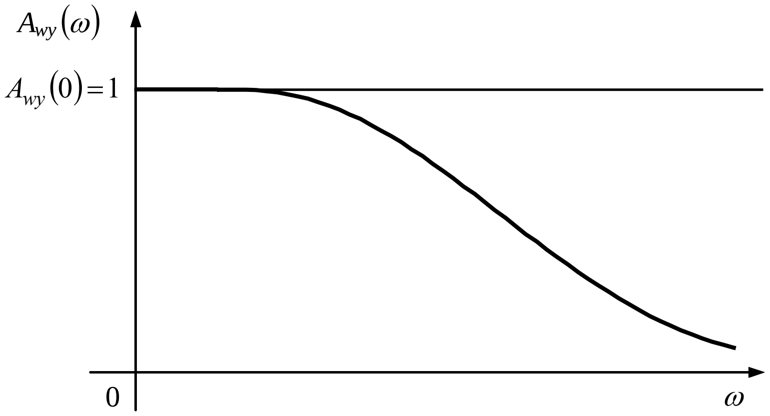

Fig. 6.25 Desired course of the modulus of frequency control system transfer function for the modulus optimum method

It is obvious that it holds

$$A_{wy}(\omega) \to 1 \Leftrightarrow A_{wy}^2(\omega) \to 1.$$

This is important because with the square power it is easier to work and the equalities

$$(\alpha + \mathrm{j}\omega)(\alpha - \mathrm{j}\omega) = \alpha^2 + \omega^2 = |\alpha + \mathrm{j}\omega|^2$$

hold and therefore for the control system transfer function

$$G_{wy}(s) = \frac{b_m s^m + b_{m-1}s^{m-1} + \ldots + b_1 s + b_0}{a_n s^n + a_{n-1}s^{n-1} + \ldots + a_1 s + a_0}, \qquad n \ge m \tag{6.88}$$

it is possible to write

$$A_{wy}^2(\omega) = G_{wy}(\mathrm{j}\omega)G_{wy}(-\mathrm{j}\omega) = \frac{B_m\omega^{2m} + B_{m-1}\omega^{2(m-1)} + \ldots + B_1\omega^2 + B_0}{A_n\omega^{2n} + A_{n-1}\omega^{2(n-1)} + \ldots + A_1\omega^2 + A_0}, \tag{6.89}$$

where

$$\begin{aligned}
A_0 &= a_0^2 & B_0 &= b_0^2\,, \\
A_1 &= a_1^2 - 2a_0a_2 & B_1 &= b_1^2 - 2b_0b_2\,, \\
A_2 &= a_2^2 - 2a_1a_3 + 2a_0a_4 & B_2 &= b_2^2 - 2b_1b_3 + 2b_0b_4\,, \\
&\vdots & &\vdots \\
A_i &= a_i^2 + 2\sum_{j=1}^{i}(-1)^j a_{i-j}a_{i+j} & B_i &= b_i^2 + 2\sum_{j=1}^{i}(-1)^j b_{i-j}b_{i+j}\,, \\
&\vdots & &\vdots \\
A_{n-1} &= a_{n-1}^2 - 2a_{n-2}a_n & B_{m-1} &= b_{m-1}^2 - 2b_{m-2}b_m\,, \\
A_n &= a_n^2 & B_m &= b_m^2\,.
\end{aligned} \tag{6.90}$$

If the equalities

$$\frac{B_0}{A_0} = \frac{B_1}{A_1} = \frac{B_2}{A_2} = \cdots = \frac{B_i}{A_i} = \cdots$$

hold and the numerator degree m would be equal to the denominator degree n of the control system transfer function (6.88), then the square of modulus $A_{wy}^2(\omega)$ and hence modulus $A_{wy}(\omega)$ would be independent of the angular frequency ω. From the point of view of the physical realizability the inequality $n > m$ always holds in technical practice and therefore independency on the angular frequency ω cannot be achieved. The control process will be satisfactory if $A_{wy}^2(\omega)$ with increasing angular frequency ω it will monotonically decrease, i.e.

$$A_{wy}^2(0) = \frac{B_0}{A_0} \geq \frac{B_i}{A_i}. \tag{6.91}$$

When using the MOM the conditions (6.91) are practically used like equalities in the same number as there is in the number of adjustable controller parameters p, i.e.

$$A_i B_0 = A_0 B_i, \quad i = 1,2,\ldots,p. \tag{6.92}$$

For the control systems of the type $q = 1$ ($b_0 = a_0 \Leftrightarrow B_0 = A_0$) the equalities

$$A_i = B_i, \qquad i = 1,2,\ldots,p. \tag{6.93}$$

are used.

Since condition (6.92) or (6.93) does not consider all the coefficients of the characteristic polynomial

$$N(s) = a_n s^n + a_{n-1} s^{n-1} + \ldots + a_1 s + a_0 \tag{6.94}$$

in the denominator of the control system transfer function (6.88), the MOM generally does not guarantee the stability and therefore it must not ensure the desired control process performance. When using the MOM it is generally necessary to check stability and to verify the control process performance.

If the plant transfer function $G_P(s)$ has any of the forms mentioned in Tab. 6.12, then using the recommended controller and corresponding values of its adjustable parameters ($T = 0$), the control system transfer function will have the so called **standard form**

$$G_{wy}(s) = \frac{1}{T_w^2 s^2 + 2\xi_w T_w s + 1}, \quad \xi_w = \frac{1}{\sqrt{2}}, \qquad T_w = \sqrt{2} T_i, \tag{6.95}$$

where for rows 1 and 2 in Tab. 6.12 $i = 1$, for rows 3 and 4 $i = 2$ and for row 5 $i = 3$.

In this case it is not necessary to check the stability of the control system, because the form (6.95) is also the standard form for the ITAE criterion [see (6.3e)]. This standard form leads to the relative overshoot 4.3 %.

The compensation of the time constants, i.e. the cancellation of one or two stable binomials for PD and PI or PID controllers, was used for controller tuning on the basis of Tab. 6.12. It causes a simplification of control system dynamics but simultaneously it may lead to slower responses because the stable zeros of the numerator of the transfer function $G_{wy}(s)$ can accelerate the control process [22, 29].

Table 6.12 may be used as well for the analog controllers ($T = 0$) as for the digital controllers ($T > 0$), see Section 6.3 [27].

The MOM is used for $q \le 1$, primarily for electrical drives control, where small time constants (electrical) are substituted by the summary time constant, see Section 4.2.

Tab. 6.12 Controller adjustable parameters for the modulus optimum method (MOM)

Plant transfer function		Controller < analog $T = 0$, digital $T > 0$			
		Type	K_P^*	T_I^*	T_D^*
1	$\dfrac{k_1}{T_1 s + 1}$	I	–	$2k_1(T_1 - 0.5T)$	–
2	$\dfrac{k_1}{s(T_1 s + 1)}$	P	$\dfrac{1}{2k_1 T_1}$	–	–
3	$\dfrac{k_1}{(T_1 s + 1)(T_2 s + 1)}$ $T_1 \ge T_2$	PI	$\dfrac{T_I^*}{2k_1 T_2}$	$T_1 - 0.5T$	–
4	$\dfrac{k_1}{s(T_1 s + 1)(T_2 s + 1)}$ $T_1 \ge T_2$	PD	$\dfrac{1}{2k_1(T_2 + 0.5T)}$	–	$T_1 - 0.5T$
5	$\dfrac{k_1}{(T_1 s + 1)(T_2 s + 1)(T_3 s + 1)}$ $T_1 \ge T_2 \ge T_3$	PID	$\dfrac{T_I^*}{2k_1(T_3 + 0.5T)}$	$T_1 + T_2 - T$	$\dfrac{T_1 T_2}{T_1 + T_2} - \dfrac{T}{4}$

Procedure:

1. The plant transfer function is converted into a suitable form in accordance with Tab. 6.12 and for the recommended controller the values of its adjustable parameters are calculated.
2. If the plant transfer function cannot be converted into some of the forms in Tab. 6.12 or another controller instead of the recommended controller is used, then for the determination of the p adjustable parameters of the selected controller for $q = 0$ formulas (6.92) are used and for $q = 1$ formulas (6.93) are used. It is possible to use time constant compensation (cancellation).
3. In the case of another form of the control system transfer function than the standard form (6.95) for the MOM, it is necessary to check the stability (if the control system is unstable, the MOM cannot be used) and the control performance should be preferably verified by simulation.

Example 6.8

It is necessary to tune the PI controller by the MOM for the plant with the transfer function

$$G_P(s) = \frac{k_1}{(T_1 s + 1)(T_2 s + 1)}, \qquad T_1 \ge T_2$$

with the use of compensation.

Solution:

For the PI controller with the transfer function

$$G_C(s) = K_P\left(1 + \frac{1}{T_I s}\right) = \frac{K_P(T_I s + 1)}{T_I s}$$

the open-loop control system transfer function has the form

$$G_o(s) = G_C(s)G_P(s) = \frac{K_P k_1 (T_I s + 1)}{T_I s (T_1 s + 1)(T_2 s + 1)},$$

from which it follows that the control system type $q = 1$.

For $T_I^* = T_1$ the compensation (cancellation) of the stable binomials $T_1 s + 1$ takes place and the open-loop transfer function is essentially simplified

$$G_o(s) = \frac{K_P k_1}{T_1 s (T_2 s + 1)}.$$

The control system transfer function has the form

$$G_{wy}(s) = \frac{G_o(s)}{1 + G_o(s)} = \frac{K_P k_1}{T_1 T_2 s^2 + T_1 s + K_P k_1},$$

where $a_0 = b_0 = K_P k_1$, $a_1 = T_1$, $a_2 = T_1 T_2$.

On the basis of the relations (6.90) and (6.93) for $p = 1$ there is obtained

$$A_1 = a_1^2 - 2a_0 a_2 = T_1^2 - 2K_P k_1 T_1 T_2,$$

$$B_1 = 0,$$

$$A_1 = 0 \Rightarrow T_1^2 - 2K_P k_1 T_1 T_2 = 0 \Rightarrow K_P^* = \frac{T_1}{2k_1 T_2}.$$

The adjustable parameters for the PI controller are

$$K_P^* = \frac{T_1}{2k_1 T_2}, \qquad T_I^* = T_1.$$

The same adjustable parameters were directly obtained from Tab. 6.12 (row 3 for $T = 0$).

After substitution these parameters in the control system transfer function there is obtained

$$G_{wy}(s) = \frac{1}{2T_2^2 s^2 + 2T_2 s + 1} = \frac{1}{T_w^2 s^2 + 2\xi_w T_w s + 1},$$

where

$$\xi_w = \frac{1}{\sqrt{2}}, \qquad T_w = \sqrt{2}T_2 .$$

It is obvious that the standard form of the control system transfer function for the MOM was obtained [see (6.95)] and therefore a stability check is unnecessary.

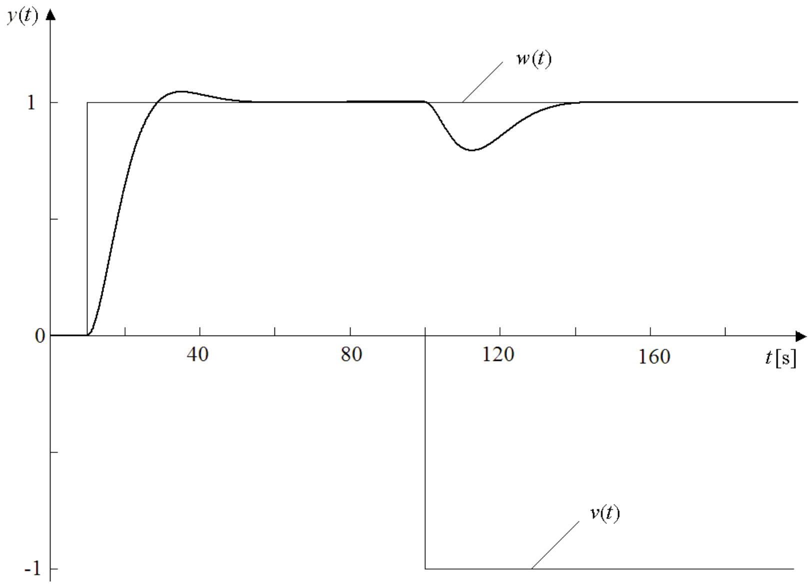

Fig. 6.26 Response of the control system with the PI controller tuned by the MOM – Example 6.8

For instance for $k_1 = 3$, $T_1 = 6$ s and $T_2 = 4$ s there is obtained

$$K_P^* = \frac{T_1}{2k_1T_2} = 0.25; \qquad T_I^* = T_1 = 6\,\mathrm{s}.$$

The response of the control system is shown in Fig. 6.26.

6.2.10 Symmetrical optimum method

The SOM (**s**ymmetrical **o**ptimum **m**ethod) is suitable for controller tuning for the control system type $q \geq 2$, and especially in the case when disturbances act on the plant input [2, 7, 21, 29]. In this paragraph $q = 2$ is assumed. Then the control system transfer function with the PI controller for the SOM has the standard form

$$G'_{wy}(s) = \frac{4T_is+1}{8T_i^3s^3 + 8T_i^2s^2 + 4T_is + 1} = \frac{4T_is+1}{(2T_is+1)(4T_i^2s^2 + 2T_is + 1)}, \tag{6.96}$$

where $i = 1$ and 2, see the corresponding row in Tab. 6.13.

To calculate the controller adjustable parameters it is necessary to solve the system of two equations [see (6.90)]

$$\left.\begin{aligned} A_1 &= 0 \\ A_2 &= 0 \end{aligned}\right\} \Rightarrow \begin{aligned} a_1^2 - 2a_0a_2 &= 0, \\ a_2^2 - 2a_1a_3 &= 0. \end{aligned} \tag{6.97}$$

For instance for the plant with the transfer function

$$G_P(s) = \frac{k_1}{s(T_1 s + 1)} \tag{6.98}$$

it is necessary to choice the PI controller (so as $q = 2$) with the transfer function

$$G_C(s) = K_P\left(1 + \frac{1}{T_I s}\right). \tag{6.99}$$

From the open-loop transfer function the closed-loop control system transfer function

$$G_C(s)G_P(s) = \frac{k_1 K_P (T_I s + 1)}{T_I s^2 (T_1 s + 1)}$$

is obtained

$$G'_{wy}(s) = \frac{G_o(s)}{1 + G_o(s)} = \frac{k_1 K_P T_I s + k_1 K_P}{T_1 T_I\, s^3 + T_I\, s^2 + k_1 K_P T_I s + k_1 K_P}. \tag{6.100}$$

From (6.100) it follows that $q = 2$ (the last two coefficients in the numerator and the denominator are the same).

For $a_0 = k_1 K_P$, $a_1 = k_1 K_P T_I$, $a_2 = T_I$ and $a_3 = T_1 T_I$ after substitution in (6.97) the adjustable parameters are obtained (see row 1 in Tab. 6.13 for $T = 0$)

$$\left.\begin{aligned} &(k_1 K_P T_I)^2 - 2k_1 K_P T_I = 0 \\ &T_I^2 - 2k_1 K_P T_1 T_I^2 = 0 \end{aligned}\right\} \Rightarrow \quad \begin{aligned} K_P^* &= \frac{1}{2k_1 T_1}, \\ T_I^* &= 4T_1. \end{aligned} \tag{6.101}$$

It is obvious that after substitution (6.101) in (6.100) for $i = 1$ the standard form (6.96) for the SOM is obtained.

Similarly, for the $T_1 >> T_2$ row 2 in Tab. 6.13 for $T = 0$ is obtained because it can be written

$$\frac{k_1}{(T_1 s + 1)(T_2 s + 1)} = \frac{\frac{k_1}{T_1}}{\left(s + \frac{1}{T_1}\right)(T_2 s + 1)} \approx \frac{\frac{k_1}{T_1}}{s(T_2 s + 1)}. \tag{6.102}$$

Since the stable zero is in the numerator of the control system transfer function (6.96) and moreover $q = 2$, in the control system a relatively large overshoot of about 43 % arises. The large overshoot may be substantially reduced to about 8% by using the input filter (see Fig. 5.5)

$$G_F(s) = \frac{1}{4T_i s + 1}, \tag{6.103}$$

which in the case of using the 2DOF PI controller can be easily realized by selecting the set-point weight value for the proportional component $b = 0$, see equation (5.36) for $T_I = 4T_i$ and $T_D = 0$.

Table 6.13 may be used as well for the analog controllers ($T = 0$) as for the digital controllers ($T > 0$), see Section 6.3 [29].

Tab. 6.13 PI controller adjustable parameters for the symmetrical optimum method (SOM)

Plant transfer function		PI controller < analog $T = 0$, digital $T > 0$		
		K_P^*	T_I^*	Filter
1	$\dfrac{k_1}{s(T_1 s+1)}$	$\dfrac{4}{k_1(8T_1+3T)}$	$4T_1-0.5T$	$\dfrac{1}{4T_1 s+1}$
2	$\dfrac{k_1}{(T_1 s+1)(T_2 s+1)}$ $T_1 >> T_2$	$\dfrac{4T_1}{k_1(8T_2+3T)}$	$4T_2-0.5T$	$\dfrac{1}{4T_2 s+1}$

The SOM, similarly as the MOM, is mainly used in electric drives, where instead of the input filter or the 2DOF PI controller the speed limiter on the input is often used [7, 21].

For instance the transfer function of the DC motor from Example 3.6 can be easily modified in the form (6.98) because motor armature circuit inductance is often negligible, i.e. $L_a \approx 0$ (see also Section 4.2).

The same form (6.98) has also the simplified linearized model of the hydraulic double acting linear motor, see Example 4.1.

Procedure:

1. The plant transfer function is converted into a suitable form in accordance with Tab. 6.13, e.g. by the approaches described in Section 4.2.
2. Based on Tab. 6.13 the values of the PI controller adjustable parameters are determined and when the 2DOF PI controller is used then $b = 0$ is set.

Example 6.9

It is necessary to tune the PI controller by the SOM for the plant with the transfer function (time constants are in seconds)

$$G_S(s) = \frac{0.05}{s(10s+1)(2s+1)}.$$

Solution:

The plant transfer function does not have a suitable form for the SOM (see Tab. 6.13), and therefore it has to be modified. For $k_1 = 0.05$; $T_{10} = 10$ and $T_{20} = 2$ on the basis of the equality of complementary areas over the plant step responses (see Section 4.2) there is obtained

$$T_1 = T_{10} + T_{20} = 12 \Rightarrow$$

$$G_P(s) = \frac{0.05}{s(10s+1)(2s+1)} \approx \frac{0.05}{s(12s+1)}.$$

From Tab. 6.13 for $k_1 = 0.05$ and $T_1 = 12$ ($T = 0$) the PI controller adjustable parameters were obtained

$$K_P^* = \frac{1}{2k_1T_1} \doteq 0.84; \; T_I^* = 4T_1 = 48\,\text{s}.$$

The servo and regulatory responses for different values of the set-point weight b are shown in Fig. 6.27. For $b = 1$ the 2DOF PI controller is the conventional (1DOF) PI controller. It is clear that by using of the 2DOF PI controller the overshoot in the servo response was significantly reduced.

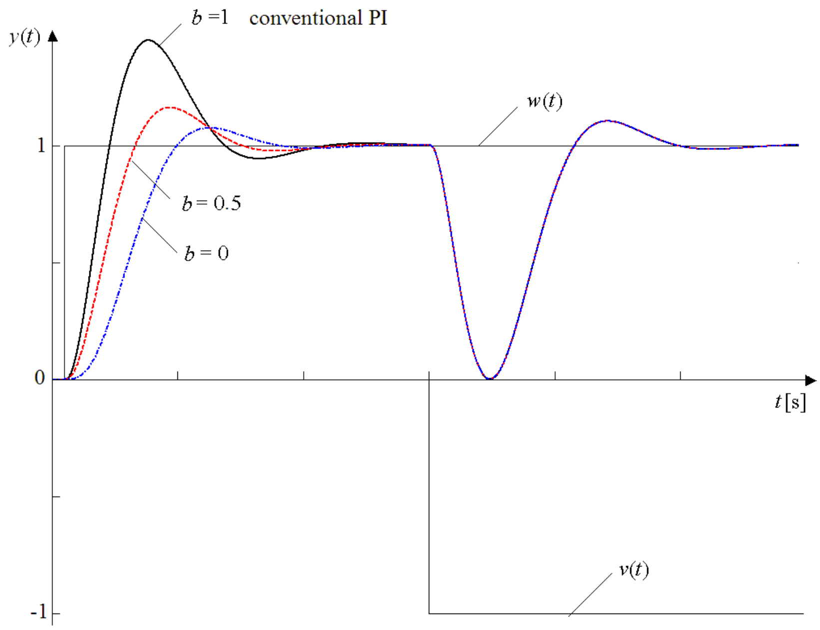

Fig. 6.27 Responses of the control system with the 2DOF PI controller tuned by the SOM for different values of weight b – Example 6.9

6.3 Digital control

With the development of digital technology and at the same time with decreasing prices digital controllers are increasingly being used in the control engineering. Digital controllers mostly implement the same control algorithms like analog ones but in discrete forms. Due to the assumed negligibly small quantization errors the terms "digital" (discrete in time and magnitude) and "discrete" (discrete in time but continuous in magnitude) are not distinguished. For instance the digital PID controller (T is the **sampling period**, kT – the **discrete time**)

$$u(kT) = K_P\left\{e(kT) + \frac{T}{T_I}\sum_{i=0}^{k} e(iT) + \frac{T_D}{T}\{e(kT) - e[(k-1)T]\}\right\}, \tag{6.104}$$

$$k = 0,1,2,\ldots,$$

corresponds to the analog PID controller.

It is obvious that for the digital controllers further adjustable parameter arises – the sampling period T. Its proper choice is very important from the point of view of the control performance. The sampling period T increases the influence of the integral (summation) component (the integral component destabilizes the control process) and reduces the effect of the derivative (difference) component (the derivative component stabilizes the control process), hence the ***impact of the sampling period T on the control performance is always negative***. This follows also from the fact that between the sampling instants $kT \le t < (k + 1)T$ the digital controller has no information on the instantaneous value of the control error $e(t)$, see Fig. 6.28.

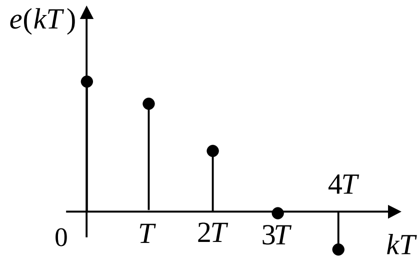

Fig. 6.28 Control error course in a control system with a digital controller

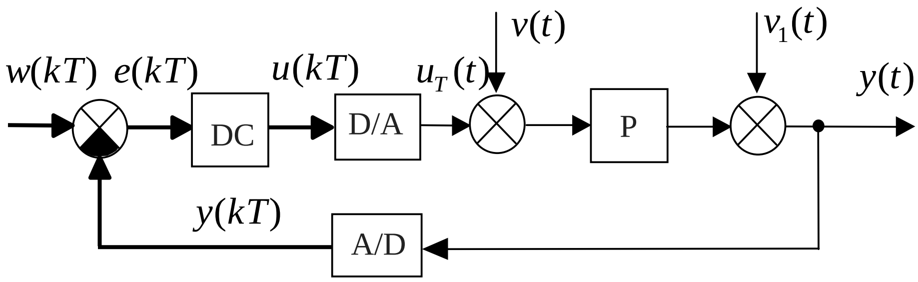

Fig. 6.29 Control system with a digital controller

The **analog-to-digital converter** (A/D converter) processes the conversion of the continuous (analog) variable into the discrete (digital) variable. It is plugged in the feedback (Fig. 6.29). The output variable of the digital controller (DC) is the discrete manipulated variable $u(kT)$ which the **digital-to-analog converter** (D/A converter) converts into the continuous in time (analog) variable $u_T(t)$, and has the most staircase course (Fig. 6.30).

The digital PID controller is one of the most complex conventional digital controllers. In practice simpler controllers are used:

- the digital PI controller

$$u(kT) = K_P\left[e(kT) + \frac{T}{T_I}\sum_{i=0}^{k} e(iT)\right], \tag{6.105}$$

- the digital PD controller

$$u(kT) = K_P\left\{e(kT) + \frac{T_D}{T}\{e(kT) - e[(k-1)T]\}\right\}, \tag{6.106}$$

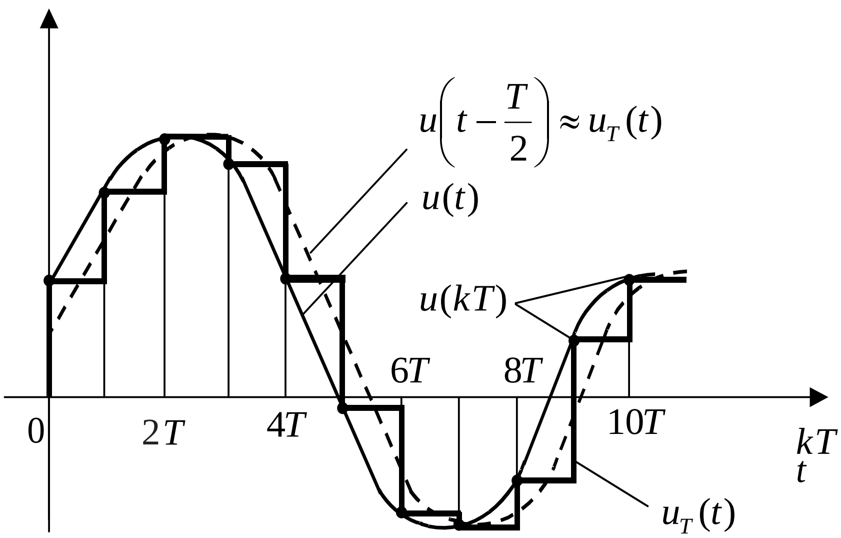

Fig. 6.30 Manipulated variable courses in a control system with a digital controller

- the digital I controller

$$u(kT)=\frac{T}{T_I}\sum_{i=0}^{k}e(iT)\,, \tag{6.107}$$

- the digital P controller

$$u(kT)=K_P e(kT)\,. \tag{6.108}$$

In practice, digital control algorithms with the summation (integral) component are implemented in **incremental forms** [unlike the **position forms** (6.104) - (6.108)], namely:

- the digital PID controller

$$\left.\begin{aligned} &u(kT)=u[(k-1)T]+q_0e(kT)+q_1e[(k-1)T]+q_2e[(k-2)T],\\ &q_0=K_P\left(1+\frac{T}{T_I}+\frac{T_D}{T}\right),\ q_1=-K_P\left(1+2\frac{T_D}{T}\right),\ q_2=K_P\frac{T_D}{T}, \end{aligned}\right\} \tag{6.109}$$

- the digital PI controller

$$\left.\begin{aligned} &u(kT)=u[(k-1)T]+q_0e(kT)+q_1e[(k-1)T],\\ &q_0=K_P\left(1+\frac{T}{T_I}\right),\ q_1=-K_P, \end{aligned}\right\} \tag{6.110}$$

- the digital I controller

$$u(kT)=u[(k-1)T]+\frac{T}{T_I}e(kT)\,. \tag{6.111}$$

Summation (integral) and difference (derivative) components are often also implemented by other methods (the forward rectangular method, trapezoidal method, etc.) and in the summation index i starts from 1 and not from 0.

For properly choosing sampling period T these differences are negligible and also manufacturers often do not give any information about summation and difference component implementation.

For the difference component the input variable must always be properly filtered [18, 22, 29]**.**

The digital controllers, similarly like the analog controllers, may also be constructed with two degrees of freedom.

When using a conventional digital controller in comparison with the same type of conventional analog controller, there is always a reduction of the control process performance. It is given by the fact that between two sampling instants the digital controller has no information on the real value of the control error $e(t)$, and in addition as mentioned above by increasing the sampling period T leads to destabilization of the control system.

Therefore it is obvious that the choice of the sampling period and the problems of the digital control are very complicated. Simplified digital controller tuning is shown below which for the ordinary control practice is fully satisfactory.

If the A/D converter is moved from the feedback in front of the digital controller (Fig. 6.31 above) then the digital controller with both converters can be approximately regarded as the analog controller (AC). Therefore, for the approximate control system synthesis with a digital controller there can be used the block diagram of the control system in Fig. 6.31 (below).

Assuming that the D/A converter has the properties of the sampler and zero-order holder the manipulated variable $u_T(t)$ has the form of the staircase time function, see Fig. 6.30.

From Fig. 6.30 it follows that the staircase manipulated variable $u_T(t)$ for sufficiently small sampling period T can be approximately expressed as $u(t - T/2)$. Therefore, the control system with the digital controller can be substituted by a continuous control system with the analog controller $G_C(s)$ and the plant with the transfer function

$$G''_P(s) = G_P(s)\mathrm{e}^{-\frac{T}{2}s} = G'_P(s)\mathrm{e}^{-T_d s}\mathrm{e}^{-\frac{T}{2}s} = G'_P(s)\mathrm{e}^{-\left(T_d + \frac{T}{2}\right)s}, \qquad (6.112)$$

where $G'_P(s)$ is the part of the plant transfer function without the time delay.

Then for this plant the appropriate analog controller $G_C(s)$ is designed and tuned. The values of its adjustable parameters, together with the sampling period T are then applied to the corresponding digital controller.

Some tuning methods are directly derived for digital controllers.

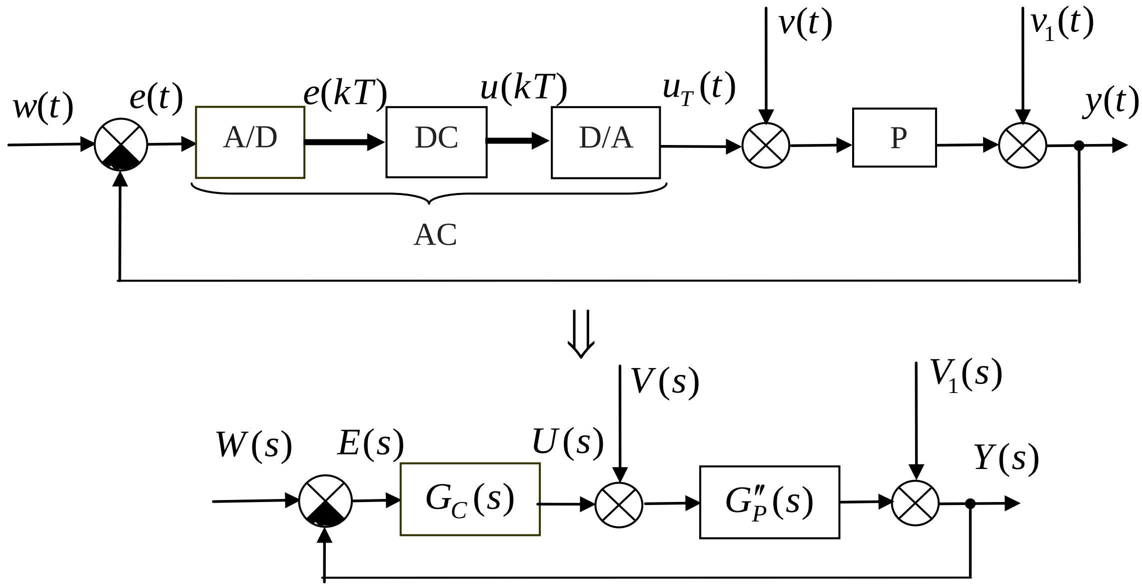

Fig. 6.31 Conversion of a control system with a digital controller on a control system with an analog controller

In this text, it relates to the MOM and SOM (Tabs 6.12 and 6.13), which are determined for plants without a time delay. Therefore, these methods can be directly used for digital controller tuning. For other methods considering plants with a time delay the approximate procedure above for conventional digital controller tuning can be used. If for the controller tuning methods mentioned in this text the inequality [29]

$$T < 0.3T_1 \quad \text{and} \quad T < 0.3T_d \tag{6.113}$$

hold then it can be assumed that the deterioration of the control performance in comparison with the corresponding analog control will not be greater than about 15 % [integral criterion IAE (6.3e)].

By the time constant T_1 in the inequality (6.113) the greatest plant time constant is to be considered.

Example 6.10

For the plant with the transfer function

$$G_P(s) = \frac{1}{(6s+1)(4s+1)}$$

it is necessary to tune the analog and digital controllers so that the relative overshoot will be about 5 % (time constants are in seconds).

Solution:

Since the MOM and DMM (also the SIMC method for this plant) are able to ensure a relative overshoot of about 5 %, both methods will therefore be used.

Modulus optimum method (MOM)

The plant transfer function has the desired form for the MOM (Tab. 6.12, $k_1 = 1$, $T_1 = 6$, $T_2 = 4$), and therefore we can write directly:

a) The analog PI controller ($T = 0$)

$$K_P^* = \frac{T_1}{2k_1T_2} = 0.75;\ T_I^* = T_1 = 6\,\mathrm{s}.$$

b) The digital PI controller

In accordance with the inequalities (6.113) we can choose e.g. T = 1 s:

$$K_P^* = \frac{T_1 - 0.5T}{2k_1T_2} \doteq 0.69;\ T_I^* = T_1 - 0.5T = 5.5\,\mathrm{s}.$$

The responses of the control system tuned by the MOM are shown in Fig. 6.32.

a)

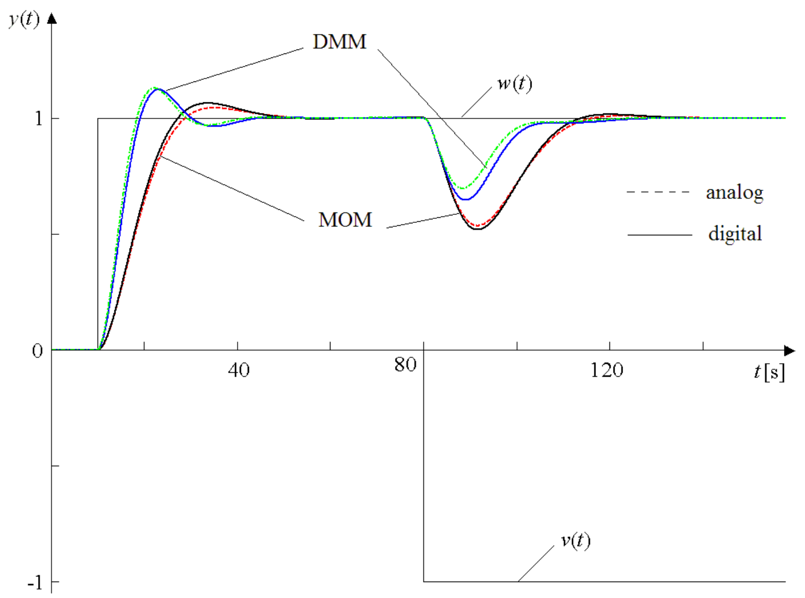

b)

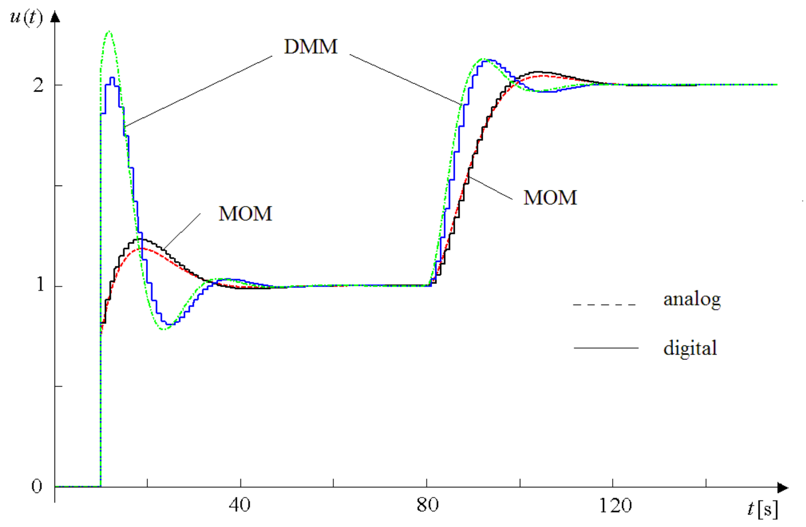

Fig. 6.32 Control system with an analog and digital PI controller – Example 6.10:
a) controlled variable responses, b) manipulated variable courses

Desired model method (DMM)

The plant transfer function has not the desired form for the DMM (Tab. 6.9), therefore we must modify it (for the "half rule": $k_1 = 1$, $T_{10} = 6$, $T_{20} = 4$).

In accordance with (4.54) we can write

$$T_1 = T_{10} + \frac{T_{20}}{2} = 8\,\mathrm{s}, \qquad T_{d1} = \frac{T_{20}}{2} = 2\,\mathrm{s},$$

$$G_P(s) = \frac{1}{(6s+1)(4s+1)} \approx \frac{1}{8s+1}\mathrm{e}^{-2s}.$$

We use Tabs 6.9 and 6.10 for the DMM ($k_1 = 1$, $T_1 = 8$, $T_d = 2$):

a) The analog PI controller ($T = 0$)

$$\kappa = 0.05 \;\Rightarrow\; \beta = 1.944,$$

$$K_P^* = \frac{T_1}{k_1 \beta T_d} \doteq 2.06; \;\; T_I^* = T_1 = 8\,\mathrm{s},$$

b) The digital PI controller

We use the same sampling period $T = 1\,\mathrm{s}$ in order to compare the MOM and DMM:

$$K_P^* = \frac{T_1}{k_1 \beta \left(T_d + \dfrac{T}{2} \right)} \doteq 1.65; \;\; T_I^* = T_1 = 8\,\mathrm{s}.$$

The responses are shown in Fig. 6.32a. There are also shown the corresponding manipulated variable courses (Fig. 6.32b).

The responses in Fig. 6.32a show that the DMM gives the faster responses with a slightly higher overshoot although a rather rough approximation of the plant transfer function was used. The overshoot for the DMM can be easily reduced by reducing the controller gain K_P. The obtained courses in Fig. 3.32 also show that simplified digital controller tuning gives acceptable results for control practice.

6.4 Cascade control

Simple control systems with conventional controllers (i.e. control systems with a simple single-loop structure) may not always ensure the desired control performance. In this case, it is possible to use controllers with a more complex structure or alternatively the control systems may have a more complex structure.

In the first case, design, tuning, and especially the later maintenance in operational conditions are very demanding from the point of view of craftsmanship as well as the financial costs. The second case of using a more complex structure of the control system is often inexpensive and feasible and it can achieve a substantial increase in the control performance. Such control systems are characterized by a more complex structure but they have only one main desired variable $w(t)$ and one main controlled variable $y(t)$.

The importance of the control system with a complex structure is currently great, because the availability of high-quality measuring and computing devices easily allows implementing these complex structures in industrial practice.

Below we will be devoted to only so called **cascade control systems**.

Since the conclusions cover both continuous control systems with analog controllers and discrete control systems with digital controllers the arguments in transfer functions and variable transforms will be omitted.

A block diagram of the cascade control system is shown in Fig. 6.33. From the block diagram it follows that the cascade control system consists of an auxiliary (slave) control system (the inner loop) and a main (master) control system (the outer loop). The controlled variable y_1 and the desired variable w_1 are called the auxiliary variables.

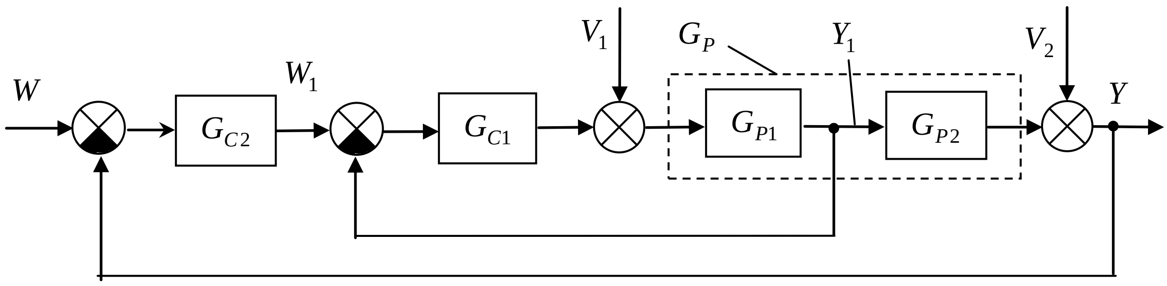

Fig. 6.33 Cascade control system

In accordance with Fig. 6.33 for the auxiliary control system there can be written

$$G_{w_1 y_1} = \frac{G_{C1}G_{P1}}{1+G_{C1}G_{P1}} = \frac{1}{\dfrac{1}{G_{C1}G_{P1}}+1}, \; G_{v_1 y_1} = \frac{G_{P1}}{1+G_{C1}G_{P1}} = (1-G_{w_1 y_1})G_{P1}, \tag{6.114}$$

then for the main control system it is possible to write

$$\left.\begin{aligned} G_{wy} &= \frac{G_{C2}G_{P2}G_{w_1 y_1}}{1+G_{C2}G_{P2}G_{w_1 y_1}}, \\ G_{v_1 y} &= \frac{(1-G_{w_1 y_1})G_{P1}G_{P2}}{1+G_{C2}G_{P2}G_{w_1 y_1}}, \\ G_{v_2 y} &= \frac{1}{1+G_{C2}G_{P2}G_{w_1 y_1}}. \end{aligned}\right\} \tag{6.115}$$

If the auxiliary control system will be properly tuned, then for the sufficiently large modulus of the open inner loop the relations hold

$$|G_{C1}G_{P1}| \to \infty \quad \Rightarrow \qquad G_{w_1 y_1} \to 1 \tag{6.116}$$

and the transfer functions of the main control system can be simplified

$$G_{wy} \approx \frac{G_{C2}G_{P2}}{1+G_{C2}G_{P2}}, \; G_{v_1 y} \approx 0, \; G_{v_2 y} \approx \frac{1}{1+G_{C2}G_{P2}}. \tag{6.117}$$

Then the desired control performance will be ensured by properly tuning the main control system (the outer loop).

From the above it is obvious that the cascade control system can be used in the case when the plant can be divided into two parts with the transfer functions G_{P1} and G_{P2} (i.e. the auxiliary variable y_1 can be measured at a suitable position). Its essential feature is that it (partially) eliminates the internal loop including the disturbances acting in this loop as well as its potential nonlinearities. The inner loop should not contain time delays and the auxiliary controller G_{C1} should be as simple as possible, i.e. the auxiliary controller G_{C1} is the P controller in the most cases. The main controller G_{C2} should include the integration component (term), and therefore it is most often the PI or PID controller.

Cascade control systems are used for controlling electrical drives and power servomechanisms. In this case, they may have more than two loops [7, 21, 22]. They are very often used for the control of boilers, destillation columns and reactors and other thermal power plants.

Procedure:

1. Primarily, the inner loop is tuned (i.e. the auxiliary control system) for the first part of the plant. The P controller is most often used (steady-state errors do not matter).
2. Then the inner loop is replaced by the simplest dynamic subsystem with the transfer function G_{w1y1} (in case of possibility $G_{w1y1} = 1$).
3. Finally, the outer loop (i.e. the main control system) is tuned using the PI or PID controller and preferably the achieved control performance is verified by the simulation.

Example 6.11

For the plant with the transfer function

$$G_P(s) = \frac{k}{s(T_1 s + 1)} \mathrm{e}^{-T_d s} = \frac{k_1}{s} \frac{k_2}{T_1 s + 1} \mathrm{e}^{-T_d s}$$

it is necessary to design such control which ensures the control process without overshoots and steady-state errors for the step change of all input variables.

Solution:

Since the integrator output variable can be measured, the plant can be described by two serially connected transfer functions

$$G_{P1}(s) = \frac{k_1}{s}, \quad G_{P2}(s) = \frac{k_2}{T_1 s + 1} \mathrm{e}^{-T_d s}$$

and then the cascade control in accordance with Fig. 6.34 can be used.

We use the P controller in the inner loop

$$G_{C1}(s) = K_{P1}$$

and the PI controller in the outer loop

$$G_{C2}(s) = K_{P2}\left(1 + \frac{1}{T_{I2}s}\right).$$

For the auxiliary control system (the inner loop) it is possible to write

$$G_{w_1y_1}(s) = \frac{G_{C1}(s)G_{P1}(s)}{1 + G_{C1}(s)G_{P1}(s)} = \frac{1}{\frac{1}{K_{P1}k_1}s + 1},$$

$$G_{v_1y_1}(s) = \frac{G_{P1}(s)}{1 + G_{C1}(s)G_{P1}(s)} = \left[1 - G_{w_1y_1}(s)\right]G_{P1}(s).$$

It is obvious, that the inner loop can be neglected theoretically for $K_{P1} \to \infty$, practically, if its time constant is much smaller than the time constant T_1, i.e.

$$\frac{1}{K_{P1}^* k_1} << T_1 \quad \Rightarrow \quad G_{w_1y_1}(s) \to 1, \; G_{v_1y_1}(s) \to 0.$$

Then the main control system (the outer loop) can be considered as a simple one-loop control system, where $G_{w1y1}(s) \approx 1$ (Fig. 6.35). In this case, the main PI controller may be tuned only for the second part of the plant with the transfer function $G_{P2}(s)$.

From the point of view of the requirements on the control performance the DMM can be used for main PI controller tuning. On the basis of Tabs 6.9 and 6.10 (for $\kappa = 0 \Rightarrow \beta = 2{,}718$) it is possible to write

$$K_P^* = \frac{T_1}{k_2 \beta T_d}; \; T_I^* = T_1.$$

For instance, for $k_1 = 2$, $k_2 = 1$, $T_1 = 5$ s, $T_d = 5$ s, based on the DMM the adjustable parameters of the both controllers were obtained: $K_{P1}^* = 5$ ($K_{P1}k_1 = 2T_1$), $K_P^* \doteq 0.368$; $T_I^* = 5$ s.

The responses of the cascade control system are shown in Fig. 6.36. It is obvious that the responses without overshoots can be obtained even for the integrating plants and conventional controllers. In most cases cascade control ensures very good control performance.

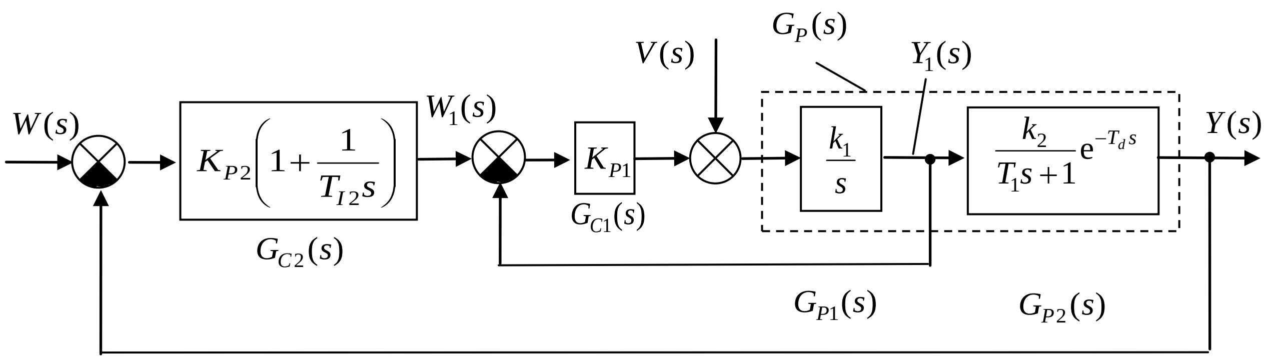

Fig. 6.34 Cascade control system – Example 6.11

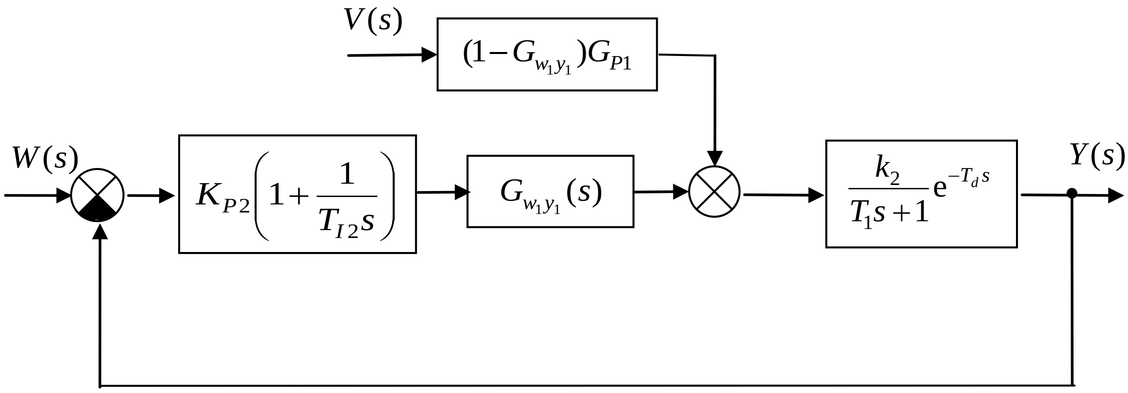

Fig. 6.35 Modified cascade control system – Example 6.11

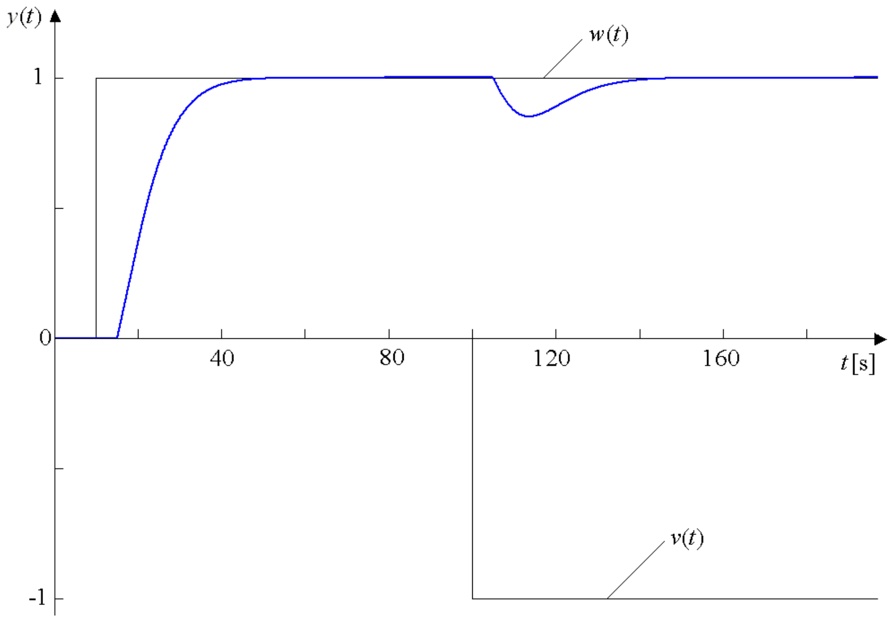

Fig. 6.36 Response of the cascade control system – Example 6.11

Example 6.12

For the DC motor from Example 3.6 it is necessary to design a position cascade control. It is assumed that the DC motor is supplied by a power amplifier.

Solution:

From equations (3.94) and the block diagram in Fig. 3.24 it follows that the motor torque $m(t)$ is directly proportional to the armature current $i_a(t)$. Therefore, it is appropriate to control this current.

Assume that the power amplifier has negligible dynamics and for the control of the current $i_a(t)$ the P controller with gain K_{Pi} will be used, see Figure 6.37a.

By moving the summation node (Tab. 3.1) we obtain the transformed block diagram in Fig. 6.37b.

In accordance with the block diagram in Fig. 6.37b for the current loop it holds

$$\frac{I_a(s)}{I_w(s)} = \frac{\dfrac{K_{Pi}}{K_{Pi}+R_a}}{\dfrac{L_a}{K_{Pi}+R_a}s+1} = \frac{k_a}{T_a s+1},$$

$$k_a = \frac{K_{Pi}}{K_{Pi}+R_a},\ T_a = \frac{L_a}{K_{Pi}+R_a}.$$

For sufficiently high K_{Pi} there is obtained

$$k_a \approx 1, \quad T_a \approx 0 \ \Rightarrow\ \frac{I_a(s)}{I_w(s)} \approx 1.$$

Because simultaneously

$$\frac{c_e}{K_{Pi}} \approx 0$$

holds (see Fig. 6.37b) the block diagram in Fig. 6.37 can be essentially simplified as it is shown in Fig. 6.38.

a)

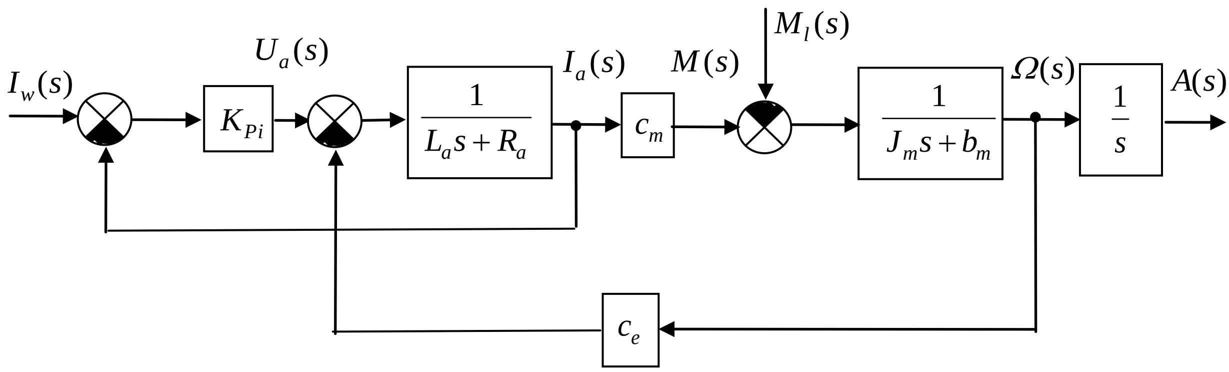

b)

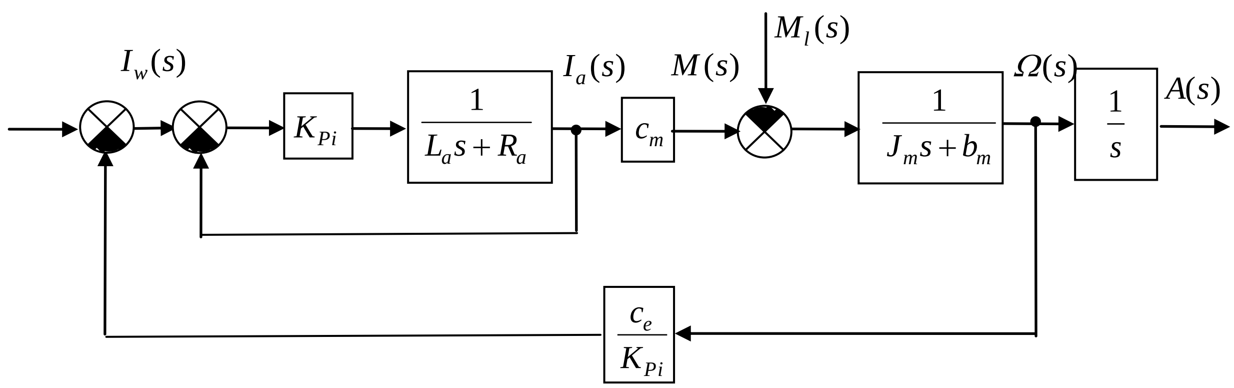

Fig. 6.37 Block diagram of the DC motor with a current loop: a) original, b) transformed – Example 6.12

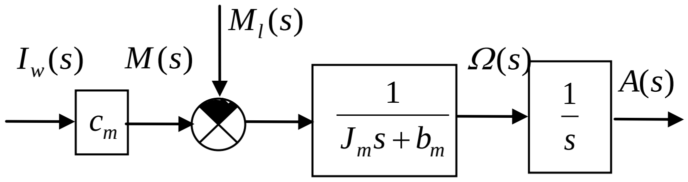

Fig. 6.38 Simplified block diagram of the DC motor with a tuned current loop – Example 6.12

For the speed loop the P controller with gain $K_{P\omega}$ is also used and in accordance with the block diagram in Fig. 6.39 we get

$$\frac{\Omega(s)}{\Omega_w(s)} = \frac{\dfrac{K_{P\omega}c_m}{K_{P\omega}c_m + b_m}}{\dfrac{J_m}{K_{P\omega}c_m + b_m}s + 1} = \frac{k_\omega}{T_\omega s + 1},$$

$$k_\omega = \frac{K_{P\omega}c_m}{K_{P\omega}c_m + b_m},\ T_\omega = \frac{J_m}{K_{P\omega}c_m + b_m},$$

$$\frac{\Omega(s)}{M_l(s)} = -\frac{\dfrac{1}{K_{P\omega}c_m + b_m}}{\dfrac{J_m}{K_{P\omega}c_m + b_m}s + 1} = -\frac{k_l}{T_\omega s + 1},$$

$$k_l = \frac{1}{K_{P\omega}c_m + b_m}.$$

Similarly like for the current loop for sufficiently high gain $K_{P\omega}$ of the P controller for the speed loop we obtain

$$k_\omega \approx 1, \qquad \frac{\Omega(s)}{\Omega_\omega(s)} \approx \frac{1}{T_\omega s + 1}.$$

In this case the time constant T_ω cannot be neglected because the total moment of inertia J_m often has a high value.

The simplified block diagram of the DC motor with a tuned current and speed loops is shown in Fig. 6.40.

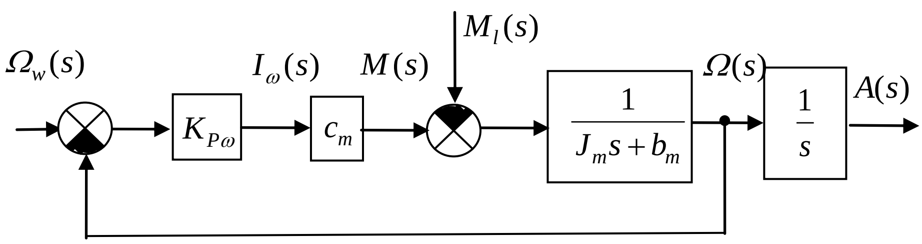

Fig. 6.39 Block diagram of the speed loop of a DC motor with a tuned current loop – Example 6.12

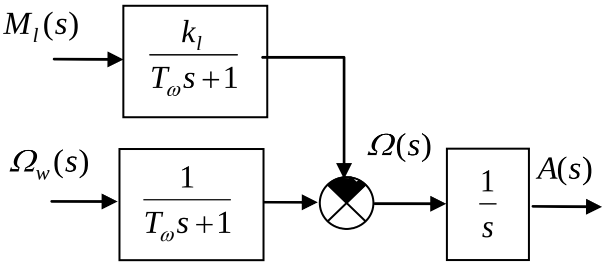

Fig. 6.40 Simplified block diagram of a speed loop of a DC motor with a tuned current loop – Example 6.12

First consider in the position loop in Fig. 6.41 the P controller with gain K_P. In accordance with Fig. 6.41 for

$$G_C(s) = K_P\,,$$

we get

$$\frac{A(s)}{A_w(s)} = \frac{1}{\frac{T_\omega}{K_P}s^2 + \frac{1}{K_P}s + 1}\,,$$

$$\frac{A(s)}{M_l(s)} = -\frac{\frac{k_l}{K_P}}{\frac{T_\omega}{K_P}s^2 + \frac{1}{K_P}s + 1}\,.$$

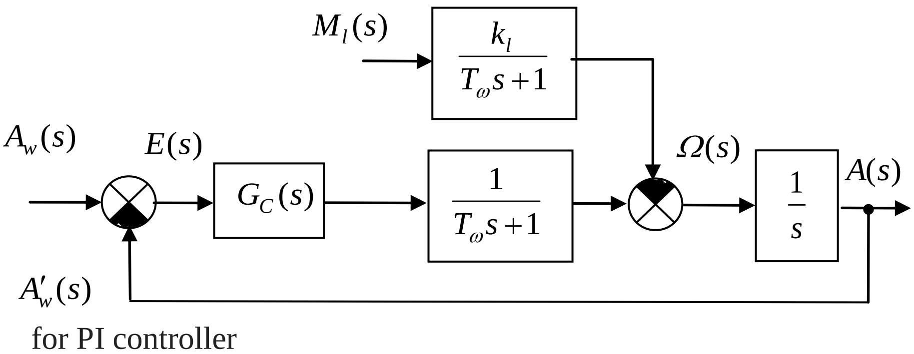

Fig. 6.41 Block diagram of a position loop of a DC motor with a tuned current and speed loops – Example 6.12

For a tuning of the P controller we will use the standard form (6.95) for the MOM, for which there holds

$$\left.\begin{aligned} T_w^2 &= \frac{T_\omega}{K_P} \\ 2\xi_w T_w &= \frac{1}{K_P} \\ \xi_w &= \frac{1}{\sqrt{2}} \end{aligned}\right\} \Rightarrow K_P^* = \frac{1}{2T_\omega}.$$

After substitution in the previous transfer functions there is obtained

$$\frac{A(s)}{A_w(s)} = \frac{1}{2T_\omega^2 s^2 + 2T_\omega s + 1},$$
$$\frac{A(s)}{M_l(s)} = -\frac{2k_l T_\omega}{2T_\omega^2 s^2 + 2T_\omega s + 1}.$$

From the last transfer function it follows that by the use of the P controller in the position loop the steady-state control error $e_m(\infty)$ remains in it for the step change of the load torque $m_l(t) = m_{l0}\eta(t)$.

Therefore there holds (see Fig. 6.41)

$$\frac{E_m(s)}{M_l(s)} = -\frac{A(s)}{M_l(s)} = \frac{2k_l T_\omega}{2T_\omega^2 s^2 + 2T_\omega s + 1},$$

the steady-state control error can be easily determined

$$e_m(\infty) = \lim_{s\to 0}\left[s\frac{E_m(s)}{M_l(s)}\frac{m_{l0}}{s}\right] = 2k_l T_\omega m_{l0}.$$

Now we will use the PI controller with transfer function

$$G_C(s) = K_P\left(1 + \frac{1}{T_I s}\right)$$

in the position loop.

Since the DC motor after tuning of the current and speed loops has the transfer function in a suitable form for the SOM, see Fig. 6.40 and Tab. 6.13, we can therefore directly write ($T = 0$, $k_1 = 1$, $T_1 = T_\omega$)

$$K_P^* = \frac{1}{2k_1 T_1} = \frac{1}{2T_\omega},$$
$$T_I^* = 4T_1 = 4T_\omega.$$

In accordance with Fig. 6.41 for the PI controller we get

$$\frac{A(s)}{A_w'(s)} = \frac{4T_\omega s + 1}{8T_\omega^3 s^3 + 8T_\omega^2 s^2 + 4T_\omega s + 1},$$
$$\frac{A(s)}{M_l(s)} = -\frac{8k_l T_\omega^2 s}{8T_\omega^3 s^3 + 8T_\omega^2 s^2 + 4T_\omega s + 1}.$$

Since in the last transfer function the complex variable *s* arises in the numerator, the step change of a load torque does not cause the steady-state control error (see the final value theorem, Appendix A).

The SOM gives a big overshoot. It is caused by the stable binomial

$$4T_\omega s + 1$$

in the numerator of the control system transfer function. That is why the 2DOF PI controller with $b = 0$ or the input filter with the transfer function (see Tab. 6.13)

$$G_F(s) = \frac{1}{4T_\omega s + 1}$$

must be used.

Then the resulting control system transfer function has the form

$$\frac{A(s)}{A_w(s)} = G_F(s)\frac{A(s)}{A'_w(s)} = \frac{1}{8T_\omega^3 s^3 + 8T_\omega^2 s^2 + 4T_\omega s + 1}.$$

On the basis of the above derived relations the simulation of the shaft (angular) position cascade control of the DC motor was performed for the following parameters: $J_m = 0.02$ kg m^2, $L_a = 0.2$ H, $R_a = 1\ \Omega$, $c_m = c_e = 0.05$ N m A^{-1} = V s rad^{-1}, $b_m = 0.01$ N m s rad^{-1}, $\alpha_{w0} = 1$ rad, $m_{l0} = 0.5$ N m.

The current loop

In the current loop the P controller with sufficiently high gain K_{Pi} is used, e.g. it is chosen as

$$K_{Pi}^* = 10 \Rightarrow k_a = \frac{K_{Pi}}{K_{Pi} + R_a} \doteq 0.91 \approx 1;$$

$$T_a = \frac{L_a}{K_{Pi} + R_a} \doteq 0.018 \approx 0;\ \ \frac{c_e}{K_{Pi}} \doteq 0.005 \approx 0.$$

The speed loop

Also in the speed loop the P controller with sufficiently high gain $K_{P\omega}$ is used, e.g. it is chosen as

$$K_{P\omega}^* = 10 \Rightarrow k_\omega = \frac{K_{P\omega}c_m}{K_{P\omega}c_m + b_m} \doteq 0.98 \approx 1;$$

$$T_\omega = \frac{J_m}{K_{P\omega}c_m + b_m} \doteq 0.039;\ \ k_l = \frac{1}{K_{P\omega}c_m + b_m} \doteq 1.96.$$

The position loop

a) P controller

In the block diagrams in Figs 6.41 and 6.42 the P controller

$$G_C(s) = K_P$$

and in Fig. 6.42 the transfer function

$$G_F(s) = 1$$

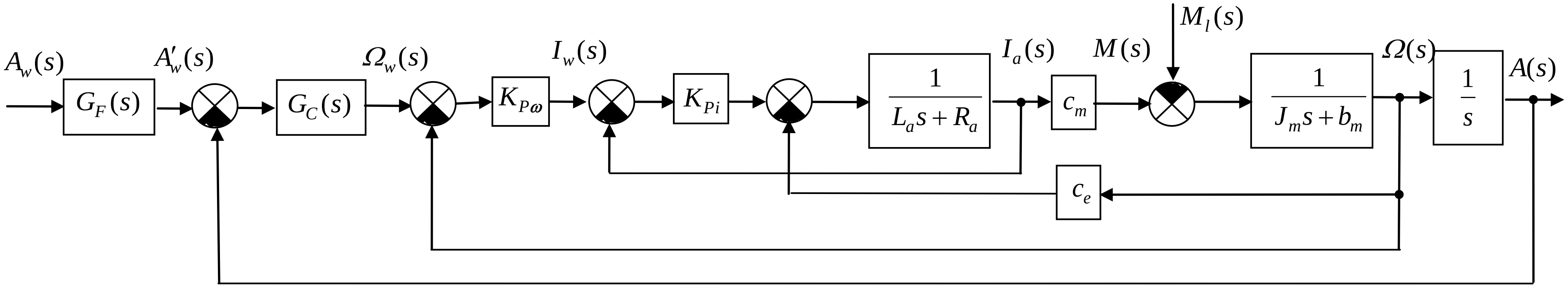

Fig. 6.42 Block diagram of angular position cascade control of a DC motor – Example 6.12

should be considered.

In accordance with the previous relations we can write

$$K_P^* = \frac{1}{2T_\omega} \doteq 12.82\,;$$

$$e_m(\infty) = 2k_l T_\omega m_{l0} \doteq 0.077\,\text{rad}.$$

The response of the DC motor with the cascade control for the P controller in the position loop is shown in Fig. 6.43.

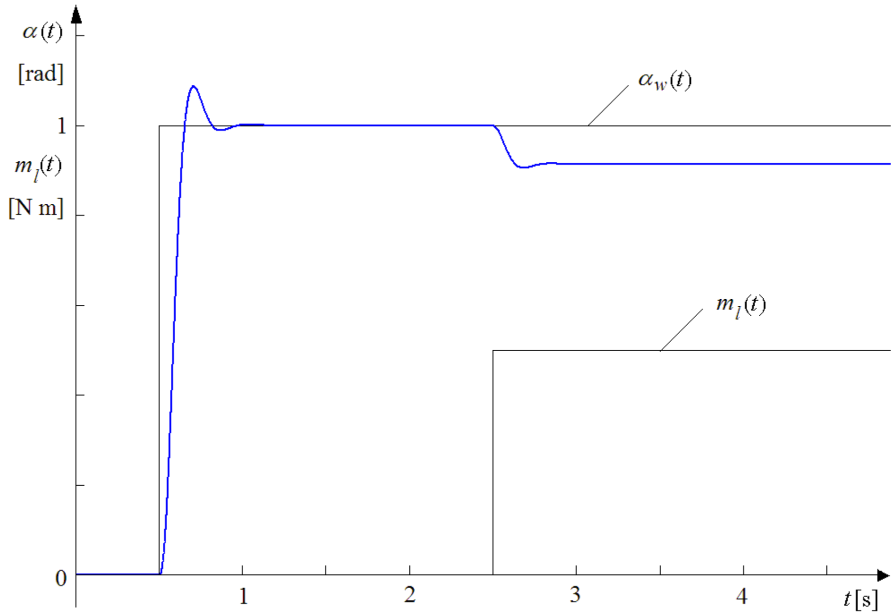

Fig. 6.43 Response of the DC motor with cascade control for the P controller in a position loop – Example 6.12

b) PI controller

In the block diagrams in Figs 6.41 and 6.42 the PI controller

$$G_C(s) = K_P\left(1 + \frac{1}{T_I s}\right)$$

and in Fig. 6.42 the transfer function

$$G_F(s) = \frac{1}{4T_\omega s + 1}$$

should be considered.

We will determine the adjustable parameters of the PI controller

$$K_P^* = \frac{1}{2T_\omega} \doteq 12.82;\; T_I^* = 4T_\omega \doteq 0.16\,.$$

The response of the DC motor with the cascade control for the PI controller in the position loop is shown in Fig. 6.44.

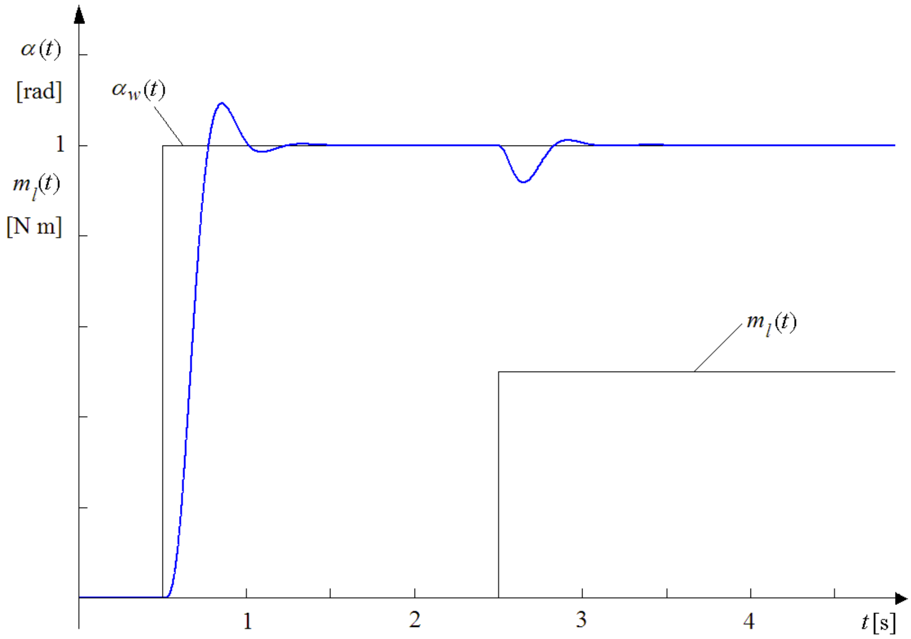

Fig. 6.44 Response of the DC motor with cascade control for the PI controller in a position loop – Example 6.12

Both Figs 6.43 and 6.44 show that even for large simplifications the results of the simulation illustrate good agreement with assumptions.

The real cascade control of the DC motor must consider the maximum permissible current in the current loop and the maximum permissible angular velocity in the speed loop. These restrictions cause significant nonlinearities of the cascade control. Most often PI controllers are used in current and speed loops, because it is necessary to consider the dynamics of power amplifiers, sensors and filters. In the position loop a P or PI controller is used.

7 STATE SPACE CONTROL

The chapter briefly describes the design of a state controller and observer for the SISO linear dynamic system.

7.1 State space controller

Development of a **state space control** is associated with the development of aeronautics and astronautics. It allows control very complex and unstable systems, where classical control with 1DOF and 2DOF controllers does not give satisfactory results.

Consider the SISO controlled linear dynamic system (in state space methods the name "controlled system" is most often used instead of the plant)

$$\dot{\boldsymbol{x}}(t) = \boldsymbol{A}\boldsymbol{x}(t) + \boldsymbol{b}u(t), \quad \boldsymbol{x}(0) = \boldsymbol{x}_0, \tag{7.1a}$$

$$y(t) = \boldsymbol{c}^T \boldsymbol{x}(t), \tag{7.1b}$$

which is controllable, observable and strongly physically realizable [see (3.36) and (3.37)]. Its characteristic polynomial has the form

$$\begin{aligned} N(s) = \det(s\boldsymbol{I} - \boldsymbol{A}) &= s^n + a_{n-1}s^{n-1} + \ldots + a_1 s + a_0 = \\ &= (s - s_1)(s - s_2)\ldots(s - s_n), \end{aligned} \tag{7.2}$$

where $s_1, s_2, \ldots, s_n$ are the system poles.

The task of the **state space controller** (state feedback, feedback controller) represented by the vector (Fig. 7.1)

$$\boldsymbol{k} = [k_1, k_2, \ldots, k_n]^T, \tag{7.3}$$

is to ensure for the closed-loop control system its characteristic polynomial

$$\begin{aligned} N_w(s) = \det(s\boldsymbol{I} - \boldsymbol{A}_w) &= s^n + a_{n-1}^w s^{n-1} + \ldots + a_1^w s + a_0^w = \\ &= (s - s_1^w)(s - s_2^w)\ldots(s - s_n^w) \end{aligned} \tag{7.4}$$

with given poles $s_1^w, s_2^w, \ldots, s_n^w$.

The vector of the state space controller can be obtained by comparing the coefficients of the control system characteristic polynomial with the corresponding coefficients of the desired control system characteristic polynomial at the same powers of complex variable s. In such a way the system of n linear equations is obtained for n unknown components k_i of the vector $\boldsymbol{k}$. For large n, this procedure is demanding.

The closed-loop control system with the state space controller in accordance with Fig 7.1 may be described by the equations

$$\dot{\boldsymbol{x}}(t) = \boldsymbol{A}_w\boldsymbol{x}(t) + \boldsymbol{b}w'(t), \quad \boldsymbol{x}(0) = \boldsymbol{x}_0, \tag{7.5a}$$

$$y(t) = \boldsymbol{c}^T \boldsymbol{x}(t), \tag{7.5b}$$

where the system matrix is given (see Fig. 7.1b)

$$\boldsymbol{A}_w = \boldsymbol{A} - \boldsymbol{b}\boldsymbol{k}^T \,. \tag{7.6}$$

The dependence between output $y_w(t)$ and input $w'(t)$ in the steady state ($t \to \infty$) can be determined on the basis of (3.39), i.e.

$$y_w = \lim_{s\to 0}[\boldsymbol{c}^T(s\boldsymbol{I} - \boldsymbol{A}_w)^{-1}\boldsymbol{b}]w' \;\Rightarrow$$

$$y_w = -\boldsymbol{c}^T\boldsymbol{A}_w^{-1}\boldsymbol{b}\,w' \,. \tag{7.7}$$

In order to in the steady state the equality

$$y_w = w \tag{7.8}$$

holds, the correction

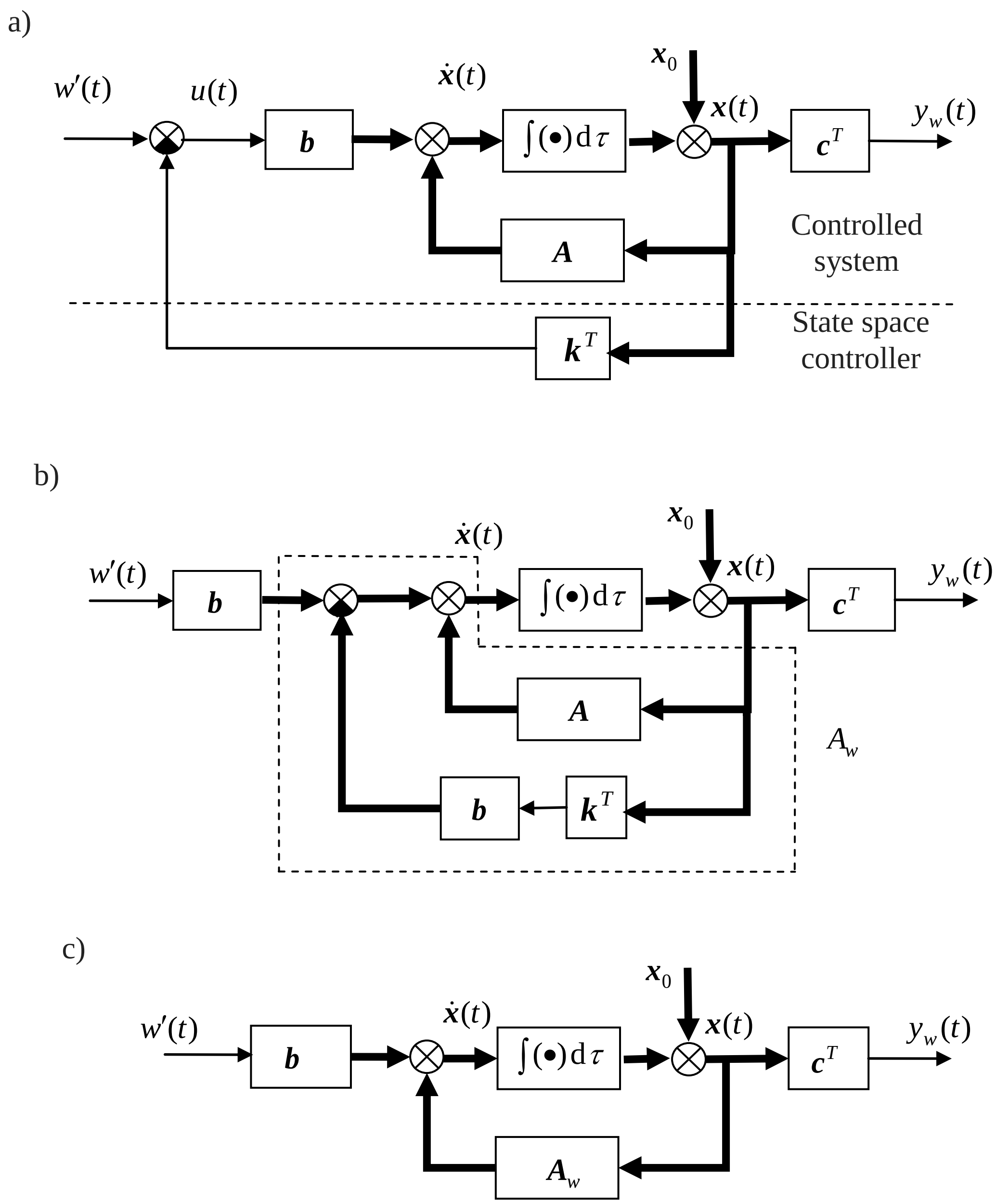

Fig. 7.1 Block diagram of the control system with a state space controller without input correction: a) original, b) modified, c) resultant

$$k_w = -\frac{1}{\boldsymbol{c}^T \boldsymbol{A}_w^{-1} \boldsymbol{b}} \tag{7.9}$$

in the input must be placed (Fig. 7.2).

The state space controller design is easy for the state space model of the controlled system in the canonical controller form (3.42).

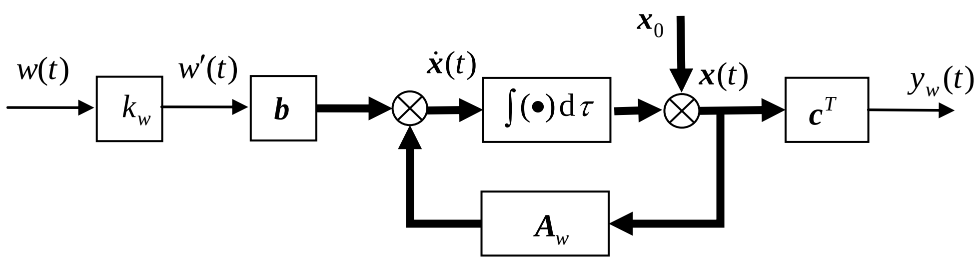

Fig. 7.2 Block diagram of the control system with a state space controller

Consider that the matrices $\boldsymbol{A}$ and $\boldsymbol{A}_w$ are transformed into canonical controller forms in accordance with the relations (3.36), (3.47), (3.49) and (3.50), then equation (7.6) can written in the canonical controller form

$$\boldsymbol{A}_{wc} = \boldsymbol{A}_c - \boldsymbol{b}_c \boldsymbol{k}_c^T \,. \tag{7.10a}$$

i.e.

$$\begin{bmatrix} 0 & 1 & 0 & \dots & 0 \\ 0 & 0 & 1 & \dots & 0 \\ \dots & \dots & \dots & \dots & \dots \\ 0 & 0 & 0 & \dots & 1 \\ -a_0^w & -a_1^w & -a_2^w & \dots & -a_{n-1}^w \end{bmatrix} = \\ = \begin{bmatrix} 0 & 1 & 0 & \dots & 0 \\ 0 & 0 & 1 & \dots & 0 \\ \dots & \dots & \dots & \dots & \dots \\ 0 & 0 & 0 & \dots & 1 \\ -a_0 & -a_1 & -a_2 & \dots & -a_{n-1} \end{bmatrix} - \begin{bmatrix} 0 \\ 0 \\ \vdots \\ 0 \\ 1 \end{bmatrix} [k_{c1}, k_{c2}, \dots, k_{cn}]. \tag{7.10b}$$

We can see that the equalities hold

$$-a_{i-1}^w = -a_{i-1} - k_{ci} \;\Rightarrow$$

$$k_{ci} = a_{i-1}^w - a_{i-1} \quad \text{for} \quad i = 1, 2, \dots, n. \tag{7.11}$$

The last equalities can be written in the vector form

$$\boldsymbol{k}_c = \boldsymbol{a}^w - \boldsymbol{a} \,, \tag{7.12}$$

where

$$\boldsymbol{a}^w = [a_0^w, a_1^w, \dots, a_{n-1}^w]^T \,, \tag{7.13a}$$

$$\boldsymbol{a} = [a_0, a_1, \ldots, a_{n-1}]^T \tag{7.13b}$$

are the vectors of the coefficients of the characteristic polynomials $N_w(s)$ and $N(s)$ [see (7.4) and (7.2)].

We have received the vector $\boldsymbol{k}_c$ of the feedback state space controller in the canonical controller form, and we must therefore transform it back for the original controlled system (7.1). We can write

$$\left.\begin{aligned} \boldsymbol{k}_c^T \boldsymbol{x}_c &= \boldsymbol{k}^T \boldsymbol{x} \\ \boldsymbol{x}_c &= \boldsymbol{T}_c^{-1} \boldsymbol{x} \end{aligned}\right\} \Rightarrow \boldsymbol{k}^T = \boldsymbol{k}_c^T \boldsymbol{T}_c^{-1} \Rightarrow$$

$$\boldsymbol{k}^T = (\boldsymbol{a}^w - \boldsymbol{a})^T \boldsymbol{T}_c^{-1}, \tag{7.14}$$

where the transformation matrix $\boldsymbol{T}_c$ is given by the relations [see (3.47), (3.49) and (3.50)]

$$\boldsymbol{T}_c = \boldsymbol{Q}_{co}(\boldsymbol{A}, \boldsymbol{b}) \boldsymbol{Q}, \tag{7.15a}$$

$$\boldsymbol{Q}_{co}(\boldsymbol{A}, \boldsymbol{b}) = [\boldsymbol{b}, \boldsymbol{Ab}, \ldots, \boldsymbol{A}^{n-1}\boldsymbol{b}], \tag{7.15b}$$

$$\boldsymbol{Q} = \begin{bmatrix} a_1 & a_2 & \ldots & a_{n-1} & 1 \\ a_2 & a_3 & \ldots & 1 & 0 \\ \ldots & \ldots & \ldots & \ldots & \ldots \\ a_{n-1} & 1 & \ldots & 0 & 0 \\ 1 & 0 & \ldots & 0 & 0 \end{bmatrix}. \tag{7.15c}$$

The state space controller is able to ensure the required pole placement of the control system, i.e. it is able to ensure its dynamic properties, but it cannot remove the harmful effect of disturbance variables.

In the case of the existence of the disturbances $\boldsymbol{v}(t)$, the state space model of the controlled system will be as follows

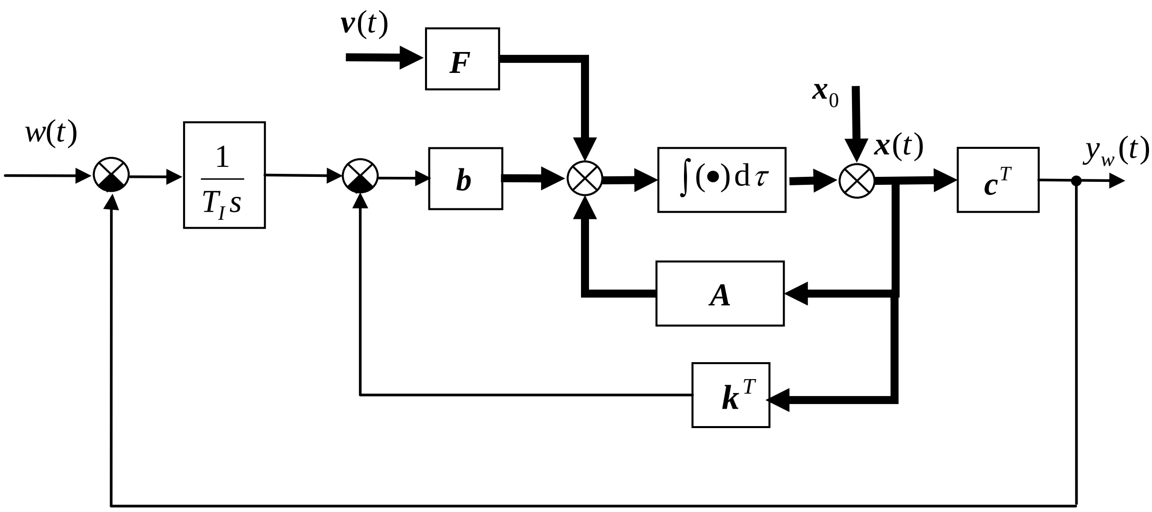

Fig. 7.3 Block diagram of a control system with a state space controller and additional loop with an I controller for disturbance attenuation

$$\dot{\boldsymbol{x}}(t) = \boldsymbol{A}\boldsymbol{x}(t) + \boldsymbol{b}u(t) + \boldsymbol{F}\boldsymbol{v}(t), \quad \boldsymbol{x}(0) = \boldsymbol{x}_0,$$

$$y(t) = \boldsymbol{c}^T \boldsymbol{x}(t),$$

where $\boldsymbol{v}(t)$ is the disturbance vector of the dimension p, $\boldsymbol{F}$ – the matrix of the dimension $(n \times p)$.

In order to eliminate disturbances $\boldsymbol{v}(t)$ an additional loop with a I or PI controller is added, see Fig. 7.3. It is obvious that the number of poles is increased by 1. This case is not further considered in the text.

Procedure:

1. Check the controllability and the observability of the controlled system (plant) [relations (3.36) and (3.37)].
2. Formulate the requirements for the control performance and express it by the desired pole placement of the control system.
3. Determine the coefficients of the characteristic polynomials $N(s)$ and $N_w(s)$ [relations (7.2) and (7.4)].
4. Compare the coefficients of the control system characteristic polynomial with the corresponding coefficients of the desired control system characteristic polynomial at the same powers of complex variable s and solve the system of n linear equations for n unknown components of the vector $\boldsymbol{k}$. In the case of high n use the transformation matrix (7.15) and the formula (7.14).
5. On the basis of the relation (7.9) determine the input correction k_w.
6. Verify the received control performance by a simulation.

Example 7.1

For the SISO linear dynamic controlled system (plant)

$$\begin{aligned}
\dot{x}_1 &= -x_1 - 4x_3 + 2u, \\
\dot{x}_2 &= 2x_1 - 2x_2 - 2x_3 + u, \\
\dot{x}_3 &= -4x_3 - 2u, \\
y &= -2x_1 + 4x_2 + x_3
\end{aligned}$$

it is necessary to design the state space controller which ensures for the closed-loop control system the poles

$$s_1^w = s_2^w = s_3^w = -2\,.$$

Solution:

It is obvious that for the controlled system the relations hold

$$\boldsymbol{x} = \begin{bmatrix} x_1 \\ x_2 \\ x_3 \end{bmatrix}, \; \boldsymbol{A} = \begin{bmatrix} -1 & 0 & -4 \\ 2 & -2 & -2 \\ 0 & 0 & -4 \end{bmatrix}, \; \boldsymbol{b} = \begin{bmatrix} 2 \\ 1 \\ -2 \end{bmatrix}, \; \boldsymbol{c}^T = \begin{bmatrix} -2 & 4 & 1 \end{bmatrix}.$$

Controllability verification:

$$\boldsymbol{Q}_{co}(\boldsymbol{A},\boldsymbol{b}) = [\boldsymbol{b}, \boldsymbol{Ab}, \boldsymbol{A}^2\boldsymbol{b}] = \begin{bmatrix} 2 & 6 & -38 \\ 1 & 6 & -16 \\ -2 & 8 & -32 \end{bmatrix},$$

$$\det \boldsymbol{Q}_{co}(\boldsymbol{A},\boldsymbol{b}) = -504 \neq 0 \;\Rightarrow\; \text{The controlled system is controllable.}$$

Observability verification:

$$\boldsymbol{Q}_{ob}(\boldsymbol{A},\boldsymbol{c}^T) = \begin{bmatrix} \boldsymbol{c}^T \\ \boldsymbol{c}^T\boldsymbol{A} \\ \boldsymbol{c}^T\boldsymbol{A}^2 \end{bmatrix} = \begin{bmatrix} -2 & 4 & 1 \\ 10 & -8 & -4 \\ -26 & 16 & -8 \end{bmatrix},$$

$$\det \boldsymbol{Q}_{ob}(\boldsymbol{A},\boldsymbol{c}^T) = 432 \neq 0 \;\Rightarrow\; \text{The controlled system is observable.}$$

From the controlled system transfer function

$$G_{uy}(s) = \frac{Y(s)}{U(s)} = \frac{\det(s\boldsymbol{I} - \boldsymbol{A} + \boldsymbol{bc}^T) - \det(s\boldsymbol{I} - \boldsymbol{A})}{\det(s\boldsymbol{I} - \boldsymbol{A})} = \frac{-2s^2 + 6s + 92}{s^3 + 7s^2 + 14s + 8}$$

it follows: $a_0 = 8$, $a_1 = 14$, $a_2 = 7$, $a_3 = 1$, $b_0 = 92$, $b_1 = 6$, $b_2 = -2$, i.e.

$$\boldsymbol{a} = [8,\quad 14,\quad 7]^T,\; \boldsymbol{c}_c = [92,\quad 6,\quad -2]^T.$$

The desired control system characteristic polynomial has the form

$$N_w(s) = (s+2)^3 = s^3 + 6s^2 + 12s + 8,$$

and therefore the vector of its coefficients is

$$\boldsymbol{a}^w = [8,\quad 12,\quad 6]^T.$$

The transformation matrix (7.15) has the form

$$\boldsymbol{T}_c = \boldsymbol{Q}_{co}(\boldsymbol{A},\boldsymbol{b})\boldsymbol{Q} = [\boldsymbol{b}, \boldsymbol{Ab}, \boldsymbol{A}^2\boldsymbol{b}] \begin{bmatrix} a_1 & a_2 & 1 \\ a_2 & 1 & 0 \\ 1 & 0 & 0 \end{bmatrix} = \begin{bmatrix} 32 & 20 & 2 \\ 40 & 13 & 1 \\ -4 & -6 & -2 \end{bmatrix} \Rightarrow$$

$$\boldsymbol{T}_c^{-1} = \begin{bmatrix} -\dfrac{5}{126} & \dfrac{1}{18} & -\dfrac{1}{84} \\ \dfrac{19}{126} & -\dfrac{1}{9} & \dfrac{2}{21} \\ -\dfrac{47}{126} & \dfrac{2}{9} & -\dfrac{16}{21} \end{bmatrix}.$$

On the basis of the relations (7.14) there is obtained

$$\boldsymbol{k}^T = \left(\boldsymbol{a}^w - \boldsymbol{a}\right)^T \boldsymbol{T}_c^{-1} = \left[\frac{1}{14},\quad 0,\quad \frac{4}{7}\right].$$

The state space model of the closed-loop control system without the input correction will be in the form

$$\boldsymbol{A}_w = \boldsymbol{A} - \boldsymbol{b}\boldsymbol{k}^T = \begin{bmatrix} -\frac{8}{7} & 0 & -\frac{36}{7} \\ \frac{27}{14} & -2 & -\frac{18}{7} \\ \frac{1}{7} & 0 & -\frac{20}{7} \end{bmatrix},$$

$$\boldsymbol{b} = [2, \quad 1, \quad -2]^T, \ \boldsymbol{c} = [-2, \quad 4, \quad 1]^T,$$

i.e.

$$\dot{x}_1 = -\frac{8}{7}x_1 - \frac{36}{7}x_3 + 2w',$$
$$\dot{x}_2 = \frac{27}{14}x_1 - 2x_2 - \frac{18}{7}x_3 + w',$$
$$\dot{x}_3 = \frac{1}{7}x_1 - \frac{20}{7}x_3 - 2w',$$
$$y_w = -2x_1 + 4x_2 + x_3.$$

The input correction is given by the formula (7.9)

$$k_w = -\frac{1}{\boldsymbol{c}^T \boldsymbol{A}_w^{-1} \boldsymbol{b}} = \frac{2}{23}.$$

and the corresponding state space model of the control system with the input correction has the form

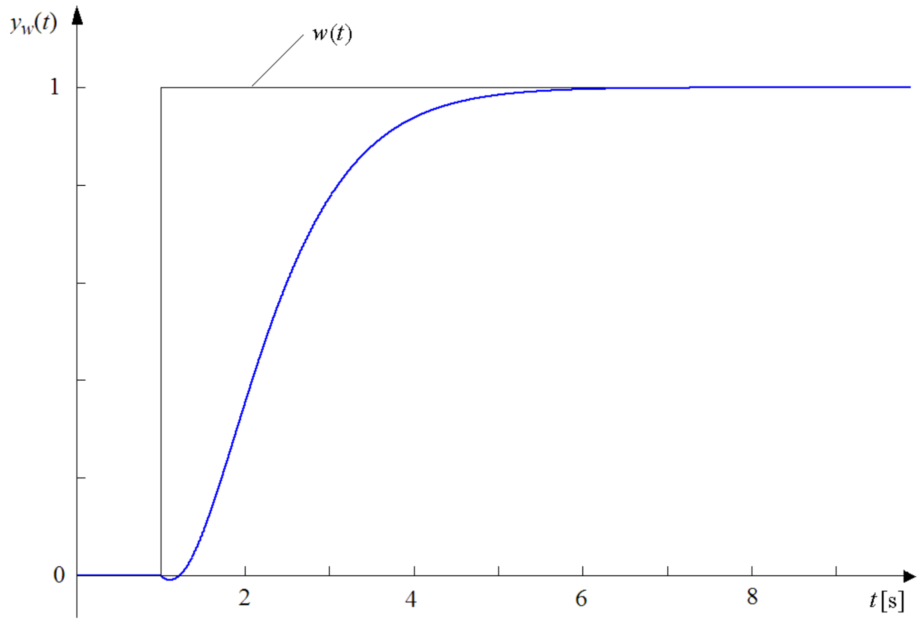

Fig. 7.4 Step response of a control system with a state space controller and input correction – Example 7.1

$$\begin{aligned}
\dot{x}_1 &= -\frac{8}{7}x_1 - \frac{36}{7}x_3 + \frac{4}{23}w,\\
\dot{x}_2 &= \frac{27}{14}x_1 - 2x_2 - \frac{18}{7}x_3 + \frac{2}{23}w,\\
\dot{x}_3 &= \frac{1}{7}x_1 - \frac{20}{7}x_3 - \frac{4}{23}w,\\
y_w &= -2x_1 + 4x_2 + x_3.
\end{aligned}$$

The step response of the control system with the state space controller and the input correction is shown in Fig. 7.4. The initial undershoot is caused by the unstable zero ($s_1^0 \doteq 8.446$).

7.2 State observer

The state variables in real dynamic system cannot often be measured due to their unavailability or high measuring costs. In these cases it is necessary to use the **state observer** (estimator).

We will focus on the design of the **Luenberger asymptotic full order observer** (further only the observer), i.e. such the observer which estimates the state variables which are asymptotically approaching the real state variables.

Consider the SISO linear dynamical system (7.1), which is controllable, observable and strongly physically realizable with the characteristic polynomial (7.2).

For this linear dynamic system the Luenberger observer has the form (Fig. 7.5)

$$\begin{aligned}
\dot{\hat{\boldsymbol{x}}}(t) &= \boldsymbol{A}_l\hat{\boldsymbol{x}}(t) + \boldsymbol{b}_l u(t) + \boldsymbol{l}y(t), \quad \hat{\boldsymbol{x}}(0) = \hat{\boldsymbol{x}}_0,\\
\hat{y}(t) &= \boldsymbol{c}_l^T\hat{\boldsymbol{x}}(t),
\end{aligned} \tag{7.16}$$

where $\boldsymbol{A}_l$ is the square observer matrix of order n [($n\times n$)], $\boldsymbol{b}_l$ – the vector of observer input of the dimension n, $\boldsymbol{c}_l$ – the vector of observer output of the dimension n, $\boldsymbol{l}$ – the vector of observer correction of the dimension n, by „^“ are marked the asymptotic estimates of the corresponding variables.

After the definition of the state error vector $\boldsymbol{\varepsilon}(t)$ by the relation

$$\boldsymbol{\varepsilon}(t) = \boldsymbol{x}(t) - \hat{\boldsymbol{x}}(t) \tag{7.17}$$

and considering the relations (7.1) and (7.16) we get

$$\dot{\boldsymbol{\varepsilon}}(t) = (\boldsymbol{A} - \boldsymbol{l}\boldsymbol{c}^T)\boldsymbol{x}(t) - \boldsymbol{A}_l\hat{\boldsymbol{x}}(t) + (\boldsymbol{b} - \boldsymbol{b}_l)u(t). \tag{7.18}$$

It is clear that the state error vector $\boldsymbol{\varepsilon}(t)$ should not depend on the input variable $u(t)$ and the estimate $\hat{y}(t)$ for the real state $\boldsymbol{x}(t)$ should be $\boldsymbol{c}^T\boldsymbol{x}(t)$, and therefore it must hold

$$\boldsymbol{b}_l = \boldsymbol{b}, \ \ \boldsymbol{c}_l = \boldsymbol{c}. \tag{7.19}$$

If we choose

$$\boldsymbol{A}_l = \boldsymbol{A} - \boldsymbol{l}\boldsymbol{c}^T \tag{7.20}$$

then for the assumption (7.19) the linear differential equation

$$\dot{\boldsymbol{\varepsilon}}(t) = \boldsymbol{A}_l \boldsymbol{\varepsilon}(t), \quad \boldsymbol{\varepsilon}_0 = \boldsymbol{x}_0 - \hat{\boldsymbol{x}}_0 \tag{7.21}$$

is obtained which describes the time course of the state error $\boldsymbol{\varepsilon}(t)$. The initial estimate $\hat{\boldsymbol{x}}_0$ is supposed zero in most cases.

It is clear that for the asymptotic state estimate $\hat{\boldsymbol{x}}(t)$ it must hold

$$t \to \infty \;\Rightarrow\; \hat{\boldsymbol{x}}(t) \to \boldsymbol{x}(t) \;\Rightarrow\; \boldsymbol{\varepsilon}(t) \to \boldsymbol{0}, \tag{7.22}$$

i.e. the linear differential equation (7.21) must be asymptotically stable.

It is obvious that in order for the state estimate $\hat{\boldsymbol{x}}(t)$ to be sufficiently accurate and fast for the changes of the real state $\boldsymbol{x}(t)$, the observer dynamics described by (7.16) and expressed by the characteristic eigenvalues of the matrix $\boldsymbol{A}_l$ must be faster than the dynamics of the observed system (7.1), expressed by the characteristic eigenvalues of the matrix $\boldsymbol{A}$. In the case of state space control the dynamics of the observer must be faster than the dynamics of the closed-loop control system.

The observer characteristic polynomial is

$$\begin{aligned} N_l(s) &= \det(s\boldsymbol{I} - \boldsymbol{A}_l) = \\ &= s^n + a_{n-1}^l s^{n-1} + \ldots + a_1^l s + a_0^l = (s-p_1)(s-p_2)\ldots(s-p_n), \end{aligned} \tag{7.23}$$

$$\boldsymbol{a}^l = [a_0^l, a_1^l, \ldots a_{n-1}^l]^T, \tag{7.24}$$

where p_i are the characteristic eigenvalues of the matrix $\boldsymbol{A}_l$ (the observer poles), $\boldsymbol{a}^l$ – the vector of the observer characteristic polynomial coefficients.

Similarly, the characteristic polynomial of the observed system (7.1) is given by (7.2) and the vector $\boldsymbol{a}$ is given by its coefficients (7.13b).

The observer asymptotic stability demands fulfilment of the conditions

$$\operatorname{Re} p_i < 0 \quad \text{pro} \quad i = 1, 2, \ldots, n \tag{7.25}$$

and furthermore, in order for the observer to have faster dynamics than the observed system, its all poles p_i must lie to the left of all poles s_i of the observed system, i.e.

$$\min_{1 \le i \le n} |\operatorname{Re} p_i| > \max_{1 \le i \le n} |\operatorname{Re} s_i|. \tag{7.26}$$

The convergence $\hat{\boldsymbol{x}}(t) \to \boldsymbol{x}(t)$ will be faster, if there will be greater margin in the inequality (7.26). It is often stated ten times, but too great a margin in the inequality (7.26) leads to large values of the components l_i of the state correction vector $\boldsymbol{l}$, and therefore to a large amplification of noise. Therefore, this margin shall be chosen from twice to five times (it does not apply for integrating systems).

The observer poles are usually chosen as multiple real

$$p_i = -p, \tag{7.27}$$

and therefore the conditions (7.26) can be written in the form

$$|p| > \max_{1 \le i \le n} |\operatorname{Re} s_i|. \tag{7.28}$$

In this case, the observer characteristic polynomial in accordance with the binomial theorem has the form

$$N_l(s) = (s+p)^n = \sum_{j=0}^{n} \binom{n}{j} p^j s^{n-j} = s^n + nps^{n-1} + \ldots + np^{n-1}s + p^n. \tag{7.29}$$

Using the observer multiple real pole it ensures the convergence (7.22) with the relative damping equal 1. If it is possible to have very suitable multiple pairs, the selection of multiple pairs

$$-(1 \pm j)p \tag{7.30}$$

will guarantee that the convergence (7.22) will be ensured with the relative damping equal $1/\sqrt{2} \doteq 0.707$. This choice ensures fast convergence and also reduces the value of p. The partial characteristic polynomial

$$s^2 + 2ps + 2p^2. \tag{7.31}$$

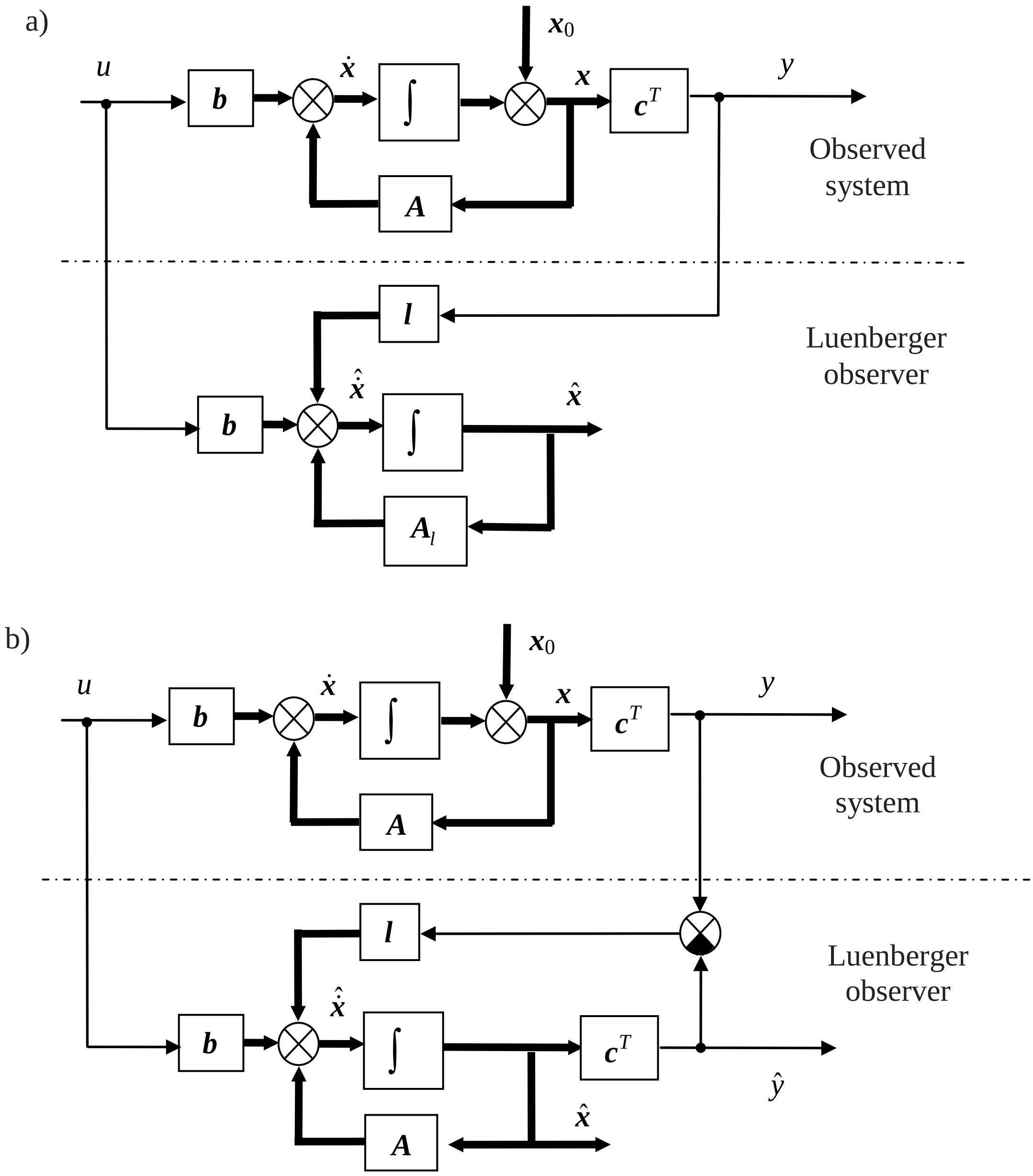

Fig. 7.5 Block diagram of the Luenberger observer: a) original, b) transformed

corresponds to the pair (7.30).

The block diagram in Fig. 7.5a can be transformed in the equivalent block diagram in Fig 7.5b, from which follows the operation of the observer. On the basis of the difference of the output variables $y(t)-\hat{y}(t)$ the state estimate $\hat{\boldsymbol{x}}(t)$ is corrected. It is clear that the Luenberger observer is in fact the model of the observed system with the running feedback correction

$$\dot{\hat{\boldsymbol{x}}}(t)=\boldsymbol{A}\hat{\boldsymbol{x}}(t)+\boldsymbol{b}u(t)+\boldsymbol{l}[y(t)-\hat{y}(t)]. \tag{7.32}$$

It is in principle a control system which tries to nullify the difference $y(t)-\hat{y}(t)$, and thus the state error vector $\boldsymbol{\varepsilon}(t)=\boldsymbol{x}(t)-\hat{\boldsymbol{x}}(t)$. Fig. 7.6 shows it clearly. The vector $\boldsymbol{l}$ is therefore also called the Luenberger observer gain vector.

When designing the observer in accordance with the relations (7.16) and (7.19) it is necessary to determine the unknown correction vector $\boldsymbol{l}$. It can be determined by comparing the coefficients of the observer characteristic polynomial with the corresponding coefficients of the desired observer characteristic polynomial at the same powers of the complex variable s. In such a way the system of n linear equations is obtained for n unknown components l_i of the vector $\boldsymbol{l}$. For large n, this procedure is demanding.

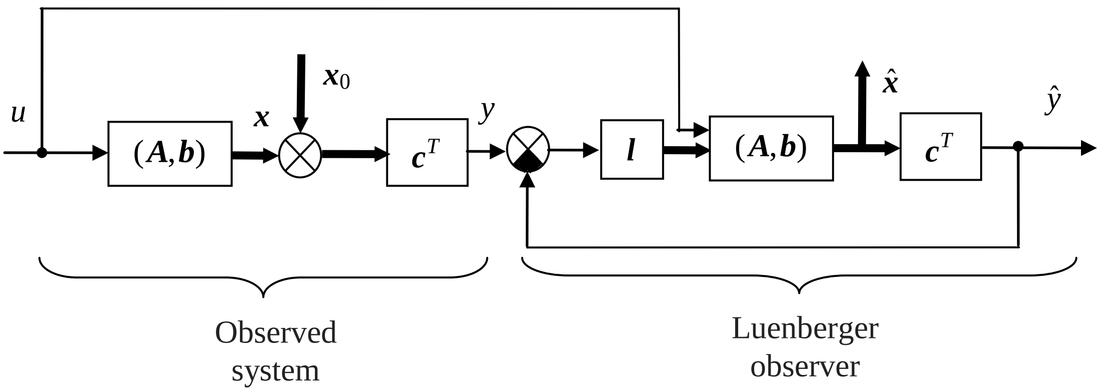

Fig. 7.6 Interpretation of the Luenberger observer

The design of the observer can be easily solved if the model of the observed system (7.1) has the canonical observer form (3.44)

$$\begin{aligned}\dot{\boldsymbol{x}}_o(t)&=\boldsymbol{A}_o\boldsymbol{x}_o(t)+\boldsymbol{b}_o u(t),\\ y(t)&=\boldsymbol{c}_o^T\boldsymbol{x}_o(t),\end{aligned} \tag{7.33a}$$

where

$$\boldsymbol{A}_o=\begin{bmatrix}0 & 0 & \dots & 0 & -a_0\\ 1 & 0 & \dots & 0 & -a_1\\ 0 & 1 & \dots & 0 & -a_2\\ \dots & \dots & \dots & \dots & \dots\\ 0 & 0 & \dots & 0 & -a_{n-2}\\ 0 & 0 & \dots & 1 & -a_{n-1}\end{bmatrix}, \tag{7.33b}$$

$$\boldsymbol{b_o} = [b_0, b_1, \ldots, b_{n-2}, b_{n-1}]^T, \tag{7.33c}$$

$$\boldsymbol{c}_o^T = [0, 0, \ldots, 0, 1]. \tag{7.33d}$$

The canonical observer form can be obtained directly from knowledge of the transfer function (3.41) or using the transformation (3.51)

$$\boldsymbol{x}_o(t) = \boldsymbol{T}_o^{-1}\boldsymbol{x}(t), \quad \boldsymbol{A}_o = \boldsymbol{T}_o^{-1}\boldsymbol{A}\boldsymbol{T}_o, \quad \boldsymbol{b}_o = \boldsymbol{T}_o^{-1}\boldsymbol{b}, \quad \boldsymbol{c}_o^T = \boldsymbol{c}^T\boldsymbol{T}_o, \tag{7.34}$$

where the transformation matrix of the order n [$(n \times n)$]

$$\boldsymbol{T}_o^{-1} = \boldsymbol{Q}\boldsymbol{Q}_{ob}(\boldsymbol{A}, \boldsymbol{c}^T) \tag{7.35}$$

is given by the observability matrix of the observed system (7.1), i.e. (3.37) and the matrix $\boldsymbol{Q}$ is given by the relation (7.15c) [see also (3.49)].

The observer (7.16) for (7.19) can also be expressed in the canonical observer form

$$\begin{aligned} \dot{\hat{\boldsymbol{x}}}_o(t) &= \boldsymbol{A}_{lo}\hat{\boldsymbol{x}}_o(t) + \boldsymbol{b}_o u + \boldsymbol{l}_o y(t), \\ \hat{y}(t) &= \boldsymbol{c}_o^T\hat{\boldsymbol{x}}_o(t), \end{aligned} \tag{7.36a}$$

where

$$\boldsymbol{A}_{lo} = \begin{bmatrix} 0 & 0 & \ldots & 0 & -a_0^l \\ 1 & 0 & \ldots & 0 & -a_1^l \\ 0 & 1 & \ldots & 0 & -a_2^l \\ \ldots & \ldots & \ldots & \ldots & \ldots \\ 0 & 0 & \ldots & 0 & -a_{n-2}^l \\ 0 & 0 & \ldots & 1 & -a_{n-1}^l \end{bmatrix} \tag{7.36b}$$

is the square observer matrix of the order n, in which the negative coefficients of the observer characteristic polynomial (7.23) appear in the last column.

The block diagrams for the canonical observer forms are the same as in Fig. 7.5, but all vectors and matrices must be provided with subscript "o".

In accordance with the relation (7.20) we can write

$$\boldsymbol{A}_{lo} = \boldsymbol{A}_o - \boldsymbol{l}_o\boldsymbol{c}_o^T = \begin{bmatrix} 0 & 0 & \ldots & 0 & -a_0 - l_{o1} \\ 1 & 0 & \ldots & 0 & -a_1 - l_{o2} \\ 0 & 1 & \ldots & 0 & -a_2 - l_{o3} \\ \ldots & \ldots & \ldots & \ldots & \ldots \\ 0 & 0 & \ldots & 0 & -a_{n-2} - l_{o,n-1} \\ 0 & 0 & \ldots & 1 & -a_{n-1} - l_{on} \end{bmatrix}. \tag{7.37}$$

From a comparison of the relations (7.36b) and (7.37) it follows

$$l_{oi} = a_{i-1}^l - a_{i-1} \quad \text{for} \quad i = 1, 2, \ldots, n,$$

i.e. in accordance with (7.24) and (7.13b)

$$\boldsymbol{l}_o = \boldsymbol{a}^l - \boldsymbol{a}, \tag{7.38}$$

where $\boldsymbol{l}_o$ is the observer correction vector in the canonical observer form.

Therefore (7.34) holds, it is possible to write

$$\begin{aligned} &\boldsymbol{l}_o y = \boldsymbol{T}_o^{-1}\boldsymbol{l}y \;\Rightarrow \\ &\boldsymbol{l} = \boldsymbol{T}_o\boldsymbol{l}_o = \boldsymbol{T}_o(\boldsymbol{a}^l - \boldsymbol{a}) \end{aligned} \tag{7.39}$$

Consider now, that the state space controller uses the state estimate $\hat{\boldsymbol{x}}(t)$ for control (Fig. 7.7), i.e.

$$\dot{\boldsymbol{x}}(t) = \boldsymbol{A}\boldsymbol{x}(t) - \boldsymbol{b}\boldsymbol{k}^T\hat{\boldsymbol{x}}(t)\,.$$

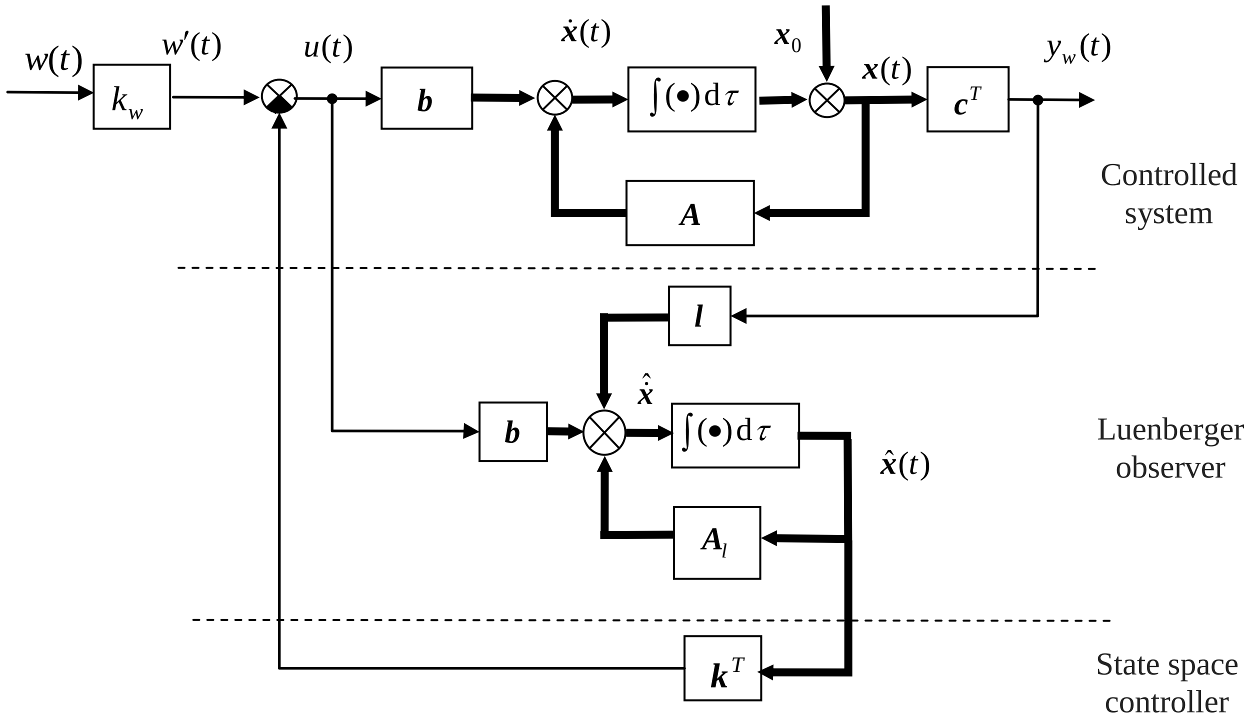

Fig. 7.7 Block diagram of a control system with a state space controller and Luenberger state observer

Therefore the equality holds

$$-\boldsymbol{b}\boldsymbol{k}^T\hat{\boldsymbol{x}}(t) = -\boldsymbol{b}\boldsymbol{k}^T\boldsymbol{x}(t) + \boldsymbol{b}\boldsymbol{k}^T\boldsymbol{\varepsilon}(t)\,,$$

we can write the state equation of the control system with state space controller and the Luenberger observer in the form [see (7.6)]

$$\begin{aligned} &\dot{\boldsymbol{x}}(t) = \boldsymbol{A}_w\boldsymbol{x}(t) + \boldsymbol{b}\boldsymbol{k}^T\boldsymbol{\varepsilon}(t), \\ &\dot{\boldsymbol{\varepsilon}}(t) = \boldsymbol{A}_l\boldsymbol{\varepsilon}(t), \end{aligned} \tag{7.40a}$$

or

$$\begin{bmatrix} \dot{\boldsymbol{x}}(t) \\ \dot{\boldsymbol{\varepsilon}}(t) \end{bmatrix} = \begin{bmatrix} \boldsymbol{A}_w & \boldsymbol{b}\boldsymbol{k}^T \\ \boldsymbol{0} & \boldsymbol{A}_l \end{bmatrix} \begin{bmatrix} \boldsymbol{x}(t) \\ \boldsymbol{\varepsilon}(t) \end{bmatrix}. \tag{7.40b}$$

It is the upper block triangular matrix, whose characteristic polynomial is given by the relation

$$N_w(s)N_l(s) = \det(sI - \boldsymbol{A}_w)\det(sI - \boldsymbol{A}_l)\,. \tag{7.41}$$

This means that the dynamic properties of the control system with the state space controller and the Luenberger state observers are mutually independent.

It is the so called **separation principle**.

It is very important because the state observer and the state space controller can be design independently. We can design a state space controller that ensures the required control performance and then we can separately design the Luenberger state observer, which ensures the correct state variable estimates. A well-designed state observer deteriorates the resulting dynamics of a control system with a state space controller very little.

Procedure:

1. Check the controllability and observability of the controlled system (plant) [relations (3.36) and (3.37)].
2. Determine the coefficients of the characteristic polynomials $N(s)$ and $N_l(s)$ [relations (7.2) and (7.23)].
3. On the basis of the pole of the control system with the largest absolute real part determine the multiple pole (7.27) or multiple pairs of poles (7.30) in such a way to ensure the sufficiently fast dynamics of the observer.
4. Compare the coefficients of the observer characteristic polynomial with the corresponding coefficients of the desired observer characteristic polynomial at the same powers of the complex variable s and the solution of the system of n linear equations is obtained for n unknown components l_i of the vector $\boldsymbol{l}$. For large n, use the transformation matrix (7.35) and the formula (7.39).
5. Verify by simulating the received estimates of the state variables

Example 7.2

For the control system with the state space controller from Example 7.1 it is necessary to design the Luenberger state observer.

Solution:

In the Example 7.1 it was shown that the controlled system is controllable and observable, and that its characteristic polynomial has the form

$$N(s) = \det(s\boldsymbol{I} - \boldsymbol{A}) = s^3 + 7s^2 + 14s + 8 = (s+1)(s+2)(s+4)\,,$$

where

$$s_1 = -1,\ \ s_2 = -2,\ \ s_3 = -4$$

are the controlled system poles and

$$a_0 = 8,\ a_1 = 14,\ a_2 = 7 \ \ \Rightarrow \ \ \boldsymbol{a} = [8,\ 14,\ 7]^T$$

are its characteristic polynomial coefficients or the vector of these coefficients.

Since

$$\max_{1\le i\le 3}|s_i| = 4$$

it is possible to choose

$$p_1 = p_2 = p_3 = p = -8$$

i.e. the observer characteristic polynomial and its coefficients are

$$N_l(s) = (s-p)^3 = (s+8)^3 = s^3 + 24s^2 + 192s + 512 \Rightarrow$$

$$a_0^l = 512,\ a_1^l = 192,\ a_2^l = 24 \Rightarrow \boldsymbol{a}^l = [512, \quad 192, \quad 24]^T .$$

a) Direct solution

The observer matrix is

$$\boldsymbol{A}_l = \boldsymbol{A} - \boldsymbol{l}\boldsymbol{c}^T = \begin{bmatrix} -1 & 0 & -4 \\ 2 & -2 & -2 \\ 0 & 0 & -4 \end{bmatrix} - \begin{bmatrix} l_1 \\ l_2 \\ l_3 \end{bmatrix} \begin{bmatrix} -2 & 4 & 1 \end{bmatrix} =$$

$$= \begin{bmatrix} 2l_1 - 1 & -4l_1 & -l_1 - 4 \\ 2l_2 + 2 & -4l_2 - 2 & -l_2 - 2 \\ 2l_3 & -4l_3 & -l_3 - 4 \end{bmatrix}.$$

After unpleasant computations the observer characteristic polynomial

$$N_l(s) = \det(s\boldsymbol{I} - \boldsymbol{A}_l) =$$
$$= s^3 + (-2l_1 + 4l_2 + l_3 + 7)s^2 + (-4l_1 + 20l_2 + 3l_3 + 14)s + 16l_1 + 16l_2 - 22l_3 + 8$$

was determined.

Comparing the coefficients at the same powers of the complex variable s for both of the observer characteristic polynomials, the system of linear algebraic equations with respect to unknown components l_1, l_2 and l_3 of the observer correction vector $\boldsymbol{l}$ was obtained, i.e.

$$\left.\begin{aligned} 16l_1 + 16l_2 - 22l_3 &= 504 \\ -4l_1 + 20l_2 + 3l_3 &= 178 \\ -2l_1 + 4l_2 + l_3 &= 17 \end{aligned}\right\} \Rightarrow \begin{aligned} l_1 &= \frac{773}{54}, \\ l_2 &= \frac{332}{27}, \\ l_3 &= -\frac{32}{9}. \end{aligned}$$

b) Solution by transformation

In accordance with (7.15c) there is obtained

$$\boldsymbol{Q} = \begin{bmatrix} a_1 & a_2 & 1 \\ a_2 & 1 & 0 \\ 1 & 0 & 0 \end{bmatrix} = \begin{bmatrix} 14 & 7 & 1 \\ 7 & 1 & 0 \\ 1 & 0 & 0 \end{bmatrix}.$$

The transformation matrix can now be determined

$$\boldsymbol{T}_o^{-1} = \boldsymbol{Q}\boldsymbol{Q}_{ob}(\boldsymbol{A},\boldsymbol{c}^T) = \begin{bmatrix} 16 & 16 & -22 \\ -4 & 20 & 3 \\ -2 & 4 & 1 \end{bmatrix} \Rightarrow$$

$$\boldsymbol{T}_o = \begin{bmatrix} -\frac{1}{54} & \frac{13}{54} & -\frac{61}{54} \\ \frac{1}{216} & \frac{7}{108} & -\frac{5}{54} \\ -\frac{1}{18} & \frac{2}{9} & -\frac{8}{9} \end{bmatrix}.$$

After substituting into the relation on the observer correction vector $\boldsymbol{l}$, the same result

$$\boldsymbol{l} = \boldsymbol{T}_o(\boldsymbol{a}^l - \boldsymbol{a}) = \begin{bmatrix} \frac{773}{54} \\ \frac{332}{27} \\ -\frac{32}{9} \end{bmatrix}$$

is obtained as for the direct solution.

The step response of the control system with a state space controller with and without the Luenberger state observer is shown in Fig. 7.8.

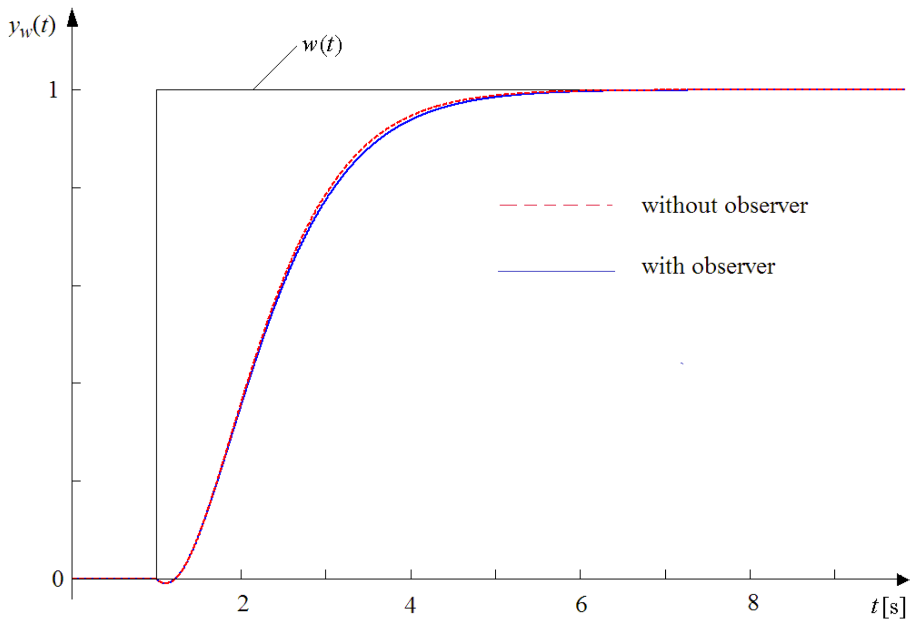

Fig. 7.8 Influence of the Luenberger state observer on the step response of a control system with a state space controller – Example 7.2

APPENDIX – A

LAPLACE TRANSFORM

The Laplace transform is a very effective tool for the description, analysis and synthesis of continuous (analog) control systems.

The purpose of a transform is the transfer of a complex problem from the original domain in the transform domain, where this problem can be easily solved and then it can be transferred back in the original domain in accordance with Fig. A. 1.

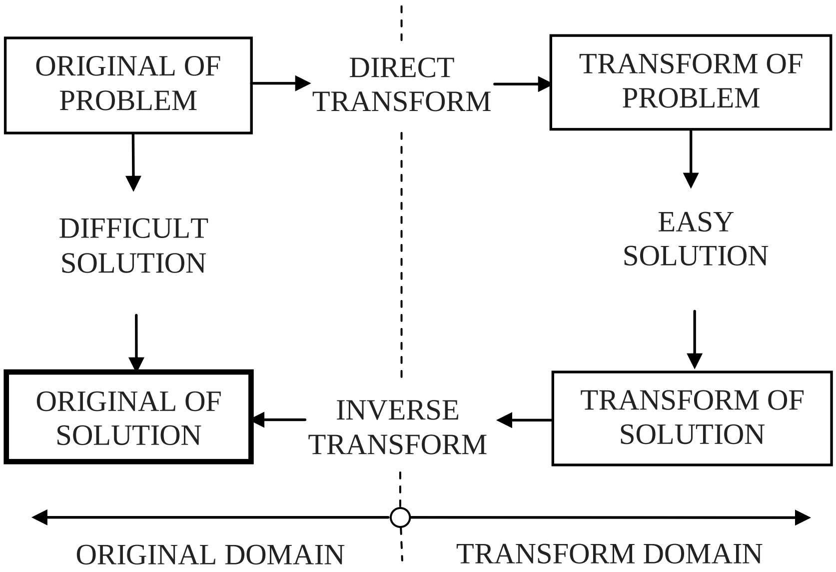

Fig. A.1 General diagram for solving problems by means of a transform

In our case the original domain is the time domain and the transform domain is the complex variable domain. For example, a differentiation and an integration in the time domain are difficult problems, i.e. they are difficult mathematical operations. These difficult operations in the time domain correspond to simple algebraic operations in the complex variable domain. Similarly a solution of linear differential equations in the time domain corresponds to an easy solution of algebraic equations in a complex variable domain.

The **Laplace transform** is defined by the formulas

$$X(s) = \mathrm{L}\{x(t)\} = \int_0^\infty x(t)\mathrm{e}^{-st}\,\mathrm{d}t \ , \tag{A.1}$$

$$x(t) = \mathrm{L}^{-1}\{X(s)\} = \frac{1}{2\pi\mathrm{j}}\int_{c-j\infty}^{c+j\infty} X(s)\,\mathrm{e}^{st}\mathrm{d}s \ , \tag{A.2}$$

where $s = \alpha + \mathrm{j}\omega$ is the complex variable ($\alpha = \operatorname{Re} s$, $\omega = \operatorname{Im} s$), t – the real variable (in our case – **time**), $x(t)$ – the **original** – the real function defined in the time domain for $t \in \langle 0,\infty)$, $X(s)$ – the **transform** – the complex variable function defined in the complex variable domain, $\mathrm{j} = \sqrt{-1}$ – the imaginary unit, L – the operator of the direct Laplace transform, L^{-1} – the operator of the inverse Laplace transform, c – the real constant selected so as to the function $X(s)$ has no any singular points in the half plane for $\operatorname{Re} s > c$.

From formula (A.1) it follows that the Laplace transform maps the function of the real variable $x(t)$ on the complex function of the complex variable $X(s)$. The value of the original $x(t)$ for $t \geq 0$ represents in physical interpretations a magnitude of the given physical quantity in the time t. Therefore the physical dimension of the complex variable s is time^{-1}. The imaginary part of the complex variable s, i.e. $\omega = \operatorname{Im} s$ has the physical interpretation of the angular frequency with the physical dimension time^{-1}. The time t changes continuously and therefore the Laplace transform is a continuous transform. It is obvious that the Laplace transform is first of all suitable for linear continuous systems which can be described by means of linear differential, integral and integrodifferentilal equations with constant coefficients.

In order for the time function $x(t)$ to be original it must be:

a) equal to zero for the negative time, i.e.:

$$x(t) = \begin{cases} x(t) & t \geq 0, \\ 0 & t < 0; \end{cases} \tag{A.3}$$

b) of the exponential order, i.e. it must satisfy the inequality

$$\left.\begin{aligned} &|x(t)| \leq M\,\mathrm{e}^{\alpha_0 t}, \\ &M > 0, \alpha_0 \in (-\infty, \infty), t \in \langle 0, \infty); \end{aligned}\right\} \tag{A.4}$$

c) piecewise continuous.

In most of time functions used in engineering the last two conditions are fulfilled. For example, function $x(t) = \mathrm{e}^{t^2}$ does not hold the second condition.

The first condition can be held by the multiplication of the given time function by the **unit Heaviside step** defined by the formula

$$\eta(t) = \begin{cases} 1 & t \geq 0, \\ 0 & t < 0. \end{cases} \tag{A.5}$$

Before using the Laplace transform every continuous function $x(t)$ must be multiplied by the unit Heaviside step, and that is why notation $x(t)\eta(t)$ is mostly simplified and the symbol $\eta(t)$ is omitted.

An original is indicated by a small letter and its transform is indicated by a capital letter. The relation between an original and its transform is called a **correspondence** and it is written in the form

$$x(t) \mathrel{\hat{=}} X(s). \tag{A.6}$$

The correspondence between an original and its transform is single valued in a Laplace transform if we consider time functions equivalent, in this case when their values differ by finite values in finite isolated points.

In the Laplace transform in the case that the function $x(t)$ is not continuous in the point $t = 0$ the initial value $x(0)$ is considered as the right-hand limit.

$$x(0) = x(0_+) = \lim_{t \to 0_+} x(t). \tag{A.7}$$

The same is applied for a derivative of the function $x(t)$ and therefore the values $x(0),\ \dfrac{\mathrm{d}x(0)}{\mathrm{d}t},\ldots$ must be considered as the right-hand limits.

Example A.1

By the help of the direct Laplace transform definition formula (A.1) it is necessary to determine the transforms of the given time functions (originals):

a) $\eta(t-T_d)$, b) t, c) e^{-at}, d) $\sin\omega t$, e) $\delta(t)$ (a, ω, T_d are the constants).

Solution:

a) $$\mathrm{L}\{\eta(t-T_d)\}=\int_0^\infty \eta(t-T_d)\mathrm{e}^{-st}\mathrm{d}t=\int_{T_d}^\infty \mathrm{e}^{-st}\mathrm{d}t=\left[-\frac{1}{s}\mathrm{e}^{-st}\right]_{T_d}^\infty=\frac{1}{s}\mathrm{e}^{-T_d s},$$

$$\eta(t-T_d)\,\hat{=}\,\frac{1}{s}\mathrm{e}^{-T_d s}\ . \tag{A.8}$$

We can see that the time delay T_d of the original corresponds to the multiplication of the transform by the exponential function $\mathrm{e}^{-T_d s}$.

b) $$\mathrm{L}\{t\}=\int_0^\infty t\,\mathrm{e}^{-st}\mathrm{d}t=\left[t\left(-\frac{1}{s}\mathrm{e}^{-st}\right)\right]_0^\infty-\int_0^\infty\left(-\frac{1}{s}\mathrm{e}^{-st}\right)\mathrm{d}t=\left[-\frac{1}{s^2}\mathrm{e}^{-st}\right]_0^\infty=\frac{1}{s^2},$$

$$t\,\hat{=}\,\frac{1}{s^2}\quad . \tag{A.9}$$

The integration method by parts was used

$$\int_a^b u\dot{v}\,\mathrm{d}t=[uv]_a^b-\int_a^b \dot{u}v\,\mathrm{d}t, \tag{A.10}$$

where $u = t,\ \dot{v}=\mathrm{e}^{-st}$.

c) $$\mathrm{L}\{\mathrm{e}^{-at}\}=\int_0^\infty \mathrm{e}^{-at}\,\mathrm{e}^{-st}\mathrm{d}t=\int_0^\infty \mathrm{e}^{-(s+a)t}\,\mathrm{d}t=\left[-\frac{1}{s+a}\mathrm{e}^{-(s+a)t}\right]_0^\infty=\frac{1}{s+a},$$

$$\mathrm{e}^{-at}\,\hat{=}\,\frac{1}{s+a}\ . \tag{A.11}$$

d) $$\mathrm{L}\{\sin\omega t\}=\int_0^\infty(\sin\omega t)\mathrm{e}^{-st}\mathrm{d}t=\int_0^\infty\frac{1}{2\,\mathrm{j}}\left(\mathrm{e}^{\mathrm{j}\omega t}-\mathrm{e}^{-\mathrm{j}\omega t}\right)\mathrm{e}^{-st}\,\mathrm{d}t=$$

$$=\frac{1}{2\,\mathrm{j}}\left[\int_0^\infty \mathrm{e}^{-(s-\mathrm{j}\omega)t}\,\mathrm{d}t-\int_0^\infty \mathrm{e}^{-(s+\mathrm{j}\omega)t}\,\mathrm{d}t\right]=$$

$$\frac{1}{2\,\mathrm{j}}\left\{\left[-\frac{1}{s-\mathrm{j}\omega}\mathrm{e}^{-(s-\mathrm{j}\omega)t}\right]_0^\infty+\left[\frac{1}{s+\mathrm{j}\omega}\mathrm{e}^{-(s+\mathrm{j}\omega)t}\right]_0^\infty\right\}=$$

$$=\frac{1}{2\mathrm{j}}\left(\frac{1}{s-\mathrm{j}\omega}-\frac{1}{s+\mathrm{j}\omega}\right)=\frac{\omega}{s^2+\omega^2},$$

$$\sin\omega t \mathrel{\hat{=}} \frac{\omega}{s^2+\omega^2} \quad . \tag{A.12}$$

The Euler formula was used

$$\sin\omega t=\frac{1}{2\mathrm{j}}\left(\mathrm{e}^{\mathrm{j}\omega t}-\mathrm{e}^{-\mathrm{j}\omega t}\right). \tag{A.13}$$

e) The symbol $\delta(t)$ represents the **unit Dirac impulse** defined by the relations

$$\begin{aligned}&\int_{-\infty}^{\infty}\delta(t)x(t)\,\mathrm{d}t=x(0),\\ &\delta(t)=0\ \text{for}\ t\neq 0,\end{aligned} \tag{A.14}$$

$$\mathrm{L}\{\delta(t)\}=\int_0^{\infty}\delta(t)\mathrm{e}^{-st}\mathrm{d}t=\mathrm{e}^0=1,$$

$$\delta(t)\mathrel{\hat{=}}1 \quad . \tag{A.15}$$

Example A.2

By the help of the direct Laplace transform definition formula (A.1) it is necessary to determine the transforms of the given mathematical operations: a) $a_1x_1(t)\pm a_2x_2(t)$, where a_1, a_2 are any real or complex constants b) $\frac{\mathrm{d}x(t)}{\mathrm{d}t}$, c) $\int_0^t x(\tau)\mathrm{d}\tau$.

Solution:

a) $$\mathrm{L}\{a_1x_1(t)\pm a_2x_2(t)\}=\int_0^{\infty}[a_1x_1(t)\pm a_2x_2(t)]\mathrm{e}^{-st}\mathrm{d}t=$$

$$=a_1\int_0^{\infty}x_1(t)\mathrm{e}^{-st}\mathrm{d}t\pm a_2\int_0^{\infty}x_2(t)\mathrm{e}^{-st}\mathrm{d}t=a_1X_1(s)\pm a_2X_2(s),$$

$$a_1x_1(t)\pm a_2x_2(t)\mathrel{\hat{=}}a_1X_1(s)\pm a_2X_2(s) \quad . \tag{A.16}$$

The derived correspondence (A.16) expresses the **linearity** of the Laplace transform.

b) $$\mathrm{L}\left\{\frac{\mathrm{d}x(t)}{\mathrm{d}t}\right\}=\int_0^{\infty}\frac{\mathrm{d}x(t)}{\mathrm{d}t}\mathrm{e}^{-st}\mathrm{d}t=\left[x(t)\mathrm{e}^{-st}\right]_0^{\infty}+\int_0^{\infty}sx(t)\mathrm{e}^{-st}\mathrm{d}t=sX(s)-x(0),$$

$$\frac{\mathrm{d}x(t)}{\mathrm{d}t}\mathrel{\hat{=}}sX(s)-x(0). \tag{A.17}$$

The integration method by parts (A.10) was used, where $u=\mathrm{e}^{-st}$, $\dot{v}=\frac{\mathrm{d}x(t)}{\mathrm{d}t}$.

Similarly the transform from the n-th order derivative can be determined

$$\frac{\mathrm{d}^n x(t)}{\mathrm{d}t^n} \mathrel{\hat{=}} s^n X(s) - s^{n-1}x(0) - s^{n-2}\frac{\mathrm{d}\,x(0)}{\mathrm{d}t} - \ldots - \frac{\mathrm{d}^{n-1}x(0)}{\mathrm{d}t^{n-1}} \quad . \tag{A.18}$$

For zero initial conditions a simple and very important formula holds

$$\frac{\mathrm{d}^n x(t)}{\mathrm{d}t^n} \mathrel{\hat{=}} s^n X(s)\,. \tag{A.19}$$

We can see that the n-th order derivative in the time domain corresponds to the multiplication of the transform by the n-th power of the complex variable s in the complex variable domain.

c)

$$\mathrm{L}\left\{\int_0^t x(\tau)\mathrm{d}\tau\right\} = \int_0^\infty\left[\int_0^t x(\tau)\mathrm{d}\tau\right]\mathrm{e}^{-st}\mathrm{d}t = \left[\left[\int_0^t x(\tau)\mathrm{d}\tau\right]\left(-\frac{1}{s}\mathrm{e}^{-st}\right)\right]_0^\infty - \int_0^\infty x(t)\left(-\frac{1}{s}\mathrm{e}^{-st}\right)\mathrm{d}t =$$

$$= 0 + \frac{1}{s}\int_0^\infty x(t)\mathrm{e}^{-st}\mathrm{d}t = \frac{1}{s}X(s),$$

$$\int_0^t x(\tau)\mathrm{d}\tau \mathrel{\hat{=}} \frac{1}{s}X(s)\,. \tag{A.20}$$

The integration method by parts (A.10) was used, where $u = \int_0^t x(\tau)\mathrm{d}\tau,\ \ \dot{v} = \mathrm{e}^{-st}$.

We can see that the integration in the time domain corresponds to the division of the transform by the complex variable s in the complex variable domain.

In the Examples A.1 and A.2 transforms of some simple time functions were derived on the basis of the direct Laplace transform definition formula (A.1). The use of the inverse Laplace transform definition formula (A.2) is time consuming and labour intensive. It demands very good knowledge of the theory of complex variables. Therefore the Laplace transform definition formulas (A.1) and (A.2) are not often used in practice. The **Laplace transform tables** are used advantageously in practice. The basic correspondences are given in these tables, see Tabs A.1 and A.2.

Example A.3

On the basis of the correspondence [see (A.11)]

$$\mathrm{e}^{-at} \mathrel{\hat{=}} \frac{1}{s+a} \tag{A.21}$$

and properties of the Laplace transform from Tab. A.1 it is necessary to derive further correspondences.

Solution:

a) For $a = 0$ (property 19 in Tab. A.1) from the correspondence (A.21) we can obtain

$$\mathrm{e}^0 = 1 \mathrel{\hat{=}} \frac{1}{s}\ ,$$

$$\eta(t) \mathrel{\hat{=}} \frac{1}{s} \quad . \tag{A.22}$$

b) On the basis of the linearity (property 3 in Tab. A.1) and the correspondences (A.21) and (A.22) we can write

$$\eta(t) - \mathrm{e}^{-at} \mathrel{\hat{=}} \frac{1}{s} - \frac{1}{s+a} = \frac{a}{s(s+a)} \ ,$$

$$1 - \mathrm{e}^{-at} \mathrel{\hat{=}} \frac{a}{s(s+a)} \ . \tag{A.23}$$

c) By differentiation of the correspondence (A.21) with respect to the parameter a (property 20 in Tab. A.1) we obtain

$$\frac{\mathrm{d}}{\mathrm{d}a}\left(\mathrm{e}^{-at}\right) = -t\,\mathrm{e}^{-at} \mathrel{\hat{=}} \frac{\mathrm{d}}{\mathrm{d}a}\left(\frac{1}{s+a}\right) = -\frac{1}{(s+a)^2} \ ,$$

$$t\,\mathrm{e}^{-at} \mathrel{\hat{=}} \frac{1}{(s+a)^2} \quad . \tag{A.24}$$

d) From the correspondence (A.24) for $a = 0$ (property 19 in Tab. A.1) we obtain [see (A.9)]

$$t \mathrel{\hat{=}} \frac{1}{s^2} \quad . \tag{A.25}$$

e) On the basis of the integration in the time domain (property 12 in Tab. A.1) we can get from the correspondence (A.25) the new correspondence

$$\int_0^t \tau \,\mathrm{d}\tau \mathrel{\hat{=}} \frac{1}{s}\left(\frac{1}{s^2}\right),$$

$$\frac{t^2}{2} \mathrel{\hat{=}} \frac{1}{s^3} \ . \tag{A.26}$$

f) From the correspondence (A.26) by the help of property 8 in Tab. A.1 we obtain

$$\frac{t^2}{2}\mathrm{e}^{-at} \mathrel{\hat{=}} \frac{1}{(s+a)^3} \ . \tag{A.27}$$

g) From the correspondence (A.21) for $a = \pm\,\mathrm{j}\omega$ we get

$$\mathrm{e}^{\pm \mathrm{j}\omega t} \mathrel{\hat{=}} \frac{1}{s \mp \mathrm{j}\omega} \ .$$

On the basis of the Euler formulas [see also (A.13)]

$$\sin \omega t = \frac{1}{2\,\mathrm{j}}\left(\mathrm{e}^{\mathrm{j}\omega t} - \mathrm{e}^{-\mathrm{j}\omega t}\right) , \qquad \cos \omega t = \frac{1}{2}\left(\mathrm{e}^{\mathrm{j}\omega t} + \mathrm{e}^{-\mathrm{j}\omega t}\right).$$

we obtain the further two important correspondences [compare with (A.12)]:

$$\sin \omega t \mathrel{\hat{=}} \frac{1}{2\mathrm{j}}\left(\frac{1}{s-\mathrm{j}\omega}-\frac{1}{s+\mathrm{j}\omega}\right)=\frac{\omega}{s^2+\omega^2} \ ,$$

$$\sin \omega t \mathrel{\hat{=}} \frac{\omega}{s^2+\omega^2} \ , \tag{A.28}$$

$$\cos \omega t \mathrel{\hat{=}} \frac{1}{2}\left(\frac{1}{s-\mathrm{j}\omega}+\frac{1}{s+\mathrm{j}\omega}\right)=\frac{s}{s^2+\omega^2} \ ,$$

$$\cos \omega t \mathrel{\hat{=}} \frac{s}{s^2+\omega^2} \ . \tag{A.29}$$

h) We directly get two further important correspondences on the basis of the last two correspondences (A.28) and (A.29) and property 8 in Tab. A.1

$$\mathrm{e}^{-at}\sin \omega t \mathrel{\hat{=}} \frac{\omega}{(s+a)^2+\omega^2} \ , \tag{A.30}$$

$$\mathrm{e}^{-at}\cos \omega t \mathrel{\hat{=}} \frac{s+a}{(s+a)^2+\omega^2} \ . \tag{A.31}$$

We can easily verify by comparison with Tabs A.1 and A.2 that all the derived correspondences are correct. In the similar way it is possible to obtain further correspondences. We can see that by making practical use of the Laplace transform it is enough to have knowledge of a few basic properties and several important correspondences.

Determining originals from transforms

We can directly use the Laplace transform tables in cases where we find originals or transforms in the suitable forms. We mostly make do with simple modifications. Problems can arise for the inverse Laplace transform because some transforms are complex and we must decompose them to their simplest expressions which can be found in the Laplace transform tables. We very often use partial-fraction expansion and residual methods.

In practical cases the transform has mostly the form of the **strictly proper function**

$$X(s)=\frac{M(s)}{N(s)}=\frac{b_m s^m+\ldots+b_1 s+b_0}{a_n s^n+\ldots+a_1 s+a_0}, \quad n>m. \tag{A.32}$$

If the denominator degree n is not greater than the nominator degree m it is necessary to divide the nominator by the denominator.

We can simplify the transform in the form of the strictly proper function (A.32) by the partial-fraction expansion in expressions which may be found in the Laplace transform tables.

For the polynomial in the denominator (A.32) the relation holds

$$N(s)=a_n s^n+\ldots+a_1 s+a_0=a_n(s-s_1)(s-s_2)\ldots(s-s_n), \tag{A.33}$$

where $s_1, s_2, ..., s_n$ are the **roots** of the polynomial $N(s)$ and they are simultaneously the **poles** (singular points) of the transform $X(s)$.

The poles s_i may be simple or multiple. At first consider the simple poles, which can be real or complex. If they are complex then they arise in complex conjugate couples, e.g.

$$s_i = \alpha + \mathrm{j}\beta, \qquad s_{i+1} = \alpha - \mathrm{j}\beta. \tag{A.34}$$

For the complex conjugate couple (A.34) the relation holds

$$(s - s_i)(s - s_{i+1}) = s^2 - 2\alpha s + \alpha^2 + \beta^2 = s^2 + cs + d. \tag{A.35}$$

The couple of the strictly imaginary poles

$$s_i = \mathrm{j}\beta, \qquad s_{i+1} = -\mathrm{j}\beta \tag{A.36}$$

is the special case of (A.34) or (A.35) for $\alpha = c = 0$.

Now consider the multiple poles. For the r-multiple real pole s_i it is possible to write

$$(s - s_i)^r. \tag{A.37}$$

Similarly in accordance with (A.35) we may also write for the r-multiple complex conjugate couple poles s_i and s_{i+1}

$$(s - s_i)^r (s - s_{i+1})^r = \left(s^2 + cs + d\right)^r. \tag{A.38}$$

The transform $X(s)$ of the strictly proper function (A.32) for the given types of poles can be written in the form (for $a_n = 1$)

$$X(s) = \frac{M(s)}{N(s)} = \frac{M(s)}{(s-a)(s-b)^r\left(s^2 + cs + d\right)\left(s^2 + es + f\right)^q}, \tag{A.39}$$

where $(s - a)$ corresponds to the simple real pole a,
$(s - b)^r$ corresponds to the r-multiple real pole b,
$(s^2 + cs + d)$ corresponds to the simple complex conjugate couple

$$\frac{1}{2}\left(-c \pm \sqrt{c^2 - 4d}\right), \tag{A.40}$$

$(s^2 + es + f)^q$ corresponds to the q-multiple complex conjugate couple

$$\frac{1}{2}\left(-e \pm \sqrt{e^2 - 4f}\right). \tag{A.41}$$

The transform $X(s)$ expressed by the relation (A.39) may be written in the decomposed form

$$\begin{aligned} X(s) = {} & \frac{A}{s-a} + \frac{B_1}{s-b} + \frac{B_2}{(s-b)^2} + \ldots + \frac{B_r}{(s-b)^r} + \\ & + \frac{Cs + D}{s^2 + cs + d} + \frac{E_1 s + F_1}{s^2 + es + f} + \frac{E_2 s + F_2}{(s^2 + es + f)^2} + \ldots + \frac{E_q s + F_q}{(s^2 + es + f)^q}, \end{aligned} \tag{A.42}$$

where constants $A, B_1, B_2, ..., B_r, C, D, E_1, E_2, ..., E_q, F_1, F_2, ..., F_q$ are determined, e.g. by the substitution method, the method of indefinite coefficients or the residual method.

The introduced procedure is called the **partial-fraction expansion**.

Example A.4

It is necessary to find the original $x(t)$ from the its transform

$$X(s)=\frac{2s^3+7s^2+4s+1}{s^2(s+1)^2}. \tag{A.43}$$

Solution:

The transform (A.43) is a strictly proper function and therefore in accordance with (A.42) we can write

$$\frac{2s^3+7s^2+4s+1}{s^2(s+1)^2}=\frac{A_1}{s}+\frac{A_2}{s^2}+\frac{B_1}{s+1}+\frac{B_2}{(s+1)^2}. \tag{A.44}$$

a) Substitution method

After multiplying the equation (A.44) by the denominator of its left side we get

$$2s^3+7s^2+4s+1=A_1s(s+1)^2+A_2(s+1)^2+B_1s^2(s+1)+B_2s^2. \tag{A.45}$$

The equation (A.45) holds for any s and therefore it must hold also for the poles of the transform $X(s)$, i.e.:

$$s=s_1=0 \quad \Rightarrow \quad 1=A_2,$$
$$s=s_2=-1 \quad \Rightarrow \quad 2=B_2.$$

As further values of the complex variable s we select

$$s=1 \quad \Rightarrow \quad 14=4A_1+4A_2+2B_1+B_2$$

and using the determined constants A_2, B_2 after modification we get

$$2A_1+B_1=4.$$

We select further

$$s=-2 \quad \Rightarrow \quad 5=-2A_1+A_2-4B_1+4B_2$$

and similarly as in the previous case we use the determined constants A_2 and B_2, and after modification we get

$$A_1+2B_1=2.$$

By solving the simple equation system

$$2A_1+B_1=4,$$
$$A_1+2B_1=2$$

we obtain $A_1 = 2$ a $B_1 = 0$.

The partial-fraction expansion of the transform (A.43) has the form

$$X(s) = \frac{2}{s} + \frac{1}{s^2} + \frac{2}{(s+1)^2}.$$

By the help of the Laplace Transform Table A.2 we easily obtain the original

$$x(t) = 2\eta(t) + t + 2t\,\mathrm{e}^{-t} = 2 + t + 2t\,\mathrm{e}^{-t}, \quad t \ge 0. \tag{A.46}$$

b) Method of indefinite coefficients

We modify the relation (A.45) with respect to the powers of the complex variable s and we get

$$2s^3 + 7s^2 + 4s + 1 = (A_1 + B_1)s^3 + (2A_1 + A_2 + B_1 + B_2)s^2 + (A_1 + 2A_2)s + A_2.$$

The coefficients for the same powers of the complex variable s must be the same and therefore these relations hold

$$2 = A_1 + B_1,$$
$$7 = 2A_1 + A_2 + B_1 + B_2,$$
$$4 = A_1 + 2A_2,$$
$$1 = A_2.$$

By solving the equation system we get the coefficient values: $A_1 = 2$, $A_2 = 1$, $B_1 = 0$ and $B_2 = 2$. The next steps are identical like in case a.

c) Residual method

We use the formula 22 (row) from Tab. A.1

$$x(t) = \sum_i \frac{1}{(r_i - 1)!} \lim_{s \to s_i} \frac{\mathrm{d}^{r_i - 1}}{\mathrm{d}\, s^{r_i - 1}} \left[(s - s_i)^{r_i} X(s) \mathrm{e}^{st} \right],$$

where $i = 1, 2$; $s_1 = 0$, $r_1 = 2$; $s_2 = -1$, $r_2 = 2$ ($n = r_1 + r_2 = 4$).

After substitution (A.43) we successively obtain:

$$x(t) = \lim_{s \to 0} \frac{\mathrm{d}}{\mathrm{d}\, s} \left[\frac{2s^3 + 7s^2 + 4s + 1}{(s+1)^2} \mathrm{e}^{st} \right] + \lim_{s \to -1} \frac{\mathrm{d}}{\mathrm{d}\, s} \left[\frac{2s^3 + 7s^2 + 4s + 1}{s^2} \mathrm{e}^{st} \right] =$$

$$= \lim_{s \to 0} \left[\frac{6s^2 + 14s + 4}{(s+1)^2} \mathrm{e}^{st} - 2\frac{2s^3 + 7s^2 + 4s + 1}{(s+1)^3} \mathrm{e}^{st} + \frac{2s^3 + 7s^2 + 4s + 1}{(s+1)^2} t\,\mathrm{e}^{st} \right] +$$

$$+ \lim_{s \to -1} \left[\frac{6s^2 + 14s + 4}{s^2} \mathrm{e}^{st} - 2\frac{2s^3 + 7s^2 + 4s + 1}{s^3} \mathrm{e}^{st} + \frac{2s^3 + 7s^2 + 4s + 1}{s^2} t\,\mathrm{e}^{st} \right] =$$

$$= (4 - 2 + t) + \left(-4\mathrm{e}^{-t} + 4\mathrm{e}^{-t} + 2t\,\mathrm{e}^{-t}\right) = 2 + t + 2t\,\mathrm{e}^{-t}.$$

We can see that the result is the same like (A.46).

Example A.5

It is necessary to determine the original $x(t)$ for the transform

$$X(s) = \frac{3s^2 + 22s + 13}{s\left(s^2 + 6s + 13\right)}. \tag{A.47}$$

Solution:

The polynomial in the denominator of the transform (A.47) has complex conjugate poles and therefore its partial-fraction expansion has the form

$$\frac{3s^2 + 22s + 13}{s\left(s^2 + 6s + 13\right)} = \frac{A}{s} + \frac{Bs + C}{s^2 + 6s + 13}. \tag{A.48}$$

a) Substitution method

We multiply the equation (A.48) by the denominator of its left side and then we get

$$3s^2 + 22s + 13 = A\left(s^2 + 6s + 13\right) + \left(Bs + C\right)s. \tag{A.49}$$

This equation holds for any s, therefore we select 3 different values and then we obtain

$$s = s_1 = 0 \;\Rightarrow\; 13 = 13A \;\Rightarrow A = 1,$$
$$s = 1 \quad \Rightarrow\; 38 = 20A + B + C \;\Rightarrow\; B + C = 18,$$
$$s = -1 \;\Rightarrow -6 = 8A + B - C \;\Rightarrow\; B - C = -14.$$

We get the linear equation system

$$B + C = 18,$$

$$B - C = -14,$$

which has the solution $B = 2$ and $C = 16$.

In accordance with (A.47) and (A.48) we can write

$$X(s) = \frac{1}{s} + \frac{2s + 16}{s^2 + 6s + 13}.$$

Now we use results (A.30) and (A.31) from the example A.3.

$$X(s) = \frac{1}{s} + \frac{2(s+3) + 2\cdot 5}{(s+3)^2 + 2^2} = \frac{1}{s} + \frac{2(s+3)}{(s+3)^2 + 2^2} + \frac{2\cdot 5}{(s+3)^2 + 2^2}.$$

and we obtain the original

$$\begin{aligned} x(t) &= \eta(t) + 2\,\mathrm{e}^{-3t}\cos 2t + 5\,\mathrm{e}^{-3t}\sin 2t = \\ &= 1 + 2\,\mathrm{e}^{-3t}\cos 2t + 5\,\mathrm{e}^{-3t}\sin 2t, \quad t \geq 0. \end{aligned} \tag{A.50}$$

b) Method of indefinite coefficients

The relation (A.49) after modification has the form

$$3s^2 + 22s + 13 = (A + B)s^2 + (6A + C)s + 13A.$$

The coefficients at the same powers must be the same and therefore it may be written

$$3 = A + B,$$

$$22 = 6A + C,$$

$$13 = 13A.$$

From this equation system there is the result $A = 1$, $B = 2$ and $C = 16$.

The next steps are the same as in previous case a).

The use of the residual method for complex conjugate poles is more elaborate and therefore it is not used in this case.

Example A.6

It is necessary to derive formulas for the initial and final values of the time original (property 16 and 17 in Tab. A.1).

Solution:

a) Initial value

We expand the original $x(t)$ in the MacLaurin series

$$x(t) = x(0) + \frac{\dot{x}(0)}{1!}t + \frac{\ddot{x}(0)}{2!}t^2 + \frac{\dddot{x}(0)}{3!}t^3 + \dots$$

and then we use the Laplace transform

$$X(s) = \frac{x(0)}{s} + \frac{\dot{x}(0)}{s^2} + \frac{\ddot{x}(0)}{s^3} + \frac{\dddot{x}(0)}{s^4} + \dots$$

It is obvious that after multiplication of the left and right side by the complex variable s the relation holds (if it exists)

$$x(0) = \lim_{s\to\infty} sX(s) \quad . \tag{A.51}$$

b) Final value

For the transform of the derivative $\dot{x}(t)$ it holds [see (A.17)]:

$$\mathrm{L}\{\dot{x}(t)\} = \int_0^\infty \dot{x}(t)\mathrm{e}^{-st}\mathrm{d}t = sX(s) - x(0),$$

$$\lim_{s\to 0}\int_0^\infty \dot{x}(t)\mathrm{e}^{-st}\mathrm{d}t = \lim_{s\to 0}[sX(s) - x(0)],$$

$$\int_0^\infty \dot{x}(t)\mathrm{d}t = \lim_{s\to 0} sX(s) - x(0),$$

$$x(\infty) - x(0) = \lim_{s\to 0} sX(s) - x(0).$$

Therefore we obtain (if it exists)

$$x(\infty) = \lim_{s\to 0} sX(s) \quad . \tag{A.52}$$

Example A.7

It is necessary to derive the transforms of the original multiplied by the exponential function (complex shifting in the complex domain) and the delayed original (property 8 and 6 in Tab. A.1).

Solution:

a) Multiplication by exponential function

$$\mathrm{L}\left\{\mathrm{e}^{\mp at}\,x(t)\right\}=\int_0^\infty x(t)\mathrm{e}^{-(s\pm a)t}\mathrm{d}t=\int_0^\infty x(t)\mathrm{e}^{-ut}\mathrm{d}t=X(u)=X(s\pm a),$$

$$\mathrm{e}^{\mp at}\,x(t)\,\hat{=}\,X(s\pm a)\ . \tag{A.53}$$

The substitution $u = s \pm a$ was used.

b) Delayed original $x(t-a)$, $a \geq 0$

$$x(t-a)=\begin{cases}0 & t<a,\\ x(t-a) & t\geq a,\end{cases}$$

$$\mathrm{L}\{x(t-a)\}=\int_0^\infty x(t-a)\mathrm{e}^{-st}\mathrm{d}t=\int_0^\infty x(u)\mathrm{e}^{-s(u+a)}\mathrm{d}u=$$

$$=\mathrm{e}^{-as}\int_0^\infty x(u)\mathrm{e}^{-su}\mathrm{d}u=\mathrm{e}^{-as}\,X(s),$$

$$x(t-a)\,\hat{=}\,\mathrm{e}^{-as}\,X(s)\ . \tag{A.54}$$

The substitution $u = t - a$ was used.

Tab. A.1 Laplace transform - definition formulas and basic properties

	Definition formulas
1	$X(s)=\mathrm{L}\{x(t)\}=\int_0^\infty x(t)\mathrm{e}^{-st}\mathrm{d}t$
2	$x(t)=\mathrm{L}^{-1}\{X(s)\}=\frac{1}{2\pi j}\int_{c-j\infty}^{c+j\infty} X(s)\mathrm{e}^{st}\mathrm{d}s$
	Linearity
3	$\mathrm{L}\{a_1x_1(t)\pm a_2x_2(t)\}=a_1X_1(s)\pm a_2X_2(s)$
	Similarity
4	$\mathrm{L}\{ax(at)\}=X\left(\frac{s}{a}\right), a>0$
	Convolution in time domain
5	$\mathrm{L}\left\{\int_0^t x_1(t-\tau)x_2(\tau)d\tau\right\}=\mathrm{L}\left\{\int_0^t x_2(t-\tau)x_1(\tau)d\tau\right\}=X_1(s)X_2(s)=X_2(s)X_1(s)$
	Real shifting on the right in time domain (time delay)
6	$\mathrm{L}\{x(t-a)\}=\mathrm{e}^{-as}X(s), a\geq 0$
	Real shifting on the left in time domain (lead)
7	$\mathrm{L}\{x(t+a)\}=\mathrm{e}^{as}\left[X(s)-\int_0^a x(t)\mathrm{e}^{-st}\mathrm{d}t\right], a\geq 0$
	Complex shifting in a complex domain
8	$\mathrm{L}\left\{x(t)\mathrm{e}^{\mp at}\right\}=X(s\pm a)$
	Derivative in time domain
9	1-st order derivative $\quad \mathrm{L}\left\{\frac{\mathrm{d}x(t)}{\mathrm{d}t}\right\}=sX(s)-x(0)$
10	*n*-th order derivative $\quad \mathrm{L}\left\{\frac{\mathrm{d}^n x(t)}{\mathrm{d}t^n}\right\}=s^nX(s)-\sum_{i=1}^{n}s^{n-i}\frac{\mathrm{d}^{i-1}x(0)}{\mathrm{d}t^{i-1}}$
	Derivative in a complex domain
11	$\mathrm{L}\{tx(t)\}=-\frac{\mathrm{d}X(s)}{\mathrm{d}s}$

	Integral in time domain
12	$\mathrm{L}\left\{\int_0^t x(\tau)\,\mathrm{d}\tau\right\} = \frac{1}{s}X(s)$
	Integral value
13	$\int_0^\infty x(t)\,\mathrm{d}t = \lim_{s\to 0} X(s)$
14	$\int_0^\infty t x(t)\,\mathrm{d}t = -\lim_{s\to 0} \frac{\mathrm{d}X(s)}{\mathrm{d}s}$
	Periodical function transform
15	$\mathrm{L}\{x(t)+x(t-a)+x(t-2a)+\ldots\} = X(s)\frac{1}{1-\mathrm{e}^{-as}}$ a – period, $a > 0$
	Initial value in time domain (if it exists)
16	$x(0) = \lim_{t\to 0_+} x(t) = \lim_{s\to\infty} sX(s)$
	Final value in time domain (if it exists)
17	$x(\infty) = \lim_{t\to\infty} x(t) = \lim_{s\to 0} sX(s)$
	Mathematical operation with respect to an independent parameter
18	$\mathrm{L}\{x(t,a)\} = X(s,a)$
19	$\mathrm{L}\{\lim_{a\to a_0} x(t,a)\} = \lim_{a\to a_0} X(s,a)$
20	$\mathrm{L}\left\{\frac{\partial x(t,a)}{\partial a}\right\} = \frac{\partial X(s,a)}{\partial a}$
21	$\mathrm{L}\left\{\int_{a_1}^{a_2} x(t,a)\,\mathrm{d}a\right\} = \int_{a_1}^{a_2} X(s,a)\,\mathrm{d}a$
	Inverse transform by residues
22	$x(t) = \sum_i \operatorname{res}_{s=s_i}\left[X(s)\mathrm{e}^{st}\right] = \sum_i \left\{\frac{1}{(r_i-1)!}\lim_{s\to s_i}\frac{\mathrm{d}^{r_i-1}}{\mathrm{d}s^{r_i-1}}\left[(s-s_i)^{r_i}X(s)\mathrm{e}^{st}\right]\right\}$ r_i – the multiplicity of transform pole s_i $n = \sum_i r_i$ – the polynomial degree in the transform denominator

Tab. A.2 Laplace transform - correspondences

	Transform $X(s)$	Original $x(t)$
1	s	$\dot{\delta}(t)$
2	1	$\delta(t)$
3	$\frac{1}{s}$	$\eta(t)$
4	$\frac{1}{s^n},\quad n=1,2,\ldots$	$\frac{t^{n-1}}{(n-1)!}$
5	$\frac{s}{T_1 s+1}$	$\alpha_1\left[\delta(t)-\alpha_1 \mathrm{e}^{-\alpha_1 t}\right],\qquad \alpha_1=\frac{1}{T_1}$
6	$\frac{1}{T_1 s+1}$	$\alpha_1 \mathrm{e}^{-\alpha_1 t},\qquad \alpha_1=\frac{1}{T_1}$
7	$\frac{1}{s(T_1 s+1)}$	$1-\mathrm{e}^{-\alpha_1 t},\qquad \alpha_1=\frac{1}{T_1}$
8	$\frac{1}{s^2(T_1 s+1)}$	$\frac{1}{\alpha_1}\left(\mathrm{e}^{-\alpha_1 t}-1\right)+t,\qquad \alpha_1=\frac{1}{T_1}$
9	$\frac{b_1 s+1}{s(T_1 s+1)}$	$1+(\alpha_1 b_1-1)\mathrm{e}^{-\alpha_1 t},\qquad \alpha_1=\frac{1}{T_1}$
10	$\frac{b_1 s+1}{s^2(T_1 s+1)}$	$C_1\left(1-\mathrm{e}^{-\alpha_1 t}\right)+t,\ C_1=b_1-\frac{1}{\alpha_1},\quad \alpha_1=\frac{1}{T_1}$
11	$\frac{s}{(T_1 s+1)^2}$	$\alpha_1^2(1-\alpha_1 t)\mathrm{e}^{-\alpha_1 t},\qquad \alpha_1=\frac{1}{T_1}$
12	$\frac{1}{(T_1 s+1)^2}$	$\alpha_1^2 t\,\mathrm{e}^{-\alpha_1 t},\qquad \alpha_1=\frac{1}{T_1}$
13	$\frac{1}{s(T_1 s+1)^2}$	$1-(1+\alpha_1 t)\mathrm{e}^{-\alpha_1 t},\qquad \alpha_1=\frac{1}{T_1}$
14	$\frac{1}{s^2(T_1 s+1)^2}$	$t-\frac{2}{\alpha_1}+\left(\frac{2}{\alpha_1}+t\right)\mathrm{e}^{-\alpha_1 t},\qquad \alpha_1=\frac{1}{T_1}$
15	$\frac{b_1 s+1}{(T_1 s+1)^2}$	$\alpha_1^2[b_1+(1-\alpha_1 b_1)t]\mathrm{e}^{-\alpha_1 t},\qquad \alpha_1=\frac{1}{T_1}$

	Transform $X(s)$	Original $x(t)$
16	$\dfrac{b_1 s+1}{s(T_1 s+1)^2}$	$1-[1+\alpha_1(1-\alpha_1 b_1)t]\mathrm{e}^{-\alpha_1 t}, \quad \alpha_1=\dfrac{1}{T_1}$
17	$\dfrac{b_1 s+1}{s^2(T_1 s+1)^2}$	$t+C_1-(C_1-C_2 t)\mathrm{e}^{-\alpha_1 t}$ $C_1=b_1-\dfrac{2}{\alpha_1},\ C_2=1-\alpha_1 b_1,\ \alpha_1=\dfrac{1}{T_1}$
18	$\dfrac{s}{(T_1 s+1)^n},\quad n=2,3,\ldots$	$\alpha_1^n\dfrac{t^{n-2}}{(n-1)!}(n-1-\alpha_1 t)\mathrm{e}^{-\alpha_1 t}, \quad \alpha_1=\dfrac{1}{T_1}$
19	$\dfrac{1}{(T_1 s+1)^n},\quad n=1,2,\ldots$	$\alpha_1^n\dfrac{t^{n-1}}{(n-1)!}\mathrm{e}^{-\alpha_1 t}, \quad \alpha_1=\dfrac{1}{T_1}$
20	$\dfrac{1}{s(T_1 s+1)^n},\quad n=1,2,\ldots$	$1-\mathrm{e}^{-\alpha_1 t}\sum_{i=0}^{n-1}\alpha_1^i\dfrac{t^i}{i!}, \quad \alpha_1=\dfrac{1}{T_1}$
21	$\dfrac{1}{s^2(T_1 s+1)^n},\quad n=1,2,\ldots$	$t-\dfrac{n}{\alpha_1}+\mathrm{e}^{-\alpha_1 t}\sum_{i=0}^{n-1}\alpha_1^{i-1}(n-i)\dfrac{t^i}{i!}, \quad \alpha_1=\dfrac{1}{T_1}$
22	$\dfrac{s}{(T_1 s+1)(T_2 s+1)},\quad T_1\neq T_2$	$C_1\,\mathrm{e}^{-\alpha_1 t}-C_2\,\mathrm{e}^{-\alpha_2 t},\ \alpha_1=\dfrac{1}{T_1},\ \alpha_2=\dfrac{1}{T_2}$ $C_1=\dfrac{1}{T_1(T_2-T_1)},\ C_2=\dfrac{1}{T_2(T_2-T_1)}$
23	$\dfrac{1}{(T_1 s+1)(T_2 s+1)},\quad T_1\neq T_2$	$C_1\left(\mathrm{e}^{-\alpha_1 t}-\mathrm{e}^{-\alpha_2 t}\right),\ C_1=\dfrac{1}{T_1-T_2},\ \alpha_1=\dfrac{1}{T_1},\ \alpha_2=\dfrac{1}{T_2}$
24	$\dfrac{1}{s(T_1 s+1)(T_2 s+1)},\quad T_1\neq T_2$	$1+C_1\,\mathrm{e}^{-\alpha_1 t}-C_2\,\mathrm{e}^{-\alpha_2 t},\ \alpha_1=\dfrac{1}{T_1},\ \alpha_2=\dfrac{1}{T_2}$ $C_1=\dfrac{T_1}{T_2-T_1},\ C_2=\dfrac{T_2}{T_2-T_1}$
25	$\dfrac{1}{s^2(T_1 s+1)(T_2 s+1)},\quad T_1\neq T_2$	$t-C_0+C_1\,\mathrm{e}^{-\alpha_1 t}-C_2\,\mathrm{e}^{-\alpha_2 t},\ C_0=T_1+T_2$ $C_1=\dfrac{T_1^2}{T_1-T_2},\ C_2=\dfrac{T_2^2}{T_1-T_2},\ \alpha_1=\dfrac{1}{T_1},\ \alpha_2=\dfrac{1}{T_2}$
26	$\dfrac{b_1 s+1}{(T_1 s+1)(T_2 s+1)},\quad T_1\neq T_2$	$C_1\,\mathrm{e}^{-\alpha_1 t}-C_2\,\mathrm{e}^{-\alpha_2 t},\ \alpha_1=\dfrac{1}{T_1},\ \alpha_2=\dfrac{1}{T_2}$ $C_1=\dfrac{T_1-b_1}{T_1(T_1-T_2)},\ C_2=\dfrac{T_2-b_1}{T_2(T_1-T_2)}$

	Transform $X(s)$	Original $x(t)$
27	$\dfrac{b_1 s+1}{s(T_1 s+1)(T_2 s+1)},\ T_1 \neq T_2$	$1+C_1\,\mathrm{e}^{-\alpha_1 t}+C_2\,\mathrm{e}^{-\alpha_2 t},\ \alpha_1=\dfrac{1}{T_1},\ \alpha_2=\dfrac{1}{T_2}$ $C_1=\dfrac{b_1-T_1}{T_1-T_2},\ C_2=\dfrac{T_2-b_1}{T_1-T_2}$
28	$\dfrac{b_1 s+1}{s^2(T_1 s+1)(T_2 s+1)},\ T_1 \neq T_2$	$t+C_0+C_1\,\mathrm{e}^{-\alpha_1 t}+C_2\,\mathrm{e}^{-\alpha_2 t},\ C_0=-T_1-T_2+b_1$ $C_1=\dfrac{(b_1-T_1)T_1}{T_2-T_1},\ C_2=\dfrac{(T_2-b_1)T_2}{T_2-T_1},\ \alpha_1=\dfrac{1}{T_1},\ \alpha_2=\dfrac{1}{T_2}$
29	$\dfrac{s}{\prod\limits_{i=1}^{n}(T_i s+1)},\ n=2,3,\dots\ T_i-\text{different}$	$-\sum\limits_{i=1}^{n} C_i\,\mathrm{e}^{-\alpha_i t},\ C_i=\dfrac{T_i^{n-3}}{\prod\limits_{k=1,k\neq i}^{n}(T_i-T_k)},\ \alpha_i=\dfrac{1}{T_i}$
30	$\dfrac{1}{\prod\limits_{i=1}^{n}(T_i s+1)},\ n=2,3,\dots\ T_i-\text{different}$	$\sum\limits_{i=1}^{n} C_i\,\mathrm{e}^{-\alpha_i t},\ C_i=\dfrac{T_i^{n-2}}{\prod\limits_{k=1,k\neq i}^{n}(T_i-T_k)},\ \alpha_i=\dfrac{1}{T_i}$
31	$\dfrac{1}{s\prod\limits_{i=1}^{n}(T_i s+1)},\ n=2,3,\dots\ T_i-\text{different}$	$1-\sum\limits_{i=1}^{n} C_i\,\mathrm{e}^{-\alpha_i t},\ C_i=\dfrac{T_i^{n-1}}{\prod\limits_{k=1,k\neq i}^{n}(T_i-T_k)},\ \alpha_i=\dfrac{1}{T_i}$
32	$\dfrac{1}{s^2\prod\limits_{i=1}^{n}(T_i s+1)},\ n=2,3,\dots\ T_i-\text{different}$	$t-C_0+\sum\limits_{i=1}^{n} C_i\,\mathrm{e}^{-\alpha_i t},\ \alpha_i=\dfrac{1}{T_i}$ $C_i=\dfrac{T_i^{n}}{\prod\limits_{k=1,k\neq i}^{n}(T_i-T_k)},\ C_0=\sum\limits_{i=1}^{n} T_i$
33	$\dfrac{\omega}{s^2+\omega^2}$	$\sin\omega t$
34	$\dfrac{s}{s^2+\omega^2}$	$\cos\omega t$
35	$\dfrac{s}{T_0^2 s^2+2\xi_0 T_0 s+1},$ $0\le\xi_0<1$	$-C_1\,\mathrm{e}^{-\gamma t}\sin(\omega t-\varphi),\ C_1=\dfrac{1}{\omega T_0^3},\ \gamma=\dfrac{\xi_0}{T_0}$ $\omega=\dfrac{1}{T_0}\sqrt{1-\xi_0^2},\ \varphi=\mathrm{arctg}\,\dfrac{\omega}{\gamma}$

	Transform $X(s)$	Original $x(t)$
36	$\dfrac{1}{T_0^2 s^2 + 2\xi_0 T_0 s + 1}$, $0 \le \xi_0 < 1$	$C_1 \mathrm{e}^{-\gamma t} \sin \omega t,\ C_1 = \dfrac{1}{\omega T_0^2},\ \gamma = \dfrac{\xi_0}{T_0},\ \omega = \dfrac{1}{T_0}\sqrt{1-\xi_0^2}$
37	$\dfrac{1}{s\left(T_0^2 s^2 + 2\xi_0 T_0 s + 1\right)}$, $0 \le \xi_0 < 1$	$1 - C_1 \mathrm{e}^{-\gamma t} \sin(\omega t + \varphi),\ C_1 = \dfrac{1}{\omega T_0},\ \gamma = \dfrac{\xi_0}{T_0}$ $\omega = \dfrac{1}{T_0}\sqrt{1-\xi_0^2},\quad \varphi = \operatorname{arctg}\dfrac{\omega}{\gamma}$
38	$\dfrac{1}{s^2\left(T_0^2 s^2 + 2\xi_0 T_0 s + 1\right)}$, $0 \le \xi_0 < 1$	$t - C_0 + C_1 \mathrm{e}^{-\gamma t} \sin(\omega t + 2\varphi),\ C_0 = 2\xi_0 T_0^2$ $C_1 = \dfrac{1}{\omega}, \gamma = \dfrac{\xi_0}{T_0},\ \omega = \dfrac{1}{T_0}\sqrt{1-\xi_0^2},\ \varphi = \operatorname{arctg}\dfrac{\omega}{\gamma}$
39	$\dfrac{b_1 s + 1}{T_0^2 s^2 + 2\xi_0 T_0 s + 1}$, $0 \le \xi_0 < 1$	$C_1 \mathrm{e}^{-\gamma t} \sin(\omega t + \varphi),\ C_1 = \dfrac{1}{\omega T_0^3}\sqrt{(1-2b_1\gamma)T_0^2 + b_1^2}$ $\gamma = \dfrac{\xi_0}{T_0},\ \omega = \dfrac{1}{T_0}\sqrt{1-\xi_0^2},\ \varphi = \operatorname{arctg}\dfrac{\omega b_1}{1-\gamma b_1}$
40	$\dfrac{b_1 s + 1}{s\left(T_0^2 s^2 + 2\xi_0 T_0 s + 1\right)}$, $0 \le \xi_0 < 1$	$1 + C_1 \mathrm{e}^{-\gamma t} \sin(\omega t - \varphi),\ C_1 = \dfrac{1}{\omega T_0^2}\sqrt{(1-2b_1\gamma)T_0^2 + b_1^2}$ $\gamma = \dfrac{\xi_0}{T_0},\ \omega = \dfrac{1}{T_0}\sqrt{1-\xi_0^2},\ \varphi = \operatorname{arctg}\dfrac{\omega T_0^2}{b_1 - \gamma T_0^2}$

b_1, b_2 – the real constants, $T_i > 0$, $i = 0, 1, \ldots$

REFERENCES

[1] ALFARO, V. M. *Evolución y tendencies en el desarrollo de los métodos de sintonizació de controladores PID.* Departamento de Automática, Esculea de Ingeniera Electrica Universidad de Costarica, 2004, 77 p.

[2] ASTROM, K. J., HAGGLUND, T. *Advanced PID Control*. ISA – Instrumentation, Systems, and Automation Society, Research Triangle Park, 2006, 460 p.

[3] DORF, R.C., BISHOP, R. *Modern Control Systems.* 12th Edition. Prentice-Hall, Upper Saddle River, New Jersey 2011, 1082 p.

[4] FINDEISEN, W. *Automatic Control Technology (in Polish).* 2nd Edition. Panstwowe Wydawnictwo Naukowe, Warszawa, 1969, 441 p.

[5] FRANKLIN, G. F., POWELL, J. D., EMAMI-NAEIMI, A. *Feedback Control of Dynamic Systems*. Fourth Edition. Prentice-Hall, 2002, 910 p.

[6] HAUGEN, F. *The Good Gain method for PI (D) controller tuning*. Tech Teach, http://techteach.no (19. July 2010), 7 p.

[7] KALAS, V., JURISICA, L., ZALMAN, M. *Technical Cybernetics of Electrical Drives (in Slovak).* Alfa, Bratislava, 1978, 390 p.

[9] KOPELOVIC, A. P. *Automatic Control in Metallurgy (in Russian).* Gosudarstvennoje naucno-techniceskoje izdatelstvo literatury po cernoj i cvetnoj metallurgii. Moskva, 1963, 408 p.

[10] KOWAL, J. *Basis of Automatic Control (in Polish).* Volume 1, Uczelniane wydawnictwa naukovo-dydaktyczne AGH, Krakow, 2006, 301 p.

[11] KOZAKOVA, A. Tuning decentralized PID controllers for performance and robust stability. */ICIC Express Letters: Int. Journal of Research and Surveys/,* vol. 2, No.2 (June 2008), p. 117-122.

[12] KROKAVEC, D., FILASOVA, A. *Discrete Systems (in Slovak).* 2nd Edition. Elfa, Kosice, 2008, 334 p.

[13] LANDAU, I. D., ZITO, G. *Digital Control Systems. Design, Identification and Implementation*. Springer – Verlag, London, 2006, 484 p.

[14] MATUSU, R., PROKOP, R. Robust Tuning of PI Controllers for Interval Systems. *Transactions of the VSB – Technical University of Ostrava, Mechanical Series*, No. 2, 2010, vol. LVI, article No. 1790, p. 123-130

[15] NISE, N. S. *Control Systems Engineering*. 6th Edition. John Wiley and sons, Hoboken, New Jersey, 2011, 926 p.

[16] NOSKIEVIC, P. *Modelling and System Identification (in Czech).* Montanex, Ostrava, 1999, 276 p.

[17] O´DWYER, A. *Handbook of PI and PID Controller Tuning Rules*. Third Edition. Imperial College Press, London, 2009, 608 p.

[18] PIVONKA, P., SCHMIDT, M. Comparative Analysis of Discrete Derivative Implementations in PID Controllers. In: *Proceedings of the 11th WSEAS International Conference on SYSTEMS*, Agios Nikolaos, Crete Island, Greece, July 23-25, 2007, p. 33-37

[19] ROSINOVA, D. Robust Decentralized PID Controller: A Case Study. *Transactions of the VSB – Technical University of Ostrava*, Nr. 2/2008, volume LIV, Mechanical Series, article Nr. 1631, p. 115-120

[20] SKOGESTAD, S. Simple analytic rules for model reduction and PID controller tuning. *Modeling, Identification and Control*, 2004, Vol. 25, No. 2, p. 85-120

[21] SZKLARSKI, L., JARACZ, K., VITECEK, A. *Optimization of Electrical Drives (in Polish).* Panstwowe Wydawnictwo Naukowe, Warszawa, 1989, 291 p.

[22] SULC, B., VITECKOVA, M. *Theory and practice of control system design (in Czech)*. CTU Publishing House, Prague, 2004, 333 p.

[23] VASEK, V., KOLOMAZNIK, K., JANACOVA, D. Optimization and Automatic Control of Chromium Recycling. Technology. In "*Proceedings of the 5th WSEAS Int. Conf. on Simulation, modeling and optimization*". Corfu, Greece, August 17-19, 2005, p. 391-394

[24] VISIOLI, A. *Practical PID Control*. Springer – Verlag, London, 2006, 310 p.

[25] VISIOLI, A. ZHONG, Q. *Control of Integral Processes with Dead Time*. Springer – Verlag, London, 2011, 251 p.

[26] VITECKOVA, M., VITECEK, A., LANDRYOVA, L. *Basic Principles of Automatic Control*. Technical University of Ostrava, 2012, 115 p.

[27] VITECKOVA, M., VITECEK, A. Modulus optimum for Digital Controllers. *Acta Montanistica Slovaca*. Ročník 8, 4/2003, p. 214-216

[28] VITECKOVA, M., VITECEK, A. 2DOF PI and PID Controllers Tuning. In *Proceedings of the 9th IFAC Workshop on Time Delay Systems (TDS),* Prague, June 7-9, 2010, 6 p. on CD

[29] VITECKOVA, M., VITECEK, A. *Selected Controller Tuning Methods (in Czech)*. Technical University of Ostrava, 2011, 230 p.

[30] VITECKOVA, M., VITECEK, A. Unified Approach to Digital and Analog 2DOF PI Controller Tuning for Integrating Plants. In *Proceedings of the 12th International Carpathian Control Conference* ICCC´2011. Velke Karlovice, Czech Republic, VSB- Technical University of Ostrava, May 25-28, 2011, p. 437-440

[31] ZIEGLER, J. G., NICHOLS, N. B. Optimum Setting for Automatic Controllers. *Transactions of the ASME*, 64, 1942, p. 759-768

[32] ZITEK, P. *Time Delay Control System Design Using Functional State Models*. CTU Publishing House, Prague, 1998, 93p.

Authors:	Prof. Ing. Antonín Víteček, CSc., Dr.h.c. Prof. Ing. Miluše Vítečková, CSc.
Department:	Control Systems and Instrumentation
Title:	Closed-Loop Control of Mechatronic Systems
Place, Year, Edition:	Ostrava, 2013, 1st
Pages:	204
Published:	VŠB - Technical University of Ostrava 17. listopadu 15/2172 708 33 Ostrava - Poruba
Printed:	REPRONIS, s.r.o. Teslova 2, 702 00 Ostrava
Number of copies:	70

Not for sale

ISBN 978-80-248-3149-7